Endocannabinoid hydrolases in human blood fractions

Nuha Anajirih, MSc.

Thesis submitted to the University of Nottingham for the degree of Doctor of Philosophy

March 2019

Abstract

Despite extensive studies of the cardiovascular effects of cannabinoids and evidence that endocannabinoid levels in the blood can be influenced by diet and metabolic state, there has been no investigation of the activities of endocannabinoid hydrolases (fatty acid amide hydrolase, FAAH, and monoacylglycerol lipase, MAGL, which hydrolyse anandamide, AEA, and 2-arachidonoylglycerol, 2AG, respectively), their variation in human blood, and which methods can be used to monitor them. This thesis had the aim of identifying the activity levels of these enzymes in human blood fractions and the influence of clotting processes.

To characterise enzyme activities, multiple assay styles (a radiometric assay, activity-based protein profiling, ABPP, and a spectrophotometric assay) were utilized with blood vessels and blood samples from Wistar rats. Functional expression of MAGL and FAAH in these samples was measured using the Gold Standard technique of the radiometric assay; the results of which agreed broadly with ABPP. By contrast, the spectrophotometric assay used for MAGL activity detection was not suitable for enzyme detection using complex samples. In rat mesenteric arteries, MAGL was not affected, whereas FAAH activity increased with age of the donor animals, which suggests that FAAH may either be a potential therapeutic target or biomarker for vascular dysfunction associated with age. The activity levels of these enzymes were higher in circulating blood

compared to vascular tissue, suggesting a potentially greater influence on circulating endocannabinoid levels.

In a human study, overnight fasting blood samples were obtained on three different occasions from healthy volunteers of both genders within the University of Nottingham (n=18). Studies provided evidence that MAGL and FAAH activities were measurable and reproducible in healthy human blood. Platelets contained a higher proportion of MAGL activity while erythrocytes contained a higher proportion of FAAH activity compared to other blood fractions, which predicts their roles; MAGL may be involved in the platelet aggregation process, while FAAH may be involved in the turnover of erythrocytes. There was no difference in the level of MAGL and FAAH activities when comparing activity over the three visits for individual donors or between male and female donors. The stability of enzyme activities within an individual suggests that the activity level of these enzymes could be used as a biomarker in the future. However, these studies identified that enzyme activity of isolated platelets and erythrocytes degraded after short term storage at -80 ^{o}C, but was retained after storage in liquid nitrogen. Clearly, this has implications for the archiving of material for subsequent enzyme analysis.

A second human study collected blood samples on one occasion from eight volunteers to investigate the influence of clotting processes. Clot formation was initiated by addition of thrombin and enzyme activity was measured in the supernatant layer following centrifugation at low speed equivalent to that used to separate serum. The clotting process altered enzyme distribution, where

FAAH in the serum-like fraction could be liberated from either platelets or erythrocytes, while MAGL activity was not present in the supernatant layer and was only marginally reduced by the direct proteolytic effects of thrombin. ABPP was able to detect multiple serine hydrolase enzymes with higher activity such as MAGL, but not those with marginal activity, such as FAAH, in these blood fractions.

Finally, the functional impact of extended inhibition of MAGL and FAAH activities on proliferation and migratory activity were investigated with the MCF-7 breast adenocarcinoma cell line using MTT and cell exclusion assays, respectively. Although MCF-7 cells were found to express FAAH, but not MAGL, inhibition of FAAH activity did not have any functional impact on proliferation or migration of these cells. Thus, FAAH inhibition could be considered not useful as a therapeutic target for breast cancer.

These findings provide evidence, for the first time, of the reproducible detection of MAGL and FAAH activities in human blood samples, how their functional expression changes during normal patho/physiological processes such as clotting, and how neither longer term FAAH nor MAGL inhibition has any effects on MCF-7 cell proliferation or migration. This research sets the foundation for future clinical studies using the expression of these enzymes as a potential biomarker for dysfunction or disease.

Meeting Abstracts

Anajirih N, O'Sullivan SE and Alexander SPH (2018) The derivation of serum FAAH activity, 28th Annual Symposium on the Cannabinoids (Leiden) **28**: P2-55.

Anajirih N, O'Sullivan SE and Alexander SPH (2017) Endocannabinoid hydrolase activities are differentially expressed in human blood fractions 27th Annual Symposium on the Cannabinoids (Montreal) **27**: P1-23.

Anajirih NA, Alexander SP and O'Sullivan SE (2017) A pilot study on measuring the activity level of fatty acid amide hydrolase (FAAH) in human blood Proceedings of the British Pharmacological Society (London) **18**: 170P http://www.pA2online.org/abstracts/Vol18Issue1abst170P.pdf

Anajirih NA, Alexander SP and O'Sullivan SE (2017) Characterization of monoacylglycerol hydrolysis in human platelets proceedings on the 8th workshop on cannabinoid research, British Pharmacological Society (London).

Anajirih N, Ho W-SV, O'Sullivan S and Alexander SPH (2016) 2-Oleoylglycerol hydrolysis in the rat vasculature by monoacylglycerol lipase activity, 26th Annual Symposium on the Cannabinoids (Zakopane) **26**: P1-18.

Acknowledgement

First, I would like to thank Allah for giving me the strength and determination to continue working to reach my dream, and thank Allah for everything that I am blessed with.

I would like to thank my supervisors Dr. Stephen Alexander and Dr. Saoirse O'sullivan sincerely for their advice, support, and direction throughout my PhD. I genuinely mean this, I have truly enjoyed my time and I have learned a great deal from them. Thanks also to the other staff at the Life Science school, particularly Michael Garle and Paul Millns ; without their help, my work would not have been possible.

My never-ending love and appreciation go to my family, parents, and siblings, for their support and trust, so I dedicate this thesis to them. Finally, I am grateful to the Government of Saudi Arabia for their financial support and the chance to study at the University of Nottingham.

Abbreviation

AA	Arachidonic acid
AA	Abdominal aortae
ABPP	Activity based protein profiling
ADBH6/12	α/β hydrolase domain enzymes 6/12
AEA	Anandamide
ApoA-1	Apolipoprotein A1
ATG	Arachidoic-1-thioglycerol
ATP	Adenosine triphosphate
2-AG	2-Arachidoiniglycerol
CB1/CB2	Cannabinoids receptors
CNS	Central nerve system
COX-2	Cyclooxygenase-2
DAGLα/β	Diacylglycerol lipase α and β
DTNB	5,5′-dithiobis(2-dinitrobenzoic acid)
eCBs	Endocannabinoid system
E2	17-β-oestradiol
EMT	Putative endocannabinoid membrane transporter
ER	Estrogen receptor

FAAH	Fatty acid amide hydrolase
HER2	Human epithelial receptor 2
HSCs	Haematopoietic stem cells
MA	Mesenteric arteries
MAFP	Methylarachidonoylfuorophosphonate
MAGs	Monoacglycerols
MAGL	Monoacglylcerol lipase
NAPE-PLD	N-acylphosphatidylethanolamine phospholipase
NO	Nitric oxide
2-OG	2-oleolglycerol
PGE2	Prostaglandin-E_2
PR	Progesterone receptor
PRP	Platelets-rich-plasma
SH	Serine hydrolase
TA	Thoracic aortae
1-TG	1- Thioglycerol
THC	Δ^9-tetrahydrocannabinol
TxA2	Thromboxane-2

Table of Contents

Table of Figures

Chapter 1 General introduction

1.1 The Endocannabinoid system

The endocannabinoid system (eCB) is an intricate endogenous signalling structure that is named after the Cannabis plant. The eCB is composed of cannabinoid (CB) receptors, endocannabinoid ligands, and enzymes that regulates the biosynthesis, cellular uptake and metabolism of these ligands (Pertwee et al., 2010). The cannabinoid receptors (CB_1 and CB_2) are members of the superfamily of G protein-coupled receptors (GPCR) (Pertwee et al., 2010), and their natural ligands are lipophilic, derived from fatty acids, particularly arachidonic acid (Reggio, 2010). The main endocannabinoids documented and thoroughly investigated are long chain polyunsaturated fatty acid (PUFA) amides, such as N-arachidonoylethanolamine (anandamide, AEA) and glycerides, such as sn-2-arachidonoylglycerol (Pertwee, 2008). Endocannabinoids bind and stimulate CB receptors (Di Marzo et al., 2004), mimicking the pharmacological activities of the psychoactive principle of the Cannabis plant, Δ^9-tetrahydrocannabinol (THC), first isolated over 50 years agofrom hashish, a resinous extract from the plant (Gaoni et al., 1964).

The CB_1 cannabinoid receptor is distributed in multiple regions of the brain, and acts to impair cognition and memory, and alter the perception of pain (Pertwee et al., 2010). CB_1 receptors have been observed in a number of peripheral tissues in humans, such as liver, cardiac, adipose, and the gastrointestinal tract (Kurz et al., 2008), functioning to control several physiological processes such as blood pressure and energy control. In contrast, comparatively low levels of CB_2 receptors are present in the central nervous

system (CNS); higher expression has been identified in cells of immune origin, including peripheral macrophages (Cabral et al., 2008), producing immunomodulatory effects. CB receptors are also located on peripheral blood mononuclear cells, where the levels of CB_2 receptor are reportedly higher than the CB_1 receptor (Nong et al., 2001).

AEA and 2-AG are described as endogenous neuromodulatory lipids as a reflection of their location in the CNS. Based on tissue and cellular responses, AEA acts as a partial agonist of CB_1 receptors, while 2-AG is a full agonist of CB_1 and CB_2 receptors. 2-AG and AEA both have higher affinities for the CB_1 than the CB_2 receptor (Muccioli, 2010; Pertwee et al., 2010)

1.2 The biosynthesis of eCBs

2-AG and AEA are arachidonate derivatives, known as eicosanoids, which are synthesised upon demand via the hydrolysis of cell membrane phospholipid precursors (Pertwee, 2008).

1.2.1 AEA synthesis

AEA is generated from an N-acyl phosphatidylethanolamine (NAPE), a precursor that is formed as a result of the transacylation of membrane phosphatidylethanolamine-containing phospholipids via a calcium-dependent N-acyl transferase (Fowler et al., 2017). NAPE is subsequently hydrolysed by an N-acylphosphatidylethanolamine phospholipase D (NAPE-PLD) to AEA (Liu et al., 2006). The pharmacological effects of AEA on CB receptors rely on the lifespan of the eCB in the extracellular space, that is restricted by rapid cellular uptake, before the intracellular hydrolysis of AEA to ethanolamine and arachidonic acid (AA) primarily by the serine hydrolase fatty-acid amide

hydrolase (FAAH) (Ahn et al., 2009). N-Acylethanolamine-selective acid amidase (NAAA) (Ueda et al., 1999), a cysteine amidase, and a second serine hydrolase amidase known as FAAH-2 (Wei et al., 2006) also contribute to the hydrolysis of AEA, albeit in a relatively minor way compared to FAAH (see Figure 1.1).

Endocannabinoids are poorly water soluble requiring a transmembrane protein transporter to pass through lipid membrane to degrade inside the cell (Deutsch, 2016). *In vitro* and *in vivo* studies suggested a putative endocannabinoid membrane transporter (EMT) (Chicca et al., 2012). Other EMT-independent mechanisms have been reported, such as binding to cytoplasmic proteins (FABPs) or the uptake of AEA facilitated by FAAH degradation which facilitates the uptake of AEA (Deutsch, 2016).

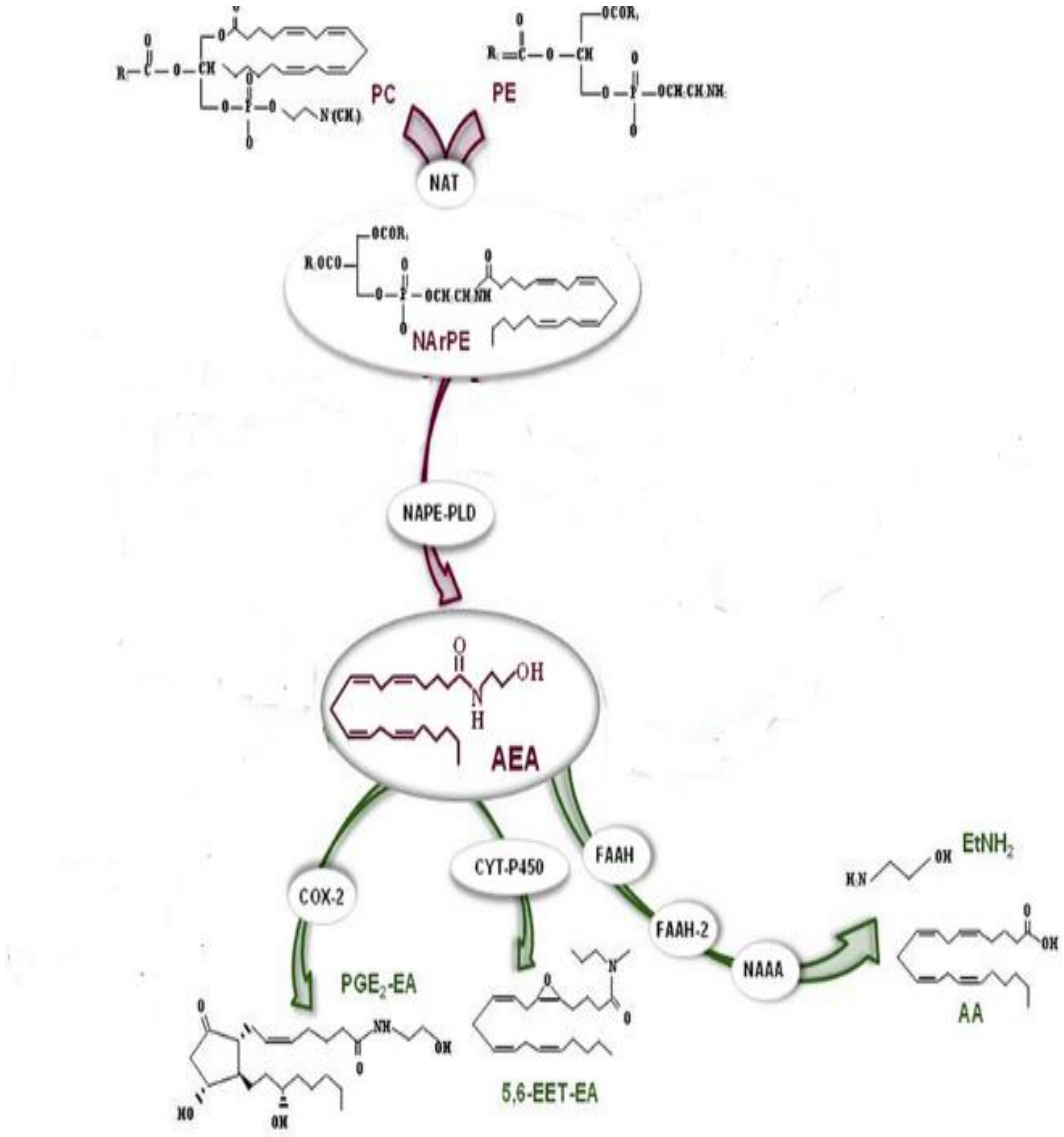

Figure 1.1: **Biosynthetic and degradation pathways of AEA.** N-arachidonoylphosphatidylethanolamine (NArPE) is generated from the hydrolysis of 1,2-sn-di-arachidonoylphosphatidylcholine (PC) by N-acyltransferase (NAT). Subsequently, N-acyl-phosphatidylethanolamine (NAPE)-specific phospholipase D (NAPE-PLD) is hydrolysed by NArPE, leading to the release of AEA. AEA is hydrolysed mainly by FAAH into arachidonic acid (AA) and ethanolamine (EtNH2) or by FAAH-2 and N-acylethanolamine-hydrolyzing acid amidase (NAAA). Alternatively, AEA is transformed to PGE_2-ethanolamide (PGE_2-EA) via cyclooxygenase-2 (COX-2), or to 5,6-epoxyeicosatrienoic acid ethanolamide (5,6-EET-EA) via cytochrome P450 (CYT-P450) .

1.2.2 2-AG synthesis

2-AG is potentially synthesised from multiple pathways. The synthesis pathway believed to be most physiologically relevant in the majority of cells is the conversion of diacylglycerol (DAG) to 2-AG by two serine hydrolases (the sn-1-selective DAG lipase α and β) (Bisogno et al., 2003). In turn, DAG is generated from the hydrolysis of phosphatidylinositol 4,5-bisphosphate by phospholipase C-β (PLC-β) (Bisogno et al., 2005) . The DAGLα isoform is the most significant enzyme in the brain for 2-AG synthesis. On the other hand, DAGLβ is the most abundant enzyme in the liver (Piyanova et al., 2015) (see figure 1.2). Additionally, it is probable that, at least in adipocytes, a percentage of 2-AG synthesis occurs due to triglyceride lipolysis through adipose triglyceride lipase (ATGL) and hormone sensitive lipase (HSL) (Zechner et al., 2009).

Like AEA, 2-AG appears to be accumulated into cells through EMT (Chicca et al., 2012), and hydrolysed by serine hydrolase enzymes. By using an activity-based protein profiling (ABPP) approach, it was reported that 85% of 2-AG in mouse brain membranes is hydrolysed by monoacylglycerol lipase (MAGL) and beyond this 13% is hydrolysed by two α/β hydrolase domain enzymes (ADBH6 or ABHD12) (Blankman et al., 2007). In addition, 2-AG and AEA can be metabolized by other enzymes such as cyclooxygenase-2 (COX-2) to produce prostaglandin analogues and by cytochrome P450 to produce epoxy derivatives (Pertwee et al., 2002; Snider et al., 2010)(see figure 1.1 and 1.2).

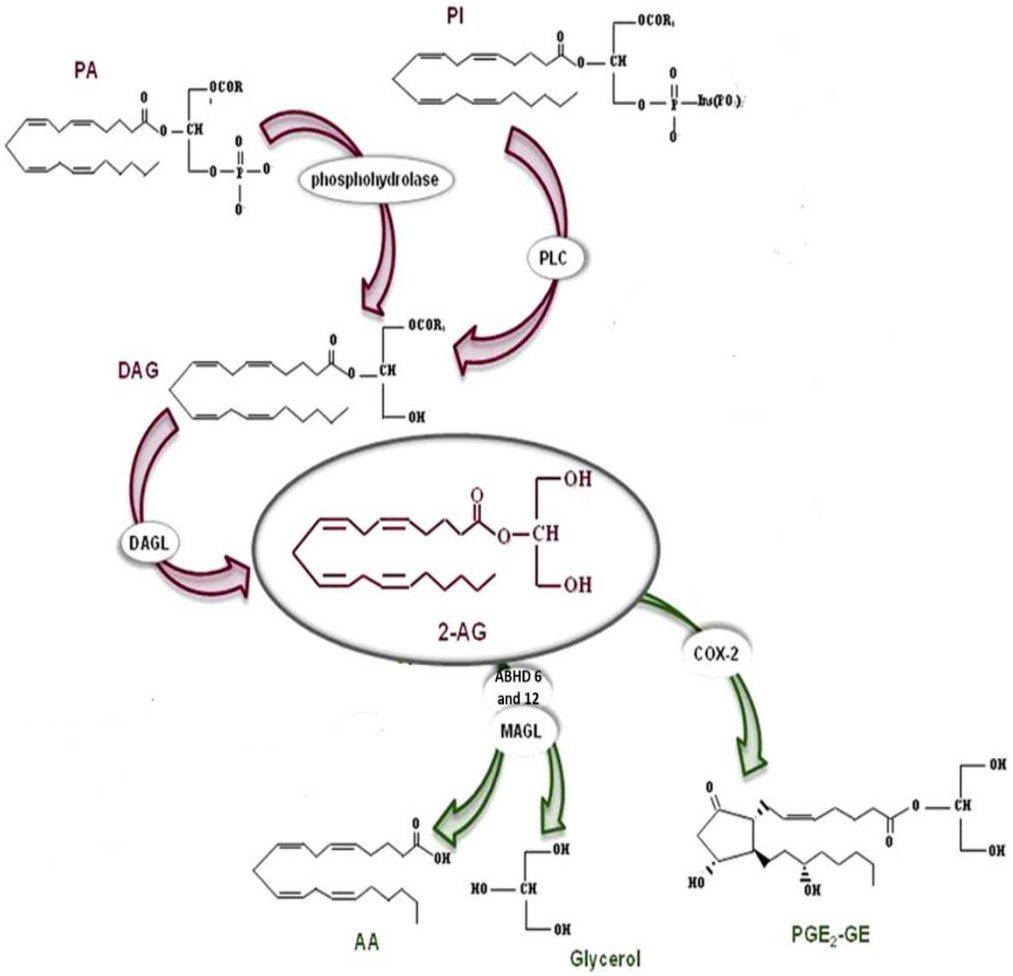

Figure 1.2: Biosynthetic and degradation pathways of 2-AG. The precursor diacylglycerol (DAG) is generated by either phosphatidic acid (PA) that is degraded by PA-phosphohydrolase or from inositol phospholipids (PI) degraded by a phospholipase C (PLC). Then, DAG is converted to 2-AG via a sn-1-DAG lipase (DAGL). 2-AG is mainly metabolised by MAGL to arachidonic acid (AA) and glycerol, and also ABHD6 and 12 enzymes involved in this pathway. Alternatively, 2-AG is metabolized by COX-2 to PGE_2 glyceryl-ester (PGE_2-GE).

1.3 ECB hydrolysis pathways

1.3.1 MAGL enzyme

MAGL is a 33 kDa soluble enzyme (Blankman et al., 2007), which associates with membranes, that belongs to the ester-signature class of enzymes, a subclass of serine hydrolase that has a unique Ser-Ser-Lys catalytic triad (Bertrand et al., 2010; Labar et al., 2010). Human MAGL has a catalytic triad (Ser122-His269-Asp239), where the Ser122 position is a nucleophilic serine that is responsible for cleaving the ester bond of the preferred substrate 2-AG. Human MAGL shares 84% structure sequence identity with rat MAGL and 92% identity with mouse MAGL (Blankman et al., 2007). MAGLX2, a second variant, differs from MAGLX1 in that it lacks 30 amino acids from a region that is vital for recognising and selecting substrates, which subsequently affects its activity (Labar et al., 2010b). However, the physiological function of this splice variant is still unknown.

MAGL's principle physiological functional responsibility includes catalysing the terminal step in the triglyceride hydrolysis in the adiposity. Hormone sensitive lipase (HSL) cleaves triglyceride to MAGs (including 2-AG and 2-OG), which is further converted by MAGL to glycerol and fatty acids, and then fatty acids are released into the blood circulation to maintain energy homeostasis (Chen et al., 2014). MAGL is localized in human brain presynaptic terminals close to CB_1 receptors in the axon terminals, such that its localization is optimal for termination of 2-AG-CB_1 signalling (Ludanyi et al., 2011).

The degradation of 2-AG by MAGL releases AA, a precursor for pro-inflammatory eicosanoid synthesis in the brain, liver and lung (Nomura et al.,

2011a). Since the level of 2-AG is two hundred times higher than AEA in the brain (Fagundo et al., 2013), MAGL largely contributes to determining free AA levels in brain. AA is oxygenated by COX-2, leading to the production of neuro-inflammatory prostaglandins E_2 and D_2, which regulate pain and inflammation (Hu et al., 2008). In addition, MAGL leads to the release of free fatty acids for the synthesis of pro-tumorigenic signalling lipids, including prostaglandins, in proliferative cancer cells (Mulvihill et al., 2013).

Therefore, pharmacological inhibitors of MAGL offer useful tools not only for characterizing MAGL, but also to identify its physiological and potential therapeutic roles.

1.3.1.1 MAGL inhibitors

JZL184, a piperazine carbamate, is a potent and irreversible MAGL inhibitor with an IC_{50} value of 8 nM in mouse (Pan et al., 2009), and in human blood and platelet-rich-plasma (PRP) (Brantl et al., 2014a). It does not interact with CB receptors and it does not inhibit the 2-AG synthesis activities of DAGLα and -β (Long et al., 2009a). Inhibition of MAGL by JZL184 *in vivo* exerts CB-dependent anti-inflammatory effects by elevating the level of 2-AG via preventing its hydrolysis, without interfering with the AEA and prostaglandin pathways in the digestive system, and without causing toxicity in the gastrointestinal system (Nomura et al., 2011a)

However, at a high concentration(>10 μM) JZL184 inhibits FAAH in addition to MAGL (Long et al., 2009a), and also it exerts lower potency for rat MAGL than mouse and human MAGL (Scalvini et al., 2015). More recently, JJKK-048 (a piperidine triazole urea), was identified as a highly potent and selective MAGL inhibitor, without inhibiting other serine hydrolases such as ABDH6/12

and FAAH, with equivalent potency of IC_{50} value of 214-275 pM at human, mouse or rat enzymes (Aaltonen et al., 2013; Korhonen et al., 2014). In common with JZL184, JJKK-048 inhibited MAGL through irreversibly binding to the active site Ser122 of MAGL to prevent access of substrate (Aaltonen et al., 2013). An *in vivo* study has shown that blocking MAGL by JJKK-048 exerts anti-nociceptive effects (Aaltonen et al., 2016).

1.3.2 FAAH enzyme

FAAH is a 61 kDa serine hydrolase belonging to the amidase-signature subclass that has a Ser241-Ser217-Lys142 catalytic triad. It is an integral membrane enzyme localized in the endoplasmic reticulum (Patricelli et al., 1999; McKinney et al., 2003). It also metabolises several other lipid signalling molecules such as the sleep-inducing substance 9(Z)-octadecenamide (oleamide) (Cravatt et al., 1995), the satiety signal N-oleoyl ethanolamine (OEA)(De Fonseca et al., 2001), and the analgesic anti-inflammatory factor N-palmitoyl ethanolamine (PEA) (Lambert et al., 2002). These lipid transmitters, unlike AEA, exert their effects through non-CB receptor pathways. FAAH, also described as FAAH-1, is found in different patterns across human tissues, mainly expressed in the brain, kidneys, liver, small intestines, lungs, and prostate (Wei et al., 2006). FAAH knockout mice are viable and have been found to display analgesia and an anti-inflammatory profile, without disruptions in motility, cognition, or body temperature (Cravatt et al., 2001). The distribution and concentration of FAAH-1 enzyme is similar in the brain of rats and humans (Romero et al., 2002; Rusjan et al., 2013).

A second isoform FAAH-2 differs from FAAH-1 by molecular size (58 kDa), localization (within lipid rafts (Kaczocha et al., 2010)), and is also widely distributed in mammalian tissues, mostly found in the kidneys, liver, lungs, prostate, heart and ovaries. Intriguingly, the enzyme is not expressed in rodents. FAAH-2 has lower AEA hydrolytic activity than FAAH-1, while ODA is the preferred substrate (Wei et al., 2006). The general term of FAAH enzyme, has been commonly used in human tissue investigations, and may be used to refer to the two isoforms of FAAH.

These data together suggest that FAAH/AEA pathways regulate a distinct subset of behavioural processes; thus, developing selective pharmacological inhibition of FAAH is a potential strategy to raise AEA levels and maintain the advantageous effects of CB receptor activation in a selectively amplificatory manner, whilst preventing the unwanted effects of direct, indiscriminate CB_1 agonists. Notably, however, FAAH inhibitors have not transitioned to clinical use to date.

1.3.2.1 FAAH inhibitors

There has been a great advancement in the development of FAAH inhibitors in recent years, including irreversible and reversible covalent inhibitors. Developing irreversible inhibitors also gets more interest due to the fact that they lead to the long-lasting and complete inactivation of target proteins, therefore maximising the pharmacological effects from one administration (Alexander et al., 2005). Almost 30% of enzymes which are targeted by drugs in clinical use today, are inhibited by a covalent irreversible mechanism (Robertson, 2005).

Mor et al. (2004) were the first to describe the alkylcarbamic acid ester (URB597) as a potent FAAH inhibitor that irreversibly inactivates the enzyme

by the formation of a covalent bond with Ser241 of the FAAH active site (Mor et al., 2004). URB597 displays nanomolar potency to inhibit both FAAH isoforms (FAAH-1/-2) in ABPP, and around 20 fold selectivity for FAAH-2 over FAAH-1 (Wei et al., 2006). An *in vitro* study found that URB597 exhibited high potency in human liver microsomes and rat brain membranes with IC_{50} values of 2.5 and 5 nM, respectively. In addition, URB597 has been shown to be efficacious in the treatment of pain in rat and mice models, which is reflected in sustained inhibition of brain FAAH and elevation of AEA levels associated with enhancing local activation of the CB_1 receptor. This amplificatory effect helps to avoid the motor impairment related to direct CB_1 activation (Piomelli et al., 2006).

However, at a high concentration (10 µM), URB597 is reported to interact with several targets in addition to FAAH (Ahn et al., 2011), inhibiting around 42% of other rat liver esterase activity, such as carboxylesterase (Keith et al., 2008; Karbarz et al., 2009). In addition, Ahn et al. (2011) found that by using the ABPP technique, 10 µM of URB597 completely blocked the FP-labelling of several serine hydrolase in addition to FAAH in membrane proteomes of liver, brain and heart from human and mice.

Although URB597 is the most commonly used inhibitor of FAAH activity, more selective FAAH-1 inhibitors would clearly be useful. JNJ1661010, a piperazinyl phenyl urea, is a potent and selective FAAH-1 inhibitor, which also forms a covalent bond at the active site of the enzyme. It inhibits human recombinant FAAH with an IC_{50} value of 12 nM. JNJ1661010 displays limited inhibition of FAAH-2 and a >100-fold selectivity for FAAH-1 compared to FAAH-2 (Karbarz et al., 2009).

In addition, PF-3845, a biaryl ether piperidine, is a high potent and selective inhibitor of FAAH-1 with a covalent, irreversible mechanism of action similar to URB597 and JNJ1661010. It has negligible activity against the FAAH-2 variant (IC_{50} value >10 μM), and exerts anti-nociceptive effects *in vivo* (Ahn et al., 2009).

These features make JNJ-1661010 and PF-3845 well-suited to discriminate and investigate the role of FAAH-1 in both central and peripheral patho/physiological processes.

1.3.2.1.1 Therapeutic potential of FAAH inhibitors

It has been argued that inhibiting FAAH activity could bring new therapeutic benefits to treat certain disease conditions where increased eCB activity would be advantageous. URB59 (Fegley et al., 2005; Piomelli et al., 2006), JNJ-1661010 (Kono et al., 2014) and PF-3845 have all been found to exhibit analgesic pharmacology in various animal models (J Alvarez-Jaimes et al., 2011), and do not cause classical cannabinoid-like effects such as hypothermina, catalepsy, and hyperphagia, or predicted abuse liability. URB597 results in a crucial loss of inflammatory and neuropathic pain in experiments on animals (Pertwee, 2014). URB597 has also been shown to reduce signs of nausea in rats and emesis in shrews produced by Morphine-6-glucuronide (Parker et al., 2011), secondly to reverse abuse-related behavioural effect of nicotine in rats (Forget et al., 2009), thirdly to increase wakefulness in rats (Murillo-Rodríguez et al., 2007), and finally to reduce blood pressure and cardiac contractility in hypertensive rats (Godlewski et al., 2010). Treated mice with URB579 showed a major reduction in gastric irritation caused by non-steroidal anti-inflammatory drug (diclofenac) suggesting potential therapeutic benefits of dual COX-

2/FAAH inhibition. In spite of all that, the effect of URB597 in neuropathic models is rather inconsistent as a result of its sub-optimal selectivity profile.

Furthermore, PF-3845 is more potent for FAAH-1 compared to URB579, producing hypothermia and anti-allodynic like effects in mice (Schlosburg et al., 2010), and showing efficacy similar to naproxen in the rat model of hyperalgesia and inflammatory pain. However, the therapeutic utility of FAAH inhibitors in humans have not yet evaluated. Nevertheless, there has only been minor human application of FAAH inhibitors, one of which was cancelled due to low efficacy in knee osteoarthritis (Huggins et al., 2012). Thus, FAAH inhibitors are far from being exploited therapeutically in the endocannabinoid system.

1.4 The role of endocannabinoids in the circulatory system

1.4.1 Vascular Function

In a healthy cardiovascular system, key characteristics of arterial blood vessels are to guarantee efficient propagation of the pressure wave in the arterial tree and then, at the arteriolar level, a normal endothelial and smooth muscle cell function to permit vascular tone and blood flow to be properly regulated. The endothelial layer of the blood vessels regulates the production of vasoactive substances or endothelial-derived relaxing factors (EDRFs). For instance, when endothelial cells are subject to a rise in shear stress, they form and release EDRFs including nitric oxide (NO) and prostacyclin, and subsequently these substances pass into the nearby vascular smooth muscle cells (VSMCs) causing VSMC relaxation/vasodilation (Vanhoutte et al., 2017). Early studies found that, in rat mesenteric arteries (Randall et al., 1996) and in bovine coronary arteries (Pratt et al., 1998), AEA is synthesised and released by endothelial cells that serve as

a precursor of prostacyclin. AEA hydrolysis is catalysed intracellularly by FAAH to AA, which is further converted to vasodilatory eicosanoids such as prostacyclin or epoxyeicosatrienoic acids (Pratt et al., 1998). Since then, extensive research has shown that AEA induces the relaxation of blood vessels *in vitro*, with conflicting results reviewed by Stanley et al. (2014a). For instance, AEA stimulated relaxation in human (Stanley et al., 2012) and rat (O'Sullivan et al., 2004) mesenteric arteries, acting on the CB_1 receptor in the endothelium, leading to phosphorylation of endothelial nitric oxide (eNOS) for the production of NO. However, AEA stimulates endothelium relaxation in the rat aorta by an FAAH and COX-2 metabolism pathway. AEA is hydrolysed to AA by FAAH, then AA is further metabolised by COX-2 to PGE_2 that binds to the prostaglandin E receptor type 4 (EP_4) in VSM and causes vasorelexation (Herradón et al., 2007). It may be that two pathways exist at the same time, as the interrelation between these two endothelium pathways has been reported. NO regulates PGE_2 production by stimulating the activation of COX-2 enzymes (Martín Giménez et al., 2018). Therefore, AEA plays a critical role in arterial hypertension. Inhibition of FAAH by URB597 leads to normalising blood pressure and heart rate by decreasing cardiac contractility of hypertensive rats (Bátkai et al., 2004; Godlewski et al., 2010). In humans, elevating the AEA level in plasma was linked to a reduction of blood pressure in young males with the functional FAAH gene variant, resulting in decreased enzyme activity (Sarzani et al., 2008).

2-AG is also released by endothelium cells and induces vasodilation (Hillard, 2000). In human isolated mesenteric arteries, the vasodilation effect of 2-AG was mediated by metabolism by COX-2 (Stanley et al., 2014b), and caused a CB_1-dependent vasorelaxation in the same arterial bed from rabbits, and induced

a weak relaxation in rat aorta independent of both CB_1 and COX-2 metabolism (Stanke-Labesque et al., 2004). 2-AG has generally received less attention than AEA because 2-AG is less stable *in vitro* and *in vivo,* it undergoes spontaneous intramolecular migration to 1-AG that has lower affinity for the CB_1 receptor compared to 2-AG (Hillard, 2000).

Taken together, AEA and 2-AG inducing vasodilation may be through different mechanisms depending on animal species, vascular beds, and in humans, the medical background. However, less is known about the expression of FAAH and MAGL activities in regulating this mechanism, and which factors may influence them.

1.4.2 The eCBs and blood cells

1.4.2.1 Haematopoiesis

Blood cells derived from haematopoietic stem cells (hemocytoblast, HSCs) (see figure 1.3), a subtype of the cells in the bone marrow of adult mammals residing in a specialized microenvironment 'niche', provided via stromal matrix to support stem cell differentiation and proliferation. HSCs give rise to two lineages: lymphoid progenitor cells and myeloid progenitor cells, the latter of which give rise to CFU-GEMM (Colony-forming unit: erythrocyte, granulocyte, monocyte and megakaryocyte) colonies (see figure 1.3). The mobilization of HSCs is regulated by specific transcription factors, cytokines and growth factors such as erythropoietin (Epo) and interleukin-3 (IL-3) (Hoffbrand et al., 2011). An *in vitro* study showed that AEA at a low micromolar concentration, acting at CB_2 receptors, stimulates the proliferation of HSC lines and normal mouse bone marrow cells, and this effect was synergistic with Epo and IL-3 (Valk et al.,

1997). In contrast, AEA inhibits the migration of bone marrow cells, while 2-AG acts via CB_2 receptors to enhance the migration of these cells (Patinkin et al., 2008), and the effect was also synergistic with Epo and IL-3 (Jordà et al., 2002). This suggests a role of eCBs in the regulation of blood cell production.

The appearance of eCB in the blood stream has been ascribed to their movement from blood cells and peripheral tissues (Randall, 2007), and their levels is argued to illustrate the general levels of eCB in all of the body (Fanelli et al., 2012). Some of the constituents of blood are described briefly below.

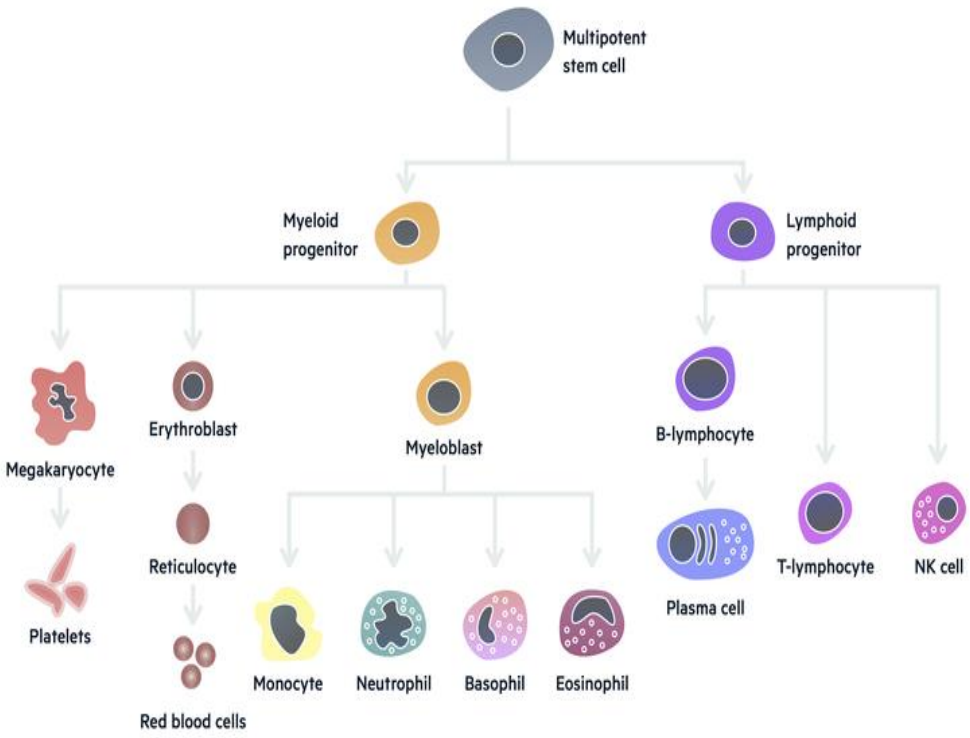

Figure 1.3: Illustration of the hematopoietic stem cells and the blood cell lines that arise from it. The figure was adapted from (Hoffbrand et al., 2011).

1.4.2.2 Plasma

Plasma is a liquid extracellular matrix that contains an unquantified number of proteins (around 289 proteins have been documented)(Anderson et al., 2002; Anderson, 2010), which are mainly secreted by the liver and the intestine. In addition, plasma carries other secretion products and proteins derived from cell leakage (Anderson et al., 2002), which may only occur transiently by release from damaged cells or tissues during disease, representing potential diagnostic biomarkers.

2-AG and AEA levels were detected in human blood (Vogeser et al., 2006; Brantl et al., 2014a) and plasma (Jian et al., 2010; Pastor et al., 2014), where the level of 2-AG is one hundred times greater than AEA, similar to the situation reported in brain (Nomura et al., 2008). The higher concentration of 2-AG may mean that it is a more "important" eCB in tissues as it demonstrates higher efficacy at CB receptors compared to AEA (Sugiura et al., 1999; Sugiura et al., 2002). However, their levels are of limited use as potential biomarkers because of their instability in plasma (Pastor et al., 2014).

There is, as yet, limited data about the activities of MAGL and FAAH in healthy human plasma. A MAGL-like activity was identified to be present in plasma in 1969, initially measured in human post-heparin plasma using a radiometric assay using moneoylglycerol as substrate (Greten et al., 1969). A MAGL activity was also purified from healthy human post-heparin plasma (Noma et al., 1976). In contrast to MAGL as a cytosolic enzyme, FAAH is a membrane-bound enzyme; FAAH activity is not present in plasma, but may be released by blood cells (Jian et al., 2010).

1.4.2.3 Erythrocytes

Erythrocytes represent 96% of the total number of blood cells (Hoffbrand et al., 2011). They are formed from the precursor proerythroblast, which is formed from the transformation of myeloid stem cells, which have a large nucleus and stippled chromatin. In 15 days proerythroblast develops into basophilic, which are smaller and the nuclear chromatin becomes coarser where the ribosomes synthesis occurs. A polychromatic normoblast is then formed followed by the formation of orthochromatic erythroblasts (see figure 1.3). These stages contain haemoglobin and the chromatin in the nuclei becomes clumped and dark. This is then converted into reticulocytes where the nuclei are ejected (young RBC). The two main factors that regulate erythropoiesis are sensing hypoxia and the erythropoietin (Epo)- Epo receptor signalling pathway. Epo is a hormone produced by the kidneys that regulates the differentiation of proerythroblasts (Hoffbrand et al., 2011). Intriguingly, *in vitro* low 2-AG (at low micromolar concentrations) increased the proliferation of erythroid cells in culture in the absence of Epo (Patinkin et al., 2008). Eventually, mature erythrocytes are formed which require nutritional factors and cofactors such as iron, vitamin B12 and folate (Hoffbrand et al., 2011).

The primary functions of the red blood cells are to transport oxygen from pulmonary capillaries to peripheral tissues, eliminate carbon dioxide from the body via the systemic capillaries, and maintain pH (Jagger et al., 2001).

As there is no nucleus in erythrocytes, they are not involved in protein synthesis (Jagger et al., 2001). A study by Boyer in 1981 was able to detect membrane-bound MAGL-like activity in healthy human erythrocytes using a radiometric assay with ethyloleate as substrate (Boyer et al., 1981). Fourteen

years later, a MAGL activity was purified from human erythrocyte membranes (Somma-Delpero et al., 1995). Thereafter, there have been no published data on the presence or role of MAGL in erythrocytes. One possible explanation is the difficulty in detecting MAGL activity in human erythrocytes due to its relative instability and scarcity. The low activity of MAGL may be due to its proportional inhibition by Apolipoprotein A-1 (ApoA-1), which is found in erythrocytes (Somma-Delpero et al., 1995), and inhibits MAGL in rat hearts (Vérine et al., 1989).

In common with MAGL, one published study stated that FAAH may be released from blood cells (Yapa et al., 2012). Utilising human erythrocyte ghosts, Bojesen et al. (2005) described that AEA in less than one second passes through erythrocytes membranes, and is then degraded by FAAH, through a saturable mechanism that does not require ATP. Erythrocyte membrane ghosts from human erythrocytes were produced by light water hemolysis until totally free of haemoglobin. At a higher concentration than that found in circulating plasma of heathy subjects, AEA induces eryptosis (Bentzen et al., 2007). Nevertheless, there are no data available to-date about the stability and reproducibility of FAAH activity in erythrocytes.

1.4.2.4 Platelets

Platelets are small, discoid, enucleated cell fragments, hence lacking gene transcription, which are produced in the bone marrow by fragmentation of megakaryocytes. Megakaryocytes release platelets into the blood stream (Gasperi et al., 2014c), see figure 1.3. Nascent platelets contain mRNA from megakaryocytes that are used for protein synthesis (Rowley et al., 2013). 2-AG,

acting through $CB_{1/2}$ receptors, is reported to enhance the differentiation of megakaryocytes and production of platelets. Differentiation can be described as losing rounded morphology and the addition of a spinous phenotype with extended cytoplasmic protrusions, and via the release of particular markers for late-stage megakaryocyte maturation. In addition, megakaryocytes have the capacity to control 2-AG tone by raising the activity of MAGL and lowering expression of both CB receptors on plasma membrane during differentiation (Gasperi et al., 2014a). 2-AG is also synthesised and released from platelets (Maccarrone et al., 2002a).

After circulating for around 10 days, platelets are destroyed in the liver and spleen (Catani et al., 2010). In healthy individuals, platelet counts are between 150 and 400 x 10^9/L, being higher in females than males (Becker et al., 2006), which plays a critical role in hemostasis by regulating the creation of thrombus and vascular tone.

The hydrolysis of MAGs by MAGL was first demonstrated experimentally by Bry et al. (1979) using 3×10^8 /mL of human platelets, which corresponds to the normal concentration of platelets in blood (Bry et al., 1979). Following this observation, it was concluded that the activity of MAGL was 100-times higher in human platelets compared to other lipases (Chau et al., 1988), and was found in platelet membranes (Gkini et al., 2009). Like MAGL, FAAH activity was also detected in human platelets (Maccarrone et al., 1999; Fasia et al., 2003). Since human platelets showed MAGL and FAAH activities, platelets might be counted as a potential source of releasing these enzymes into blood circulation. Since then, to-date there have been no data or information about the reproducibility between individuals or stability of these enzymes in human blood.

1.4.2.4.1 ECBs and thrombus formation

In comparison with other blood cells, platelets can be considered as one of the sources of circulating eCBs, which may participate in many pathophysiological responses. Maccarrone and colleagues carried out the early work about the role of eCBs and platelets function. In 2001, Maccarrone et al. (2001b) reported that low concentration of 2-AG (~400 nM) caused activation of human platelets (Malorni et al., 2004). Continuing with this work, it was found that the action of 2-AG was enhanced by serotonin while it was reduced by ADP and collagen (Maccarrone et al., 2003a).

Since then, a large body of evidence has shown that 2-AG is an agonist induced platelet activation in different species, such as rat (Shearer et al., 2018), rabbit (Gkini et al., 2009), and human (Malorni et al., 2004; Baldassarri et al., 2008; Keown et al., 2010; Grazia Signorello et al., 2011; Signorello et al., 2011a; Signorello et al., 2013; Brantl et al., 2014b; Brantl et al., 2014a). However, in independent research to-date, 2-AG induces platelet aggregation through two different pathways; CB_1/CB_2-dependent mechanism, or an AA-dependent pathway.

Data presented by Maccarrone et al. (2001b) and Signorello et al. (2011a) in platelet-rich-plasma (PRP) have shown that 2-AG induced platelet activation through CB receptors, where the CB_1 antagonist rimonabant decreased thrombin induced platelet aggregation (Signorello et al., 2011a). In contrast, other studies used whole blood aggregometry, reporting that 2-AG induced platelet aggregation via a MAGL triggered mechanism, resulting in AA, which was then further metabolised by COX-2 to thromboxane2 (TxA_2) (Keown et al., 2010; Brantl et al., 2014a). TxA_2 controls platelet aggregation through TP prostanoid

receptors. Pharmacological inhibition of MAGL by JZL184 partially inhibited platelet aggregation in human blood and PRP (Brantl et al., 2014b) (see figure 1.4). This discrepancy may be explained by different methodologies of platelet aggregation. The Maccarrone and Signorello studies used PRP to promote platelet aggregation, and indeed human platelets are reported to highly express $CB_{1/2}$ receptors (V Catani et al., 2010). In contrast, studies by Keown and Brantl used whole blood aggregometry to permit platelet activation to be assessed in its physiological environment, in the presence of leukocytes and erythrocytes that can modulate platelet aggregation.

2-AG also induces platelet aggregation by lowering the intracellular level of cAMP, which reduces platelet activation (Signorello et al., 2016). Therefore, inappropriate activation of coagulation cascade leads to pathophysiological response such as destructive blood clots that can cause a heart attack, stroke, or other vascular diseases. 2-AG and AEA do not behave interchangeably as regulators, yet they possess unique biological functions, particularly in megakaryocyte/platelet biology. Unlike 2-AG, AEA induces platelet activation at a micromolar concentration *in vitro* in the presence of other stimuli such as collagen, thrombin, and fibrinogen, independent of hydrolysis by FAAH; thus, AEA is not an individual influence on platelet function but rather a co-agonist, playing a role other than activation and aggregation (Maccarrone et al., 1999; Maccarrone et al., 2001a; Brantl et al., 2014b). For instance, it was reported that AEA in the blood could be one of several factors that are required for platelet survival by stimulating eNOS activity, consequently increasing both the levels of platelet NO and cyclic GMP (Signorello et al., 2011b). AEA regulates NO increase that in turn contributes to platelet survival and relaxation of vascular

tone (Kunos et al., 2000; Signorello et al., 2011b). However, there is an interrelationship; NO enhances uptake of AEA by endothelial cells (Maccarrone et al., 2000a), leading to the removal of AEA from the extracellular space, which results in a reduction in the abnormal formation of the thrombus (Maccarrone et al., 1999).

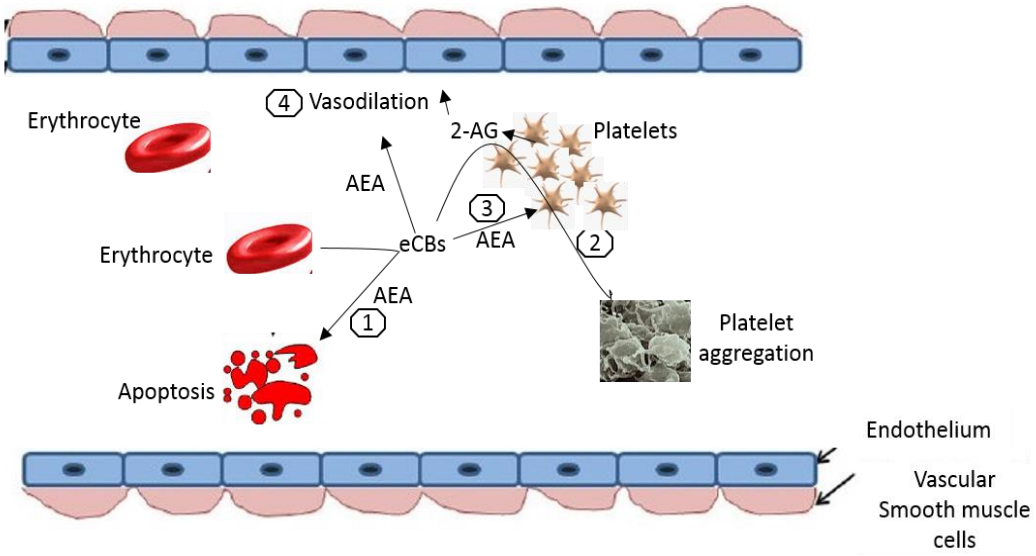

Figure 1.4: Effects of eCBs on blood cells; 1) AEA induces apoptosis of erythrocytes, 2) 2-AG enhances platelet activation, while 3) AEA enhances platelet survival, 4) AEA and 2-AG enhance vasodilation.

1.5 Factors affecting MAGL and FAAH activities from healthy species

1.5.1 Age and Gender

Despite the importance of the endocannabinoid system, there remains a lack of evidence on the influence of age and gender variations on the activities of MAGL and FAAH. Not accounting for sex as a significant reason for variability

in circulated molecule concentrations may induce confusion of these variables with disease status and decrease ability to identify differences, contributing to the low performance of biomarker tests in preliminary and follow-up studies (Ramsey et al., 2016). A study by Tanaka et al. (2007) found that there is no difference in the levels of FAAH mRNA in blood samples between male and female healthy donors. Another large scale human cohort study found that there was no sexual dimorphism of AEA levels in plasma, whereas the level of 2-AG was 20% higher in male than in female heathy subjects (Fanelli et al., 2012). A study reported that the level of MAGL gene expression in the rat brain was higher in adolescent females than adolescent males (Marco et al., 2014).

Regarding ageing, Piyanova et al. (2015) found that MAGL activity was increased in the hippocampi in old mouse brains (12-15 months old) compared to young mice (2-3 months old), without any significant change observed in FAAH activity (Piyanova et al., 2015). A human study found that level of 2-AG in plasma correlated positively with age in female subjects, whereas no change in 2-AG and AEA circulating level was detected in males of different ages (Fanelli et al., 2012). However, numerous circulating biomarkers evolve with age irrespective of disease. Characterizing of biomarkers in different healthy age groups would be essential to diagnose more specifically, guide treatment and prevention, and reduce unnecessary processes and treatments (Sebastiani et al., 2016).

Further study needs to be done with human studies to identify whether circulating MAGL and FAAH activities vary according to age and gender.

1.5.2 Alcohol

Alcohol, one of the most established misused substances globally, continues to be a cause of financial and health issues around the world. However, there are very limited studies, with conflicting data, that have examined the influence of alcohol consumption on MAGL and FAAH activity levels. A reduction of MAGL and FAAH activities was observed in different brain region of rats after short-term exposure to alcohol, respectively (Hansson et al., 2007; Rubio et al., 2009). These results parallel what was observed in alcoholic humans, where the protein levels and activity of MAGL and FAAH were reduced (Hansson et al., 2007). Acute administration of the URB597 inhibitor or genetic deletion of FAAH, can lead to greater alcoholic consumption in mice (Basavarajappa et al., 2006; Blednov et al., 2007), and in Wistar rats (Hansson et al., 2007). In addition, mutation of the FAAH gene was associated with increasing vulnerability to alcohol abuse in humans (Sipe et al., 2002; Chiang et al., 2004). Conversely, a post mortem study, in part conducted locally in Nottingham, was undertaken on alcoholic individuals who either committed suicide or did not. The activity of MAGL was decreased significantly in the post-mortem alcoholic prefrontal cortex without changing the protein levels, however no change was observed in FAAH activity (Erdozain et al., 2014). Similarly, Basavarajappa et al. (2003) found that chronic administration of alcohol had no effects on the FAAH activity level in the neuronal cells.

Together, these studies indicate that the activity level of MAGL and FAAH fluctuated as a result of alcohol consumption. Further study on the relationship between alcohol on the activity of MAGL and FAAH in blood samples are warranted to clarify these results.

1.5.3 Physical exercise

Humans can do physical exercise in different ways that vary by type, duration and intensity. For example, resistance training boosts power and strength in the muscles by utilising smaller muscle groups, whereas aerobic training encompasses the dynamic usage of large muscle groups. The intensity of the exercise is also influential as glycogen is the main source of fuel for high intensity exercises, while fatty acids become the main energy source for low to moderate intensities (Howley, 2001). The first investigation on the influence of physical exercise has on eCBs in humans was carried out by Sparling et al. (2003), which found increasing AEA level in plasma following 45 minutes of medium intensity training on a cycle ergometer (Sparling et al., 2003). Following that, other human studies confirmed increasing plasma content of AEA following medium intense aerobic training, whereas 2-AG concentrations remained stable (Feuerecker et al., 2012; Heyman et al., 2012; Raichlen et al., 2013). Since endogenous cannabinoids are lipids with the ability to rapidly cross the blood-brain barrier, it is conceivable that increased AEA concentration in the blood during exercise may be effective in the CNS to change pain perception contributing to an immediate feeling of well-being (Tantimonaco et al., 2014). Recently, it was found that cycling for 30 minutes increased the level of AEA in healthy postmenopausal females, which in turn enhanced mood (Stone et al., 2018). Since FAAH is the main enzyme which hydrolyses AEA, it is speculated that possibly an increase in the level of AEA in blood is parallel to a reduction in FAAH enzyme activity. However, the FAAH activity was significantly higher in T lymphocytes (but not in the other blood compartments) in healthy individuals who practiced moderate aerobic exercise for about 8 hours per week,

compared to sedentary group, who did exercise with 30 min treadmill exercise per week (Gasperi et al., 2014b). It appears that moderate exercise leads to an increased FAAH activity and AEA level, but the conflict of the result may be because the FAAH and AEA were measured in different blood fractions during different duration of exercises.

1.5.4 Stress

Stress can be defined as mental, emotional or physical factors that cause mental or bodily tension. The gene and protein expressions of FAAH and MAGL were raised within the hippocampus region of adolescent male and female rats reared in maternal deprivation as a type of early life stress, compared to adolescent rats reared under normal conditions (Marco et al., 2014). A clinical study involving healthy men and women demonstrated that the serum concentration of AEA increases in response to acute psychosocial stress along with rises in blood pressure and heart rate. Consequently, increased AEA concentration in the circulation can protect against anxiety (Dlugos et al., 2012). This is in agreement with findings in the murine model, blocking FAAH with URB597 exerted anti-depressant-like and anxiolytic-like effects in chronically and mildly stressed rats: " a behavioural model with high isomorphism to human depression" (Bortolato et al., 2007). It is speculated that increasing the serum level of AEA might be a biomarker for depression and anxiety; whether stress can affect the activity levels of MAGL and FAAH in human body remains to be investigated.

1.6 ECBs and cancer

The correlation between cancer and the haemostatic system is well recognized as an essential mediator of cancer progression. Breast cancer is the most prevalent cancer in women both in the developed and developing world. In fact, platelets, one component of the haemostatic system, since 1968 have been proved to contribute to breast cancer metastasis. The count of circulating platelets is greater in women in breast cancer patients, which in turn is related to poor cancer prognosis (Lal et al., 2013). Platelets directly shield tumour cells, protect them from tumour necrosis factor-alpha (NTF-α)-mediated cytotoxic, and inhibit immunoreceptor natural killer, which increases the survival of cancer cells within the circulation (Wojtukiewicz et al., 2017). Since the number of platelets is increased during the disease progression, platelets undergo a process of activation that leads to the release of their granules. P-selection is a cell adhesion molecule stored in α-granule of platelets, realised after platelets are activated to facilitate cancer cell adhesion to the endothelium (Sabrkhany et al., 2011). Also, cancer growth relies on the creation of new blood vessels (angiogenesis). More than thirty angiogenesis-regulating factors are stored in platelets such as vascular endothelial growth factor (VEGE) and insulin-like growth factor (IGF). In fact, platelet pool contains over 80% of total circulating VEGE in heathy subjects and patients with cancer, including those with breast cancer(Sabrkhany et al., 2011; Wojtukiewicz et al., 2017). Platelets release their pro-angiogenic proteins after activation to induce migration and proliferation of endothelial cells (process of angiogenesis), and finally tumour cell growth at metastatic site (Wojtukiewicz et al., 2017).

However, blood cells such as platelets and erythrocytes are anucleate cells or cell fragments classified as terminally differentiated cells incapable of cellular division, which means they are not able to be investigated over extended periods. Cell culture has been a hugely beneficial technique for preclinical drug testing. MCF-7 cells are a breast cancer line, which are very well characterized with an impressive number of publication describing them (Ayakannu et al., 2013; Comşa et al., 2015). Despite that, there is very limited data about the role of FAAH and MAGL inhibitors on these cell types.

1.6.1 Breast cancer

Breast cancer is the most frequent malignancy in women that mainly depends on two hormones, estrogen and progesterone, for initial growth and survival. Higher hormone levels, lower fertility, iodine deficiency, no breastfeeding and genetic predisposition count as major risk factors for the development of breast cancer. It generally grows from ductal neoplasm or lobular neoplasm, although lung, lymph node, and bone are the sites that breast cancer may spread to (Comşa et al., 2015) .

Progesterone, a C-21 steroid hormone generated by the ovarian corpus luteum following ovulation, possibly plays a role in the regulation of FAAH signalling. It upregulates FAAH activity in human lymphocytes (Maccarrone et al., 2001c; Maccarrone et al., 2003b), and in platelets (Cupini et al., 2006), hence decreasing plasma AEA levels. However, progesterone has been shown to downregulate FAAH activity in mouse uterus (Maccarrone et al., 2000b).

Estrogens are steroid hormones too, generated by the ovarian follicle in the early part of the menstrual cycle and oestrous cycle. In addition, a comparatively

low amount of estrogen is made by breast, liver and the adrenal glands. When estrogen is inside the cell, it binds to estrogen receptors, resulting in the regulation of several process such as cellular apoptosis and proliferation (Ayakannu et al., 2013). 17β-estradiol (E2) is the most powerful growth-stimulating estrogen, which regulates the levels of AEA. E2 directly stimulates the generation and release of AEA from endothelial cells by inhibiting FAAH and stimulating the precursor NAPE-PLD (Maccarrone et al., 2002a). Another study also confirmed E2 downregulating FAAH activity in the mouse uterus (Maccarrone et al., 2002b).

There are at least 51 different breast cancer cell lines. Among them, MCF-7 and MDA-MB-231 cells are extensively used as feasible models of breast cancer because of the consistent molecular characterization in different literature. They are classified as dependent on the expression of three important markers; progesterone receptor (PR), estrogen receptors (ER) and human epithelial receptor 2 (HER2) (Dai et al., 2017). MDA-MB-231 belongs to basal tumour subtype and triple negative (ER-, PR- and HER2 negative), over-express several genes associated with tumour invasive features such as vimentin and moesin. MCF-7 cells are ER and PR positive, and HER2 negative, belonging to a Luminal A subtyping classification. They have a high propensity for differentiation, with a lesser ability to migrate owing to tight cell-cell junctions. Since they are poorly aggressive, they have a better prognosis. Indeed, MCF-7 is proven to be a suitable model cell line for breast cancer investigation worldwide (Dai et al., 2017).

CB_1 and CB_2 receptors are expressed in MCF-7 and MDA-MB-231 cells (Ayakannu et al., 2013), while FAAH activity was detected in MCF-7 (Wei et

al., 2006). In addition, AEA has been shown, at low micromolar concentration, inhibits MCF-7 cells growth by reducing prolactin, through binding to CB_1 receptors, independent of FAAH activity. No interaction between AEA and estrogen receptor was detected. Prolactin is a hormone that behaves as an autacoid proliferative agent as a result of its ability to accelerate the G1/S transition of the cell mitotic cycle (De Petrocellis et al., 1998). The role of FAAH on MCF-7 cell proliferation remains an open question.

MAGL was found to be highly expressed in aggressive forms of breast cancer compared to nonaggressive forms (e.g MCF-7), which regulate migration and tumour growth via the fatty acid network. MAGL, through metabolism of MAGs, produced AA that is further converted into prostaglandin E_2 (PGE_2) (Nomura et al., 2010). PGE_2 enhanced the generation of pro-angiogenic factors such as VEGF to stimulate the migration of cancer cells (Baenke et al., 2013). Higher level of VEGF expression was observed in MDA-MB-231 cells compared to MCF-7, which have less capabilities for migrating and invasion. Blocking of MAGL by JZL184 in various malignant breast cancer cell lines suppressed migration, and survival; thus, MAGL is an exciting target for breast cancer therapy (Nomura et al., 2010). However, it has been demonstrated that MCF7 cells produce metastases to local and distant lymph nodes by the stimulation of VEGF, which is regulated by ER (Comşa et al., 2015). Whether or not blocking MAGL affects proliferation or migration of MCF-7 remains untested.

1.7 Hypothesis and objectives

The eCBs are shown to have a role in the circulatory system, but as yet, it is unknown how the level of eCBs is regulated by MAGL and FAAH in the haematological system. This thesis, therefore, explores the hypothesis that FAAH and MAGL enzymes are present and have a potential role in the function of blood cells to help maintain homeostasis. In order to test this hypothesis, several specific aims were set and explored using rat vascular and blood samples, human blood samples and breast cancer cell lines (MCF-7).

In the first study described in Chapter 3, the primary endpoints were to investigate the activity of MAGL and FAAH and whether their activities differ in mesenteric arteries between young and old by using a radiometric assay. Following that, validation of the radiometric assay protocol to measure enzyme activities in rat blood samples was assessed, as the activity of these enzymes had not yet been measured in whole blood samples. Secondary objectives were to use rat tissues to assess sensitivity and reliability of ABPP to detect MAGL and FAAH activities, and to assess the validity of a spectrophotometric assay to detect MAGL, as validation of these techniques helps to overcome the drawback of using a costly radiometric assay.

Following the validation of assays, the aims of the second study in Chapter 4 were to investigate MAGL and FAAH activities in human isolated blood, as eCB studies have been inconclusive. The primary aim was to determine the variation and reproducibility of these enzymes on three different occasions. In line with this aim, the secondary objectives were to identify which blood fractions contain high and low activities, and to examine the stability of enzyme activity after storage conditions. As a consequence of the results from Chapter

4, a third study was undertaken, with work presented in the third study in Chapter 5, to explore the potential impact of clot formation on the activities of MAGL and FAAH, in which blood fractions are responsible for releasing their activities during serum formation. As an additional objective, human platelet and erythrocyte samples were used to explore whether the enzyme protein level can be used as a marker of its activity level.

The final set of aims involved human breast cancer cell line (MCF-7) in culture, with work presented in the fourth study of Chapter 6, to directly determine the functional impact of inhibition of MAGL and FAAH on cell proliferation and migration. This study was conducted because the aim could not be achieved using human platelets and erythrocytes, as these cells are anucleate and as a result are considered incapable of generating a new population.

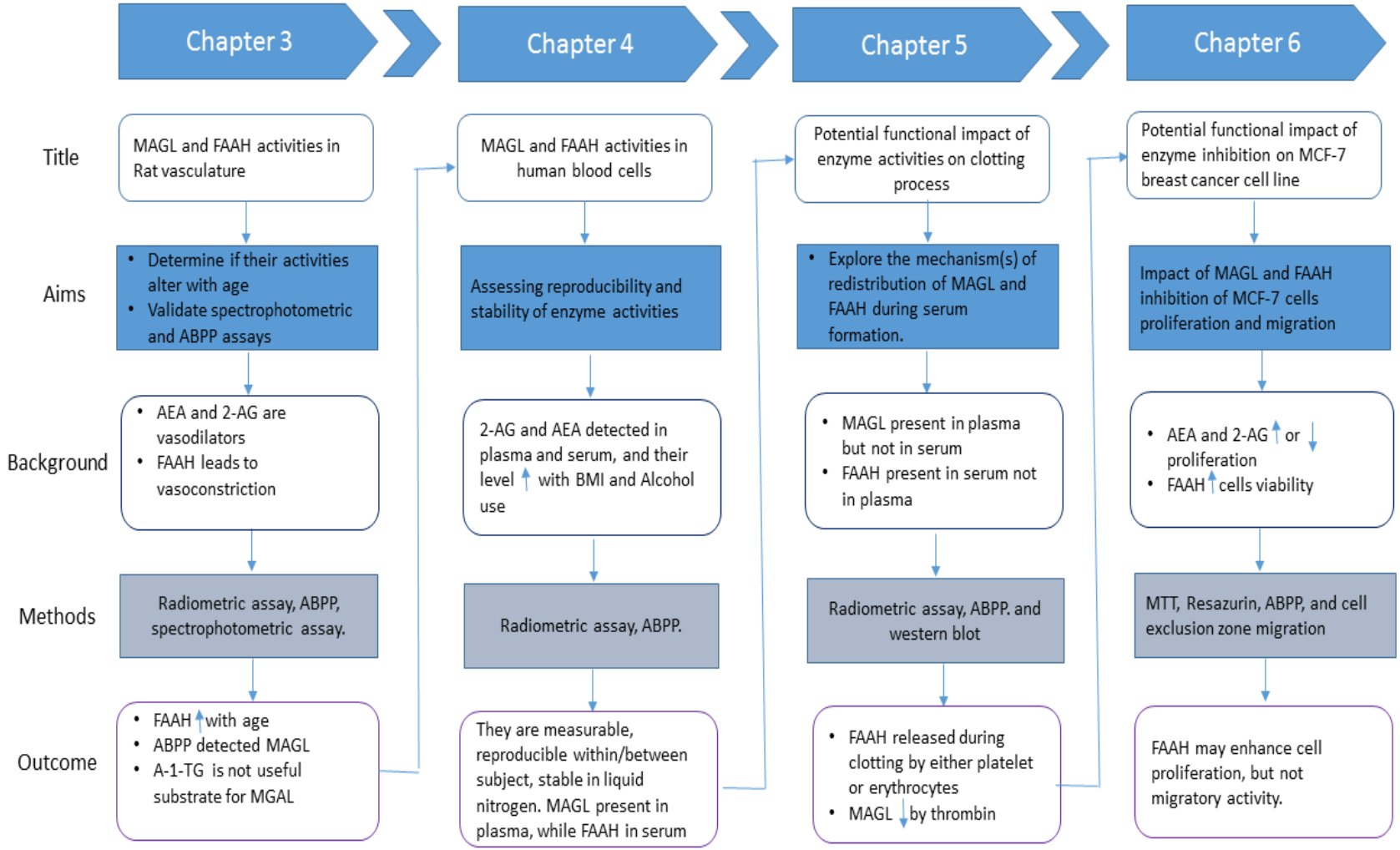
Chapter 3
Chapter 4
Chapter 5
Chapter 6
Title
Aims
Background
Methods
Outcome
MAGL and FAAH activities in Rat vasculature
• Determine if their activities alter with age
• Validate spectrophotometric and ABPP assays
• AEA and 2-AG are vasodilators
• FAAH leads to vasoconstriction
Radiometric assay, ABPP, spectrophotometric assay.
• FAAH ↑ with age
• ABPP detected MAGL
• A-1-TG is not useful substrate for MGAL
MAGL and FAAH activities in human blood cells
Assessing reproducibility and stability of enzyme activities
2-AG and AEA detected in plasma and serum, and their level ↑ with BMI and Alcohol use
Radiometric assay, ABPP.
They are measurable, reproducible within/between subject, stable in liquid nitrogen. MAGL present in plasma, while FAAH in serum
Potential functional impact of enzyme activities on clotting process
• Explore the mechanism(s) of redistribution of MAGL and FAAH during serum formation.
• MAGL present in plasma but not in serum
• FAAH present in serum not in plasma
Radiometric assay, ABPP. and western blot
• FAAH released during clotting by either platelet or erythrocytes
• MAGL ↓ by thrombin
Potential functional impact of enzyme inhibition on MCF-7 breast cancer cell line
Impact of MAGL and FAAH inhibition of MCF-7 cells proliferation and migration
• AEA and 2-AG ↑ or ↓ proliferation
• FAAH ↑ cells viability
MTT, Resazurin, ABPP, and cell exclusion zone migration
FAAH may enhance cell proliferation, but not migratory activity.

Chapter 2 General Methodology

In this chapter, the experimental procedures of radiometric assay and an competitive activity based protein profiling are described in details. Generally, the same methodology is used in all chapters unless otherwise stated.

2.1 Chemicals and Reagents:

Table 2.1 Sources of the chemical used in this project

Chemicals	Company
2-oleoyl-[^{3}H]-glycerol N-arachidonoyl-[^{3}H]-ethanolamine	American Radiochemicals Company via Hartmann (Germany)
2-oleoylglycerol Anandamide JNJ1661010 WWL70 Methylarachidonyl fluorophosphonate (MAFP) JZL184	Tocris (Bristol, UK),
Scintillation fluid (ULTIMA GOLD XR)	PerkinElmer (Poole, Dorset, USA).
Trizma base EDTA (diaminoethanetetra-acetic acid disodium salt) sodium carbonate (Na_2CO_3) dimethyl sulfoxide (DMSO) copper sulphate ($CuSO_4$) sodium hydroxide (NaOH) hydrochloric acid (HCl) ethanol	BDH Laboratory Supplies (Poole, Dorset, UK)
Bovine Serum Albumin (BSA) JJKK048 URB597 PF3845 30% polyacrylamide mix, 10% sodium dodecyl sulphate (SDS) 10% Ammonium persulphate (APS) Tetramethylethylenediamine (TEMED)	Sigma-Aldrich (UK).
ActivX TAMRA-FP Serine Hydrolase Probe	ThermoFisher Scientific (UK)
Amersham ECL Full-Range Rainbow Molecular Weight Marker	GE heathcare office, UK.
Mini-PROTEAN TGXTM	BIO-RAD, UK

2.1.1 Determination of protein level

The protein concentration in each sample was determined using a Lowry assay (Lowry et al., 1951). The BSA standards were prepared at 0-300 µg/mL in 0.5 M sodium hydroxide. This assay uses solution A and Folin Ciocalteu's phenol reagent, which takes on a blue colour, the intensity of which is in proportion to the protein phenolic groups. Solution A was formed from a mixture of 2% (w/v) Na_2CO_3, 2% (w/v) of $CuSO_4$ and 1% (w/v) sodium potassium tartrate. Folin Ciocalteau's phenol reagent was diluted at a ratio of 1:1, with distilled water. The following volumes show how the solutions were mixed: sample/protein standard in sodium hydroxide (200 µL), solution A (1 mL), and diluted Folins reagent (100 µL). Samples were mixed, before being incubated for one hour. The optical density was noted at 750 nm on Unicam UV/Vis Spectrometer (UV4). A solubilized cytosolic sample was dissolved at a ratio of 1:100 in 0.5 M sodium hydroxide. In order to find the protein content, this solution was compared with the BSA standards.

2.2 Radiometric assays for endocannabinoid hydrolases:

2.2.1 Measuring MAGL activity using Tritiated 2-OG:

The assay method applied in this study was adapted from a published version (Boldrup et al., 2004). The assay involved incubation of a known quantity of sample homogenate in TE buffer, with substrates (2-OG/ 2-[^{3}H]-OG) for target enzyme MAGL under near physiological conditions (e.g. 37 °C and pH 7.4). We used 2-[^{3}H]-OG as a radiolabelled tracer, at very low concentration.

In this molecule, tritium was inserted into the glycerol moiety as a radiolabelled tracer. The final substrate concentration was adjusted by adding unlabelled 2-OG. Directly after incubation and enzymatic metabolism, the hydrolyzed product was separated from unhydrolyzed substrate by adding cold-acidified charcoal solution. During this step, the unhydrolyzed substrate and the liberated oleate adsorbs to the charcoal while the product, [^{3}H]-glycerol, does not. The charcoal with bound unhydrolyzed 2-OG was separated from the product, [^{3}H]-glycerol, by centrifugation. A quantity of the aqueous phase (supernatant layer) was then mixed with scintillation fluid and radioactivity was measured by liquid scintillation counting. An additional vial containing only the substrate solution was mixed with the scintillation fluid and used as a standard to determine the total activity in the substrate solution.

Although 2-AG is used as a substrate to study the physiological interest of MAGL, the analogue 2-OG was used in this study for several reasons: MAGL hydrolyzes 2-AG and 2-OG at similar rates (Labar et al., 2010a), 2-[^{3}H]-OG is commercially cheaper than 2-[^{3}H]-AG, 2-[^{3}H]-AG can be difficult to deal with because of its propensity to degrade to 1(3)-AG (Mander et al., 2010), and it was found that replacement of the arachidonoyl chain of 2-AG with a oleoyl chain did not affect the observed affinity of this substrate toward MAGL enzyme (Ghafouri et al., 2004). In these investigations, most of the samples were re-suspended in TE buffer (hypotonic buffer) because it was found that MAGL activity was higher in the TE than in the sodium phosphate buffer.

Bovine serum albumin (BSA) was used in the assay as it appears to stabilize enzyme activities by acting as a weak anti-oxidant, and preventing adhesion of enzymes (and other substances) to reaction material surfaces. Thus, BSA can act

as a reversible carrier of fatty acids (Spector et al., 1978), and endocannabinoids (Parolaro et al., 2002; Petrocellis et al., 2004).

2.2.2 Measuring FAAH activity using tritiated AEA:

The concept of the FAAH assay is the same as those described for MAGL assay, with the primary difference being the use of [^{3}H]-anandamide as a substrate. FAAH hydrolyses anandamide to ethanolamine and arachidonic acid. Unhydrolyzsed anandamide and arachidonic acid are adsorbed to activated charcoal, while ethanolamine remains in the aqueous phase separated by centrifugation.

Equipment:

Shaking incubator (Favourgen Biotech Corp, Vienna, Austria), ARE heating magnetic stirrer (VELP scientific, Shrophire, UK), Vortex/Whirlimixer (Laboratory FSA supplies, scintillation vials, liquid scintillation counter (Packard, US).

Reagents:

1. 2-Oleoylglcerol substrate mix preparation: 2-oleoyl-[^{3}H]-glycerol was mixed in absolute ethanol with 2-OG to give a final concentration of 100 µM 2-OG with 50 000-100 000 dpm of 2-[^{3}H]-OG.
2. Anandamide substrate mix preparation: [^{3}H]-AEA in absolute ethanol was mixed with AEA to give a final concentration of 2 µM AEA with 50 000-100 000 dpm of [^{3}H]-AEA.
3. Stop solution (acidified charcoal solution): 2 g of activated charcoal is added to 25 mL of 0.5 M HCl.

2.2.3 Enzyme reaction:

Homogenates were diluted in TE buffer with essentially fatty acid free albumin (1 mg/mL), unless otherwise specified. Tissue samples were diluted to elicit between 10-15 % hydrolysis of substrate, in order to maintain linearity of enzyme kinetics. 90 µL of sample aliquots were pre-incubated with 5 µL of selective inhibitor or vehicle (DMSO) at 37 ^{o}C for 15 min. Previous studies in the lab identified that enzyme activities of FAAH or MAGL were tolerant to 10 % ethanol or DMSO without significant loss of the activity. The pre-incubation step allows inhibitors to mix thoroughly with the sample, and react with the enzyme activities in a more reproducible manner.

A tissue blank sample was prepared without homogenate in order to assess non-enzymatic hydrolysis of 2-[^{3}H]-OG or [^{3}H]-AEA. After pre-incubation, 5 µL of tritiated-substrate (either 2-[^{3}H]-OG or ^{3}H-AEA) was added to each tube, making an assay volume of 100 µL. The reaction was allowed to proceed for a further 30 min at 37 ^{o}C. The reaction was stopped by addition of 400 µL of cold-acidified activated charcoal. After a short period of standing on the bench, the mixture was then centrifuged at 13 000 g for up to 5 min to pellet the charcoal, to which is bound un-hydrolysed substrate. After centrifugation, 200 µL of the supernatant layer were then removed into scintillation insert vials (6 mL capacity), to which was added 3 mL scintillation fluid, and counted for ^{3}H in a scintillation counter. 5 µL aliquots of the radiolabelled substrate were quantified as a standard to allow calculation of the % conversion of substrate to product.

2.2.4 Data Analysis.

The scintillation counter measured the number of light flashes produced from the interaction of the radioisotope with scintillators, which is proportional to the intensity of radiation emitted and expressed this intensity as disintegrations per minute (dpm). MAGL activity was typically expressed as a normalised rate in nmoles/min/mg protein or mL of blood and FAAH activity expressed as pmoles/min/mg of protein or mL of blood using the following equation:

$$= \frac{\text{Test}-\text{Blank}}{\text{Standard}} \times \frac{[\text{ nmoles of substrate }]}{[\text{Protein concentration }] \times \text{Incubation Time}}$$

The equation takes into account the background hydrolysis (Blank), the amount of tritium in each sample aliquot (Test), the maximum amount of tritium in the sample (Standard), the number of moles of substrate in each sample, the incubation time and the amount of protein in each sample. To determine IC_{50} values of inhibitors, the values of substrate hydrolysis in the presence of varying concentrations of inhibitors was plotted in GraphPad Prism software and then normalised to control levels of substrate hydrolysis in the absence of inhibitors, generating graphs as % of control activity, fitting curves to a four parameter logistic equation.

2.3 Activity based protein profiling (ABPP)

2.3.1 Concept of the assay

The ABPP technique is an approach to determine multiple enzyme activities simultaneously using chemical probes that selectively react with the catalytic site of a particular enzyme family. The serine hydrolase assay involves incubation of a known quantity of sample homogenate with ActivX^{TM} TAMRA-FP (tetramethylrhodamine-fluorophosphonate) Serine Hydrolase Probe. The TAMRA-FP probe consists of three structural elements (Figure 2.1): the reactive group, also called "warhead", the electrophilic fluorophosphonate (FP); a spacer element or linker; and a reporter tag element, the fluorophore (see figure 2.1.A)(Simon et al., 2010; Willems et al., 2014).

The FP reactive group is an irreversible serine hydrolase inhibitor that reacts covalently with the catalytic nucleophile serine residues in the active site of this enzyme family. Serine hydrolases include more than 100 enzymes that share an α/β hydrolase fold (parallel β sheets flanked by α helices) structure (Sutton, 2012). Three amino acid residues, including serine, emerging from the α/β-hydrolase fold comprise a catalytic triad site (Ollis et al., 1992). As a consequence, FP derivatives, like diisopropyl fluorophosphates, irreversibly inhibit the majority of serine hydrolases by forming a covalent bond with active site serine, which in turn prevents the binding of substrate to the active site (Liu et al., 1999).

The spacer/linker element compose of a long alkyl chain that connects between the warhead and reporter tag element (Liu et al., 1999; Everley et al., 2007). It also acts to enhance probe accessibility and decrease steric hindrance

between both groups. The reporter tag element is a fluorescent dye (rhodamine) that allows visualization of the labelled enzyme in the SDS-PAGE gel. During the incubation period, the catalytic nucleophile of the serine hydrolase enzyme cleaves the scissile bond P residues, which releases the fluoride, generating a covalent bond with the serine residue in the active site (Sieber et al., 2006). As a result, TAMRA-FP probe irreversibly binds to the enzyme proteins (figure 2.1.A).

After a period of incubation, the reaction between TAMRA-FP and target enzyme was quenched by adding Laemmli buffer. The TAMRA-tagged enzymes were then separated on SDS-PAGE gels, and observed using a Typhoon scanner (Amersham Biosciences). Light emitted from fluorescently-labelled enzymes is proportional to the amount of enzyme activity in the sample. Emitted light is converted to an electrical signal via a photomultiplier, and the signal is digitized to allow image display and quantitation using ImageStudio software.

2.3.2 Enzyme reaction

The assay method applied in this study was adapted from the manufacturer's instructions (Thermo Fisher Scientific). 20 µL of homogenised samples were pre-incubated with 1 µL of vehicle (DMSO) or selective inhibitors (e.g. 1 µM MAFP, 1 µM JZL184 or 100 nM JJKK048) at 37 ^{o}C for 15 min. Pre-incubation of sample with selective inhibitor will reduce the signal of TAMRA-FP labelling enzymes targeted via the inhibitor, and this help to identify the individual enzyme of interest. Then, 1 µL of ActivX™ TAMRA-FP Serine Hydrolase Probe (final concentration of 500 nM) was added to each tube, and incubated for 30 min at 37 ^{o}C. Following incubation, 4 µL of 6 X Laemmli

reducing sample buffer was added to quench enzyme activity and linearise proteins; labelled enzymes were separated by SDS-PAGE.

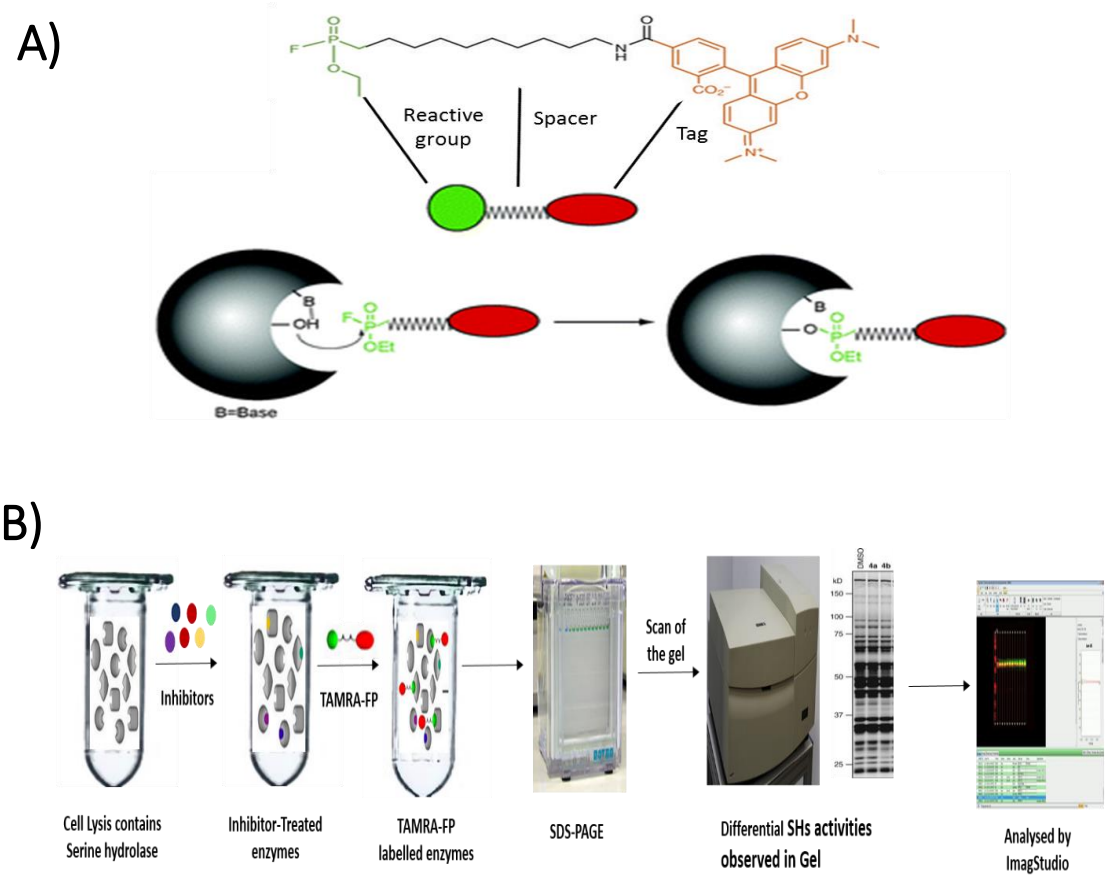

Figure 2.1. Activity based protein profiling for serine hydrolase detection. A) Structure of TAMRA-FP probe, which consists of fluorophosphonate (FP) reactive group (green), spacer (black) and a reporter tag rhodamine (red). FP reacts covalently with catalytic nucleophile serine of serine hydrolysis enzymes. B) ABPP experiment, cells or tissue samples treated with inhibitors or vehicle (DMSO), and then incubated with TAMRA-FP rhodamine. Fluorescent labelled enzymes were separated on SDS-PAGE gel and then visualized by Typhoon scanner.

2.3.3 Concept of Sodium Dodecyl Sulphate Polyacrylamide Gel Electrophoresis (SDS-PAGE):

SDS-PAGE is a technique used to separate proteins in an electric field based on their molecular sizes. The proteins in the tissue sample are first denatured by heating the sample with Laemmli buffer. Laemmli buffer consists of the ionic detergent SDS, which binds to the proteins to imparts to them a negative charge, and 2–mercaptoethanol that prevents disulphide bond formation between the amino acids. As a result, the proteins unfold into their linear structures with negative charge proportional to their molecular weights. In addition, Laemmli buffer contains the dye bromophenol blue (BPB) to aid visualization of sample movement in the gel.

Denatured proteins are loaded onto polyacrylamide gels, and are separated by electrophoresis. The concept of separation is that negatively charged particles migrate towards the positive charged cathode, with gel density allowing differentiation of proteins according to their size (Jensen, 2012). Rainbow marker ladders were also loaded onto the gel alongside the samples, allowing interpolation of the molecular sizes of bands of interest.

2.3.4 Preparation of gels for electrophoresis

Migration rates of protein depend on the concentration of the separation gel, where higher concentrations of acrylamide produce pores with smaller sizes. A focus for this method was to quantify identify FAAH (62 kDa) and MAGL (32 kDa) activities in complex mixtures. Therefore, a 10% polyacrylamide-resolving gel was chosen as appropriate for resolving these target proteins.

Although gels for immunoblotting are typically mini-gels, preliminary results (Chapter 3) indicated that these allowed insufficient resolution of enzyme activities, and so larger gel formats were investigated. A total volume of 35 mL of 10% polyacrylamide-resolving gel was made as described in Table 2.1. The resolving gel was then cast in an 18 cm Hoefer gel chamber, allowing a 10 cm space for the stacking gel and loading comb. Then, 5 mL of water-saturated butanol was poured onto the top of the gel to remove all air bubbles and to prevent it from drying out. It was left to polymerize for 30 min at room temperature to form a gel. The water-saturated butanol was poured off and the top of the gel washed three times with distilled water.

After that, 35 mL of 4% stacking gel was made as described in Table 2.2. Then, the stacking gel was poured above the resolving gel to fill the chamber, allowing space at the top to insert a 1.5 mm loading comb used to form the sample wells. The gel was allowed to polymerise for 30 min at room temperature.

Table 2.2. Reagents and quantities used to prepare the resolving and stacking gels.

Reagents	**Resolving gel**	**stacking gel**
Distilled water	14.35 mL	21.35 mL
30% acrylamide mix (37:5: 1)	11.55 mL	4.55 mL
Tris buffer	8.75 mL of 1.5 M Tris buffer (pH 8.8)	8.75 mL of 1.5 M Tris buffer (pH 6.8)
10% (w/v) sodium dodecyl sulphate (SDS)	0.35 mL	0.35 mL
10% (w/v) Ammonium persulphate (APS)	0.175 mL	175 µL
Tetramethylethylenediamine (TEMED)	17.5 µL	35 µL

2.3.5 Loading the samples and running electrophoresis

Before loading, the samples were heated to 95 °C using a heating block (Stuart Instruments) for 5 min, vortexed and centrifuged at 13 000 g for 1 min. 15 µL of an ELX rainbow molecular marker was loaded into specific lanes of the gel, then the whole sample (25 µL) was loaded onto separate wells.

The gel was run initially for 1 h at 100 V in electrophoresis buffer (0.25 M Tris, 1.92 M glycine and 0.035 M SDS in 1 litre distilled water). Then, the voltage was increased up to 170 V and the gel was run for a further 4 h. This strategy was designed to achieve better resolution of bands. When the gel had finished running, the gel electrophoresis unit was removed, and electrophoresis buffer was poured off. Then, the gel was wrapped with wet blue paper towels and

covered in cling film to prevent it from drying out. If not scanned immediately, it was stored at 4 °C until the day of imaging.

2.3.6 Imaging

A GE Typhoon Trio imager (Amersham Biosciences Unit) was used to scan the gel. The scanner glass was cleaned prior to use with dH_2O. Then, the gel was released from the two glass plates and placed gently facing down on the scanner, ensuring the gel was moist and bubbles were removed. Typhoon software was opened and Cy3 filter, Green (532), (λex 532 nm, λem 606 nm) setting was employed. Subsequently, the gel was stained with Coommassie blue to observe total protein loading in each well.

2.3.7 Data analysis

Following fluorescence imaging, MAGL and FAAH were identified based on their molecular weight. Since band density on the gel corresponds to enzyme activity, MAGL and FAAH activities were determined by quantifying the fluorescence intensity of their respective bands. An enzyme that was targeted via an inhibitor showed significantly decreased signal compared with the control. Further analysis, using GraphPad Prism software, was conducted to compare the values of MAGL or FAAH activity before and after treatment with the inhibitor. Statistical analysis was performed using two way ANOVA with Tukey's multiple comparisons test. This step was conducted to determine whether activity of the enzymes was significantly reduced in the presence of the selective inhibitors.

Chapter 3 MAGL and FAAH activities in Rat vasculature

3.1.1 Introduction

A large body of evidence has shown that endocannabinoids (AEA and 2-AG) are apotent vasodilators of blood vessels isolated from different species (Randall et al., 2002). In the early nineties, Ellis et al (1995) first showed that AEA induced relaxation of rabbit cerebral arteries (Ellis et al., 1995). Since then, AEA has become the most extensively studied endocannabinoid in the vasculature (Stanley et al., 2014a). As stated in chapter 1, the level of AEA and 2-AG are mainly regulated by FAAH and MAGL, respectively. Therefore, the inhibition of these endocannabinoids hydrolysing enzymes leads to an increase in the endogenous tone of endocannabinoid ligand in the cardiovascular system, potentially increasing their beneficial effects. Therefore, exploring and investigating the role of these enzymes in cardiovascular system will allow novel therapeutic exploitation of the endocannabinoid system. AEA was shown to induce vasorelaxation in rat aorta, mainly mediated by two pathways. One of these involves the endothelial cannabinoid CB_1 receptor (Herradón et al., 2007). In the second pathway, anandamide is metabolized by FAAH to generate arachidonic acid, a substrate of COX-2, resulting in PGE_2 formation. This, in turn, binds to the EP_2 receptor in vascular smooth muscle, causing vasorelaxation (Herradón et al., 2007). In agreement with this study, metabolism by FAAH and MAGL limits the vasorelaxation effects of AEA and 2-AG, respectively, in rat mesenteric artery (Ho et al., 2007). However, another study by the O'Sullivan group showed that inhibition of FAAH by high concentrations of a selective inhibitor (URB597, 1 μM), in rat aortae, did not limit or reduce

the AEA-mediated vasorelaxant response (O'Sullivan et al., 2009). In contrast to animal studies, study in human mesenteric artery samples reported that AEA induced vasorelaxation by acting on an endothelial CB_1 receptor, and there was no effect of FAAH metabolism (Stanley et al., 2016). Additionally, the vasorelaxant response to 2-AG in human mesenteric arteries was not mediated by MAGL metabolism, but rather by oxidation via COX1 and subsequent activation of EP_4 and IP prostanoid receptors (Stanley et al., 2014b). Thus, the mechanism of the vasorelaxant response to endocannabinoids is complex and still not fully understood, and it may well depend on vessel type and species. Despite studies to understand the role of endocannabinoids and their metabolism in vascular tissue, results have been controversial and conflicting. In addition to this, the activities of FAAH and MAGL has not been investigated to date. Measurement of FAAH and MAGL activities enables the prediction of their putative roles in vascular function. Therefore, to gain more understanding of the likely role of endocannabinoid metabolising enzymes in the cardiovascular system, and whether their activities varies with age, it is essential to investigate the activities of MAGL and FAAH, in isolated vascular tissues.

3.1.2 Aim

The primary aims for the current study were to investigate FAAH and MAGL activities in rat vascular preparations, and to examine whether the enzyme activities in the mesentery alter with age.

Activity levels of MAGL and FAAH were subsequently measured in blood circulation. The radiometric assay is a well-established assay that is widely used to measure enzyme activity. However, the high cost and hazards associated

with radiolabelled substrates lead to the investigation of alternative methods to measure enzyme activity in native tissues. Thus, the secondary objective of this study was to validate activity-based protein profiling to detect activity levels of FAAH and MAGL in rat vascular tissues. A spectrophotometric assay for MAGL activity detection was also validated by comparison with the results from the radiometric assay.

3.2 Materials & Methods

3.2.1.1 Chemicals & reagents

The following table shows chemicals that were used in the assays described in this chapter:

Chemicals or solutions	Company
Arachidonoyl-1-thio-glycerol (ATG) 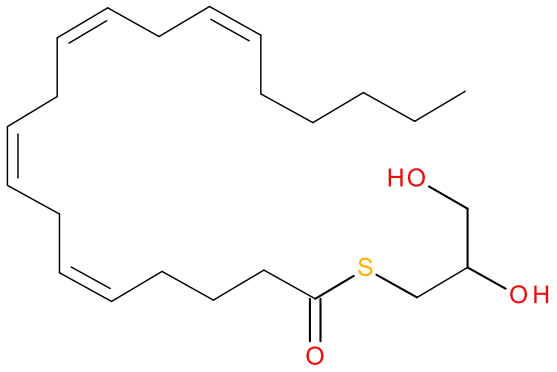	VWR, UK
Thioglycerol (TG)	Sigma-Aldrich, UK
Trichloroacetic acid (TCA) and 5,5′-dithiobis(2-dinitrobenzoic acid) (DTNB)	BDH Laboratory Supplies (Poole, Dorset, UK)

The sources of other chemicals used were identified in **chapter 2**.

3.2.1.2 Isolation and preparation of vascular tissues

Young male Wistar rats (aged 8-12 weeks, weighing 125-150 g) were stunned by a blow to the back of the head and killed by cervical dislocation by Dr Michael Garle. Internal thoracic and abdominal organs were removed, exposing the aorta. The aorta was removed and placed into ice-cold 50 mM Tris/HCl containing 1 mM EDTA buffer, pH 7.4 (TE buffer). It was then cut free and cleaned of adherent connective and adipose tissue. The thoracic aorta (TA) was dissected starting from the arch of the aorta running down to the diaphragm,

while the abdominal aorta (MA) descends from the diaphragm continues down until before the iliac bifurcation.

Superior mesenteric artery (MA) samples, from a young male Wistar rat aged 8-12 weeks and an older rat aged 6-9 months, were supplied by Dr WS Vanessa Ho (St George's, University of London). Tissues were homogenised in 1:10 weight/volume (w/v) ice-cold TE buffer by using Kit ceramic (zirconium oxide) beads in 2 mL standard tubes, Precellys (Figure 3). Ceramic beads (2.8 mm) were chosen to homogenise the thoracic and abdominal aorta (sample size ~ 200 mg), while smaller ceramic beads (1.4 mm) were used to homogenise the mesenteric artery (sample size between 15 and 20 mg). Ceramic beads were used to homogenise vascular tissues as preliminary investigations using prolonged homogenisation with glass:glass or glass:Teflon homogenisers resulted in uneven aggregates which were resistant to disaggregation.

Tubes containing the tissue and the beads were placed in a Precellys® 24 Tissue Homogenizer (US) and homogenised at 9 000 rpm × 15 seconds × 8 cycles. A five min interval was allowed between each cycle, with the homogenates being placed on ice to ensure the disruption of tissue with minimal denaturing of proteins.

Samples were then centrifuged at 33 000 g for 45 min, at 4 °C. Subsequently, the supernatant layer (cytosolic fractions) was transferred into Eppendorf tubes and stored at -80 °C. The pellet was re-suspended in the same buffer volume and re-homogenised. A second centrifugation step was conducted and the second supernatant layer (cytosolic fraction) was discarded. The same volume of ice-cold TE buffer was added to the membrane fraction and re-homogenised

manually by repeatedly pipetting up and down. Then, the samples were transferred into Eppendorf tubes and stored at -80 °C until required.

Estimates of recovery and residue were then calculated as follows to assess the degree of homogenisation;

Residue

=

$$\frac{\text{the weight } of\ tube\ containg\ the\ beads\ and\ tissue\ after\ homogenization - the\ weight\ of\ tube\ and\ beads\ only}{\text{the weight of tube containg beads and tissue before the homogenization} - \text{the weight of tube and bead only}}$$

$$\text{Recovery} = \frac{\text{the weight } of\ tissue\ before\ homogenization - the\ weight\ of\ tissue\ after}{\text{the weight of tissue before homogenization}}$$

Equipment:

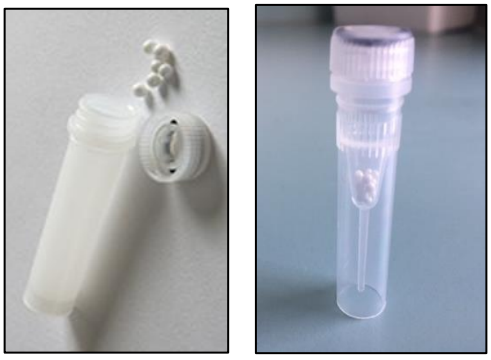

Figure 3.1. The ceramic (Zirconium oxide) bead kit (Precellys).

3.2.1.3 Isolation and preparation rat liver and brain tissues

The protocol for preparation of rat liver and brain membrane fractions was adapted from Paul et al. (2005) with modifications made by Michael Garle. Whole brain and liver tissues were dissected from young male Wistar rats (aged 8-12 weeks, weighing 125-150 g). Tissues were weighed after being washed with ice-cold TE buffer. They were roughly chopped with scissors in buffer, followed by homogenization 1:10 (w/v) in TE buffer using a glass/glass

homogenizer and a Polytron homogenizer for brain and liver, respectively. The homogenates were centrifuged at 10 000 g for 20 min at 4 °C. Then, the pellet containing the un-homogenised material and nuclei was discarded, while the supernatant layer was transferred into a clean tube and re-centrifuged at 30 000 g at 4 ^{o}C for 1 hour to obtain membrane fraction. The resulting pellet was suspended in 1:2 (w/v) of ice-cold TE buffer, and re-homogenized manually by homogenizer. Then, samples were stored at -80 ^{o}C until required.

3.2.1.4 Blood sampling from a rat:

A Wistar young male rat (aged 8-12 weeks) was killed by CO_2 (a Schedule 1 procedure conducted by Paul Millns) and then, after the heart had stopped, a needle was inserted into the left ventricle of the heart to withdraw blood. 0.5mL of blood sample was withdrawn, transferred into a tube and mixed with 5µL of Acid Citrate Dextrose (ACD) solution. The blood was immediately diluted to 1:1000 (v/v) volume in ice-cold TE buffer, and an assay was performed.

3.2.1.5 Determination of protein content:

The protein concentration of rat tissues was quantified by the Lowry method, as described in sections 2.3.

3.2.1.6 Radiometric endocannabinoid hydrolase assays

FAAH and MAGL activities were measured by radiolabelled ligands as described in section 2.1. Optimization of the assay was accomplished by using various dilutions of homogenate, until activity was measurable, ensuring that no more than 10 % of substrate was hydrolysed.

3.2.1.7 Activity based protein profiling

Homogenates were labelled with the TAMRA-FP probe as described in section 2.2. To ensure comparability of the assay, the protein content of vascular

tissue was kept identical to the amount of protein in the radiometric assay. Optimization of the protocol was achieved by using several probe concentrations, to test the visibility of enzyme activities in the subsequent scan.

3.2.1.8 Spectrophotometric assay for MAGL activity

3.2.1.8.1 Concept of the assay

Radiometric assay is a gold standard assay to measure the activity of MAGL. Nevertheless, radioactive substrates are still relatively expensive. In this study, the validity of a spectrophotometric assay to detect MAGL activity in native tissues was investigated. The assay employs a thioester-containing analog of 2-AG, arachidonoyl-1-thio-glycerol (A-1-TG), which MAGL can hydrolyze.

A spectrophotometric assay for MAGL activity based on thiolate ion quantification was adapted from (Ulloa et al., 2010), including several modifications to increase the sensitivity and stability of the assay. The assay is based on the hydrolysis of A-1-TG forming thioglycerol (1-TG), which then reacts with 5,5′-dithio- bis(2-dinitrobenzoic acid) (DTNB) generating a yellow -coloured product, 2-nitro-5-mercaptobenzoic acid (TNB) (see figure 3.2). The yellow thiolate ion is amenable to quantification by various means.

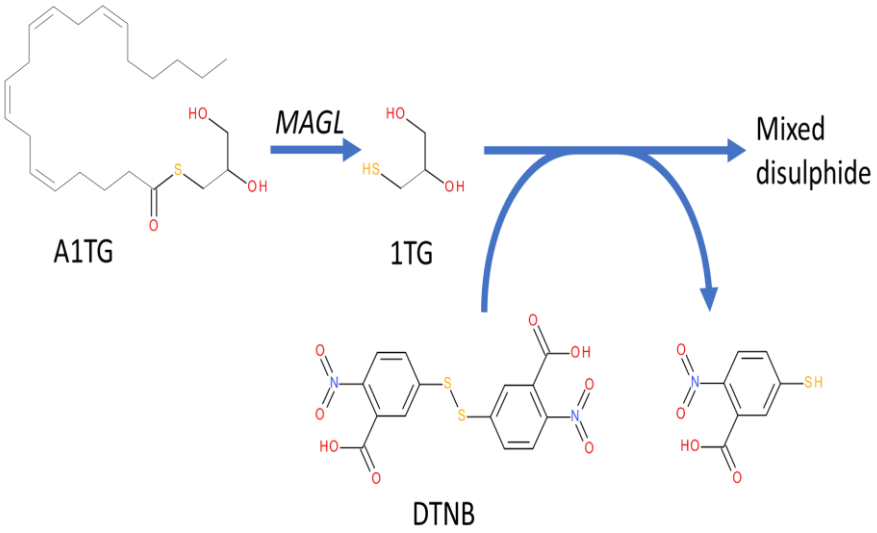

Figure 3.2. Scheme of arachidonoyl-thio-glycerol (A-1-TG) hydrolysis and detection. MAGL hydrolyses S-arachidonoyl-1-thio-glycerol to release thioglycerol (1-TG), which then reacts with DTNB generating the yellow-coloured ion, TNB.

3.2.1.8.2 Enzyme reaction

To allow direct comparisons to be made, the assay volume was kept identical to the radiometric assay volume (100 µL, see section 2.1). Cytosolic fractions were diluted in ice-cold TE buffer. The final concentration of protein in cytosolic fraction of vascular and brain tissues was 100 µg/mL and 25 µg/mL, respectively. 90 µL of cytosol/BSA/TE mix were pre-incubated with 5 µL of inhibitor (e.g. 1 µM MAFP or 2 µM JJKK-084) or vehicle (DMSO) at 37 °C for 15 min. A selective inhibitor (JJKK048) was used to define the contribution of MAGL to A-1-TG hydrolysis. 90 µL of TE/BSA only was employed as a blank. Samples were incubated for 30 min at 37 °C after the addition of 5 µL of A-1-TG (200 µM). The reaction was stopped by adding 50 µL of 20% trichloroacetic acid (TCA). 5 µL of 1-TG (200 µM) was employed as a standard diluted with

TE buffer only. Samples were then mixed by vortex and centrifuged at 3 000 g for 5 min to pellet the precipitated protein. 100 µL of the supernatant layer was transferred into a 96 well microtiter plate (obtained from Nunc Roskilde, Denmark), followed by the addition of 200 µL DTNB: 0.4M TE buffer pH 9 (final concentration of DTNB was 135 µM). TE buffer with alkaline pH 9 was used to make the environment more alkaline for substrate and subsequently reduced the background. 1-TG reacts with DTNB generating a yellow-coloured product, 2-nitro-5-mercaptobenzoic acid (TNB). Absorbance was read at 412 nm using a SPECTRA MAX, 340pc microplate reader (Molecular Device, US).

3.2.1.8.3 Data Analysis

Enzyme activity was expressed in nmoles/min/mg using the equation described in sections 2.2, while in rat blood samples the activity was expressed as nmole/min/ml of blood. The total blood volume (TBV) in rat was calculated from the following equation:

TBV = 0.06 X BW + 0.77

where 0.06 is the volume of RBC and 0.77 is the volume of plasma (Lee et al., 1985). BW is the body weight.

Then data were further analysed using GraphPad Prism software (7.04, US). Concentration response curves were modelled using the four-parameter logistic equation:

$$Y = \text{bottom} - \frac{(\text{Top}-\text{bottom})}{1+10(\log EC50-x)nH}$$

Bottom of the curve is the maximum inhibition effect of drug, top of the curve is the minimal inhibition effect of drug, Y is the level of the response, EC_{50} is the curve midpoint, x is the log concentration of inhibitors and nH is the curve slope.

3.2.1.8.4 Statistics

Data were represented as MEAN ± SEM of at least three independent experiments. Statistical differences were determined using a paired Students two-tailed t test or one-way ANOVA followed by Tukey's multiple comparison, as appropriate. A P value of <0.05 was considered as significant.

3.3 Results

3.3.1 Measurement of MAGL and FAAH activities in rat vascular preparation using radiometric assay

2-Oleoyl-[^{3}H]-glycerol ([^{3}H]-2-OG) and N-[^{3}H]-arachidonoylethanolamine ([^{3}H]-AEA) were used as radiolabeled substrates to detect the activity of MAGL and FAAH enzymes, respectively. Selective inhibitors, such as JJKK048 and URB597, were used to identify the contributions of MAGL and FAAH to the hydrolysis of 2-OG and AEA, respectively, in rat vascular preparations.

The recovery, the amount of protein, was calculated for each tissue cytosol and membrane fractions. The recovery from thoracic and abdominal aorta was 92%, while from mesenteric artery the recovery was 94%. Initially, optimization was carried out, which included alterations in the duration of incubation period and protein concentrations (described below). The goal of these optimization procedures was to achieve no greater that 10% hydrolysis of the substrate.

3.3.2 Effect of incubation time and protein concentration on the rate of 2-OG hydrolysis

The longer the incubation time of an enzyme with its substrate, the larger the amount of product produced. In balance, an excessive incubation period could lead to enzyme denaturation and product inhibition (Sharma et al., 2001). Therefore, the rate of 2-OG hydrolysis was investigated up to 60 min using the cytosolic fraction of the superior rat mesenteric artery from young male Wistar rat (aged 8-12 weeks) (Figure 3.3). The rate of 2-OG hydrolysis was found to increase linearly with incubation up to 60 min (R^2 = 0.95). However, the incubation period was optimized at 30 min to compensate for variation in enzyme activity.

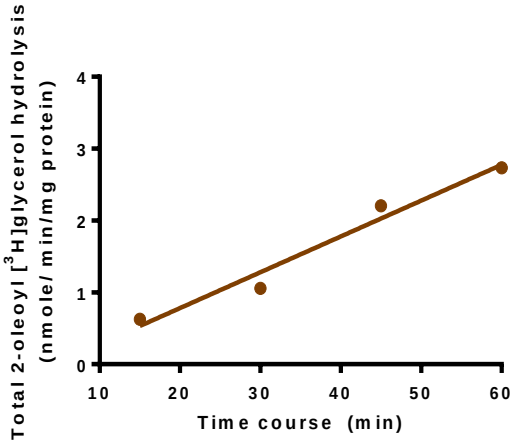

Figure 3.3. Effect of incubation time on the hydrolysis rate of 2-OG. Cytosolic fractions from rat superior mesenteric artery (MA) was incubated at 37 ºC for the indicated incubation periods. Data, measured in duplicate, are expressed as the mean ± SEM from three independent experiments. The line was fitted by linear regression test using GraphPad Prism 7.04 software.

For a given substrate concentration, the rate of an enzyme catalyzed reaction increases with increasing protein concentration, as more active sites become available to bind substrate molecules and convert them to products. The

optimum concentration of protein in cytosolic fractions from vascular tissues was determined (Figure 3.4). MAGL activity was found to increase linearly up to 200 µg of vascular tissue proteins (R^2 = 0.99). However, 100 µg of vascular tissue proteins was chosen for further experiments, as this amount of protein was capable of hydrolyzing ~10% of the substrate over the 30 min incubation period.

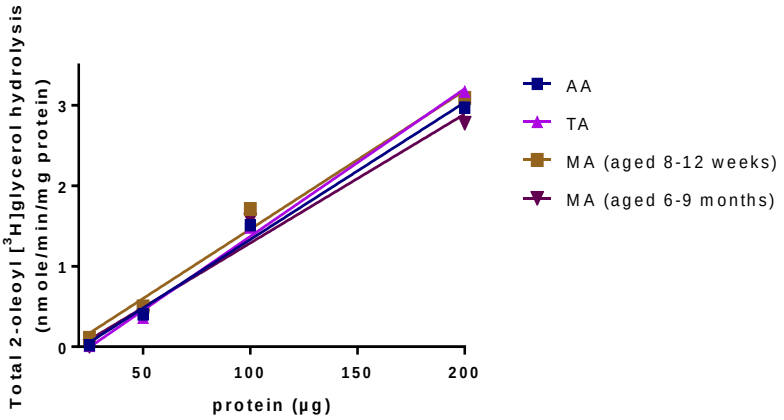

Figure 3.4 Influence of protein concentration on 2-oleoyl-[^{3}H]-glycerol hydrolysis. 2-OG/^{3}H-2-OG was incubated with increasing amounts of sample protein (5-200 µg) from abdominal aorta (AA), thoracic aorta (TA), and superior mesenteric small artery (MA). Data, measured in duplicate, are expressed as the mean ± SEM from three independent experiments. Line was fitted using linear regression test.

3.3.3 MAGL and FAAH activities in rat vasculature

After identifying the optimum protein concentration and incubation period, the activities of MAGL and FAAH in rat vascular tissue preparations were investigated. Rat brain cytosol is widely used as a source of endocannabinoid metabolising enzymes (Blankman et al., 2007), and to investigate the hydrolysis of ^{3}H-2-OG by MAGL (Ghafouri et al., 2004) . Therefore, homogenized whole rat brain was used as a positive control in this

experiment. MAGL activity can be detected in both the cytosolic and the membrane fractions of tissues (Bertrand et al., 2010; Labar et al., 2010a). Therefore, the functional expression of MAGL was investigated in both cytosol and membrane fractions (containing 100 µg of protein). In contrast to MAGL localization, FAAH is a membrane-bound enzyme (Fegley et al., 2005), therefore, only membrane fractions were used to investigate FAAH activity. JJKK048 or URB597 (1 µM) were employed as selective inhibitors to identify the activity of MAGL and FAAH enzymes, respectively (Figure 3.5).

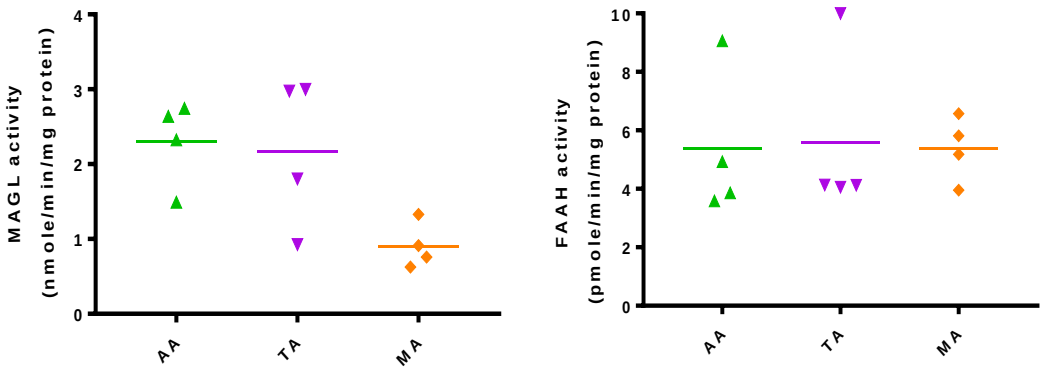

Figure 3.5. Activities of MAGL and FAAH in thoracic, abdominal aortae and mesenteric arteries from young rats (aged 8-12 weeks). Homogenized whole brain was used as a positive control. Data, measured in duplicate, are expressed as the MEAN ± SEM from four independent experiments and were analyzed using one-way Anova with Tukey's multiple comparisons test. There was no significant difference of MAGL and FAAH activities among the three blood vessels with P=0.097 and P=0.75, respectively.

Table 3.1 Summary of the activity level of MAGL and FAAH in the blood vessels compared to the brain.

Tissue	MAGL activity (nmole/min/mg protein)		FAAH activity (pmole/min/mg protein)
	Cytosol	Membrane	Membrane
Brain	13.7 ± 2.4	8.7 ±1.7	291.4 ± 67.2
TA	1.8 ±0.3	2.2 ± 0.5	5.4 ± 2
AA	0.9 ±0.1	2.1 ± 0.2	5.5 ± 1
MA	1.4 ± 0.1	1.0 ±0.2	4.3± 1

Data represented as MEAN ± SEM from four independent experiments and then the comparison was conducted using one-way Anova with Tukey's multiple comparisons test.

FAAH and MAGL activities could be measured in the cytosol and membrane fractions of rat vascular tissues although their activities were lower than activities in the rat brain. The activity level of FAAH and MAGL was significantly higher in brain comparing to blood vessels **P=0.0013. Rat brain possessed ~ 7 fold greater MAGL activity, while ~ 50 fold greater FAAH activity than blood vascular tissues. These data suggest important difference in the activities of FAAH and MAGL between brain and vascular tissue, where the high activity of FAAH and MAGL in brain reflect their involvement in the physiological process of the brain. Nevertheless, among the vascular fractions, there was no significant difference observed in either MAGL or FAAH activities among the three blood vessels.

In order to identify whether MAGL was the predominant 2-OG hydrolase activity in the cytosolic fraction of vascular tissue, the effect of JJKK048 on MAGL activity was investigated (Figure 3.6). The yield of material from membrane fractions was not sufficient for pharmacological characterization of individual tissues using this assay.

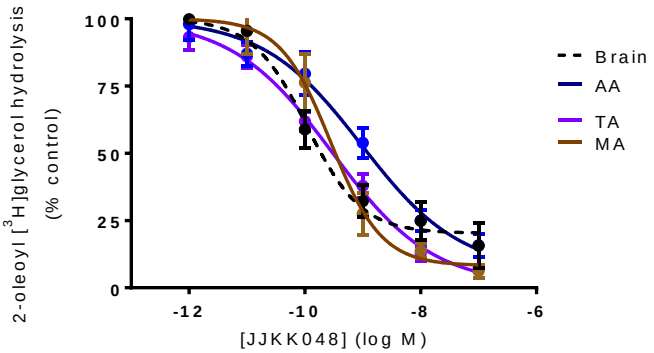

Figure 3.6. The effect of JJKK048 on MAGL activity in cytosolic fractions of vascular tissues. Data were collected in duplicate from four individual experiments and expressed as a % of control 2-OG hydrolysis. Curve was fitted using non-linear regression to a four-parameter logistical equation.

Table 3.2. The inhibitory potency of JJKK-048 to inhibits rat MAGL enzyme in brain and blood vessels

cytosol	Potency of JJKK048 logIC_{50}	JJKK048-insensitive % control	Slope
Brain	9.9 ± 0.1	21 ± 7	-1.0 ± 0
TA	9.4 ± 0.2	4 ± 1	-0.9 ± 0.1
AA	9.1 ± 0.1	20.2 ± 4	-0.9 ± 0.2
MA	9.2 ± 0.2	5.7 ± 1.7	-0.9 ± 0.3

Data are represented as a MEAN ± SEM from four individual experiments.

JJKK048 exhibited a concentration-dependent inhibition of 2-OG hydrolysis in all tissues from younger animals, with pIC_{50} mean values of 9.4 (see Table 3.2). The Hill slope of JJKK-048 across all tissues was suggesting a homogeneous interaction with the enzyme sources. The maximal inhibitions in the presence of JJKK048 were not different from the blanks, indicating that MAGL was the predominant 2-OG-hydrolyzing enzyme in vascular tissues.

3.3.4 *In vitro* enzymatic activity of MAGL and FAAH in rat blood

Enzyme activity is influenced by several factors such as pH and temperature. The impact of these factors was considered using rat vascular tissue in the previous section. Therefore, the same assay condition was applied to measure MAGL and FAAH activities using blood samples from young male rats (aged 8-12 weeks) (Table 3.3). As a result, enzyme activity was measurable under assay conditions.

Table 3.3: MAGL and FAAH enzyme activities in blood samples from young rat (aged 8-12 week).

	MAGL activity nmole/min/mL		FAAH activity pmole/min/mL	
Samples	blood	TBV	blood	TBV
whole blood	204 ±2	1628.9 ±20	3.1 ± 0.9	24.5 ±7

TBV: total blood volume, was calculated using the equation described in section 1.3.9. Values are the MEAN ± SEM obtained from five independent experiments.

3.3.5 Age-related differences in MAGL and FAAH activities in rat mesenteric arteries

As shown above, no differences were observed in MAGL and FAAH activities between the three blood vessels from young rats. Thereafter, the effect of age on MAGL and FAAH functional expression in the superior mesenteric artery was examined in young (8-12 weeks) and old (6-9 months) rats (Figure 3.7, and table 3.4). There was no significant difference observed in MAGL activity between young and older rats (with $P < 0.1$). In contrast to MAGL, FAAH activity was significantly higher in MA from older rats than from younger rats (with $^{**}P < 0.001$).

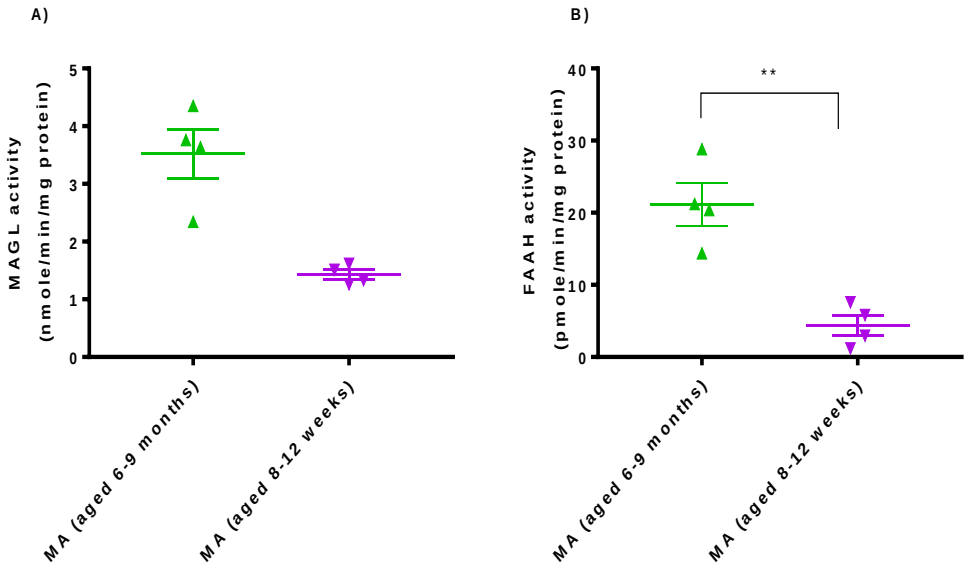

.**Figure 3.7. A) MAGL and B) FAAH activities in mesenteric artery (MA) from young (aged 8-12 weeks) and old (aged 6-9 months) Wistar rats**. Data were collected in duplicate, expressed as MEAN ± SEM from four individual experiments, and analyzed using student unpaired, two tailed t test. ** denotes p <0.001.

Table 3.4. The activity level of MAGL and FAAH in MA from young and old rats.

	MAGL activity (nmol/min/mg protein) Mean ± SEM		FAAH activity (pmole/min/mg protein) Mean ± SEM
	Cytosol	Membrane	Membrane
MA (young aged 8-12 weeks)	1.4 ± 0.1	1.3 ± 0.2	4.4 ± 1
MA (old 6-9 months	2.1 ± 0.2	2.6 ± 0.7	21.2 ± 4

Data are represented as a MEAN ± SEM from four individual experiments.

3.3.6 *In vitro* ABPP of rat mesenteric arteries expressed MAGL activity

Even though the radiometric assay is the most accurate and sensitive method for measurement of MAGL activity, the use of radiolabeled substrate has the drawback of being expensive. Activity based protein profiling (ABPP) provides an alternative to enable functional analysis of FAAH and MAGL activities in complex proteomes. We investigated whether the ABPP approach was sensitive enough to detect the modest activities of MAGL and FAAH enzymes in MA in comparison to previous results from radiometric assay. Additionally, we examined the selectivity of JJKK-048 inhibitor against MAGL in rat tissues. In this method, we employed TAMRA-FP, as an active site directed probe with broad target selectivity among serine hydrolase enzymes, to visualize changes in the activity of the enzymes in tissues. Initially, optimization of probe concentration was carried out using whole rat brain membrane fractions. Around 10 µg of sample was incubated with different concentration of TAMRA-FP for 30 min (Figure 3.8). As seen in Figure 3.7, no visible difference on band patterns or intensities were observed upon use of different concentrations of TAMRA-FP.

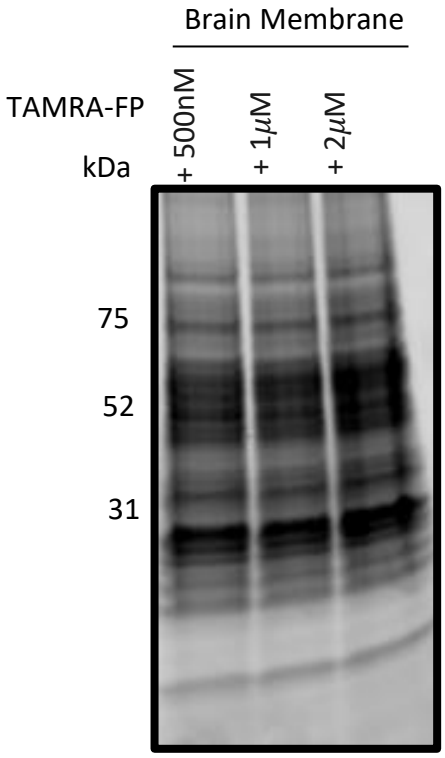

Figure 3.8. TAMRA-FP concentration effects in ABPP using whole rat brain membrane fractions.

Since no apparent differences were observed upon use of different concentrations of TAMRA-FP, we decided to use 500 nM TAMRA-FP to detect MAGL and FAAH activities in subsequent assays (Figure 3.9).

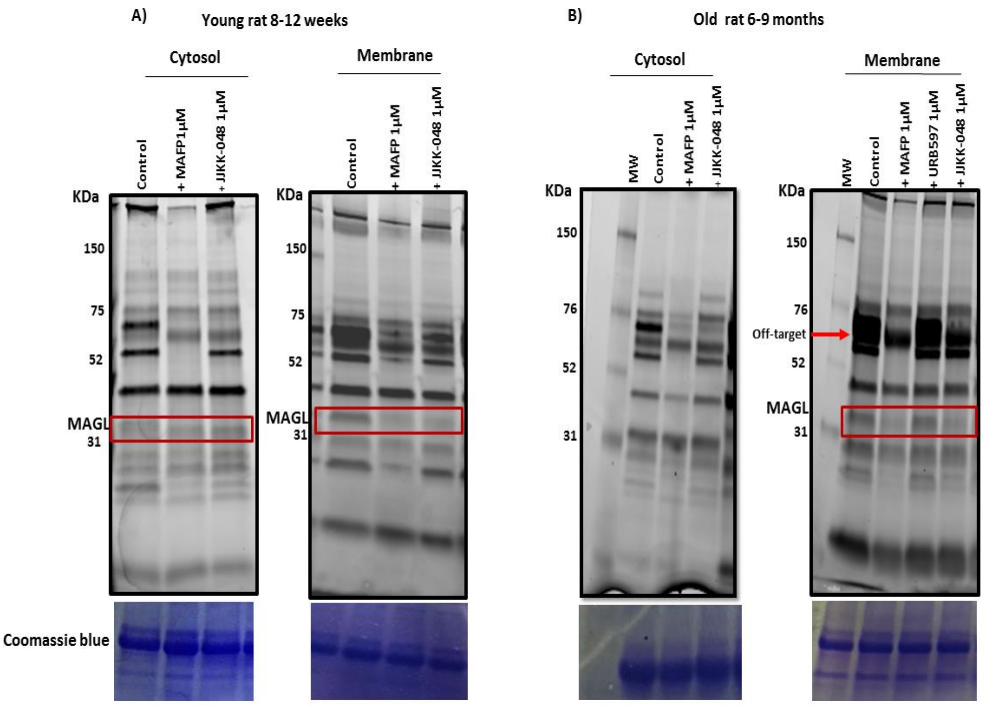

Figure 3.9. ABPP analysis of subcellular fractions from younger and older animals. Cytosol and membrane fractions were pre-incubated with DMSO (vehicle control) or selective inhibitors (1µM JJKK048 and URB597), followed by the addition of 500 nM of TMRA-FP and resolved using SDS-PAGE (100 µg protein per lane). ECL Plex Fluorescent Rainbow standard was used as a molecular marker. Coomassie blue staining was applied to confirm the loading control. The experiment was repeated three times and each time the result followed the same trend.

As mini-SDS PAGE gel was used in this assay. However, the resolution of the gel was insufficient to separate some of the enzyme activities (appearance of grouped bands); therefore, the quantification of individual bands was difficult and has not been conducted here. Nevertheless, this assay was conducted to validate the sensitivity of ABPP for detection of serine hydrolase activities. Hence, the low resolution of the gel did not impede the validation or importance of these results. Multiple fluorescent enzyme protein bands were observed; these indicated labelled serine hydrolases in rat MA. The labelled protein band was approximately 33 kDa; this band was reduced or absent when samples were pre-incubated with 1 µM of JJKK-048 or MAFP, indicating that this labelled 33 kDa

protein is MAGL. MAGL activity was detected in membrane fractions of MA from young rats. In contrast, MAGL activity in samples from older rats was detected only in the membrane fraction. The FAAH activity, unlike MAGL, was too low to be detected by ABPP in the rat MA. These results both cytosolic and membrane were similar to that obtained from the radiometric assay.

In addition, although JJKK-048 potently inhibited MAGL in the rat vasculature, at a high concentration (1 μM), it also diminished or inhibited the labelling of another enzyme bands, which was approximately 65–70 kDa, in the membrane fraction of MA from older rats. A similar reduction/inhibition was also seen following treatment with 1 μM MAFP. However, this 65–70 kDa enzyme protein remained largely unaffected by treatment with 1 μM URB597. It is therefore speculate that at high concentrations, JJKK-048 may exert inhibitory effects on serine hydrolase enzymes other than MAGL (Figure 3.9).

3.3.7 Spectrophotometric assay for MAGL activity:

3.3.7.1 Optimizing kinetic analysis of A-1-TG hydrolysis

First, a standard curve was prepared using a range of concentrations of a standard solution of the reaction product. Serial dilutions of A-1-TG (processed as the samples) were used as to generate a standard curve for this assay. The standard curve presented a straight line (figure 3.10), indicating that the signal from the assay was dependent on the amount of product in this assay.

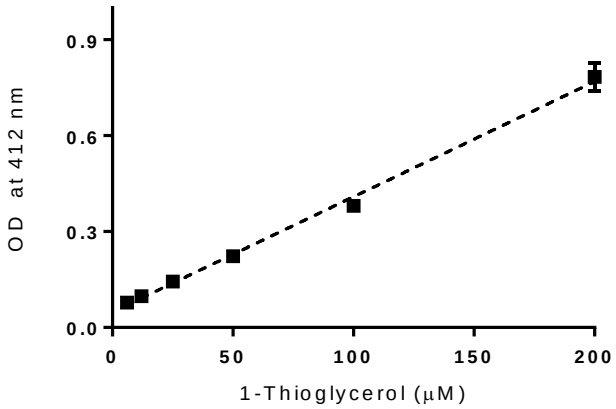

Figure 3.10. Standard Curve of 1-Thioglycerol (1-TG) DTNB absorbance. Data, acquired in triplicate, are expressed as the mean ± SEM from three independent experiments and were analyzed using linear regression ($R^2 = 1$).

The second investigation measured enzyme kinetics in a tissue rich in MAGL Increasing amounts of protein from rat brain cytosol fraction was incubated with 200 μM A-1-TG. Activity rate was found to increase linearly up to 25 μg of protein ($R^2 = 0.92$, Figure 3.11).

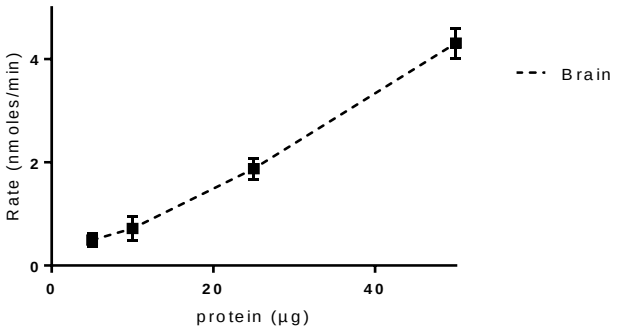

Figure 3.11. Influence of protein concentration on A-1-TG hydrolysis. Arachidonoyl-1-thioglycerol (200 μM) was incubated with increasing amounts of rat brain cytosol**.** Data, obtained in duplicate, are expressed as the mean ± SEM from four independent experiments, and were analyzed by linear regression.

Subsequently, Michaelis-Menten analysis of A-1-TG hydrolysis in rat brain cytosol was examined; estimates of an apparent V_{max} of 1669 ± 30 nmol/min/mg and K_m value of 38 ± 2 μM were obtained (Figure 3.12). In the presence of the

non-selective enzyme inhibitor, MAFP, A1TG hydrolysis was greatly reduced but not abolished (Figure 3.12).

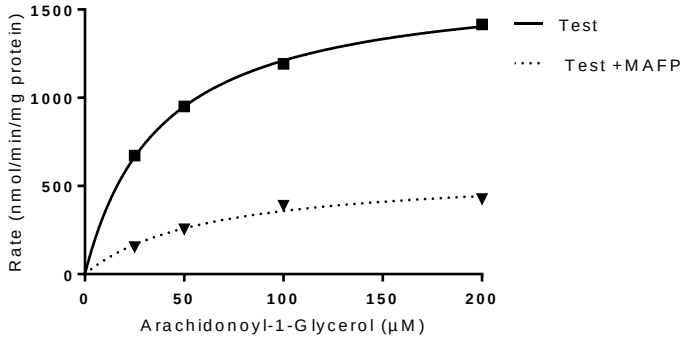

Figure 3.12. Michaelis-Menten kinetics for A1TG hydrolysis. Homogenized rat brain cytosol was incubated with increasing concentrations of A1TG in the absence and presence of 1 µM methyl arachidonoyl fluorophosphonate (MAFP). Data, obtained in duplicate, are expressed as the mean ± SEM from four independent experiments.

3.3.7.2 The effects of JJKK048 in spectrophotometric and radiometric assays.

FAAH and MAGL enzymes are highly expressed in brain and liver (Cravatt et al., 1996; Nomura et al., 2011b; Taschler et al., 2011). The effects of JJKK048 and MAFP were, therefore, investigated on liver and brain cytosolic A-1-TG hydrolysis, in order to identify the contribution of MAGL. Spectrophotometric assays (using A1TG) and radiometric assays (using 2-oleoyl-[^{3}H]-glycerol) were conducted in parallel to test the usefulness of A-1-TG as a substrate for MAGL (Figure 3.13).

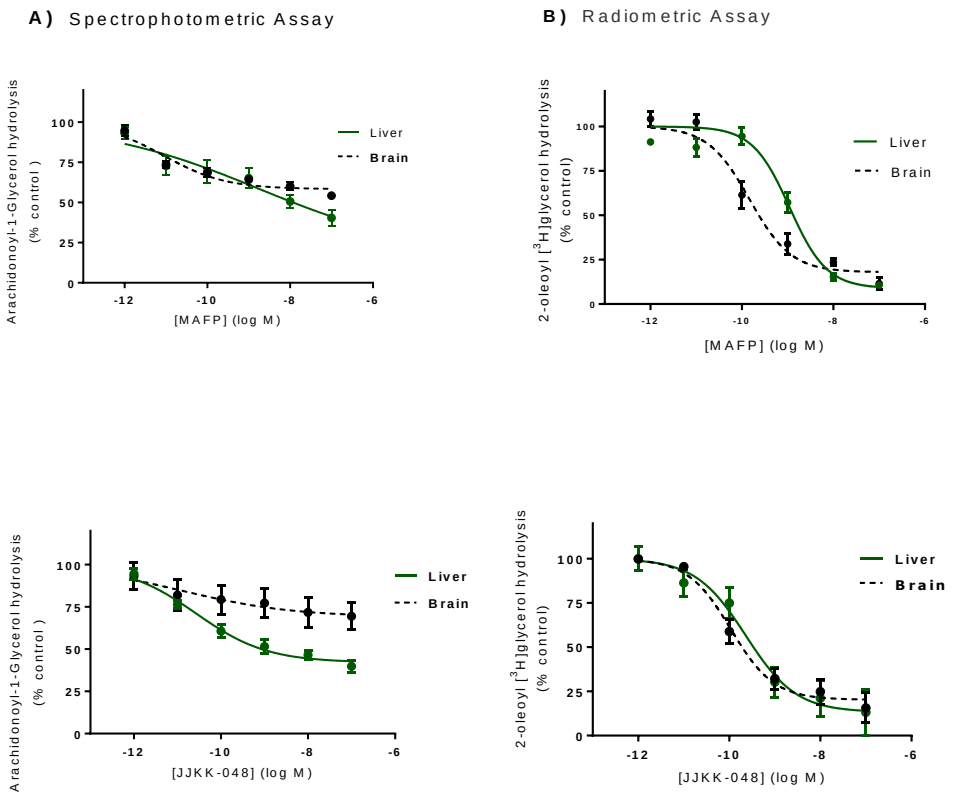

Figure 3.13. Effect of MAFP and JJKK048 on MAGL activity in cytosolic fraction of liver and brain tissues from young rats. Homogenates were pre-incubated with increasing amounts of MAFP or JJKK048 for 15 min and then incubated with: A) A1TG (spectrophotometric assay) or B) [^{3}H]-2OG (radiometric assay) for 30 min. Data were collected in duplicate from four individual experiments, and normalized as a % control substrate hydrolysis.

Table 3.5. pIC$_{50}$ values of A-1-TG hydrolysis by MAFP and JJKK-048 in both brain and liver cytosolic fraction by spectrophotometric assay.

	MAFP			JJKK-048		
	pIC50	Slope	MAFP-insensitive % control	pIC50	Slope	JJKK-048-insensitive % control
Brain	10±0.5	0.5±0.2	56±5	10 ±0.9	0.8±0.3	69±8
Liver	9.4±1	0.5±0.2	29±7	10 ±0.1	0.6±0.1	42±3

Data, conducted in duplicates, are expressed as the mean±SEM from four individual experiments.

Table 3.6. Identification of enzymes contributed to the A-1-TG hydrolysis (expressed as a fraction of total activity).

	Total A-1-TG hydrolysis %	MAGL activity %	Other serine hydrolysis %	Other protein %
Brain	100	31 ± 0.1	15±0.02	54±0.02
Liver	100	58 ± 0	9 ±0.02	33±0.02

Data, conducted in duplicates, are expressed as the mean±SEM from four individual experiments.

The pIC_{50} values calculated by radiometric assays for MAFP and JJKK-048 were consistent in brain and liver tissues, with a potency of -9 ± 0.1 and -9.7± 0.1, respectively. The potency of JJKK-048 in the brain was similar to that in peripheral tissue (see section 1.4.1), despite the targeting of other serine hydrolases, which was observed using the competitive ABPP technique (in previous section). MAFP showed excellent potency towards serine hydrolase in rat tissues with approximately 94% inhibition of 2-OG hydrolysis in the brain and liver. High concentrations of JJKK-048 elicited ~ 90% inhibition of 2-OG hydrolysis in the brain and liver. There was no significant difference between the inhibitory potency of MAFP and JJKK-048, indicating that MAGL is the predominant 2-OG-hydrolysing enzyme in the brain and liver.

The pIC_{50} values of MAFP and JJKK-048 inhibitors, as determined by spectrophotometric analysis, were reasonably similar to those determined by the radiometric assay. The Hill slope of the inhibitors was less than 1, indicating that at least one ternary complex enzymatic activity. Ternary complexes refer to three different molecules bound together; these may comprise, two enzymes bound to a single substrate, or an inhibitor and a substrate bound to an enzyme (Prinz,

2010) . In this case, the result of the Hill slope of both MAFP and JJKK-048 suggests that two or more proteins were bound to A-1-TG (see Table 3.5).

A large percentage of the residual of A-1-TG hydrolytic activity detected by spectrophotometric assay was not inhibited by inhibitors. MAFP is an irreversible inhibitor that inhibits all members of the serine hydrolase family, while JJKK-048 is selective for MAGL. Around 56% of the total A-1-TGhydrolase activities was 1µM MAFP-insensitive, whereas 69% residual activity was 1µM JJKK-048-isenstive. In contrast, in the rat liver cytosol, only 29 % and 42% residual activities were observed following treatment with the same concentrations of MAFP and JJKK-048-, respectively (Table 3.5). As stated previously, MAFP was used to investigate the contribution of serine hydrolases, including MAGL, in A-1-TG hydrolysis, while JJKK-048 was used to determine the contribution of MAGL. Therefore, based on the residual activity after treatment with JJKK-048, 31 % of total A-1-TG hydrolase activity in rat brain was attributable to MAGL activity. Similarly, considering the residual activities after treatment by both inhibitors, 15 % of the total activity was attributable to other serine hydrolyses that contributed toward A-1-TG hydrolysis. Thus, upon treatment with MAFP, the majority (54%) of total activity was due to non-serine hydrolases. In contrast, 58 % of the total A-1-TG hydrolysis activity in the liver was attributable to MAGL activity, while 9% of the total activity was attributable to other serine hydrolases and 33% to non-serine hydrolases (see Table 3.6).

3.4 Discussion

The activity level of MAGL and FAAH can be measured in rat blood vessels and blood samples using the radiometric assay. The FAAH activity increased with the age of the rat while MAGL activity remained unaffected by age. The ABPP technique can be used to detect MAGL activity, whereas it is not capable of detecting the low level of FAAH. In addition, the use of A-1-TG as a substrate to determine the activity of MAGL is not useful in native tissue, which is a complex mixture, unless the enzyme is purified.

3.4.1 Measurement of MAGL and FAAH activities in rat vascular preparation using radiometric assay

Data from this study showed that low levels of MAGL and FAAH activity were measurable by the radiometric assay. This study is one of the first to determine the activity level of FAAH and MAGL in vascular tissues. The measurement of enzyme activity can yield important insights into their physiological roles. A study by Herradón et al. (2007) demonstrated that, in aortae from rats, the relaxant effects of AEA were attenuated via the FAAH inhibitor URB597 (Herradón et al., 2007). Similarly, another study demonstrated that vasorelaxation of rat mesenteric arteries induced by AEA and 2-AG was mediated by the activity of endocannabinoid hydrolases and COX. AEA-induced relaxation was sensitive to the inhibition of FAAH by URB597, while vasorelaxant response to 2-AG were potentiated via inhibition of MAGL and COX by MAFP (Ho et al., 2007)

It is also reported that AEA induced a slight relaxation effect (not more than 20%) in intact isolated aorta rings (O'Sullivan et al., 2005). In agreement with

this study, AEA induced a slow increase in the relaxation in rat aorta in a concentration dependent manner, achieving a maximal value of 35% compared with the vehicle control (Herradón et al., 2007). Taken together, this may explains the low activity of FAAH observed in the present study, as FAAH is the main enzyme responsible for AEA degradation. In contrast to their level in blood vessels, AEA and 2-AG are abundant in the brain, where they have beneficial roles in brain development and function (Savinainen et al., 2012). (Kathuria et al., 2003; Aguado et al., 2005; Bortolato et al., 2007)As a consequence, the deactivation of AEA and 2-AG by FAAH and MAGL, respectively, regulates their roles in the brain.

Based on the current data and previously reported observations, it is likely that AEA and 2-AG exert their vasorelaxation effect specifically in rat vasculature through several mechanisms, one of these being hydrolysis by FAAH and MAGL, to produce AA (as suggested by (Herradón et al., 2007). The low activity levels of these enzymes may explain why some studies did not detect the significant effect of endocannabinoid hydrolysing enzyme inhibition on the vasorelaxation response to endocannabinoids.

The O-aryl carbamate JZL184 is a potent MAGL inhibitor for the human and mouse enzyme, while it is less potent for the rat enzyme *in vitro* (Long et al., 2009a). JJKK-048, therefore, was selected to identify the contribution of MAGL in 2-OG hydrolysis in this study. JJKK-048, a piperidine-based triazole urea, which binds to the MAGL active site serine (S122) to form a carbamate adduct, is an irreversible inhibitor of MAGL (Aaltonen et al., 2013). The potency of JJKK-048 against MAGL activity has not yet been investigated in vascular tissue. The present results show that JJKK-048 is a potent inhibitor of MAGL,

with a pIC_{50} value of ~ 9.4 for the rat enzyme *in vitro*. This value is similar to the potency described in the literature; JJKK-048 inhibited 2-AG hydrolysis in intact human cells and rat cerebellar membrane with a pIC_{50} value of 9.67 (Aaltonen et al., 2013; Laitinen et al., 2013).

3.4.2 *In vitro* enzymatic activity of MAGL and FAAH in rat blood

The ability to measure endocannabinoid-hydrolysing enzymes in blood samples would be an important step towards understanding their function in the haematological system. The activities of MAGL and FAAH are measurable in the rat blood stream. Interestingly, the activity level of MAGL in blood from rats is relatively similar to that in human blood samples, as described in detail in the following chapter. Previous studies have reported the downstream effect of the endocannabinoid system in blood cells. MAGL, but not FAAH, plays a critical role in the platelet aggregation process (Maccarrone et al., 1999; Fasia et al., 2003). This partly explains the relatively high activity of MAGL detected in blood samples. In addition, an earlier study with isolated perfused rat heart suggested that MAGL in plasma is responsible for the hydrolysis of 2-AG in the coronary bed (Fielding, 1981).

MAGL and FAAH activities in rat blood samples displayed sensitivity towards the selective inhibitors JJKK-048 and URB597, respectively. The results from this and the previous section suggest that these inhibitors may be used to study the role of MAGL and FAAH in both central and peripheral physiological processes. High concentrations of either JJKK-048 or URB597 completely ablated the activity of MAGL and FAAH, respectively, using rat blood samples *in vitro*. As both inhibitors irreversibly bind to the enzyme, it can

be speculated that the *in vitro* inhibition may correlate with the pharmacological action *in vivo*. In support of this notion, maximal inhibition of FAAH was observed in rat brain and blood leukocyte samples after oral administration of URB597. In addition, intraperitoneal injection of JJKK-048 resulted in nearly complete inhibition of MAGL in several tissues (Aaltonen et al., 2016). However, the maximal tolerated dose and the time of recovery of enzyme after inactivation needs to be determined for each species.

The reproducible results for enzyme activity, obtained in this section, represent an initial optimization step for extensive investigation of MAGL and FAAH activities in human blood, which is described in the following chapter.

3.4.3 Age-related differences in MAGL and FAAH activities in rat mesenteric arteries

Although the level of activity of FAAH in MA of rats was modest, it underwent significant changes as a result of aging. The activity increased by 5 fold in older rats (aged 6-9 months) compared with that in younger rats (aged 8-12 weeks). In contrast, there were no changes in MAGL activity observed. This is the first study to determine the influence of age on the activities of FAAH and MAGL in MA. Similar results were observed in the rat brain region, where FAAH activity was higher in 6 week old rats compared with 4-week old rats (Lee et al., 2013). In addition, increased FAAH protein expression was observed in the cerebral cortex of male Wistar rats aged (28 months) compared with an adult rat aged (4 months), while MAGL activity did not exhibit ageing-related effects (Pascual et al., 2013).

The mechanisms underlying age-associated FAAH activity have not yet been examined. In order to investigate this further, quantitative protein expression studies using immunoblotting and gene expression analysis by reverse transcription polymerase chain reaction (RT-PCR) needs to be conducted.

Age-related increase in FAAH activity further implies a role of FAAH in vascular function. A decline in the functional of the cardiovascular system (blood pressure and heart rate) was observed in wild type aged mice (31 months old) compared with younger mice (3 months old), as a result of reduction in AEA levels (Bátkai et al., 2007). In contrast, in FAAH-/- mice, a significant increase of AEA was observed and they were more resistant to the deterioration of cardiovascular function with age. Pharmacological inhibition or genetic deletion of FAAH exerts a production effect against chronic inflammatory processes associated with cardiovascular aging (Bátkai et al., 2007). Increased AEA, as a result of FAAH inhibition, inhibits essential NF-κB-dependent pivotal inflammatory pathways through the cannabinoid receptor (Nakajima et al., 2006). Suppression of the cytokine-induced NF-κB signalling pathway exerts vasculoprotective effects via the attenuation of vascular inflammation (Spiecker et al., 2000).

The inhibition of FAAH leads to an increase in AEA, which acts as a vasodilator, and consequently improves blood flow. Consistent with this hypothesis, the Ho et at (2016) group, (who supplied mesenteric arteries tissue for work in this chapter) have shown (in 2016) that AEA can enhance vasorelaxation of MA isolated from rat and protect them against endothelial dysfunction, a key feature of ageing and cardiovascular disease (unpublished).

In the MA isolated from younger rats, a smaller degree of endothelium-dependent relaxation was observed. Further, inhibition of FAAH with 1 µM URB597 restored the relaxation of endothelium after being supressed by the muscarinic agonist carbachol in older rat but not younger rats. Carbachol appeared to induce endothelium-dependent contraction in rat vessels (ICRS 2016). In addition, potential age-specific effects of URB597 have been reported, wherein chronic administration of URB597 caused reduction of BP and HR in older hypertensive rats by 21% , while no influence of FAAH inhibition by URB597 was seen in younger rats (Toczek et al., 2016). Therefore, the inhibition of FAAH may be beneficial in age-related pathological conditions.

3.4.4 *In vitro* ABPP for detection of MAGL activity.

ABPP is a powerful technique that uses FP-rhodamine to label serine hydrolase enzyme activities. Although the radiometric assay has been a Gold Standard assay to measure the activity of an enzyme, ABPP has several advantages over the former. First, multiple enzyme activities can be labelled and detected in a single experiment (Chen et al., 2016). In this study, the resolution of mini-SDS PAGE gel was insufficient for resolution of the labelled proteins. However, this experiment was mainly conducted to assess the sensitivity of ABPP for detection of MAGL and FAAH activities. As these enzymes can be identified on the ABPP gel based on their molecular size and the effects of selective inhibitors, the results of this experiment are still valid and can be used along with the results obtained from radiometric assay. MAGL activity, which corresponded to a 33 kDa band, was visible in the cytosolic and membrane fractions of MA, which is in agreement with the results from the radiometric

assay (section 1.5.1). Thus, the ABPP results confirmed that MAGL is an amphitropic enzyme that can be detected in cytosolic and membrane fractions, consistent with the literature (Labar et al., 2010a). In contrast to MAGL, the activity level of FAAH in the rat MA membrane fraction was extremely low when detected by radiometric assay and the measured activity did not exceed 2 pmol/min/mg protein. Thus, its activity was too low to be detected by ABPP.

A second advantage of ABPP is that inhibitors can be immediately screened against many enzymes in parallel in native tissues or cells, allowing simultaneous optimization of inhibitor selectivity in a single experiment (Chen et al., 2016). Competitive ABPP was used to investigate the selectivity of JJKK-048 against MAGL. Although JJKK-048 exhibited a potent inhibition of MAGL activity (described earlier in section 1.5.1), at a high concentration (1 μM) it displayed cross-reactivity with another enzyme (migrating at 65-70 kDa) in the membrane fraction of rat vascular tissues. This enzyme was insensitive to URB597, ruling out FAAH as a possible target. Similar to the current results, ABPP studies in mice peripheral tissues (such as heart, spleen, and skeletal muscle) showed that a high concentration of JJKK-048 could inhibit the 65-70 kDa carboxylesterase 1 enzyme as an off-target, in addition to MAGL (Aaltonen et al., 2016). Like MAGL, carboxylesterases are members of the serine hydrolase family , and are intracellular proteins located mainly in the microsomal fraction (Lian et al., 2017) . As the carboxylesterases were also detected in rat aorta (Belfiore, 1980; Zhang et al., 2007), it can be speculated that the enzyme migrating at 65-70 kDa observed in this study could correspond to a carboxylesterase enzyme.

Previously, it was shown that JJKK-048, at the concentration of 229 nM, displayed an inhibitory effect against alpha/beta-hydrolase domain containing 6 (ABHD6), while a higher concentration (2 μM) displayed inhibitory effects against FAAH (Alhouayek et al., 2017). Collectively, these results indicated that a lower concentration of JJKK-048 should be used (100 nM) to selectively target MAGL activity and to avoid cross-reactivity with other enzymes.

3.4.5 Spectrophotometric assay for MAGL activity:

The experiments in this study were conducted to measure MAGL hydrolytic activity and the effect of inhibitors upon the enzyme.

3.4.5.1 Optimizing kinetic analysis of arachidonoyl-1-thio-glycerol (A-1-TG) hydrolysis

The proportion of A-1-TG hydrolysis increased linearly with increasing protein content in rat brain tissues. The A-1-TG hydrolysis saturation curve for rat tissue demonstrated that this reaction follows Michaelis-Menten kinetics.

3.4.5.2 The effects of JJKK048 in spectrophotometric and radiometric assays.

A-1-TG was identified as a useful substrate for MAGL using recombinant enzyme preparations (Ulloa et al., 2010). Inhibition studies were used to compare the precision and sensitivity of the spectrophotometric assay to a radiometric assay. MAFP and JJKK-048 displayed consistent potency, with pIC_{50} values of 9.4 and 9.7, respectively, toward MAGL, in spectrophotometric and radiometric assays. The potency of an irreversible inhibitor is largely dependent on assay conditions such as duration of incubation (Singh et al.,

2011). Thus, the highly similar values of the inhibition potency between the two independent assays could be due to identical rat tissues and incubation times being used. However, it is not yet known whether the potency of an inhibitor is influenced by substrate selection. MAFP and JJKK-048 are irreversible inhibitors and exert their inhibitory effects through their permanent covalent binding with the enzyme active site of the enzyme. Thus, it is likely that their intrinsic potency is not influenced by the choice of substrate.

Despite the consistent potency between the two assays, the inhibitory effects of both inhibitors, as observed using a spectrophotometric assay, were not comparable to those obtained with radiometric assays. In the radiometric assay, MAFP and JJKK-048 exerted concentration-dependent inhibitory effects, reaching a maximum inhibition of 94% of total 2-OG hydrolysis. This indicated that MAGL is the predominant enzyme responsible for 2-OG hydrolysis in rat brain and liver tissues. In contrast to this, the use of a high concentration of MAFP and JJKK-048 did not completely inhibit A-1-TG hydrolysis in the spectrophotometric assay. More than 50% of total substrate hydrolysis in the brain was MAFP-insensitive, while 29% of total substrate hydrolase activity in the liver was insensitive to MAFP. As MAFP is a non-selective serine hydrolase inhibitor (Deutsch et al., 1997), there could be multiple non-serine hydrolyses present in brain and liver responsible for the hydrolysis of A-1-TG.

Based on JJKK-048 sensitivity, MAGL was only responsible for 31% of total A-1-TG hydrolysis in the brain, with other serine hydrolases accounting for 15% of total hydrolysis, while the majority of A-1-TG hydrolysis (54%) was catalysed by unidentified non-serine hydrolase enzymes. In contrast to that in the brain, 54% of total A-1-TG hydrolysis in the liver was due to MAGL activity,

with other serine hydrolases responsible for only 9% of the total A-1-TG hydrolysis, and the remaining 33 % could be attributed to non-serine hydrolase enzymes.

Taken together, these observations suggest that A-1-TG is hydrolysed by non-serine hydrolases other than MAGL in native rat enzyme preparations, which appear to be proportionally more abundant in the rat brain than in the liver. In addition, It is reported that 2-AG can be hydrolysed by other non-MAGL serine hydrolase enzymes such as α/β hydrolase domain enzymes (ADBH6 or ABHD12) (Blankman et al., 2007) and carboxylesterase (Dinh et al., 2002). As A-1-TG is an analogue of 2-AG, it is possible that other non-MAGL serine hydrolase enzymes, such as ABDH6, ABDH12, or carboxylesterase contribute to A-1-TG hydrolysis in rat tissues. In order to test this hypothesis, ABPP can be used to identify active enzymes involved in A-1-TG hydrolysis. A-1-TG bound to serine hydrolase enzymes, including MAGL, and would prevent their labelling, which should enable their negative identification in comparison with a positive control.

Therefore, the utility of A-1-TG as a selective substrate in native tissue, which is a complex mixture of enzymes, is limited. These results are not consistent with those reported by Ulloa et al. (2010); this may be because the latter study used human purified recombinant MAGL. These results suggest that, although A-1-TG allows kinetic monitoring of the reactions, unless purified preparations are used, A-1-TG could be hydrolysed by MAGL and other unidentified enzymes.

It is likely that the A-1-TG substrate specificity toward MAGL can be improved by replacing the arachidonoyl chain of A-1-TG with an oleoyl chain.

This notion is based on previous studies, where 2-OG has been widely used as a substrate to measure MAGL activity *in vitro*, with many advantages over 2-AG. One of these is that 2-AG, unlike 2-OG, is metabolised by other enzymes such as lipoxygenases and cyclooxygenases, and hence can lead to an underestimation of MAGL activity (Dinh et al., 2002; Björklund et al., 2010).

Chapter 4 Endocannabinoid hydrolases in human blood

4.1 Introduction

The ability to measure MAGL and FAAH activities in rat blood samples was presented in **Chapter 3** using the Gold Standard technique of the radiometric assay. Plasma eCB levels have been described in several published studies and shown to vary with several factors. For example, Blüher et al. (2006) reported a positive correlation between plasma 2AG levels and body fat, particularly visceral fat mass. Cote et al. (2007) also reported a link between plasma 2AG levels and BMI and waist girth. A relationship with alcohol addiction has also been described. In one study by Mangieri et al. (2009), healthy 'social drinkers' exposed to alcohol cue imagery showed increased plasma levels of AEA. In alcoholics, baseline levels of AEA were reduced and were unaffected by alcohol cue images. Furthermore, plasma AEA and 2-AG levels were measured to ascertain whether they correlated with decision-making and cognitive flexibility performance (prefrontal-depended cognitive functions) in healthy female individuals. It was found that raised levels of 2-AG were associated with disrupted decision making and inhibited response capacities, while elevated levels of AEA gave the opposite result (Fagundo et al., 2013).

eCBs are a key mediator in blood, where they regulate platelet aggregation (Keown et al., 2010) and erythrocyte apoptosis (Bentzen et al., 2007), and vascular tone as described in **Chapter 3**. Despite several studies having already explained the role of blood component in the cardiovascular system, as yet there are very limited data about the presence of MAGL and FAAH activities in the circulation. MAGL was found to be present in plasma (Noma et al., 1976), and

was purified from human erythrocytes (Somma-Delpero et al., 1995). Both FAAH (Maccarrone et al., 1999) and MAGL (Gkini et al., 2009) activities have been detected in platelet membranes and human platelets, respectively. In addition, FAAH mRNA expression was detected in whole blood samples from healthy volunteers (HUNGUND et al., 2004).

However, there are no studies to-date about the possible variation of MAGL and FAAH activities in human blood in individual human volunteers, and whether or not the activity level of these enzymes can be used as potential biomarkers. The functional impact of these enzymes on the haematological system has not been identified yet. Thus, this study was designed to fill that gap.

4.2 Aim

The primary aims for the study were to examine the distribution of these enzymes in human blood fractions, and to examine whether repeated sampling from the same donors provided consistent levels of activity (reproducibility). Secondary objectives were to investigate in which constituents of the blood they are most (and least) active, and to examine whether enzyme activities are maintained after storage conditions.

4.3 Materials & Methods

4.3.1 Chemicals & reagents

The following table shows chemicals that were used in the assays described in this chapter:

Chemical and solutions	Company
N-(2-hydroxyethyppiepeazine-N-(2-ethanesulfonic acid) (HEPES)	Sigma Chemical Co
Tri-sodium citrate Citric acid Magnesium chloride ($MgCl_2$) Calcium chloride ($CaCl_2$) Potassium chloride (KCl)	Fisher Scientific U.K.
Glucose	BDH Laboratory Supplies, Poole, Dorset, U.K.

All other chemicals were identified in **Chapter 2**.

4.3.2 Ethics

This study was approved by the Research Ethics Committee of the School of Life Sciences, University of Nottingham (Ethics no. A190316SA), with volunteers recruited from within the University of Nottingham by poster (see Appendix.4). All subjects were informed of the purpose and risks of the experiment before the study and gave their written signed informed consent. All volunteer' information gathered during this study was treated with privacy, confidentiality and limited access was granted only to authorized persons. The questionnaire remained in the custody of those authorised to do so.

4.3.3 Sample size determination and statistical power

As this is the first investigation of its kind, power calculations were based on our previous studies investigating inter-individual variation in human brain

endocannabinoid metabolic enzyme activities postmortem (Erdozain et al., 2015). In this study, a 25 % change was observed in enzyme activity between subject groups with a coefficient of variation of 10-25 %. Using G*Power and these parameters, with a Wilcoxon signed-rank test, setting the Power to 0.95, indicates an a priori sample size of nine individuals. Therefore, eighteen volunteers were the target required in this study (nine male and nine female). Samples from males and females were assessed separately in order to account for potential intrinsic sex differences, with an intention to identify whether males or females or males AND females could be used in subsequent studies.

4.3.4 Study design and Blood sampling

Eighteen healthy individuals aged 23-56 years old (9 male and 9 female) from the University of Nottingham Medical School were recruited using posters. Volunteers were excluded if they had participated in a clinical trial in the previous three months, or had a history of drug abuse.

Since the level of eCB is described to be influenced acutely by exercise, food and alcohol intake (Engeli et al., 2014; Feuerecker et al., 2012; Gasperi et al., 2014), subjects were asked to fast at least 8 h prior to the blood test, abstain from exercise for the previous 12 h and abstain from alcohol intake for the previous 24 h. Also, to assess the reproducibility of endocannabinoid hydrolase enzymes, subjects were asked to attend three visits in this study with the period between each experimental visit set at 15 days.

In the first visit, subjects completed a questionnaire (see Appendix.1). The questionnaire was designed to assess some aspects of the individuals which may influence variation between subjects (e.g. weight, height, smoking, consuming

alcohol and caffeine), and to exclude subjects with pathological conditions such as asthma. We also aimed to assess whether the subjects took any medication (including the oral contraceptive pill) in the last three days, or they had medical treatment and vaccination in the last three months. Afterward, blood pressure was measured with subject rested and in the supine position by using an automatic blood pressure monitor, and a venous blood sample (30mL) was taken from the antecubital fossa using a 21G butterfly needle.

In the second and third visits, subjects completed a short questionnaire (Index 2, see below) to assess some of the variable aspects that can occur for subjects between visit periods such as infections, taking medication or, for females, the stage of the menstrual period. Then, the blood sampling process in the first visit was repeated (30 mL of blood were taken). A total of 90 mL blood were taken from each participant for this study. Samples were drawn between 8 to 10 AM to avoid any potential influence of diurnal variation.

4.3.5 Isolation and homogenisation of blood cells

A tourniquet was applied to locate the cubital vein, which was punctured and then blood was drawn using a 21G butterfly needle. When blood flow was adequate, the tourniquet was slackened to prevent platelet aggregation in the stationary venous blood. Also, blood was only extracted from the vein at a rate at which resistance was not felt in the syringe, as obtaining blood from a vein against resistance can lead to platelet aggregation (Liz Simpson, 2000).

A 30 mL blood sample was taken from each subject and was then divided into two 25 mL Universal tubes; 20 mL of blood was mixed with 2 mL of Acid Citrate Dextrose solution (ACD - 0.8% citric acid, 2.2% trisodium citrate, 2.5%

dextrose) (the mixing rate is 9:1 in volume (Keown et al., 2010)), and 10 mL of blood was collected without further additions to obtain serum. ACD was used as anticoagulant because of its negligible intrinsic effect on platelets (Keown et al., 2010).

The tube that contained blood with the anticoagulation solution was centrifuged immediately at a low speed (150 g for 20 min at 24 °C) to obtain platelet rich plasma (PRP), and a denser fraction containing both erythrocytes (red blood cells, RBC) and white blood cells (WBC). The PRP was then extracted using a polypropylene transfer pipette into a separate tube. One drop of citric acid (0.15 M) was then added per mL of PRP, acidifying it to pH 7. The acidified PRP was then centrifuged at 300 g for 10 min at 24 °C to separate platelets from plasma (see Figure 4.1).

Then, the supernatant layer (plasma) was carefully aspirated and distributed in Eppendorf tubes to allow further processing or stored at -80 ^{o}C. Then, the platelet pellet was re-suspended in HEPES washing buffer (pH 7.2) of approximately the same volume as the original PRP. The solution was centrifuged at 300 g for 10 min at 24 °C. The HEPES washing buffer contained 10 mM HEPES, 3 mM EDTA, 152 mM NaC1, 4.17 mM KCl; pH 7.2 at 25 °C. The supernatant layer was then discarded, and the washed platelet pellet was re-suspended in the same volume of HEPES washing buffer as before and distributed in aliquots for further processing or stored at -80 ^{o}C to assess the influence of storage condition on enzyme activity.

The washing buffer was employed for three major reasons; to neutralise the suspension, to remove any adenosine and surplus apyrase and to eliminate any plasma proteins. The time for centrifugation is shorter in this step to prevent

platelet aggregation by over-compression of the platelet pellet, which may occurred in extended centrifugations. We used HEPES buffer instead of TE buffer because Tris, like other amines, can modify platelet responses (Mustard et al., 1989).

The denser fractions were re-suspended twice in 172 mM Tris/HCl (pH 7.4) and re-centrifuged at 800 g for 10 min at room temperature to obtain erythrocytes. On both occasions, the upper layer of the packed cells (containing mainly leukocytes) and the supernatant layers were aspirated (Somma-Delpero et al., 1995). Following this, the separated erythrocytes were aspirated and distributed in aliquots to allow further processing or stored at -80 ^{o}C to assess the influence of storage conditions on enzyme activity.

Another 10 mL of blood was collected into a plain tube to obtain serum. It was incubated at room temperature for 30 min to allow clotting, and then it was centrifuged for 15 min at 1000 g (Ho et al., 2012).

A previous study found that whole blood samples maintained at room temperature for up to 3 h maintained FAAH activity in the leukocyte fraction subsequently isolated (Yapa et al., 2012). Therefore, isolation of different blood components and measurement of enzymes activities were processed within 2 h of blood collection to avoid a loss of enzyme activity and to minimize assay variation.

4.3.6 Determination of protein levels:

The protein concentration of platelet samples was quantified by the Lowry method, as described in section 2.3, although these were much higher than animal tissues. In the Lowry assay, the determination of protein content value of

each sample was based on the comparison of the sample value with the BSA standard.

Platelet samples were initially dissolved at a ratio of 1:100 in 0.5 M sodium hydroxide to determine the protein content as was undertaken with rat tissues, but the values of protein content were outside the standard range. To overcome this problem, platelet samples were further dissolved at a ratio of 1:10000 in 0.5 M sodium hydroxides.

4.3.7 Enzyme activity assays:

4.3.7.1 Radiometric assays

FAAH and MAGL activities were measured by radiolabelled ligands as described in section 2.1. Whole blood and RBC were resuspended in TE buffer pH 7.4 to give 1 in 500 or 1 in 50 fold dilution, respectively. Also, platelets were re-suspended in HEPES buffer pH 7.2 to give 1 in 600 fold dilution. An early study by Bry (1979) found that higher MAGL activity can be detected under conditions similar to those in the blood stream where temperature is 37^{o}C, and the pH between 7.0 and 8.0 (Bry et al., 1979). Therefore, the incubation process was carried out at 37^{o}C. Afterward, optimization of the assay was accomplished by using various protein concentrations of homogenate, until activity was measurable but to no more than 10% of substrate turnover.

4.3.7.2 Data Analysis

Enzyme activity was expressed in nmoles/min/mL of blood as described in section 2.2. GraphPad Prism (California, USA) software was then used to analyse all of the data, using coefficient of variation (CV %) and unpaired two tailed Students t-test to report the variation within subjects and between groups

(males versus females) respectively. Then, the differences in enzyme activity between male and female groups were tested using 2-way ANOVA with Turkey's multiple comparisons test and different time points as factors. In addition, the stability of enzyme activity at different storage conditions was assessed using the Ordinary One-Way ANOVA (Multiple comparison) test.

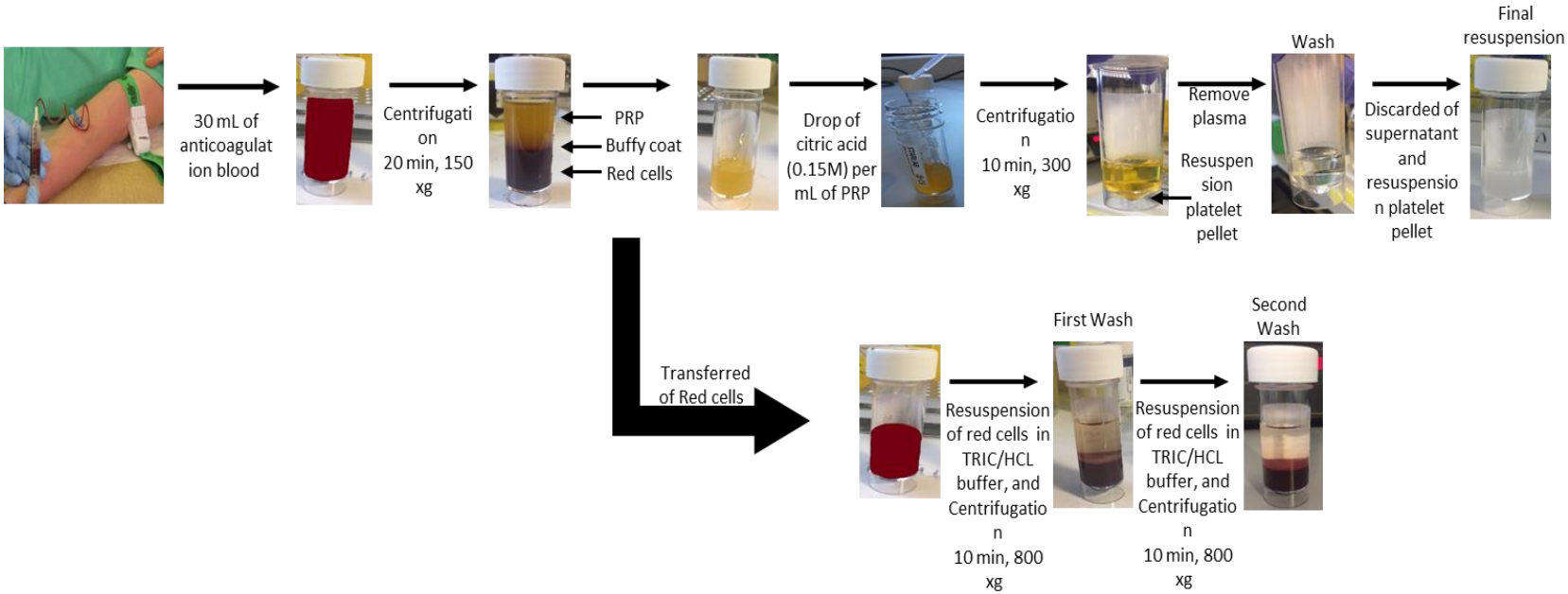

Figure 4.1: Isolation of different blood fractions. Blood was centrifuged immediately at a low speed (at 150 g, for 20 min at 24 °C) to obtain platelet rich plasma (PRP), and a denser fraction containing both erythrocytes/ red blood cells (RBC) and white blood cells (WBC). The PRP was then extracted and centrifuged at 300 g for 10 min at 24 °C to separate platelets from plasma. The denser fractions were washed twice with 172 mM TE (pH 7.4), and re-centrifuged at 800 g for 10 min at room temperature to obtain erythrocytes.

4.3.7.3 Activity based protein profiling

Immediately after isolation as described above, platelets were re-suspended in HEPES buffer pH 7.2, the enzyme assay was performed as described in section 2.2. The final amount of platelet proteins loaded onto the gel was 12 µg.

4.4 Results

4.4.1 Subjects demographics

The finding of this study was obtained from healthy subjects, and in the male group, the age ranged from 23-56 years with BMI 21.9-30.8 $kg.m^{-2}$, while in the female group, the age ranged from 23-32 years with BMI from 19.8-25.9 $kg.m^{-2}$. Descriptive data from the participants are given in Tables 4.1 & 2 below.

Table 4.1: Male subjects' descriptive data

PARTICIPANTS CODE		Age (years)	BMI ($kg.m^{-2}$)	BP (mm Hg)		Alcohol Consumption	physical activity per week
				systolic	diastolic	unit per week	
Males	7273	23	26.7	121 ± 2.9	87 ± 5.8	none	lightly active
	880	25	27.7	117 ± 4.2	65 ± 1.5	10	moderately active
	9621	26	22.6	112 ± 0.9	65 ± 3	20	moderately active
	2997	29	25.9	125 ± 1	77 ± 3.8	4	lightly active
	7251	29	29.4	127 ± 2.4	80 ± 3.4	none	sedentary
	9081	36	30.8	129± 4.6	83 ± 2.5	none	lightly active
	5349	36	23.7	111± 2.2	75 ± 1.5	none	moderately active
	4032	52	21.9	126 ± 4.7	79 ± 2.1	5	moderately active
	7350	56	29.4	109 ±0.6	71 ±3.1	5 to 10	moderately active
		34.7 ± 3.9	26.5 ± 1.1	120 ± 3	76 ± 3		

Table 4.2: Female subjects' descriptive data

PARTICIPANTS CODE		Age (years)	BMI ($kg.m^{-2}$)	BP (mm Hg)		Alcohol consumption	physical activity per week
				systolic	diastolic	unit per week	
females	5447	23	25.9	108 ± 3	69 ± 1	3	lightly active
	4485	25	23.7	107 ±2.2	65 ± 1.8	none	moderately active
	1539	25	22	96 ± 2	67 ± 1.7	3	moderately active
	5530	26	20.7	103 ± 2.7	63 ± 1.2	250 mL	moderately active
	2725	28	22.5	113 ± 0.9	65 ± 2.7	none	moderately active
	1268	28	22.7	100 ± 1.2	56 ± 2.5	100 mL	sedentary
	8953	28	19.8	97 ± 3	70 ± 2.5	rarely	lightly active
	3026	29	25.8	102 ± 4.3	73 ± 1.9	none	sedentary
	6218	32	22.5	110 ± 0.9	69 ± 2.8	none	moderately active
		27.1 ± 0.9	22.8 ± 0.7	103 ± 2	66 ± 2		

Tables 4.1 & 2: Blood pressure is expressed as mean ± SEM of three visits. BMI, body mass index. Sedentary, walking ≤30-60 min/week. Lightly active, walking 1-3 h/ week. Moderately active, walking more than 3 h per week.

4.4.2 Optimization of dilution factors

In the radiometric assay, the first optimization step was to achieve 8-10 % substrate hydrolysis (based on the standard DPM values for ^{3}H-AEA or ^{3}H-2OG), which will reflect the linear activity level of the enzymes. Whole blood sample and platelets fraction were diluted using different dilution ratios in 50 mM TE buffer as shown in figure 4.2. It was found that higher activity of MAGL was detected with the 500-fold dilution for whole blood samples, while higher activity of MAGL was detected with the 600-fold dilution for platelet samples.

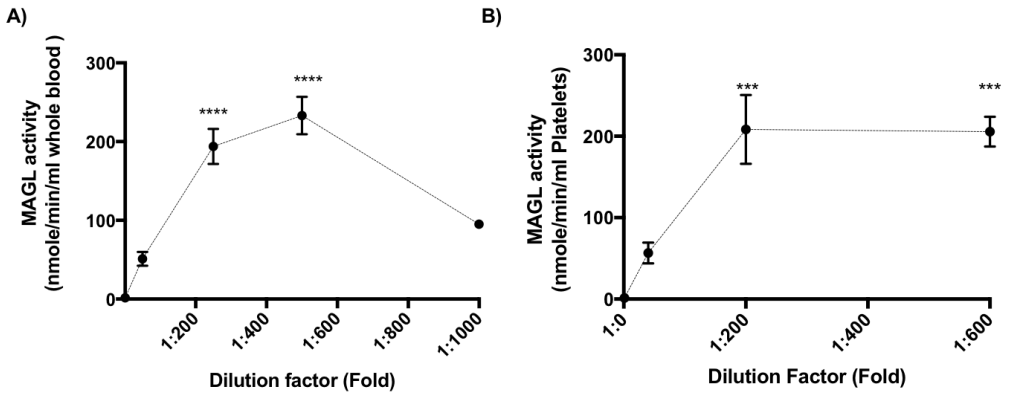

Figure 4.2: Effect of tissue dilution on the activity of MAGL in: A) whole blood samples, B) platelet samples. Samples was diluted by serial dilution methods (1 to 1000 fold) with 50 mM Tris/1 mM EDTA/ BSA 1 mg/mL and then reacted with 2-[^{3}H]-OG substrate in the radiometric assay. Samples collected from four healthy volunteers (two male and two female). Specific activity is expressed as nmole/min/mL of initial blood volume. Data are Mean ± SEM (n = 4). Significance was analyzed by one way ANOVA, Dunnett test ****$P \leq 0.0001$, *** $P \leq 0.001$.

4.4.3 Characterisation of eCB hydrolysing enzymes in human blood

4.4.3.1 Reproducibility of MAGL and FAAH enzymes in human blood:

A previous study reported that, after blood withdrawal, the chemical isomerization of 2-AG occurs during the storage and sampling process. Due to the instability of eCB concentrations in human blood, analysis needs to be performed with fresh samples in order to avoid artificial differences between samples (Pastor et al., 2014). As a consequence, this would lead to the inaccurate measurement of enzymes activities. Therefore, all the experiments were performed immediately following isolation of blood components. Initially, blood samples were treated in parallel assays with 1 µM of MAFP each time the experiments were carried out in order to ensure that the measured enzymes belonged to the serine hydrolase family. Then, specifically, a maximum

concentration of JJKK-048 (100 nM) or URB597 (1 μM) was used to evaluate the presence of MAGL and FAAH activities, respectively, in blood samples.

There was no significant difference in the level of MAGL activity in platelets between males and females for the mean data from three different time points (Males 185 ± 14; Females 153 ± 14 nmol/min/mL blood; P=0.128). It was found that the variability (CV%) of MAGL activity between subjects for males was 23% and for females was 28 % (see figure 4.3).

There was also no significant difference in the level of FAAH activity in erythrocytes between males and females from three different time points (Males 40 ± 3; Females 48 ± 3 pmol/min/mL blood; P=0.086). It was found that the variability (CV %) of FAAH activity between subjects for males was 21% and for females was 20 % (see figure 4.3).

A repeated-measures (within subjects) ANOVA with Dunnett's multiple comparison test showed that the mean levels of both FAAH and MAGL activities were not significantly different between time points (P>0.05).

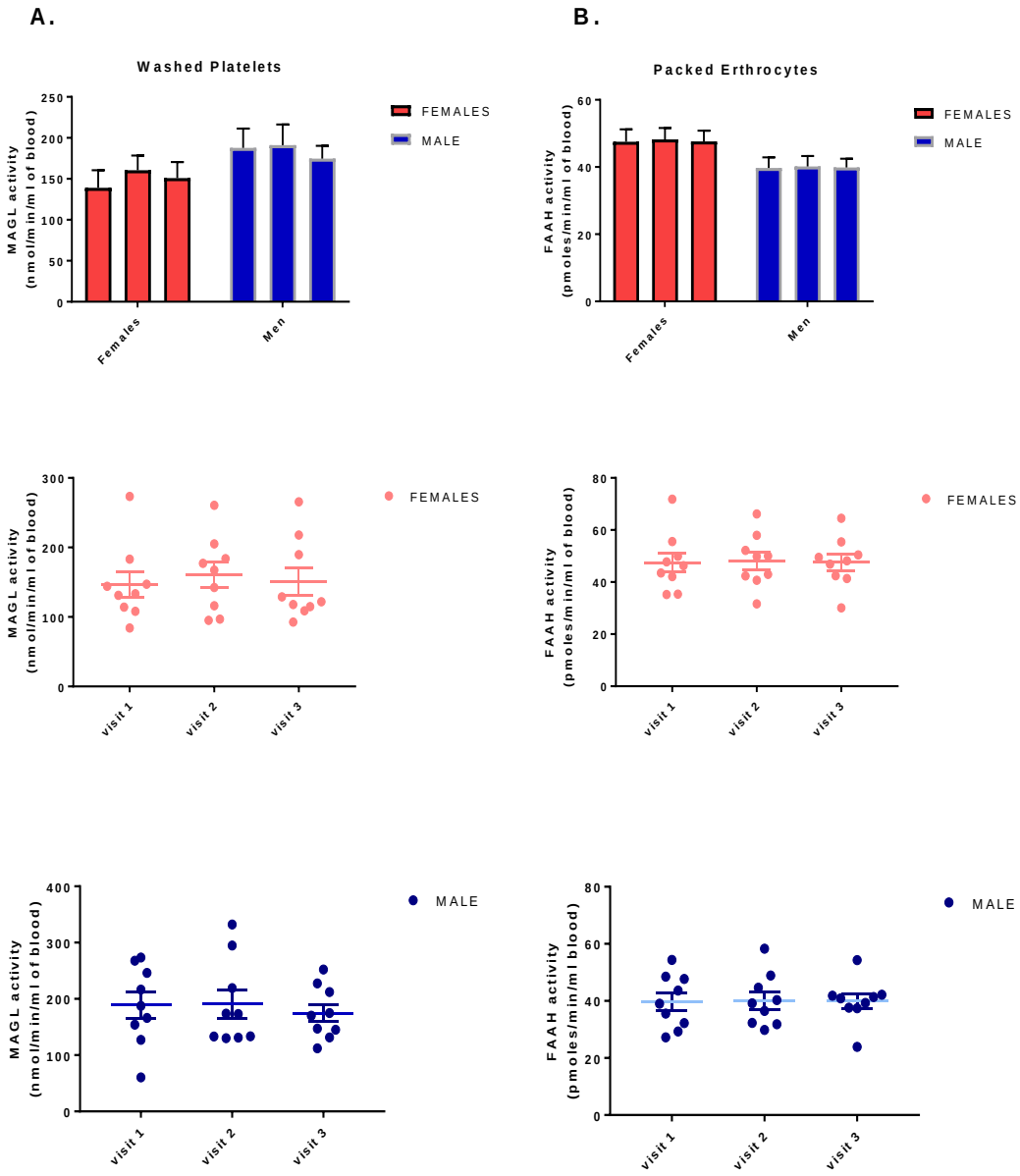

Figure 4.3: Assessing reproducibility of MAGL and FAAH enzyme activities in blood samples using radiometric assays: A) MAGL activity in washed platelet samples, B) FAAH activity in packed erythrocyte samples. Data were collected from nine females and nine males during three visits, and analysed using coefficient of variation (CV%) and Two-way Anova with Tukey's multiple comparison test and different time points as factors. Afterward, an unpaired two tailed t-test was conducted to report the variation between groups (male v. females), there was no significant difference detected in the level of enzyme activities between males and females ($P > 0.05$)

4.4.3.2 Distribution of MAGL and FAAH activities in human blood

MAGL activity was markedly higher in platelets (160 ± 13 nmol/min/mL blood) than erythrocytes (17.2 ± 1 nmol/min/mL), and much lower in plasma or serum, where it was variable or undetectable. Summing the activities from platelets, erythrocytes and plasma aggregated ~95 % of whole blood MAGL activity (188 ± 9 nmol/min/mL).

FAAH activity was highest in isolated erythrocytes (39 ± 3 pmol/min/mL), with much lower levels in platelets (1.0 ± 0.1 pmol/min/mL) and plasma (undetectable). Interestingly, FAAH activity was low, but detectable in serum (0.5 ± 0.1 pmol/min/mL). Summing the activities from platelets, erythrocytes and serum aggregated ~610 % of the FAAH activity observed in whole blood (6.6 ± 0.6 pmol/min/mL) (see figure 4.4).

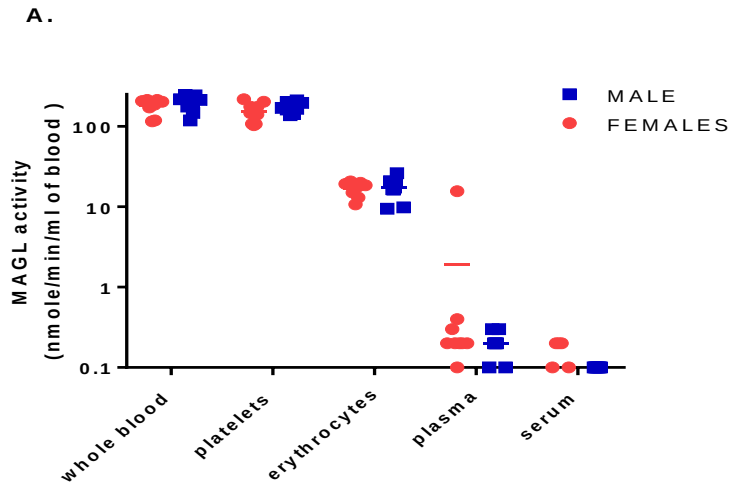

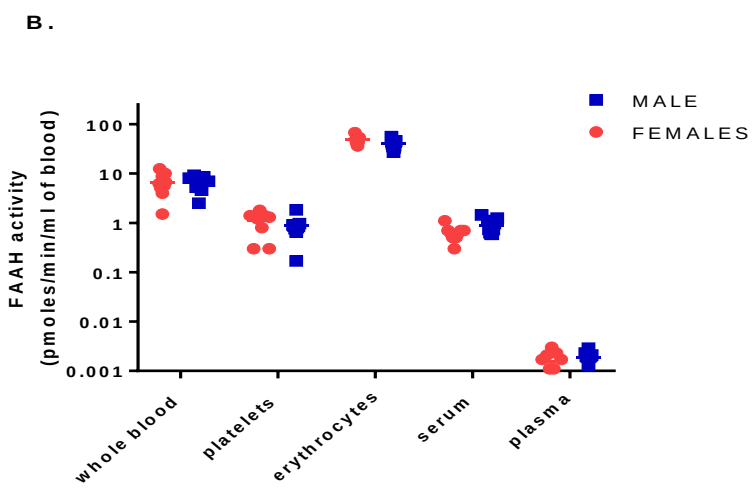

cell type	MAGL activity (nmoles/min/mL of blood)	Percentage (%)
whole blood	187.8 ± 9.4	100
platelets	160 ± 12.7	87
Erythrocytes	17.2 ±1.0	9.2
plasma	1.1 ± 0.9	0.57
serum	0.1 ± 0.0	0.040

cell type	FAAH activity (pmoles/min/mL of blood)	Percentage (%)
whole blood	6.6 ± 0.6	100
erythrocytes	39.2 ± 3.4	595
platelets	1.0 ±0.1	15
serum	0.5 ± 0.1	7.3
plasma	0.00 ± 0.0	0.03

Figure 4.4 : MAGL & FAAH activities in different blood fractions. Each point is the mean enzyme activity from the three visits for each subject. % Percentage= overall mean of each blood cells/overall mean of whole blood*100.

In addition, correlation analysis of FAAH and MAGL activities in whole blood fractions, with platelets, erythrocytes and plasma was conducted. A positive correlation was observed between the FAAH activity of whole blood and the packed erythrocytes and washed platelets (****$P \leq 0.0001$). In contrast, there was no correlation observed between the activity of MAGL measured in each blood fraction (see figure 4.5).

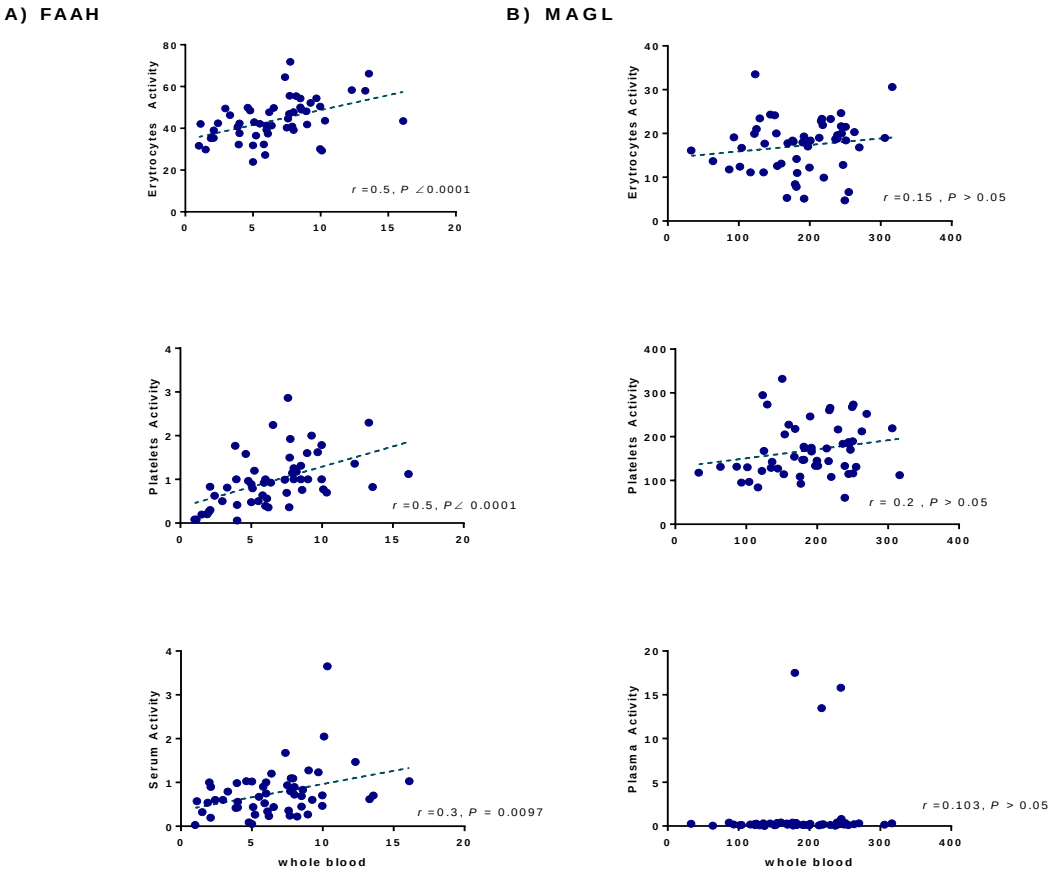

Figure 4.5: Correlation analysis of the activities of FAAH and MAGL in the whole blood fraction with packed erythrocytes, washed platelets, serum, and plasma, as determined by the radiometric assay. Each data point reflects the enzyme activity recorded per visit per subject, and the results were analysed using linear regression test

4.4.3.3 Effects of selective inhibitors on MAGL and FAAH activities

Serial dilution of the inhibitors JJKK-048 and JZL184, from 1 µM to 1 pM, was used to evaluate the contribution of MAGL to 2OG hydrolysis in different blood fractions. In the presence of a maximally-active concentration of JJKK-048 (100 nM) or JZL184 (1 µM), [^{3}H]-2OG hydrolysis level was nearly completely inhibited (4±2% and 7.4±3% control, respectively). JJKK-048 was more potent, with a pIC_{50} value of 10.4 compared to JZL184, with a pIC_{50} value of 8.2 using washed platelets (see Figure 4.6A) However, although 1 µM MAFP was able to inhibit 2OG hydrolysis completely in erythrocytes, the selective MAGL inhibitor JJKK-048 was only able to partly inhibit ^{3}H-2OG hydrolysis (29 ± 3% control, pIC_{50} 9.6 ± 0.12). Both 1 µM MAFP and 100 nM JJKK-048, produced an incomplete inhibition of plasma hydrolysis (32± 5% control) and (22 ± 5%control), respectively (see figure 4.6C). Thus, it appears that other serine hydrolases and non-serine hydrolases in addition to MAGL may contribute to 2-OG hydrolysis in plasma. For instance, by using a single concentration (1µM) of WWL70, a selective inhibitor of ABDH6, we identified that ABDH6 activity was expressed in plasma (1±0.5 nmole/min/mL), with a large variation between individuals.

Selective inhibitors were used to establish the role of FAAH in AEA hydrolysis in erythrocytes. MAFP, PF-3845, JNJ1661010, and URB597 (previously described as selective FAAH inhibitors) caused complete, potent inhibition (pIC_{50} values of 9.2 ± 0.2, 11.7 ± 0.2, 9.1 ± 0.5, and 8.5 ± 0.1 respectively). What was interesting in the inhibition graphs of JNJ1661010 and PF-3845 was the apparent discrimination of two affinity sites. By using these inhibitors, samples collected from six different donors showed a preference of

for two sites fit (6/6), with a perfect fit ($R^2 \approx 1$) (see table 4.3). JNJ1661010 showed better discrimination of the two sites with a difference of three orders of magnitude (see figure 4.7). JNJ1661010 inhibited 26% of total activity with a high potency (calculated pIC_{50} value of 13), whereas the remainder AEA hydrolysis was inhibited with a low potency (pIC_{50} of 7.8). For PF-3845, a higher fraction of the high potency hydrolysis was apparent (41% with a pIC_{50} value of 13.6), and a second low potency component with a pIC_{50} value of 10.6. In comparison, by using URB597 and MAFP, fewer samples fitted with a two sites preference (2/6 and 4/6, respectively), with many preferring one site (see table 4.3). Thus, MAFP and URB597 were not able to distinguish between two sites, possibly because these inhibitors were used over a limited concentration range (from 10^{-6} 10^{-12} M), while JNJ1661010 and PF-3845 were used from 10^{-6} to 10^{-14} M (see figure 4.7)

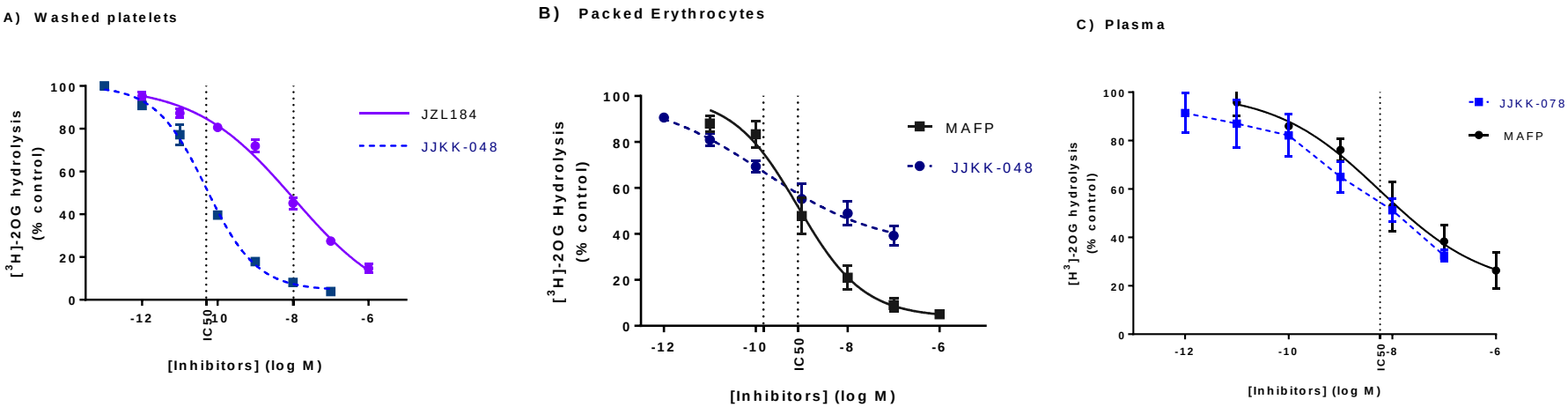

Figure 4.6: Effects of JJKK-048, JZL184 and MAFP concentration responses on MAGL activity on; A) washed platelets, B) packed erythrocytes and C) plasma. Data collected from six healthy individuals performed in duplicate. Data were normalized to values in the absence of inhibitors and expressed as a % control of ^{3}H-2-OG hydrolysis.

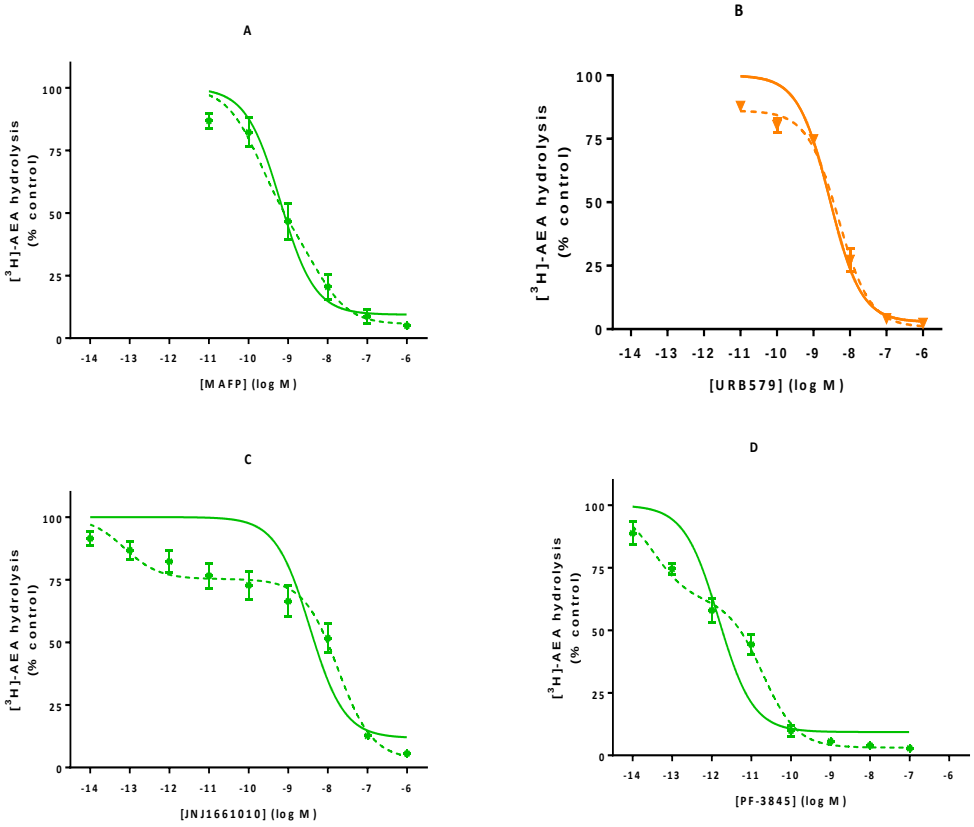

Figure 4.7: Effects of MAFP (A), URB597 (B), JNJ1661010 (C) and PF-3845 (D) concentration responses on FAAH activity on Packed Erythrocyte fractions. Data were collected from six healthy individuals performed in duplicate expressed as a % control of ^{3}H-AEA hydrolysis. Using Prism, curves were compared for fitting to one site or two site models. The solid line represents one site fit model, whereas the dotted line represents two sites fit.

Table 4.3: Inhibition of erythrocyte ^{3}H-AEA hydrolysis (n=6) using four different inhibitors, as shown in figure 4.7 (identifying One site fit and Two site fit):

Inhibitor (n)	One site fit			Two site fit					Two site preferred?
	R_{max} (% control)	pIC_{50} value	R^2	R_{max} (% control)	High potency fraction (%)	pIC_{50} value (High)	pIC_{50} value (Low)	R^2	
PF-3845	8 ± 1	11.7 ± 0.2	0.842 ± 0.035	3 ± 1	41 ± 8	13.6 ± 0.3	10.6 ± 0.1	0.986 ± 0.002	6/6
JNJ1661010	16 ± 5	9.1 ± 0.5	0.687 ± 0.097	3 ± 2	26 ± 5	13.0 ± 0.3	7.8 ± 0.1	0.979 ± 0.006	6/6
URB597	2 ± 1	8.5 ± 0.1	0.932 ± 0.018	0 ± 0	16 ± 3	11.2 ± 0.3	8.3 ± 0.1	0.990 ± 0.003	2/6
MAFP	9 ± 2	9.2 ± 0.2	0.944 ± 0.020	5 ± 2	51 ± 4	10.4 ± 0.5	8.2 ± 0.3	0.986 ± 0.006	4/6

R_{max}: the amount of activity remaining and R^2: fit of a data, and number 6 (under the column two site preferred) referees to six different donors.

4.4.3.4 The effect of storage temperature on the stability of MAGL and FAAH enzymes

The stability during short-term storage was assessed for MAGL and FAAH activities in washed platelet, packed erythrocyte and plasma samples after three and six days of storage at -80 °C or liquid nitrogen compared to activities measured on the day of harvesting (day zero samples). Enzymes activities were significantly affected by storage at -80 °C over six days. MAGL activity levels significantly decreased in washed platelet samples by 58% from 176 to 74 nmol/min/mL of blood after three days storage at -80 °C and further reduced thereafter by 73% over the next 3 days (****$P \leq 0.0001$). In contrast, MAGL activity seemed to be more stable in packed erythrocytes samples during storage, where its activity reduced by 34% after 3 days of storage (***$P \leq 0.001$), and the further reduction of activity to 72% was observed over the next 3 days (****$P \leq 0.0001$). Interestingly, MAGL activity level in plasma was stable during storage at -80 °C up to six days ($P > 0.05$) (see figure 4.8. A).

Similar to MAGL, FAAH activity in washed platelets with 3 days storage at -80 °C was significantly decreased by 58%, and by 71% after 6 days. In contrast, in packed erythrocytes, FAAH activity was observed to be reduced by only 22%, although this reduction was not statistically significant. Further storage at -80 °C, however, did evoke a significant reduction in erythrocyte FAAH activity (****$P \leq 0.0001$) (see figure 4.8.B).

By contrast, MAGL and FAAH activities in washed platelets and packed erythrocytes ($P > 0.05$) were much better maintained during storage in liquid nitrogen for up to 6 days (see figure 4.9).

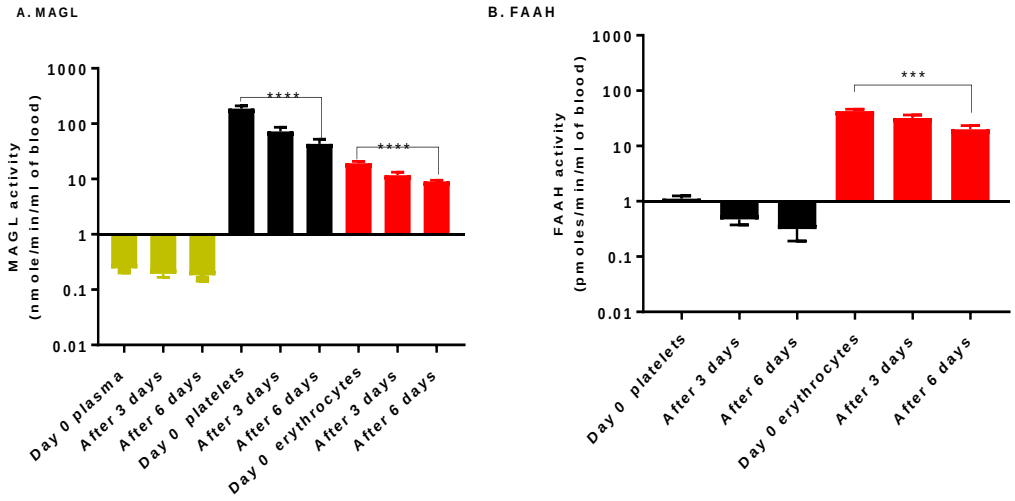

Figure 4.8: stability of FAAH and MAGL activities in plasma, platelets, and erythrocytes stored at 80 °C for up to 6 days. The activity level was measured at Day 0 or after storage for 3 and 6 days at –80°C. This experiment was conducted on samples collected from eight individuals; four females and four males, and analysed using ordinary one—way ANOVA with Dunnett's multiple comparison test.

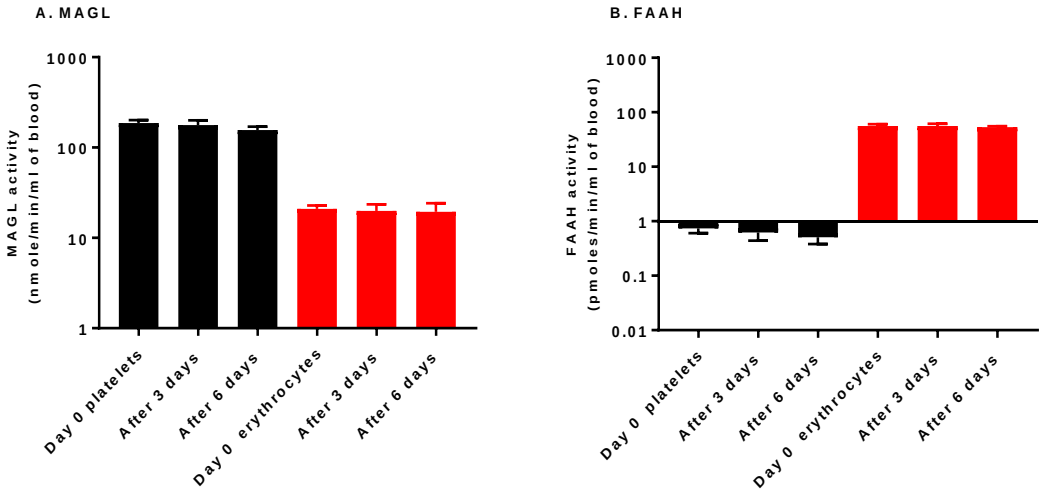

Figure 4.9: stability of FAAH and MAGL activities in platelets, and erythrocytes stored in liquid nitrogen for up to 6 days. The activity level was measured fresh or after storage for 3 and 6 days. This experiment was conducted on samples collected from eight males, and analysed using ordinary one—way Anova with Dunnett's multiple comparison test.

4.4.3.5 Competitive ABPP for detection of endocannabinoid hydrolysing enzyme in blood fractions

After the identification of MAGL and FAAH enzyme activities using the radiometric assays, an alternative method to measure these activities with higher sensitivity was available in the form of activity-based protein profiling, ABPP. Therefore, in this study, the ABPP method was used to validate the activity of serine hydrolase enzymes in platelets and erythrocytes. ABPP analysis revealed that MAGL migrated as two distinct active protein bands at ~ 33 and 28 kDa in platelet samples. The two variants were completely inhibited by MAFP (1 µM) and the MAGL selective inhibitors, JJKK048 (100 nM) and JZL148 (1 µM). FAAH activity was not detected by this technique, while other serine hydrolase enzymes were identified. Based on the molecular sizes of the active bands and the profile of serine hydrolases detected by the ABPP technique in the literature, some potential candidates for the expression of particular serine hydrolases in the blood. Among these, alpha/beta hydrolase domain containing protein 16A (ABHD16A, https://www.uniprot.org/uniprot/Q8IZ83) migrated at 63 kDa and was inhibited in the presence of MAFP or 2-OG (100 µM). Cytosolic phospholipase A2 (cPLA2, https://www.uniprot.org/uniprot/P47712) migrated at 85 kDa, acetylcholinesterase (AChE, https://www.uniprot.org/uniprot/P22303) migrated at 74 kDa, and acyl-protein thioesterase 1/ lysophospholipase I (APT1, https://www.uniprot.org/uniprot/O75608) migrated at 24 kDa, which were all inhibited by MAFP (see figure 4.10 , 4.11 and table 4.4).

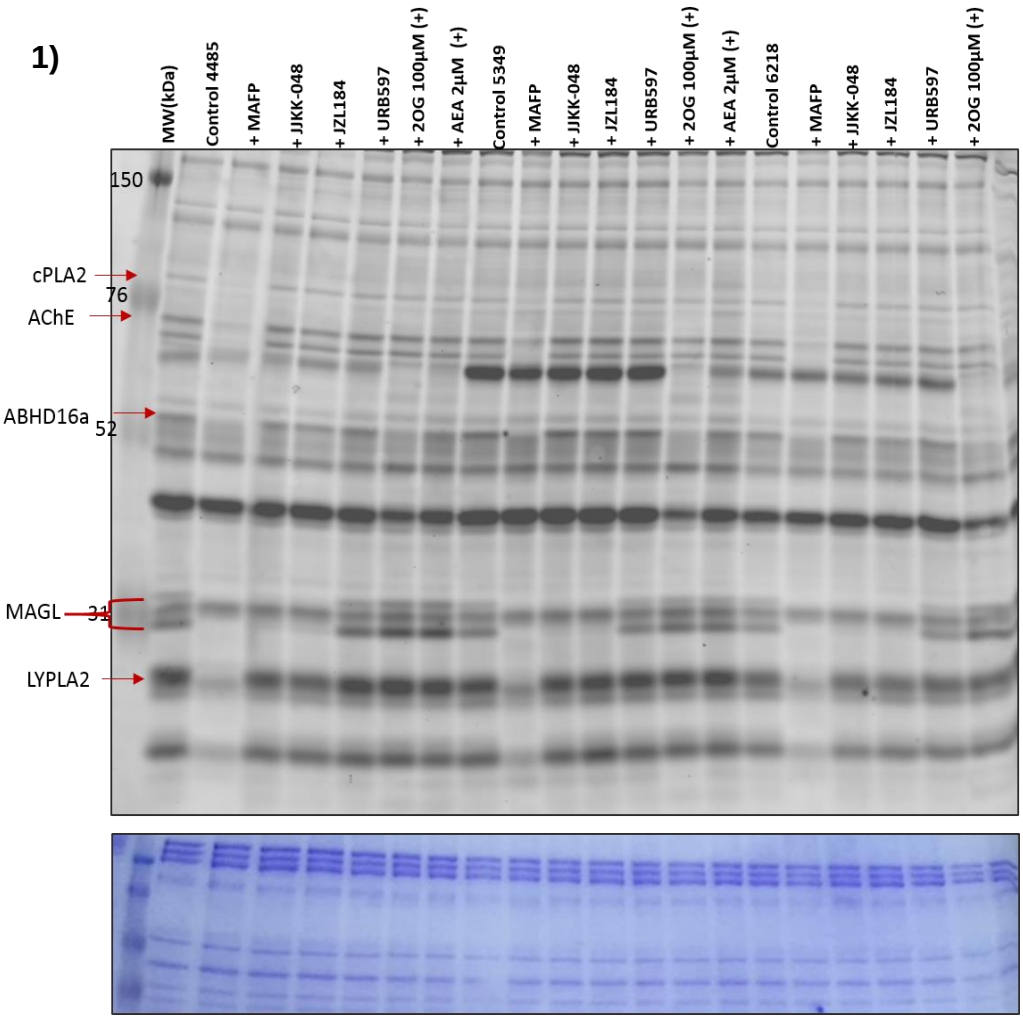
1)
MW(kDa)
Control 4485
+ MAFP
+ JJKK-048
+ JZL184
+ URB597
+ 2OG 100µM (+)
+ AEA 2µM (+)
Control 5349
+ MAFP
+ JJKK-048
+ JZL184
+ URB597
+ 2OG 100µM (+)
+ AEA 2µM (+)
Control 6218
+ MAFP
+ JJKK-048
+ JZL184
+ URB597
+ 2OG 100µM (+)
150
cPLA2
76
AChE
ABHD16a
52
MAGL
31
LYPLA2

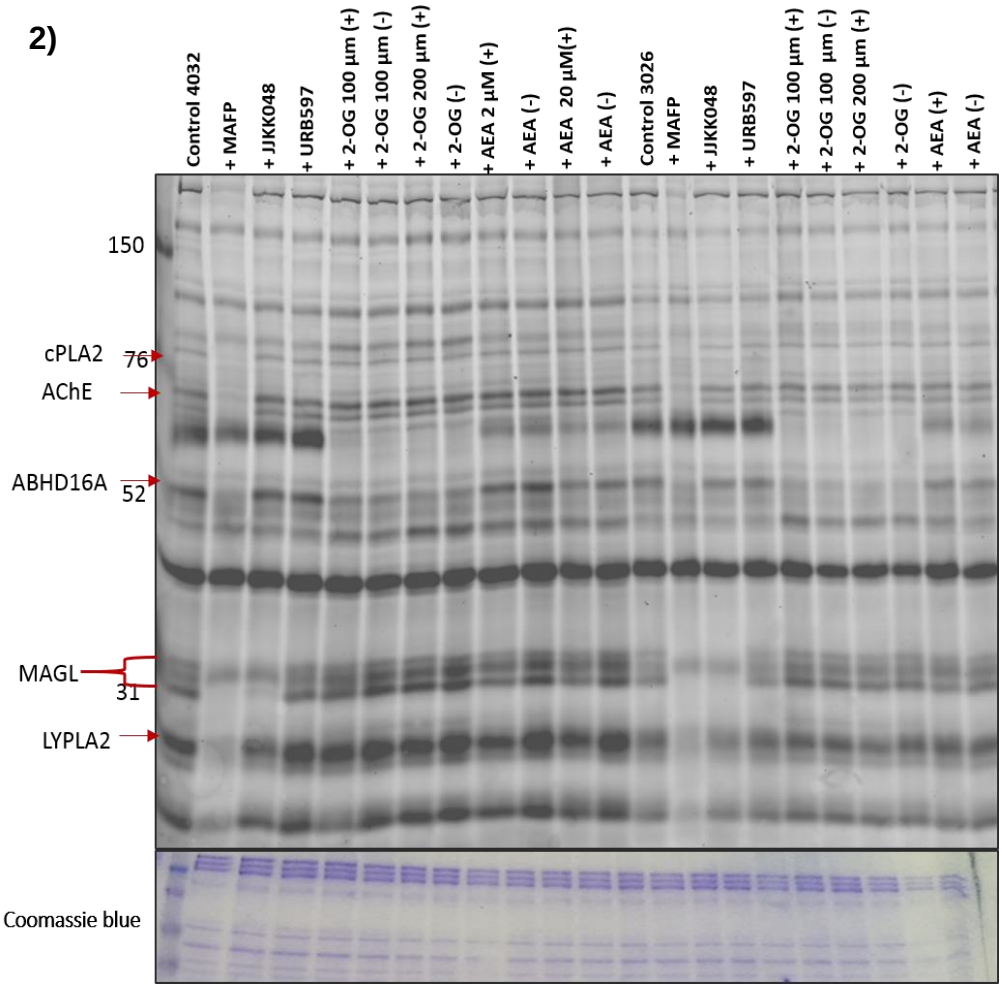
2)
Control 4032
+ MAFP
+ JJKK048
+ URB597
+ 2-OG 100 µm (+)
+ 2-OG 100 µm (-)
+ 2-OG 200 µm (+)
+ 2-OG (-)
+ AEA 2 µM (+)
+ AEA (-)
+ AEA 20 µM(+)
+ AEA (-)
Control 3026
+ MAFP
+ JJKK048
+ URB597
+ 2-OG 100 µm (+)
+ 2-OG 100 µm (-)
+ 2-OG 200 µm (+)
+ 2-OG (-)
+ AEA (+)
+ AEA (-)
150
cPLA2
76
AChE
ABHD16A
52
MAGL
31
LYPLA2
Coomassie blue

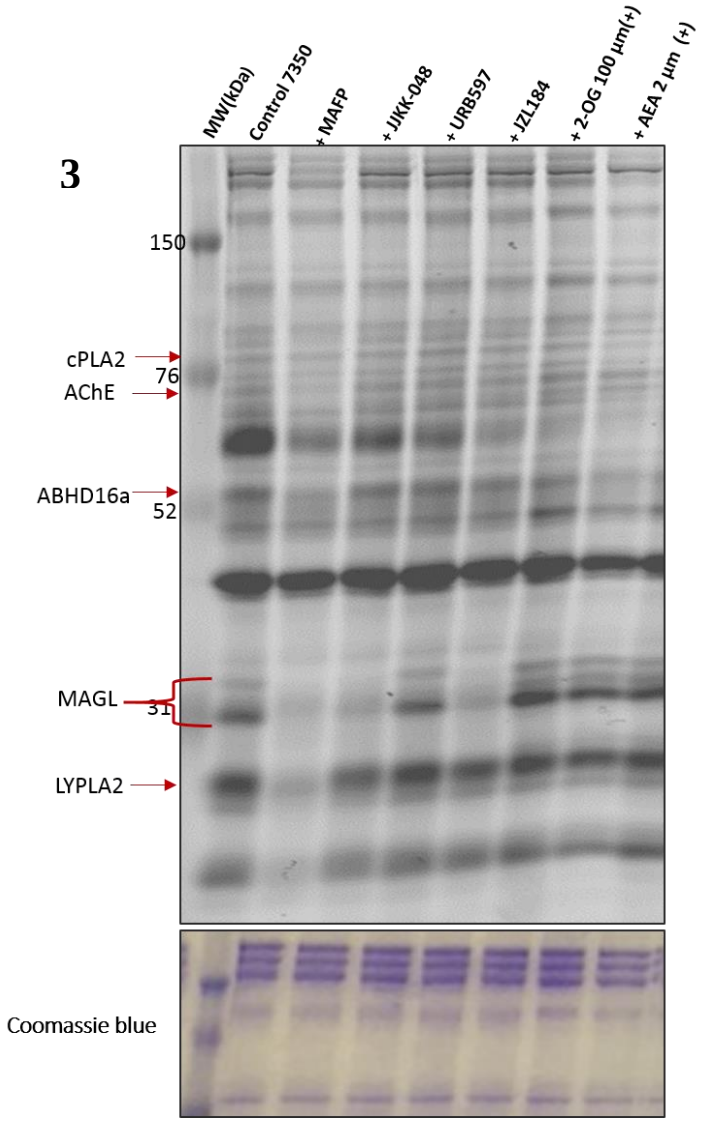

Figure 4.10: ABPP analysis of serine hydrolases in human platelet samples (1,2,3). Platelets (12 µg) were pre-treated for 15 min with DMSO or the indicated concentrations of the serine hydrolase inhibitors, after which TAMRA-FP labelling was conducted for 30 min. The reaction was stopped, 25 µL was loaded per lane and the proteins were separated on 10 % SDS-electrophoresis gels. TAMRA-FP labelling was visualized after in-gel fluorescence imaging as reported in the Methods section. Molecular weight markers are indicated on the left. Reference inhibitors MAFP, JJKK048, JZL184 and URB597 were utilised at the specified concentrations to detect the following serine hydrolases from the gel: FAAH inhibited by MAFP and URB597; MAGL inhibited by MAFP, JJKK048 and JZL184; other serine hydrolases inhibited by MAFP. Note the absence of other visible targets for MAFP at the 1 µM concentration. This experiment was conducted on samples collected from six healthy subjects (three male and three females) with similar outcomes. Multiple fluorescent enzyme protein bands were observed; these indicated labelled serine hydrolases in human platelet samples.

4.11

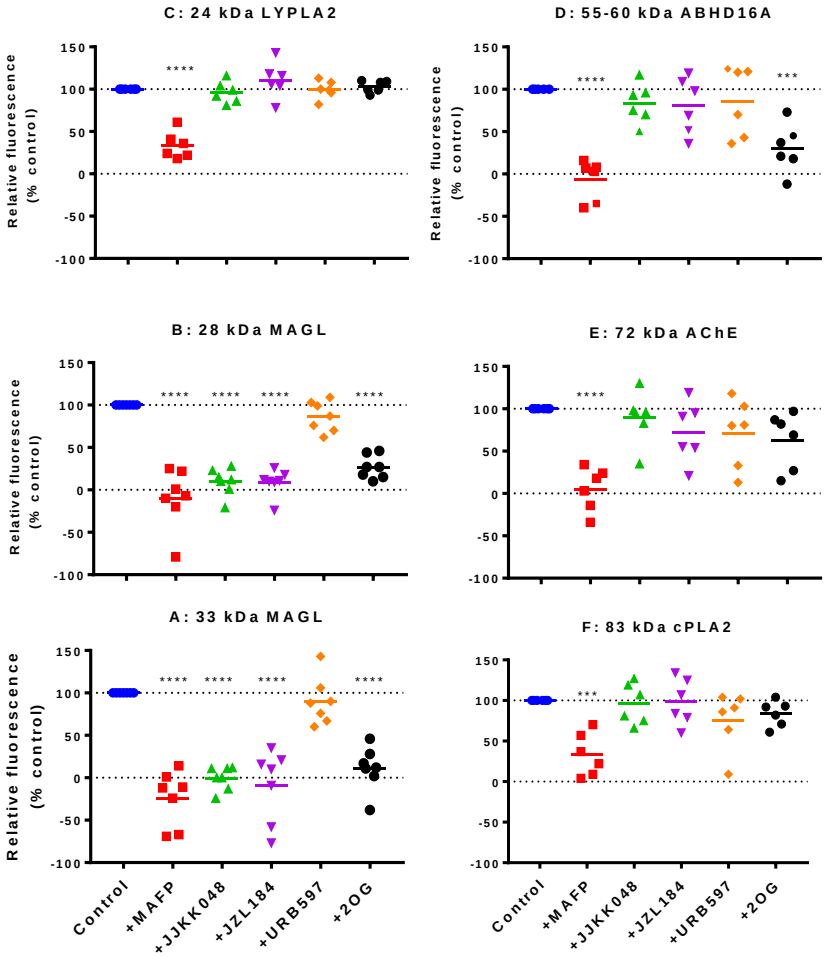
C: 24 kDa LYPLA2
D: 55-60 kDa ABHD16A
B: 28 kDa MAGL
E: 72 kDa AChE
A: 33 kDa MAGL
F: 83 kDa cPLA2
Relative fluorescence (% control)
150
100
50
0
-50
-100
****
***
Control
+MAFP
+JJKK048
+JZL184
+URB597
+2OG

4.4

Enzymes From Blankman et al., 2007	Abbreviation	MW (kDa)	Evidence for platelet expression	Inhibition profile	CV
Acetylcholinesterase	AChE	71.1, 72	Membrane (Smith et al., 1980)	inhibited by MAFP	42%
Cytosolic phospholipase A2	cPLA2G4A	83.1	Cytosol and nucleus (Börsch-Haubold et al., 1995)	MAFP	41%
Potential enzymatic regulator of immunity	ABHD16a	55-60	Plasma membrane (Lord et al., 2013)	MAFP 2OG	55 %
Monoacylglycerol lipase	MAGL	32.1	Membrane (Gkini et al., 2009)	MAFP JJKK048 JZL184 2OG	22 %
Monoacylglycerol lipase	MAGL	28			39%
Acyl-protein thioesterase 1	APT1	~ 24	Platelets (Bolen et al., 2011)	MAFP	22%

Figure 4.11 and Table 4.4: Expression of serine hydrolase enzymes in human platelets. The ABPP experiment was conducted using six platelet samples from healthy volunteers (three men and three women). Selective inhibitors were used to quantify the activities of FAAH and MAGL, and then analyzed using ImageStudio software. Following measurement of absolute band intensity, it was normalized to loading protein levels (identified by Coomassie blue staining). Enzyme activity in the control was set to 100 %, then statistical analysis was performed by one-way ANOVA with Dunnett's multiple comparison test. Six serine hydrolase enzymes were identified, as summarized in the above table. There was notable variation between the six individuals as identified by the coefficient of variation in the value of enzyme activities in platelet samples between the six tested individuals (Table 4.10.B).

However, FAAH activity was not detected in erythrocytes after haemoglobin isolation. The probable reason for this could be that during the process of eliminating haemoglobin, other enzyme proteins might have been removed (see figure 4.12).

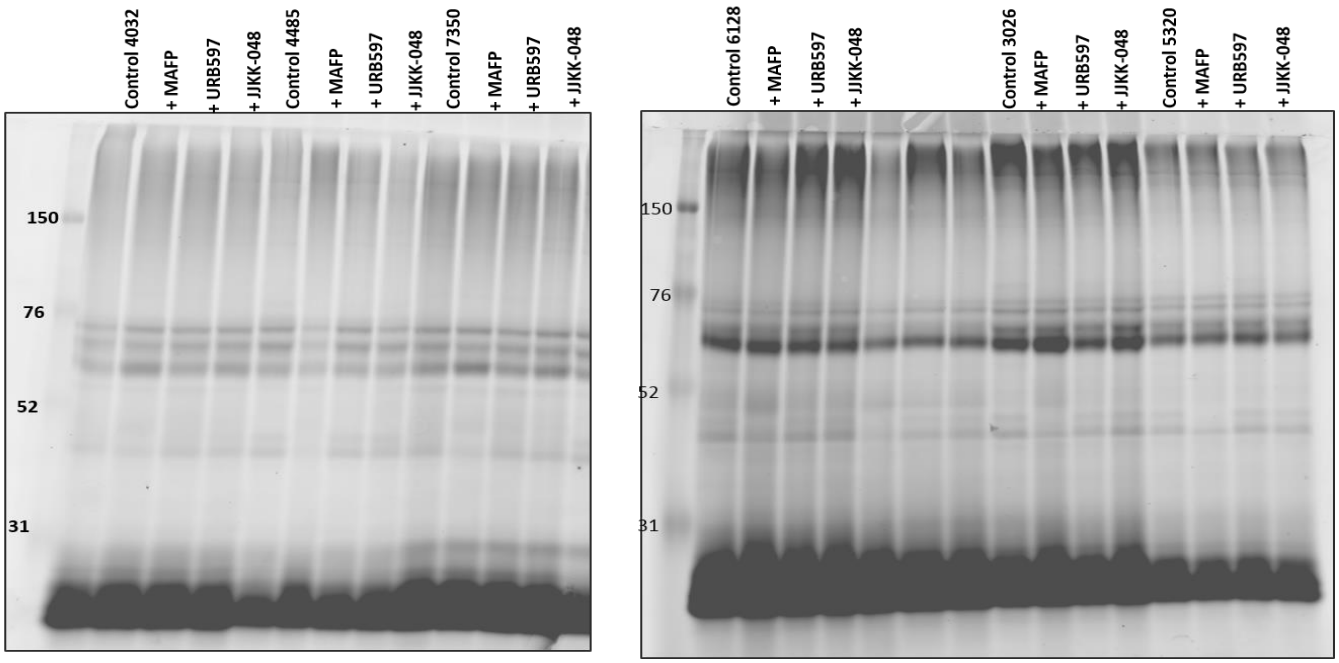

Figure 4.12: ABPP analysis of serine hydrolases in human erythrocyte membrane samples. Erythrocyte membrane fractions were isolated as outlined by Kottahachchi et al. (2015), by osmotic lysis of the washed erythrocytes utilising a lysis buffer (5 mM phosphate buffer, pH 8, 1 mM EDTA) prior to high speed centrifugation, 24000 g for 10 min. This process was performed on three occasions and haemoglobin was discarded with the supernatant on each occasion. Molecular weight markers are shown on the left. The ABPP experiment was conducted using six samples from healthy volunteers (three men and three women).

4.5 Discussion

The findings reported here provide new evidence that MAGL and FAAH activities are measurable in a reproducible manner in healthy human blood. Both MAGL and FAAH activities were stable within subjects over three visits and not different between subjects. Platelets contained a higher level of MAGL activity, while erythrocytes contained a higher activity level of FAAH compared to other blood fractions. Interestingly, MAGL activity was detectable in plasma but not in serum, while FAAH activity was detectable in serum but not in plasma. Based on these studies, blood cells should be stored in liquid nitrogen to avoid enzyme degradation during storage at -80 °C. Furthermore, ABPP is a useful technique that detects the activity of two MAGL variants and a number of other serine hydrolase enzymes in human platelets.

4.5.1 Reproducibility of FAAH and MAGL in different blood fractions

The activity of MAGL in platelets was reproducible both within subjects over three different time points and between subjects. In the male group, the variability of MAGL activity within and between subjects (CV) was 23%, while in the female group the variable was 28%. Since all blood samples were treated in the same manner including collection, preparation and enzyme assay (which gives reliable and accurately measurement), it was considered that (pre)analytical variation had a negligible effect on these results.

The range of variation observed within female subjects seems to be higher than in male subjects, which may be due to menstrual cycle variation. Scotchie et al (2014) found that MAGL protein expression increased in endometrium obtained from normal women during the secretory phase compared to the

follicular phase, (Scotchie et al., 2015). Since protein expression does not always accurately reflect enzyme activity, further study needs to be conducted to assess whether the activity level of MAGL in blood fractions decreases or increases in normal women during the menstrual cycle. However, there was no significant difference in the level of MAGL activity when comparing activity over three visits between male and female subjects ($P > 0.05$). This suggests that there may be no gender difference of MAGL activity. It also has been previously described that there was no relationship between MAGL activity and BMI in adipose tissue from 28 metabolically healthy subjects (Cable et al., 2011). Taken together, it seems that gender and BMI factors do not influence MAGL activity; however, there is insufficient knowledge of other factors influencing MAGL activity levels.

The variability of MAGL activity in platelets between subjects (23-28%) found in the current study was lower than its variability found in human brain tissue (37%) in a comparable study conducted using the same method in our laboratory (Erdozain et al., 2014).

Another important finding from the current study is that FAAH activity in erythrocytes was reproducible within and between subjects over three separate occasions. Interestingly, the range of FAAH variation between subjects in the current study was around 20% in both the female and male groups, despite the fact that four females had their blood taken on their menstrual period. However, the variability of FAAH activity (CV % of 20) between subjects in both female and male groups in the erythrocyte samples was similar to the variability observed in human brain tissue conducted by (Erdozain et al., 2014). In contrast, the variation in female platelets observed in a previous study by Maccarone 2002

was far greater (47%) than that of this study. There is no standard rate of variation applicable to this study. As this study involved individuals of different ages, weights, exercise habits, it seems reasonable in our estimation to have a rate of variation between 20% - 28%, compared to the previous studies, mentioned above.

However, there are several factors shown in previous studies to affect the level of FAAH activity in human samples. Thus, the 20% variation in erythrocytes FAAH activity levels conducted in the present study may arise from biological sources of variation. For instance, a variations of plasma AEA within and between subjects up to 10 fold were detected, variation which was attributed to food intake effects (Jian et al., 2010).

In the female group, one female (4485) had the highest FAAH activity, with a 3 fold increase, in comparison to the mean level of other females in the group, possibly as a result of suffering from menorrhagia . This finding is too preliminary to extrapolate as the present study was not designed to assess the influence of menorrhagia on FAAH activity in erythrocytes. Nevertheless, it is reported that menorrhagia is usually accompanied by a reduction of iron level, and thus decreases in the number of circulating erythrocytes, and hence it finally leads to anaemia (Cohen et al., 1980; Kim et al., 1993). In healthy subjects, there is a balance between erythropoietic output and erythrocyte turnover. Disruption of this balance leads to anaemia and is caused via three problems affecting erythrocytes: haemolysis, decreased production or haemorrhage (Sankaran et al., 2015). An interesting question raised here, which could be addressed in future, is whether FAAH activity influences the stability of erythrocytes during the

menstrual cycle. For comparison, a study by Lazzarin et al., (2004) detected different FAAH activity levels in peripheral blood lymphocytes during various phases of a menstrual cycle. The highest level was found in the luteal phase (on the 7^{th} day after ovulation) and the lowest level found in the follicular phase (on the 7^{th} day of the menstrual cycle) (Lazzarin et al., 2004). In agreement with this study, the expression of FAAH protein expression was highest in the luteal phase compared to the follicular phase in the endometrium obtained from normal women (Scotchie et al., 2015). This leads to the conclusion that the menstrual cycle is one factor which may influence FAAH activity in women.

Another factor that may influence FAAH activity in erythrocytes is BMI. In male subjects that participated in the current study, it was found that FAAH activity in erythrocytes was decreased 2 fold with increasing BMI. The FAAH activity in a man with a healthy weight (BMI=21) was 43 pmol/min/mL of blood, while the activity decreased to 27 pmol/min/mL of blood in a man with BMI=31, both subjects of similar ages. This observation was less clear in the female group because the BMI range of the female group was relatively limited (BMI 19.8 to 25.9). In support of this study, Sipe el at., (2010) assessed the relationship between the plasma levels of AEA and BMI, and found that the plasma level of AEA was slightly raised in obese subjects (BMI>30) compared to those of normal weight (BMI <26) (Sipe et al., 2010). AEA binds to CB_1 receptor resulting in increased food intake and elevated weight gain by central as well as peripheral actions (Engeli et al., 2005). It is suggested that the increase of AEA is due to the reduction of FAAH function in obese subjects (Sipe et al., 2010). However, a prior study from our labs reported that FAAH activity increased with BMI in adipocytes of healthy people (Cable et al., 2011), which may suggest the

relationship between FAAH activity and BMI is tissue-specific. There is a clear need for further human study to directly assess the relationship of circulation FAAH activity and BMI.

A linear regression test was applied to investigate potential links between recorded factors and individual MAG and FAAH activity levels in the present study, but no significant correlation was detected which may be because the number of volunteers was not sufficient (see figure in Appendix.3).

4.5.2 MAGL and FAAH activities are expressed differentially in human blood fractions

The results of this study indicated that platelets contained a higher proportion of MAGL activity, at nearly 86% of the total MAGL activity in the whole blood. This is consistent with an early study in which Chau and colleagues (1988) found that the activity of MAGL was 100-times higher in human platelets compared to other lipases (Chau et al., 1988), and was found in platelet membranes (Gkini et al., 2009).

JZL184, as a selective MAGL inhibitor, has been reported to partially inhibit platelet aggregation in human blood and PRP (Brantl et al., 2014b), which confirms the involvement of MAGL in platelet aggregation through maintaining the level of 2-AG. Alongside this role, 2-AG in platelets also stimulates endothelial nitric oxide synthase (eNOS) activity, and this contributes to vasodilation effects produced by 2-AG. These studies, together with our observation of the high level of MAGL activity, suggest that 2-AG (and potentially other monoacylglycerols) needs to be tightly controlled by MAGL to maintain normal haemostasis.

Moreover, the activity of MAGL in erythrocytes and plasma represented only 9% and 0.6% respectively of total MAGL activity in the whole blood. On the other hand, MAGL was least active in serum, or in some cases no activity was detected, which may be due to the presence of other enzymes in serum which inhibit the activity of MAGL.

The distribution of FAAH activity is different from MAGL activity, which reflects specific roles for each enzyme and their substrates/metabolites. It was found in the current study that erythrocytes expressed a higher level of FAAH activity than whole blood samples. The low activity level of FAAH detected in whole blood may be due to residual substrates retained in the unprocessed whole blood samples. Alternatively, the complex mix of proteins may result in sequestration of the radiolabelled substrate, reducing the amount available for hydrolysis. This latter alternative is supported by the work undertaken by Bojesen et al. (2003), who found that a high percentage of human plasma AEA is bound to albumin. Owing to the hydrophobic nature of AEA, it needs to be bound to specific transporter proteins such as albumin to permit both its distribution in plasma as well as intracellular trafficking (Bojesen et al., 2003; Oddi et al., 2009). Given that the concentration of albumin is as high as $7.5x10^{-4}$ M in plasma, formation of AEA:albumin complex influences AEA availability to the intended target (Leboffe et al., 2017). As a consequence, once AEA is bound to albumin, the AEA becomes less available to be metabolised by FAAH. Since the formation of products depends on the availability of substrate, this leads to a decreased amount of reaction products which subsequently underestimates the enzyme activity.

The high activity level of FAAH suggests its importance in maintaining the lifespan of RBC by regulating the level of AEA, as it is reported that AEA has an effect on erythrocyte survival. AEA stimulates the generation of PGE_2, and PGE_2 in turn increases Ca^{2+}/K^+ channel activity leading to water loss and cell shrinkage, accompanied by engulfment of RBC by macrophages, and subsequent elimination from blood circulation (Bentzen et al., 2007).

Platelets have a lower level of FAAH activity compared to erythrocytes. The low activity level of FAAH in platelets identified in this study can possibly be supported by an earlier study in which human platelets were able to inhibit FAAH activity by generating 12-(S)-hydroxy-arachidonylethanolamide (HAEA). Platelets oxygenate AEA by the lipoxygenase pathway, thus producing the oxygenated derivative 12-HAEA. The 12-HAEA compound in turn was able to inhibit FAAH activity (Edgemond et al., 1998), thus prolonging the lifespan of AEA in the bloodstream, which is an important factor that has the ability to prolong platelet lifespan. AEA promotes platelet survival through the CB_1 receptor, an interaction which regulates Akt-induced phosphorylation of pro-apopotic protein (Bad), and thus inhibits its interaction with Bcl-Xl and hence its pro-apoptotic activity. In addition, inhibition of FAAH by URB597 enhanced platelet viability (Catani et al., 2010). Therefore, it is suggested that in healthy conditions, the level of FAAH in platelets is somewhat low to maintain platelet viability.

Interestingly, FAAH activity was detected in serum but not in plasma. This finding supports published data that shows FAAH activity was not detectable in plasma (Jian et al., 2010). It is hypothesised that FAAH activity would be released during the platelet clot process into serum, an hypothesis to be tested in

the next **Chapter**. The release of FAAH activity into serum may induce further vasoconstriction by decreasing the level of AEA. This corroborates the fact that it was reported AEA promotes vasorelaxation in human mesenteric arteries mediated by the CB_1 receptor (Stanley et al., 2016).

Analysing the different distribution of FAAH activity in blood fractions, there appears to be a tendency towards positive correlation between FAAH activity in whole blood and other blood fractions such as platelets, erythrocytes, and serum. By contrast, there was no relationship between the activity of MAGL in whole blood and other blood fractions. The results suggest that the mechanism that regulates FAAH activity in humans is similar for all volunteers, whereas the mechanism that regulates MAGL in humans is different in each volunteer. Also, this indicates that MAGL is more mobile between different fractions than FAAH. As a result, it can be inferred that there is no need to isolate blood cells to compare the level of FAAH activity between subjects, if it were to be used as a biomarker of dysfunction.

4.5.3 Pharmacological tool to define the contribution of MAGL and FAAH in AEA and 2-OG hydrolysis, respectively.

Following measurement of 2OG and AEA hydrolysis in blood fractions using the classical methodologies employing radiolabelled substrates, it was essential to identify if MAGL and FAAH, respectively, were the primary enzymes responsible for the hydrolysis of these entities. This is important as the enzymes responsible for eCB hydrolysis are attractive pharmacological targets. Therefore, selective inhibitors of MGAL and FAAH were used.

It was revealed in the current study that MAGL was the predominant 2-OG hydrolyzing enzyme in platelets, where MAGL was inhibited by JJKK-048 or JZL184 with pIC_{50} values of 10.4 and 8.2. JJKK048 is reported to inhibit MAGL in intact human cells and rat cerebellar membranes with a pIC_{50} value of 9.67 (Aaltonen et al., 2013), and JZL184 inhibited MAGL in human PRP with a pIC_{50} value of 8 (Brantl et al., 2014b). This is the first study to demonstrate the potency of JJKK048 in human blood samples, showing higher potency than JZL184, such that with a concentration as low as 100 nM, nearly complete MAGL inhibition was achieved (96%). In comparison, JZL184 inhibited 92% of MAGL activity in platelets at a concentration of 1 µM.

In contrast to platelets, there appeared to be other serine hydrolase enzymes in addition to MAGL responsible for 2OG hydrolysis in erythrocytes and plasma. MAGL was responsible for 71% of total 2-OG hydrolysis in erythrocytes, while it was responsible for 78% of total 2-OG hydrolysis in plasma. Other serine hydrolases in plasma, such as ABHD6, were identified to be involved in 2-OG hydrolase, in the current study, by using the selective inhibitor WWL70. However, because there was a large variation of its level between subjects in the current study, it was difficult to determine the percentage of its involvement in 2-OG hydrolysis. It appears that the proportional contribution of different enzymes to 2-OG degradation is highly dependent upon the cell.

FAAH is the main enzyme responsible for AEA hydrolysis in erythrocytes, where high concentration (1µM) of URB597, JNJ1661010 and PF3845 completely abolished AEA metabolism. FAAH activity was inhibited by URB597 or JNJ1661010 with pIC_{50} values of 8.5 and 9, respectively, and these

figures are similar to the potency described in literature. URB597 inhibited FAAH in human liver microsomes with a pIC_{50} value of 8.5 (Piomelli et al., 2006), and JNJ1661010 inhibited human recombinant FAAH activity with a pIC_{50} value of 8 (Karbarz et al., 2009). However, it was found in the present study that PF3845 inhibited FAAH in human erythrocytes with a pIC_{50} value of 11.7, while Ahn et al. (2009) showed that PF3845 inhibited recombinant FAAH with a pIC_{50} value of 7 (Ahn et al., 2009). Whether this large discrepancy results from methodological differences seems unlikely, and so further investigations are needed to resolve the difference.

A possible explanation for the differences in inhibitor potencies is that different assays were used. In the current study, the radiometric assay was used to assess the potency of inhibitor, whereas Ahn et al. (2009) used an enzyme-coupled kinetic assay after the addition of PF-3845.

In our experiments, JNJ1661010 and PF-3845 (over concentrations ranging from 1 μM to 0.1 pM) both identified two sites for AEA hydrolysis. JNJ1661010 was better at discriminating between these two-sites than PF3845. By using JNJ1661010, 26% of total activity was due to the high potency component (pIC_{50} value of 12.95), whereas 74% of total activity was in the second low potency phase (pIC_{50} value of 7.78). These data suggest two possibilities: either two binding sites of FAAH enzyme exist or there are two FAAH isoforms present (for example, FAAH1 and FAAH2). In order to test this hypothesis in future studies, the radiometric assay should be run, as it was done in this study, using recombinant FAAH1 and 2 activities as a source of enzymes. Pre-incubation of recombinant FAAH with serial concentrations of JNJ1661010 will identify

whether FAAH 1 has two binding sites or there are actually two isoforms present in the platelet preparations.

4.5.4 Stability of MGAL and FAAH activity during storage conditions

Several studies report that the level of eCB is influenced by storage conditions (Schreiber et al., 2007; Lanz et al., 2018). It is also suggested that the biological instability of AEA and 2-AG during storage at -80 ^{o}C partially owes to the presence of catalytic activity of enzymes in blood cells (Lanz et al., 2018). However, to-date there is no literature investigating the stability of MAGL and FAAH enzymes during storage at -80 ^{o}C or in liquid nitrogen. Therefore, it is important to define reliable storage parameters that avoid the degradation of enzyme activities and hence allow consistent and reliable quantification of circulating MAGL and FAAH in human blood.

In this study, it was discovered that MAGL activity in plasma was stable after being stored at -80 °C up to 6 days. However, this may not be the case for longer storage periods. A recent study reported that 2-AG levels in plasma increased by 50% after 2 weeks of storage at -80 ^{o}C (Lanz et al., 2018). The activity of MAGL and FAAH in platelet samples was significantly decreased by more than 70% during storage at -80 °C up to 6 days. An earlier study reported that storage lesions can occur where platelets release their contents, such as ADP, leading to activation of the AA pathway and formation of thromboxane, resulting in platelet aggregation (Mustard et al., 1989). Collectively, these results suggest that low temperature (-80 °C) may be a triggering factor for platelet activation and modification of their function, and thus lead to inhibition of MAGL and FAAH activities.

In addition, ≤50% of MAGL and FAAH activities in erythrocytes were lost after 6 days of storage in this study. Erythrocyte storage at -80 °C leads to morphological changes and haemolysis Spieles et al. (1995). This suggest that the disruption of erythrocytes during storage leads to degradation of MAGL and FAAH activities.

In a follow up study, we focused on improving the storage conditions via lowering the temperature, and samples were stored in liquid nitrogen (-196 °C). Despite the instability of enzyme activity at -80 °C, MAGL and FAAH activities appeared to be stable in platelets and erythrocytes when stored in liquid nitrogen. This may be due to the high survival rates of platelets and erythrocytes samples that are frozen at liquid nitrogen. As an example, a prior study investigated whether erythrocyte haemolysis occurs during storage at -196 °C, and found there was no increase in haemolysis even after 15 years (Spieles et al., 1995). Indeed, it is notable that the storage temperature affects cell viability, as cells stored at -80 °C may allow slow chemical reactions (owing to a few portions of unfrozen water) that ultimately leads to cell death. Therefore, a very low temperature is required to completely stabilize cell function, which can be achieved by storage in liquid nitrogen (Coriell, 1979; Morris, 1995). Therefore, after blood component isolation, platelets and erythrocytes should be rapidly-stored in liquid nitrogen. These parameters are of practical importance as they will facilitate the reliable clinical profile of the circulating MAGL and FAAH activities in health and disease.

4.5.5 Identification of serine hydrolase enzymes in blood cells by ABPP

An alternative, highly selective and sensitive method was employed to quantify the activity of MAGL and FAAH in blood cells. The ABPP technique was used to quantify not only MAGL and FAAH activities, but also other serine hydrolase enzymes. This is the first study to use FP-rhodamine labelling to assess serine hydrolases of human platelet and erythrocyte samples.

FP-rhodamine labelling suggested that MAGL migrated as two distinct bands at ~ 33 and 28 kDa in platelet samples. The two variants were completely inhibited by MAFP and MAGL selective inhibitors, JJKK048 and JZL148, to a level comparable to that seen using the radiometric assay. This is consistent with previous findings that ABPP identified two bands that were attributed to MAGL in mouse (Long et al., 2009b; Aaltonen et al., 2016) and rat brain (Buczynski et al., 2016). Collectively, these data indicate that there are two MAGL protein variants expressed in human platelets, and Gkini et al., (2009) report that the presence of a second enzyme explains at least in part the higher degradation of 2-OG in human platelets (Gkini et al., 2009). However, tissue-specific activity was reported, one isoform of MAGL, migrating at 33 kDa, was detected in mice peripheral tissues such as liver, spleen and heart (Aaltonen et al., 2016). It was also reported that human MAGL shares 92% structure sequence identity with mouse MAGL (Blankman et al., 2007), suggesting a high degree of similarity between mice and humans. Therefore, it is speculated that mice brain tissue can be used to study the function of the second isoform of MAGL which may reflect its function in human platelets. Furthermore, ABPP analysis reveals that there is limited variation of MAGL activity between subjects (22-30%), which is consistent with the results obtained by radiometric assay.

ABPP identified FAAH activity in mouse brain membranes (Long et al., 2009b), and in rat brain membranes (Buczynski et al., 2016). However, in this study FAAH in platelet samples could not be detected. This is likely because the activity level of FAAH, detected in platelet by radiometric assay, was too modest (1 to 5 pmol/min/mL of blood).

Other serine hydrolase enzymes were also identified by ABPP such as alpha/beta hydrolase domain contain protein (16A) (ABHD16A), Cytosolic phospholipase A2 (cPLA2), Acetylcholinesterase (AChE), and Acyl-protein thioesterase 1/ lysophospholipase I (APT1). These enzymes have already been identified in human platelets by previous studies; however, to our knowledge this is the first study to detect their activity in this tissue using ABPP. In 2007, Blankman and her group conducted a comprehensive study to identify serine hydrolase enzyme that expressed in mice brain using the ABPP technique, and determine if the genes of these enzyme are express or found in humans. In the current study several steps were conducted or identify the serine hydrolases detected in human platelet samples. Firstly, identification of the molecular size and band signal was conducted using Image Studio software. Second, after identification of molecular size, the Blankman study was used as a reference source to suggest identification of all serine hydrolases dependent on their molecular size.

Human ABHD16A has a molecular weight of 63 kDa, also known as human lymphocytes antigen B-associated transcript 5 (BAT 5) (Lord et al., 2013; Savinainen et al., 2014; Xu et al., 2018). It was detected in mouse megakaryocytes and human platelets (Senis et al., 2007). In the current study, MAFP inhibited ABHD16A activity in platelets, where similar inhibition was

observed by Hoover et al. (2008) in native brain membrane proteomes and lysates of HEK293 cells overexpressing hBAT5 (Hoover et al., 2008). An *in vitro* study reported that ABHD16A is a genuine MAG lipase and exhibits preferential activity for MAG substrates 1-AG and 1-linoleoylglycerol (1-LG) (Savinainen et al., 2014). In addition, it was found in the current study that 100 µM of 2-OG reduced the FP probe binding to ABHD16A in platelets, confirming that monoacylglycerols (2-AG and OG) are potential substrate candidates for ABHD16A. However, there was a large variation of ABHD16A activity level in platelets between subjects (55%). A previous study showed that ABHD16A is as immunomodulator that stimulates proinflammatory cytokine release from macrophages (Kamat et al., 2015), and the degrading of prostaglandin-glycerol (PG-G) in neutrophils (Turcotte et al., 2017). However, its function in platelets is still unknown, and should be the subject of further study in this tissue.

In human platelets, cPLA2 is an enzyme with molecular size 85 kDa; cPLA2 is reported to be rapidly phosphorylated on stimulation with several platelet agonists such as collagen and thrombin (Kramer et al., 1993; Börsch-Haubold et al., 1995), leading to AA release (Hirabayashi et al., 2000). An *in vivo* study showed that the phosphorylation of cPLA2 initiated the production of TxA_2 and subsequently led to platelet activation (Canobbio et al., 2013). Indeed, subjects with inherited cPLA2 deficiency had a lower level of serum TxA_2 during clotting compared to normal subjects (Adler et al., 2008), resulting in the risk of increased bleeding time (Wong et al., 2002; Leslie, 2015). Furthermore, it was observed in the current study that there is a large variation of the cPLA2 activity level between subjects (41%). Future studies could investigate the

variation in post-translational modifications, such as phosphorylation, of cPLA2 between subjects and the influence on FP-rhodamine labelling.

AChE is another enzyme that was found to be produced in normal human bone marrow megakaryocytes and in cell lines derived thereof, which is involved in megakaryocyte proliferation (Lev-Lehman et al., 1997). The protein is reported to be expressed in human platelet membranes with molecular weight of 72 kDa (Nachman et al., 1972). The activation of AChE produced antiplatelet effects, leading to a hazard of increased bleeding (Jun et al., 2006). In our investigation, it was found that there was a large variation of AChE activity level between subjects (41%), which may be due to several factors such as age and gender. In agreement with this, a study carried out by Jha et al. (2009) has examined the effect of aging on the level of AChE activity on erythrocyte, recruiting healthy subjects of both sexes and aged between 22 and 82 years old. They found that erythrocyte AChE activity declined with increase in the age of subjects (Jha et al., 2009). This in consistent with a Das et aL., (2001) study that observed the positive relationship between ageing and AChE activity in different rat brain regions. AChE is responsible for the metabolism of acetylcholine, a neurotransmitter, which in turn plays a critical role as a cognitive enhancer. The change in activity ratio in adult and old rats was sexually dimorphic. In older male rats (8-22 months), AChE activity was decreased by 30–50% in the brain compared to younger adults (3-4 months), while in old female rats the ratio was decreased by 25-40 % (Das et al., 2001). From this, age is one factor that influences the activity level of AChE and could be investigated further in the platelet.

Acyl protein thioesterase (LYPLA-1/APT1) is an enzyme of 24 kDa (Devedjiev et al., 2000; Baumeister et al., 2018), and its activity was detected in platelets in the current study, a result which is comparable to what has been reported (Sim et al., 2007; Bolen et al., 2011a). Several studies have examined the potential role of APT1 in platelets. Among these Sim et al. (2007) found that incubation of intact platelets with APT1 inhibits agonist-induced platelet granule secretion and subsequently aggregation (Sim et al., 2007). Another study by Bolen et al., (2011) identified that APT1 released from platelets contributes to the production of phospholipid mediators (such as lysophosphatidic acid) to work as a regulator of several cellular response (Bolen et al., 2011a). A large coefficient of variation of APT1 activity level between subjects (40%) was found from the present study; however, which biological factors could influence its activity level are still undetermined.

Chapter 5 Endocannabinoid hydrolases in human blood fractions: the effects of platelet aggregation

5.1 Introduction

One, but not the only, major finding of **Chapter 4** is a differential profile of FAAH-like and MAGL activities in human blood fractions. Thus, low but measurable activity of MAGL in plasma was observed, but no measurable activity of FAAH. In contrast, serum contained measurable levels of FAAH-like activity, but no MAGL activity. Platelets appeared to have both MAGL and FAAH-like activities. Thus, these finding led us to investigate further how clotting causes these changes and precisely which enzymes are involved.

In the blood stream, platelets migrate close by the vessel wall to monitor endothelium integrity, while erythrocytes predominate in the stream. Coagulation (a process of blood clotting) is a series of events leading to hemostasis. Platelet aggregation is the primary haemostasis building a plug at the injured site of exposed endothelial cells (Palta et al., 2014; Chaudhry et al., 2018) .

Following injury to the endothelial layer, collagen is exposed and adhesion of platelets to collagen is initiated. The adhesion is mediated by von Willebrand factor (vWF), a large glycoprotein circulating in blood plasma (Ruggeri, 2003). The binding of platelets to collagen transforms their shape from resting discoid discs to activated spheres. 2-AG is thought to be taken up by platelets and then metabolised by MAGL to AA, which in turn is oxidized by cyclooxygenase-1 (COX1) to thromboxane A_2 (TxA_2) (Keown et al., 2010). In contrast to MAGL, FAAH appeared not to play a role in the production of AA despite the

appearance of FAAH activity in human platelets (Maccarrone et al., 1999; Fasia et al., 2003).

Alongside the interaction with collagen, GPIbα (as a part of the GPIb-IX-V complex) and vWF subsequently release the contents of platelet granules, including second wave mediators such as adenosine diphosphate (ADP), adenosine triphosphate (ATP), serotonin (5-HT), calcium ions (Ca^{2+}), and TxA_2. Also, platelet activation leads to activation of the pro-aggregatory agent thrombin via cleavage of prothrombin by activated Factor Xa. This results in a high local concentration of effector molecules essential for platelet aggregation. Receptors for ADP ($P2Y_1$ and $P2Y_{12}$), thrombin (protease activated receptor 1) and TxA_2 (TP prostanoid receptors) on platelets are activated. Following this, platelet surface receptors such as GPIIb/IIIa become activated, and fibrinogen binds these activated receptors leading to platelet aggregation (Andrews et al., 2004).

Subsequently, secondary haemostasis includes the two coagulation pathways; intrinsic pathway, activated by endothelial collagen, and extrinsic pathway, activated by tissue factor released via endothelial cells following external injury. Various clotting factors, known as serine proteases, are activated in these pathways; intrinsic pathway begins with factor XII, while extrinsic pathway begins with factor VII. These factors activate prothrombin into thrombin that finally activates fibrogen into fibrin subunits which bind together to stabilise the platelets plug (Palta et al., 2014; Chaudhry et al., 2018) .

Erythrocytes are also aggregated by adhesion to each other (Wagner et al., 2013) when erythrocytes bind plasma fibrinogen, a binding which leads to erythrocyte sedimentation and an increase in blood viscosity. Increasing haematocrit, in turn, leads to an elevation of the interaction and adhesion of platelets to the site of vessel injury (Byrnes et al., 2017). Aggregation can be initiated by thrombin, which converts fibrinogen to fibrin, resulting in mesh formation that traps platelets and erythrocytes (Crawley et al., 2007).

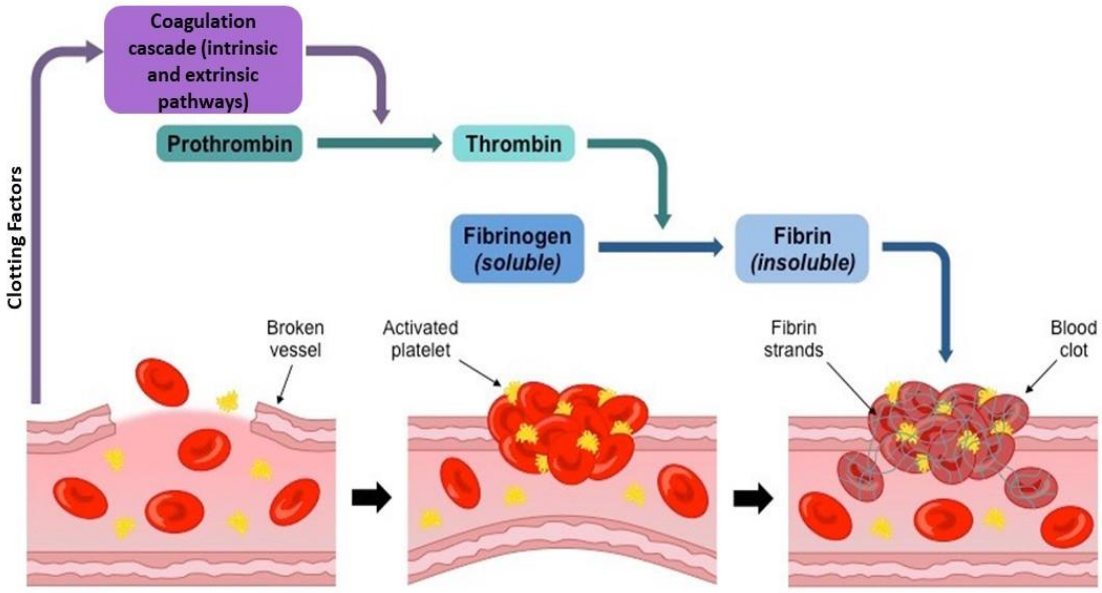

Figure 5.1: **simplified blood clotting.**

Despite the collective data described above, no studies to-date have investigated how blood clotting process changes the distribution of MAGL and FAAH activities. It would be extremely useful, therefore, to gain more understanding into how these changes in the enzyme activities might be associated with disorders such as high blood pressure and clotting problems.

5.2 Aim

This study was designed to explore the mechanism(s) of redistribution of MAGL and FAAH during serum formation. Therefore, the primary aim was to identify whether membrane fragments from platelets or erythrocytes contribute to FAAH (and/or MAGL) release into serum. This will help to identify the potential roles of these different elements in the clotting process. The secondary objective was to investigate whether MAGL and FAAH immunoreactivity was detectable in those blood fractions and could serve as a surrogate for activity levels. This would be an important step to allow an alternative, higher throughput method way to investigate the functional impact of MAGL and FAAH in blood circulation.

5.3 Materials & Methods

5.3.1 Chemicals & reagents

The following table shows chemicals that were used in the assays described in this Chapter:

Chemicals or solutions	Company	Catalogue number
Thrombin (from human plasma 2800 unit per mL)	Sigma-Aldrich (UK)	10602400001
Precision Plus protein blue standards	Bio-Rad Laboratories Ltd (UK)	#161-0373
Anti-β-actin monoclonal antibody (mouse)	Sigma-Aldrich (UK)	#A1978-100UL
Anti-MAGL polyclonal antibody (rabbit)	Cayman-chemical (USA)	100035
Anti-FAAH polyclonal antibody (rabbit)	Cayman-chemical (USA)	101600
Anti-rabbit (green, secondary antibody, IRDye 800 W)	Licor (UK)	925-32211
Anti-mouse (red, secondary antibody, IRDye 800 W)	Licor (UK)	925-32210

The sources for other chemicals are mentioned in Chapter 2.

5.3.2 Ethics

This study was approved by the research Ethics Committee of the School of Life Sciences, University of Nottingham (Ethics no. B080317SA), where volunteers were recruited from within the University of Nottingham by poster (see Appendix). All subjects were informed of the purpose and risks of the experiment before the study and gave their written signed informed consent.

5.3.3 Sample size determination and Statistical power

As this is the first investigation of its kind, power calculations were based on our previous examination of the activities of MAGL and FAAH in blood. Using G*Power with the following settings, we calculate an a priori sample size of eight (male) individuals. For the enzyme activities, we observed a coefficient of variation of 10-25 %. Radiometric assays were conducted in duplicate (measurement number).

Statistical analysis was using an ANOVA repeated measures between factors, and the power was set to 0.95. F test, One-way analysis of variance (ANOVA), was chosen because it estimates the sample size based on the ratio of variance between groups and within groups.

5.3.4 Study design and blood sampling

Eight healthy males, aged 23-54 years old, from the University of Nottingham Medical School were recruited using a poster (see Appendix.5). Exclusion criteria for this study included a current history of taking medications, recent participation in a clinical trial in the previous three months, or a history of drug abuse.

The practicalities of blood sampling were identical to the previous study that was described in **Chapter 4**. Subjects were asked to fast at least 8 h prior to the blood test, abstain from exercise for the previous 12 h and abstain from alcohol intake for the previous 24 h.

Subjects attended one visit and completed a questionnaire (see Appendix.1), which was designed to record aspects which may influence variation between subjects, and to exclude subjects with heath conditions. Then, blood pressure

was measured, a venous blood sample (50 mL) was taken using a 21G butterfly needle. Samples were drawn between 8 to 10 am to limit diurnal variation.

5.3.5 Isolation and homogenisation of blood cells

A 50 mL blood sample was taken from each subject and was then divided into three universal tubes; 1) 20 mL of blood was transferred into tubes containing 2 mL ACD, 2) another 20 mL of blood was also transferred into tubes containing 2 mL of ACD, and 3) 10 mL of blood was collected into a plain tube to obtain serum.

The first tube of 20 mL of blood sample mixed with ACD was centrifuged immediately at 150 g (low speed) for 20 min at 24 °C, to obtain platelet-rich-plasma (PRP) and a denser fraction containing both erythrocytes and buffy coat (which contains white blood cells).

The PRP was then extracted into a separate tube using a polypropylene transfer pipette, 1 unit/mL of thrombin was added to trigger clot formation and incubated at room temperature for 30 s to allow clotting.

In the tube that contained the denser fractions, buffy coat was carefully discarded using the polypropylene transfer pipette to isolate erythrocytes and avoid contamination of erythrocytes by white blood cells. At the same time, a small proportion of PRP (at the ratio of 1:10) was left on the top layer of erythrocytes because PRP contains a soluble blood protein fibrinogen. Then, 1 unit/ml of thrombin was added to erythrocytes and incubated at room temperature for 5 min to allow clotting.

Following the generation of a clot, PRP and erythrocytes fractions were centrifuged for 15 min at 1000 g (Ho et al., 2012). Then, the supernatant,

equivalent to serum, was transferred into small Eppendorfs and assayed for enzyme activity.

The second tube containing 20 mL of blood with ACD was centrifuged immediately at 150 g (low speed) for 20 min at 24 °C, to obtain platelet-rich-plasma (PRP) and denser fractions. Then, the isolation of platelets and erythrocytes was performed as described in **Chapter 4** section.

The third tube containing 10 mL of blood was incubated at room temperature for 30 min then centrifuged for 15 min at 1000 g to obtain serum.

5.3.6 Isolation of human serum particular fractions (membrane)

The serum membrane was obtained by high speed centrifugation, 1 mL of serum was transferred into Beckman Ultra-Clear tubes and then placed in a Fixed 30^{o} Angle rotor (TLA-120.2). The rotor was placed in Optima™ MAX Ultracentrifuges (BECKMAN COULTER) and serum was centrifuged at 50 000 g for 30 min at 4^{o}C. When the centrifugation process was finished, the sample tube was taken off and the supernatant was removed. The pellet that corresponded to the membrane was resuspended in TE buffer of the same volume as the original serum.

5.3.7 Radiometric assays

FAAH and MAGL activities were measured by radiolabelled ligands as described in section 2.1. Whole Blood and RBC were resuspended in TE buffer, pH 7.4, containing BSA (1 mg/mL) to give 1 in 500 or 1 in 50 fold dilutions, respectively. Platelets were re-suspended in HEPES buffer, pH 7.2, containing BSA to give a 1 in 600 fold dilution.

5.3.8 Data Analysis

Enzyme activity was expressed in nmoles or pmoles/min/mL of blood as described in section 2.2. GraphPad Prism (California, USA) software was then used to analyse all of the data, using paired t-tests to report the differences in enzyme activity between activated and inactivated samples.

5.3.9 Activity based protein profiling

Platelets were resuspended in HEPES buffer pH 7.2, the enzyme assay used was based on manufacturer's instructions (Thermos Fisher Scientific) as described in section 2.2, and the final amount of platelet proteins loaded was 12 µg.

5.3.10 Immunoblotting

As a way of corroborating the ABPP, immunoblotting was conducted as described below using platelet and erythrocyte fractions.

5.3.10.1 Sample preparation for SDS-PAGE gel

The same protein content of each platelet sample used in ABPP was used in immunoblotting.

Following protein determination, 20 µL of platelet samples was transferred into an Eppendorf tube and then 6x Laemmli buffer was added, and SDS-PAGE was conducted as described in **Chapter 2** section 2.

5.3.10.2 Running the gels

Precast Biorad gels (4-20%) were used with a Bio-Rad Mini Protean III apparatus, and precision plus protein blue standard was used as molecular weight markers. Electrophoresis tanks and modules were cleaned with IMS followed by

distilled H_2O. The platelet samples were boiled at 95 °C for 5 min, and then vortexed. After that, samples were centrifuged at 13000 g for 1 min. 1µL of colour protein marker was loaded into the first well in the gel, and the samples (20 µL) were loaded onto the gel. The gel was run for 40 min at 175V in an electrophoresis buffer solution, which contains 30.3 g Tris, 10 g SDS and 144 g glycine in 1 litre of distilled water.

5.3.10.3 Transferring the gel and blocking

Several components were used to transfer the gel including 2 pieces of filter paper, 2 scotch pads, a Biorad transfer cassette, and a piece of nitrocellulose paper. These components were soaked, and then the transfer sandwich was made; 1 scotch pad was laid on top of the cassette, and then the filter paper was placed on the top of the scotch gel. After the gel had finished running, the two plastic plates were removed to release the gel. After that, the gel was carefully placed onto the filter paper, and any bubbles were removed using a roller. The nitrocellulose membrane was placed over the gel, and then the second filter paper and scotch pad were placed over the nitrocellulose membrane. Finally, the cassette was closed and placed into the transfer module, and an ice pack was added. Notably, the black side of the cassette faced the black side of the transfer module. Then, the tank was filled with transfer buffer and the lid containing the electrodes was fitted, and a Bio-Rad power supply at a constant 100 V was used to run the transferring for 60 min at 4 °C.

When the transferring process had finished, the cassette was removed from the transfer module, which was followed by the removal of nitrocellulose from the cassette. Then, the nitrocellulose membrane was placed in a glass bowl, marker side up, and a few drops of Ponceau S solution were added onto the membrane. This step helps to confirm the successful transfer of proteins from gel into nitrocellulose membrane. The Ponceau stain was removed by washing the membrane several times with a TBST buffer. TBST was made of 30.29 g Tris and 73.12 g NaCl, both diluted in 1L distilled water, then adjusted to pH 7.6 and further diluted to 10L with the addition of Tween 20 (final concentration of 0.1 %).

Following washing with TBST, the nitrocellulose was placed in a clean glass bowl and blocking buffer (5% fat-free dried milk powder in TBST buffer) was added. It was incubated at room temperature for 60 min with gentle shaking.

5.3.10.4 Primary and secondary antibodies

The primary antibodies (either Anti-MAGL or Anti-FAAH, which crossreact with human enzymes) were diluted at the ratio of 1:200 in 5 mL of blocking buffer. β-actin was used as a loading control at the ratio of 1:50000. The nitrocellulose membrane was incubated with the primary antibody overnight in a cold room. Then, the nitrocellulose was transferred to a clean glass bowl and washed three times with 20 mL TBST. The secondary antibody was diluted at a ratio of 1:10000 in 20 mL of blocking buffer. The membrane was then incubated with the secondary antibody at room temperature for 60 min with gentle shaking. Finally, the blot was washed thoroughly three times with TBST buffer, and then washed with distilled water.

5.3.10.5 Scanning

The Licor Odyssey scanner was used to scan the nitrocellulose membrane, where it was gently placed on the scanner, facing down, ensuring the blot was wet and bubbles were removed. Odyssey software was opened and the parameters were set as follow: resolution for scanning = 84µm; offset = 0.0; 700-red image 5.0; 800-green image 7.0. The green intensity on the gel that was detected via goat anti-rabbit secondary antibody illustrated the target protein signal. The red intensity, reflecting the anti-β-actin antibody, detected via anti-mouse secondary antibody was used for normalisation of the loading variations between wells on the same gel.

5.4 Results:

5.4.1 Subjects demographics

Data were obtained from healthy male subjects ageing range from 23-54 years with BMI 22-29 $kg.m^{-2}$, with normal blood pressure, not receiving any medication (even paracetamol) at least 48 h prior to blood testing. Summary data of the participants (considering the same parameters that described in chapter 4 that have an influence on the enzyme) are given in table 5.1 below.

Table 5.1: physical data for volunteers.

PARTICIPANTS CODE		Age (years)	BMI (Kg.m2)	BP (mmHg)		Cosumeing Alcohol	physical activity per week
				systolic	Diastolic	unit per week	
Males	5280	29	28.9	124	72	none	lightly active
	4335	30	24.9	107	67	none	lightly active
	1619	23	23.6	151	69	2-3 unit per week	lightly active
	5678	23	22.9	135	70	10 unit per week	moderately active
	9322	37	28	126	77	none	Moderately active
	7377	54	22.2	126	78	4 unit per week	Moderately active
	7479	26	29.3	140	74	1-2 unit per week	moderately active
	3898	38	25.9	116	75	none	No active
		33 ± 4	26 ± 1	128 ± 5	73 ± 1		

BP, blood pressure. BMI, body mass index. Sedentary, walking ≤30-60 min/week. Lightly active, walking 1-3 h/ week. Moderately active, walking more than 3 h per week.

5.4.2 Distribution of FAAH and MAGL during serum formation:

FAAH has been shown to be a membrane enzyme in tissues and cells (Fegley et al., 2005). To further confirm that the enzyme is actively expressed in serum, high-speed centrifugation was undertaken to separate particular fractions from serum. The particulate fraction (membrane) appeared to retain the majority of FAAH activity (68-78%) in serum (see figure 5.2).

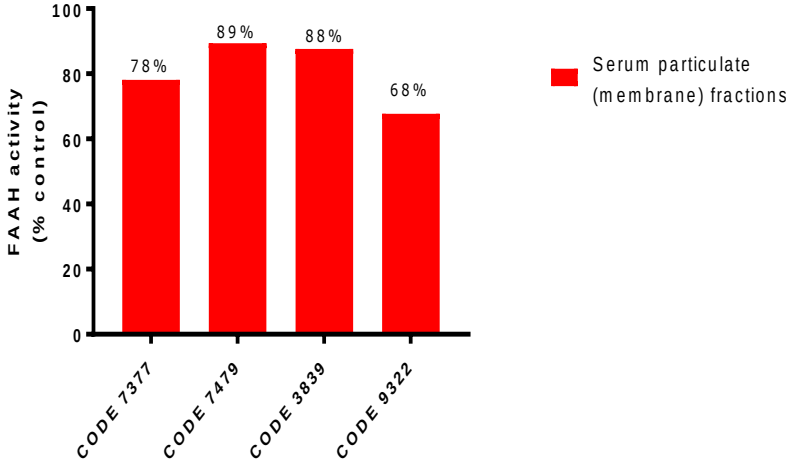

Figure 5.2: FAAH activity in serum and high speed particulate fractions. The pellet was obtained by centrifuging serum at 50 000 g for 30 min. Data are from four healthy volunteers, assayed in duplicate and analysed using a paired t test in comparison to whole serum fraction ($P > 0.05$).

It was identified in **Chapter 4** that MAGL and FAAH were measurable and reproducible in human blood samples. Knowledge or identification of which blood fractions are the source for liberating these enzymes in blood plays an important part in understanding their physiological roles. In order to answer this question, enzyme activity was measured in supernatant layers, equal to serum, obtained from erythrocytes and platelets, after clotting was initiated by thrombin referred to as a "post thrombin supernatant", and compared to original fractions erythrocytes and platelets called "prior to thrombin exposure". FAAH and

MAGL activities were measured by radiometric assays. FAAH activity was higher in erythrocytes compared to platelets, as was observed for both heathy males and females in **Chapter 4**. However, FAAH activity was decreased in erythrocytes exposed to thrombin to 80± 5% compared to erythrocytes prior to thrombin exposure (****$P \leq 0.0001$). The activity of FAAH in platelets samples was too modest; however, its activity significantly increased in post thrombin supernatant from platelets (see figure 5.2). Indeed, FAAH activity in post thrombin supernatant from platelets was 100 % higher than its value in original platelet fractions prior to thrombin exposure.

At the same time, FAAH activity in post thrombin supernatant from erythrocytes was slightly higher than its activity in post thrombin supernatant from platelets. In contrast, the activity of MAGL was significantly reduced in post thrombin supernatant from both erythrocytes and platelets compared to erythrocytes and platelets prior to thrombin exposure (****$P \leq 0.0001$) (see figure 5.3).

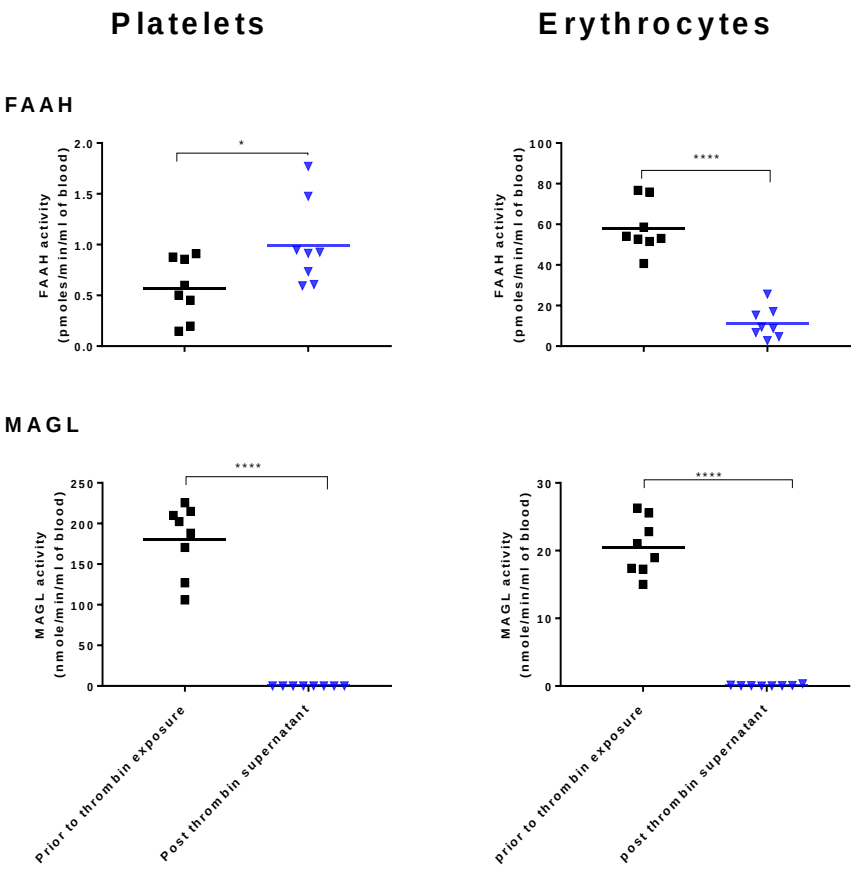

Figure 5.3: Distribution of MAGL and FAAH activities during serum formation. After isolation of blood components, thrombin (1 unit/mL) was employed to trigger clot formation with PRP and packed erythrocytes. MAGL and FAAH activities were measured by radiometric assay. Data are enzyme activities for each subject, analysed using a student's 2-tailed paired t- test (* $P \leq 0.05$, ** $P \leq 0.001$, **** $P \leq 0.0001$) .

5.4.3 Effects of thrombin on soluble MAGL activity:

Previous sections showed that MAGL activity was reduced in serum compared to plasma. Therefore, the question of which factors influence the activity level of MAGL during clotting was investigated. It was hypothesized that thrombin, activated during the clotting process, may cleave the MAGL enzyme into inactive fragments. Co-incubation of washed platelet samples with

thrombin induced a small but significant reduction (10.3% ±3) in MAGL activity (* p≤0.05) (see figure 5.4).

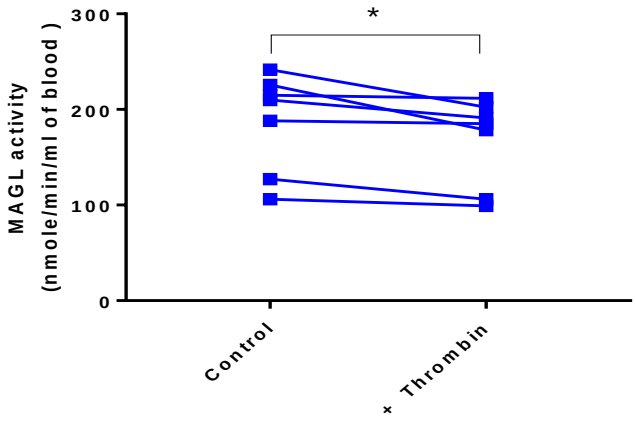

Figure 5.4: Effects of Thrombin on MAGL activity in washed platelet samples. Washed platelet samples were incubated with thrombin (as inhibitor), and DMSO was used as a vehicle in control samples. Afterword, MAGL activity was measured by radiometric assay. Data were collected from seven healthy volunteers and analysed using a student's 2-tailed paired t-test (* $P \leq 0.05$).

5.4.4 Comparison between enzyme immunoreactivity and activity level

MAGL and FAAH in platelet and erythrocyte samples were assessed using immunoblots compared to enzymatic activity measured by ABPP. Rat liver membranes and MCF-7 cell homogenates were used as positive controls for MAGL and FAAH.

As shown in figure 5.5, the expression of β-actin, loading control, was relatively similar in positive control samples (rat liver membrane and MCF-7 cells), while in platelets it had a higher proportion relative to total protein. In comparison, erythrocytes have much lower expression level of β-actin. MAGL immunoreactivity was detected as a very faint band in rat liver membranes, while

not being detectable in MCF-7 cell membranes. In comparison, it was detectable in platelet samples for each volunteer as a single band with a molecular mass of ~ 33 kDa. There was also an unidentified band at ~ 85 kDa, which appeared in human platelets and MCF-7 cell membrane (see figure 5.4). However, MAGL immunoreactivity was not detected in human erythrocytes, while a faint unidentified band with molecular mass of 58kDa was detected in erythrocytes (see figure 5.5).

FAAH immunoreactivity was detectable in positive control samples (rat liver and MCF-7 cell membranes), but was not detectable in human platelets or erythrocytes. To further identify the reason behind the absence of FAAH immunoreactivity in platelets, the rat liver membrane sample was diluted to match the equivalent FAAH activity in human platelets (indicated in figure 5.5as diluted liver membrane), as measured by radiometric assay. Thus, it was found that the diluted rat liver membrane sample did not show the expression of either β-actin or FAAH.

Furthermore, the activity expression of serine hydrolase enzymes pattern in platelet samples from different donors, detected by ABPP, was identical to what has been shown/described in **Chapter 4**. Two bands equivalent to MAGL activity were detected by the ABPP with molecular masses of ~33 and 28 kDa. These two bands were blocked by MAFP, JZL184 but not by WWL79, URB597 or JNJ1661010. However, FAAH activity was undetectable by ABPP in both platelets and erythrocytes (see figure 5.4).

As previously shown in **Chapter 4**, FAAH activity was not detectable by using ABPP with erythrocyte membrane ghosts, or in other words with haemoglobin-free white ghosts, which indicates that FAAH may degrade during the extraction

process. Therefore, in the current experiment, packed erythrocyte samples were used, without haemoglobin separation, and loaded into gel after being incubated with TAMRA-FP. However, MAGL and FAAH activities were not detectable in packed erythrocyte samples by ABPP, similar to immunoreactivity.

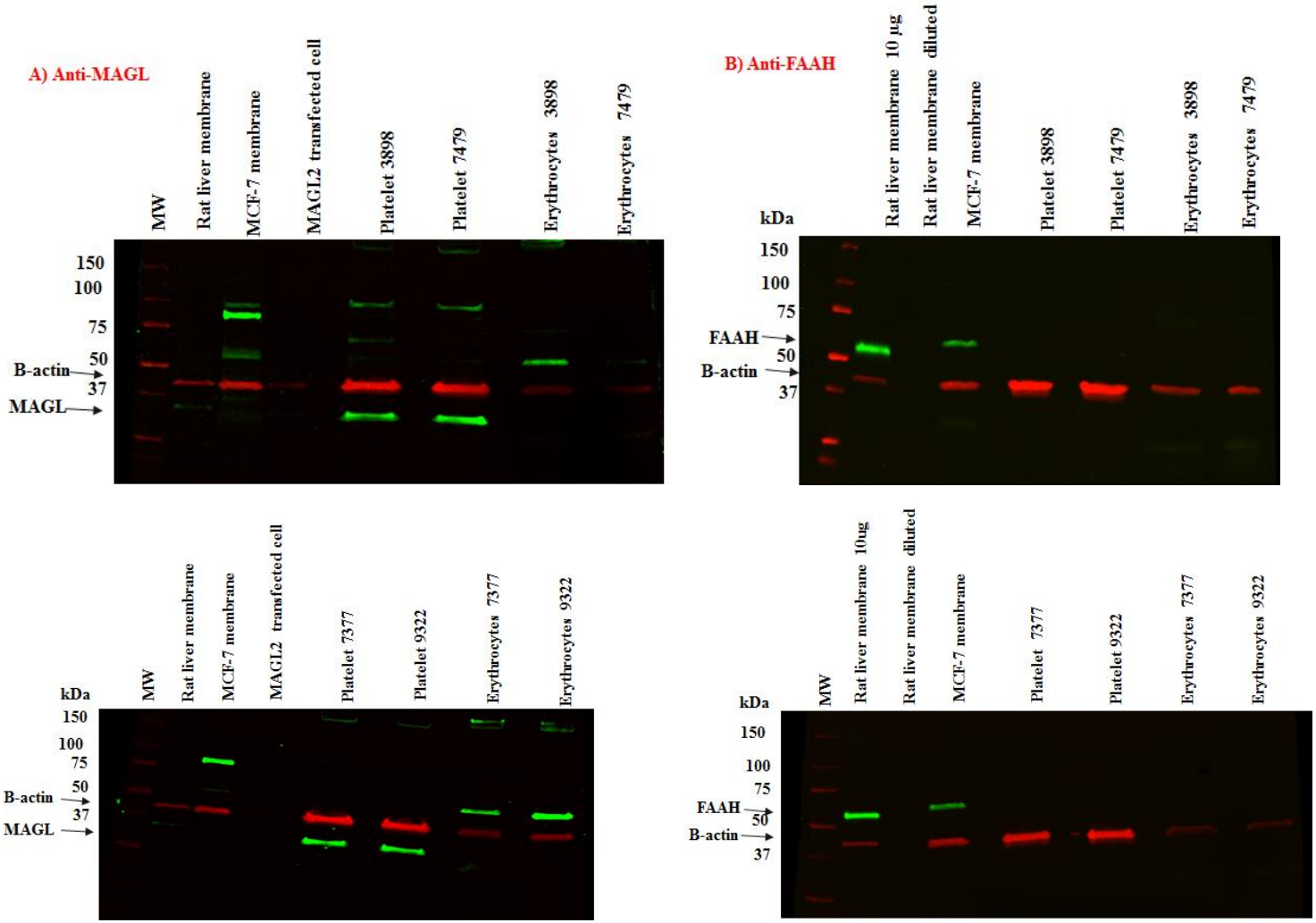

Figure 5.5: Immunoblots for FAAH and MAGL expression in washed platelet and packed erythrocyte samples from heathy males. Data represent the immunoreactivity for each target protein and the reference protein β-actin. Molecular weight ladders can be seen in the far left hand lane on each blot. Platelet and erythrocyte samples, and membrane fractions from rat liver and MCF-7 cell line was used as a positive control.

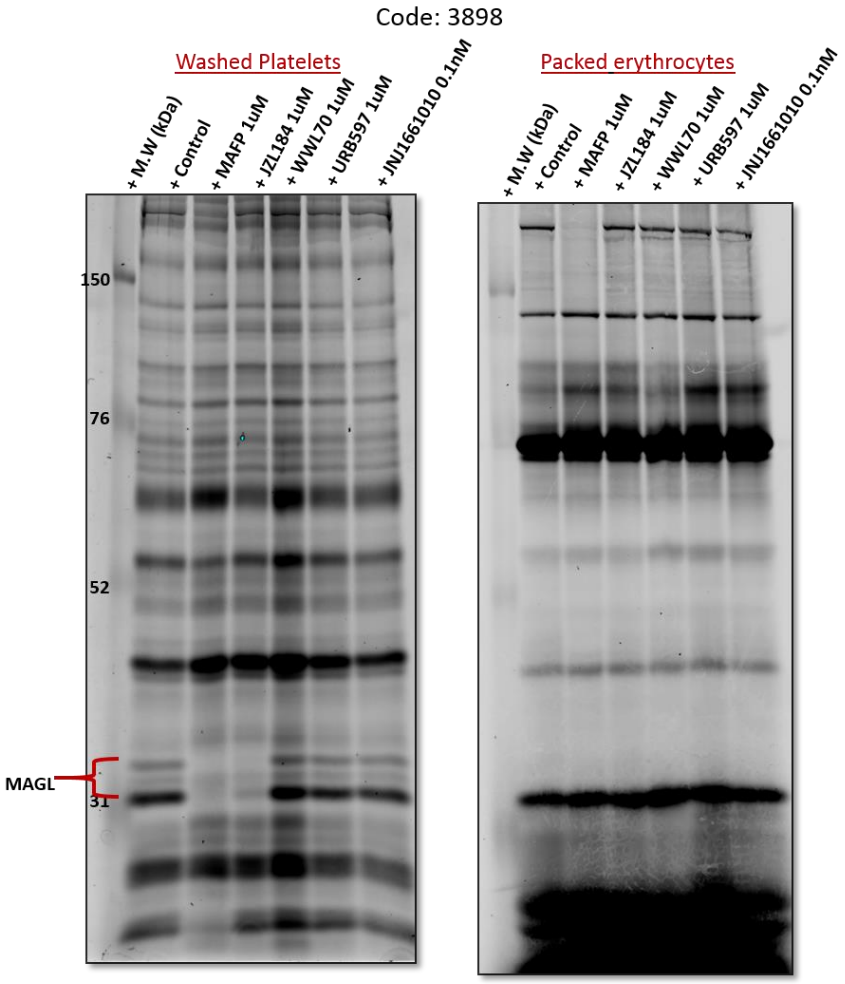
Code: 3898
Washed Platelets
Packed erythrocytes
+ M.W (kDa)
+ Control
+ MAFP 1uM
+ JZL184 1uM
+ WWL70 1uM
+ URB597 1uM
+ JNJ16610 10 0.1nM
150
76
52
31
MAGL

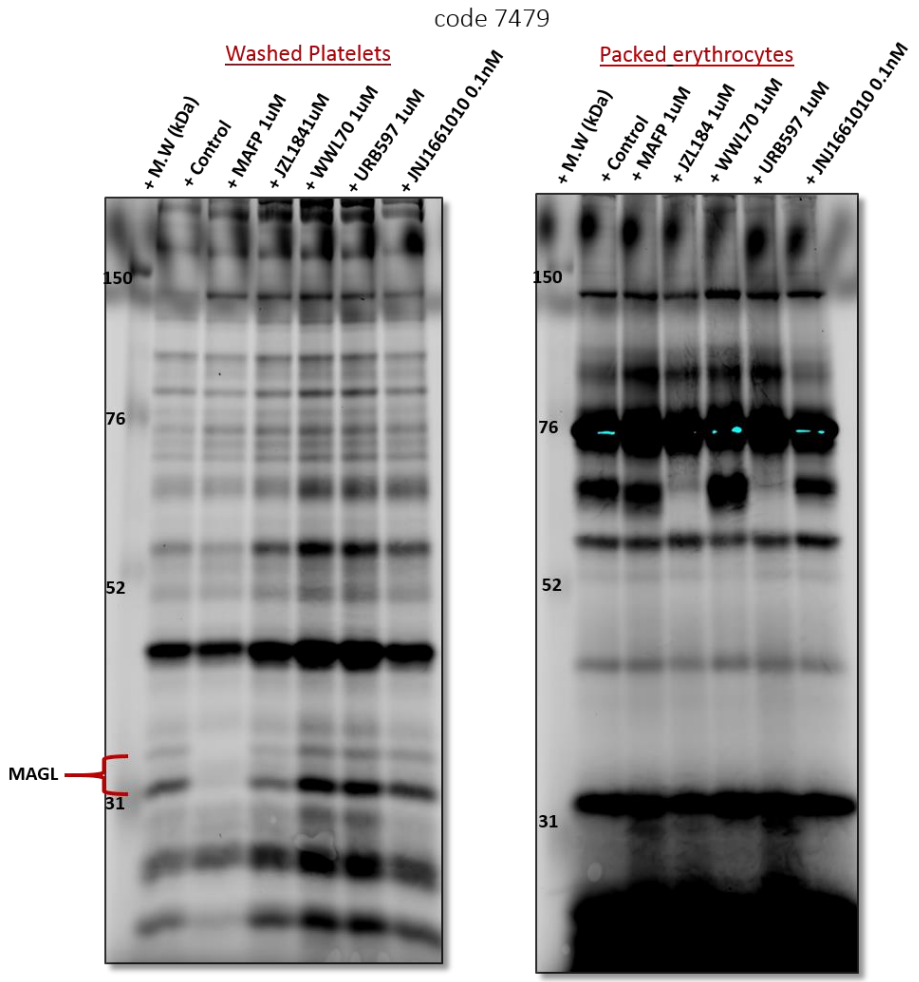
code 7479
Washed Platelets
Packed erythrocytes
+ M.W (kDa)
+ Control
+ MAFP 1uM
+ JZL1841uM
+ WWL70 1uM
+ URB597 1uM
+ JNJ16610 10 0.1nM
+ JZL184 1uM
150
76
52
31
MAGL

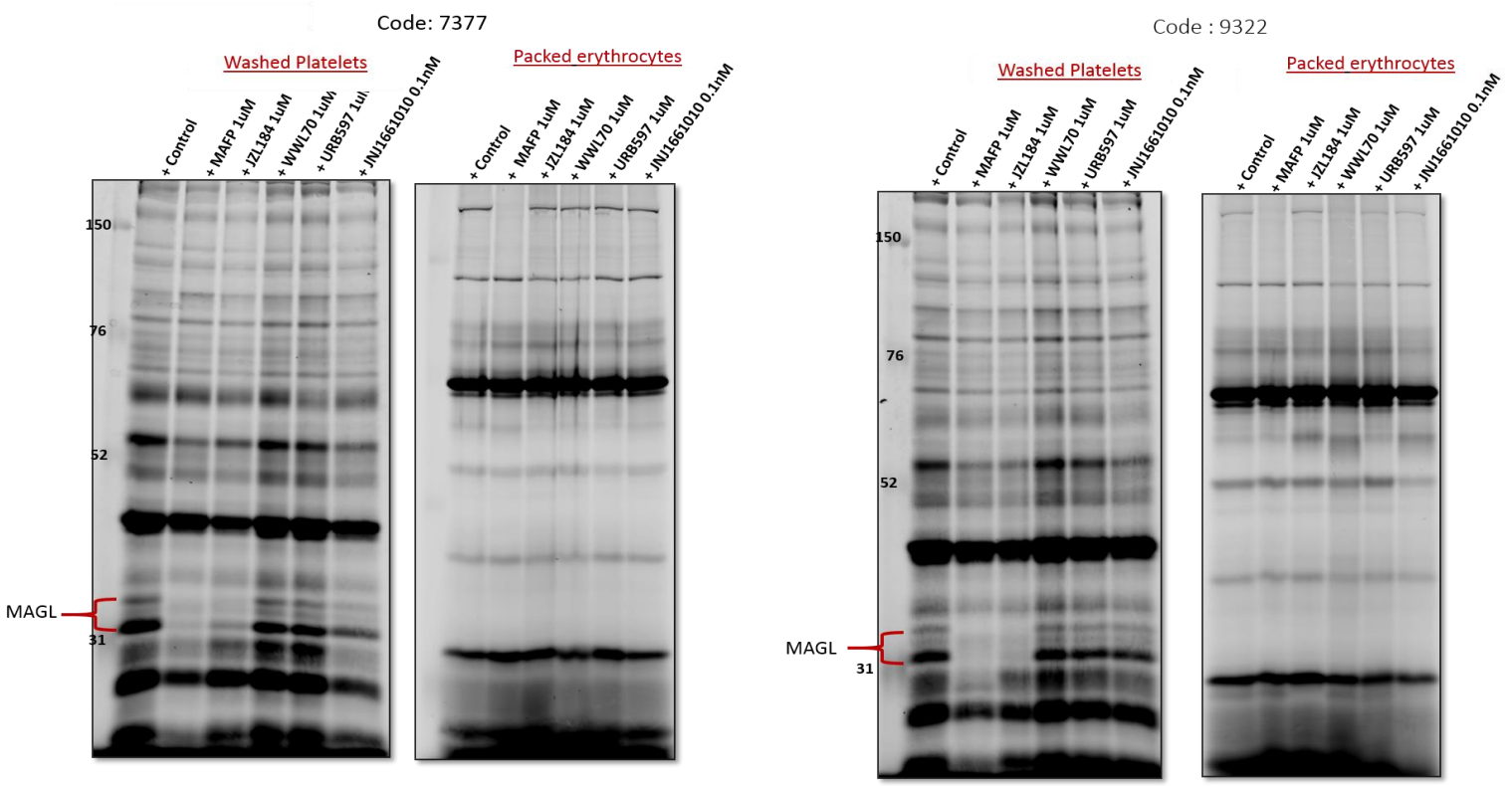

Figure 5.6: ABPP detection of MAGL and FAAH activities. Samples were labelled with FP-rhodamine in the presence or absence of MAGL and FAAH inhibitors (lane 1, DMSO; lane 2, MAFP at 1 µM; lane 3, WWWL70; lane 4, JZL184 at 1 µM ; lane 5, URB597 at 1 µM; lane 6, JNJ1661010 at 0.1 nM) as shown. A and B, gel profiles of FP-rhodamine-labeled serine hydrolases in platelets (A) and erythrocytes (B) from humans in the presence or absence of inhibitors. The bands on the gel corresponding to MAGL are highlighted, while the activity of FAAH enzyme was too low to be detected.

Analysing data from individual donors indicated that MAGL immunoreactivity and MAGL activity level in platelets samples is disconnected (see figure 5.7). However, despite using fresh platelet samples, the immunoreactivity and activity of FAAH were not detected (see figure 5.5 and 5.6).

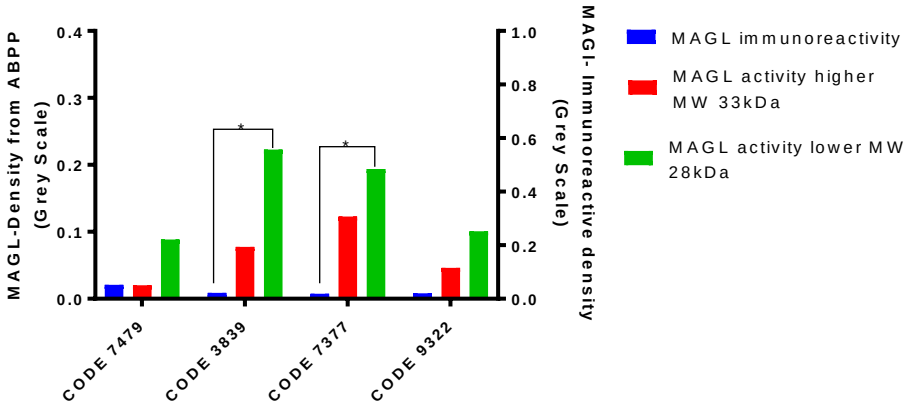

Figure 5.7: Comparison between immunoreactivity and activity level of MAGL in platelet samples. Platelets samples were collected from four healthy male volunteers, and the immunoreactivity and activity level were measured by western blot and ABPP, respectively. The density of each band was analyzed using IMAGE STUDIO Software, and subsequently, two-way ANOVA with multiple comparison was applied (**$P \leq 0.001$).There was a significant difference between the immunoreactivity and activity level of MAGL

5.5 Discussion

FAAH activity is present in serum, which is associated with particulate fractions. Given the nature of serum formation, the particulate FAAH activity originates from the proteolysis of erythrocytes, platelets or both, occurring during the clotting process. However, there are possible mechanisms other than the proteolytic effect of thrombin that lead to absence of MAGL activity in serum. MAGL immunoreactivity is detectable in human platelets but not FAAH, which is consistent with the relative activity of these two enzymes, where ABPP detected high activity of MAGL but not FAAH. Despite that, the expression of MAGL immunoreactivity is not a suitable surrogate to represent its activity levels.

5.5.1 Distribution of FAAH and MAGL during blood clotting

FAAH activity was mostly associated with particulate fractions of human serum samples. Given the nature of serum formation, it is likely that particulate FAAH activity is somehow released from the membrane fractions of the blood components involved in clot formation. However, both erythrocytes and platelets exhibited measurable FAAH activity. FAAH activity was released from platelets during clot formation. The activity level of FAAH measured in post thrombin supernatant from platelets was equivalent to its activity level in serum.

In addition, FAAH activity in erythrocytes significantly decreased after clotting initiated by thrombin. Despite that, the activity of FAAH released to the post thrombin supernatant by erythrocytes was still higher than that released by platelet activation. Therefore, this suggests that FAAH activity in serum could originate from proteolysis of either platelets, erythrocytes or both. In

comparison, after the clotting was initiated in either platelets or erythrocytes by thrombin, MAGL activity in post thrombin supernatant is significantly lower than in original fractions.

The redistribution of FAAH and MAGL activities during clot formation observed in this study is believed to be somewhat critical for regulation of 2-AG and AEA levels to maintain normal homeostasis. It has been extensively shown that during platelets activation in response to vascular injury, platelets released their granule to contribute to vasoconstriction of blood vessels and/or promotes clot formation to finally lead to wound healing. For instance, Autotoxin, is a lipid hydrolysing enzyme, mainly present in platelet α-granules, which is released by activated platelets to hydrolyse lysophosphatidic acid in order to promote platelet aggregation (Brindley et al., 2009; Bolen et al., 2011b). In the same manner, FAAH is released from platelets to serum to contribute further to vasoconstriction.

2-AG acts as an agonist of platelet activation, whereas AEA acts as antagonist for platelet activation. Prior *in vitro* studies have reported that AEA inhibits platelet aggregation by several mechanisms; in one of these, platelet-derived 2-AG binding with CB_1 receptors in endothelial cells induces AEA, which in turn inhibits ADP released from platelets binding to its receptors (P2X), subsequently inhibiting platelet activation (Maccarrone et al., 2002a). Another mechanism is that AEA inhibits platelet aggregation by decreasing the secretion of platelet granules (particularly P-selectin) (De Angelis et al., 2014). In thrombosis and inflammation, P-selectin regulates the interaction of leukocytes with platelets in the area of vessel injury (Palabrica et al., 1992). Disruption of leukocytes accumulation, as a result of P-selectin inhibition, impaired fibrin formation and

subsequently reduced thrombus stability. In contrast, an increased level of platelet leukocyte aggregate is used as a stable marker for hypercoagulability and associated with thrombo inflammatory disorder (Swystun et al., 2016). In addition, blood vessel walls get constricted in response to injury to slow the movement of blood into the damaged area while the clot forms (Hoffbrand et al., 2011), and AEA acts as a vasodilator (Herradón et al., 2007). Based on the current data and previously reported observations mentioned above, it is suggested that platelets release FAAH during clot formation to potentially inactivate AEA and subsequently inhibit either AEA vasodilator or antiplatelet activation effects.

Looking at erythrocytes, a previous study found that erythrocytes undergo eryptosis, induced by AEA (Bentzen et al., 2007). Therefore, based on the Bentzen study and the high FAAH activity in erythrocytes observed in the present study, it is speculated that under normal conditions, FAAH may prevent eryptosis by degrading AEA and subsequently maintain the life span of erythrocytes. Another study reports that aggregation of erythrocytes can be counted as a prior step to eryptosis (Mindukshev et al., 2007); thus, the reduction of FAAH activity observed in the present study after clotting may allow AEA singling to further induce eryptosis.

Enhanced erythrocyte eryptosis was observed in iron deficiency, malignancy, and hemoglobinopathies (sickle-cell anaemia)(Lang et al., 2015). Interestingly, an early study conducted by Setty et al. (1996) found that in normal healthy subjects, erythrocytes had no effects on endothelial cell phospholipid turnover. However, erythrocytes samples from patients with sickle-cell disease stimulated the production of diacylglycerol from endothelial cells (Setty et al.,

1996). Diacylglycerol is a precursor of 2-AG (Bisogno et al., 2003), and 2-AG hydrolysis leads to the production of TxA_2 (Keown et al., 2010). Therefore, this leads to an increased incidence of thrombosis, and it is reported that the high incidence of thrombosis is a pathological condition associated with sickle cell disease (Litvinov et al., 2017). It would be of interest to examine endocannabinoid hydrolase activities in subjects with sickle cell disease to identify whether turnover of AEA and/or 2AG might be altered in this pathology.

5.5.2 Proteolytic effect of thrombin on MAGL activity:

Blood clotting is a complex network of serine proteases, cofactors, and inhibitors, organized into a proteolytic cascade that ultimately leads to a plug forming to prevent the loss of blood upon vascular injury (Dashkevich et al., 2012).

Thrombin is a pluripotent enzyme that has pro and anti-coagulation mechanisms by proteolysis the induction and inhibition of fibrin proteolysis, depending on the local required conditions (Hoffbrand et al., 2011). A result from the current study found that co-incubation of platelet samples with thrombin caused a modest reduction of only 10 % in MAGL activity, while 90% was retained in platelet samples. Therefore, it suggests that the absence of MAGL activity in serum is not due to the proteolytic effect of thrombin hydrolysing MAGL into an inactive form. Taking that into consideration, there are many proteases activated during clotting process, but since thrombin is the key protease enzyme of this process (Di Cera, 2003), the undetectable MAGL activity in serum maybe because of a lack of MAGL released during clotting formation rather than effect of proteolysis.

5.5.3 No relationship between enzyme immunoreactivity and activities in human platelets

Enzyme activity does not necessarily correlate with its immunoreactivity expression. A relationship between enzyme immunoreactivity expression and its activity was examined to identify whether it might be useful to predict enzyme activity quantitatively by using its immunoreactivity expression data.

β-actin is a highly conserved protein with a molecular mass of 42kDa that is found in all eukaryotic cells (Bearer et al., 2002) as a part of the cytoskeleton that is involved in maintaining cell shape and motility, thus it is widely accepted as a loading control (Cortelazzo et al., 2014). In the current study, different expression of β-actin immunoreactivity was detected among different cell types. It was highly expressed in platelets compared to positive controls (rat liver membrane and MCF-7 cell membrane), despite loading the same amount of protein. It has been reported that platelets contains a large amount of actin roughly 15-20% of total protein, where actin reorganisation is critical in the process of shape change during aggregation (Bearer et al., 2002). Moreover, it was observed from the current study that erythrocytes have a lower β-actin expression in comparison to platelets. A previous study reported that a reduction of β-actin expression is associated with abnormal erythrocyte shape (Cortelazzo et al., 2014). Since erythrocytes are composed primarily of hemoglobin, it is assumed that β-actin may be highly diluted. However, no study to-date has made a direct comparison between the expression of β-actin in blood cells and other cell types, but our study shows that its expression varies between cell types and species.

In addition, immunoblot analysis from the current chapter revealed the presence of MAGL in platelets but not in erythrocytes as a single band. Anti-MAGL polyclonal antibody detected the band with molecular mass of 33kDa. A similar molecular mass using polyclonal antibody from the same source has been reported from MAGL in human platelets (Gkini et al., 2009). They described that the immunoreactive band was single and was abolished by the MAGL blocking peptide when using the Cayman rabbit antibody; however, when they used the Abcam chicken antibody, the immunoreactivity band was double, suggesting the presence of two isoforms (Gkini et al., 2009). A similar double band had been detected in rat brain that were attributed to two MAGL isoforms (Dinh et al., 2002), and from mouse brain (Karlsson et al., 2001). Thus, these results suggest that immunopurified polyclonal antibody is not able to detect the second variant of MAGL.

FAAH immunoreactivity was undetectable in platelet samples; despite there being a clear expression of the loading control β-actin in western blotting. The FAAH immunoreactivity was detected in control sample rat liver membrane, but when we diluted the sample to match the equivalent FAAH activity in human platelets, as measured by radiometric assay, the capacity to detect FAAH immunoreactivity by antibody was lost. Therefore, it suggests that the expression of FAAH is too modest to be detected by antibody.

In addition, the observation of serine hydrolase activities in platelet samples by ABPP in the current study was identical to what was seen in **Chapter 4**, using samples from different donors, hence identifying the validation and credibility of this approach. Although two active variants of MAGL (higher molecular mass ~ 33 and lower molecular mass 28 kDa) were identified in platelets by ABPP,

there is a disconnection between MAGL immunoreactivity and ABPP-detected MAGL activity. This could be due to the MAGL antibody not recognizing both MAGL variants equally or post-translation modification like phosphorylation of protein occurring during the process. While consistent with immunoreactivity, FAAH activity was undetectable by ABPP as the activity of FAAH was too modest to be detected.

Both the immunoreactivity and activity of FAAH and MAGL were undetectable in erythrocytes, due to the difficulty of haemoglobin extraction. The molecular size of haemoglobin is 130kDa (Yu et al., 1997) which impaired other proteins of a smaller size from migrating in the SDS-PAGE gel. Therefore, techniques such as ABPP and immunoblotting cannot be utilised to detect these enzymes in erythrocyte samples unless successful purification of proteins and absolute elimination of haemoglobin has occurred.

There is no relationship between MAGL immunoreactivity abundance and its activity in the blood fractions, which identifies that MAGL activity cannot be quantified by using immunoreactivity expression.

Chapter 6 FAAH and MAGL activities in a human breast adenocarcinoma cell line (MCF-7)

6.1 Introduction

Mature circulating human platelets and erythrocytes, unlike other cells, are anucleate and therefore are incapable of cellular division (Hoffbrand et al., 2011), as described in **Chapter 1**. Thus, these cells cannot be cultured to allow extended investigations. FAAH activity is also reported to be expressed in a model cell (MCF7 human breast cancer cells). Using the ABPP technique, Wei et al. (2006) identified the activity of two FAAH isoforms (1/2) in MCF-7 cells. Given the MCF-7 cell line is widely used as an *in vitro* model of breast cancer (Comşa et al., 2015), these cells were chosen to investigate potential functional impacts of MAGL and FAAH inhibition *in vitro*.

MCF-7 cells were originally derived from a pleural effusion from a postmenopausal woman with breast adenocarcinoma (Osborne et al., 1987). The cells express estrogen receptors (ER) and progesterone receptors (PR), which regulate cell growth. MCF-7 cells belong to the luminal A molecular subtype (Baguley et al., 2011; Done, 2011); a poorly-aggressive cancer cell line considered to have low metastatic potential.

Generally, uncontrolled cell division and cell death are key characteristics of cancer, and migration is a key event in tumour metastasis and angiogenesis. Earlier studies found that AEA, acting on the CB_1 receptor, inhibited MCF-7 cell line proliferation *in vitro* (De Petrocellis et al., 1998; Melck et al., 1999; De Petrocellis et al., 2002). The anti-proliferative effects of AEA were accompanied by either suppression of the expression of FAAH or inhibition of its activity (De

Petrocellis et al., 2002). Micromolar concentrations of 2-AG or AEA exerted a potent anti-proliferation effect on MCF-7 cancer cell line (Melck et al., 2000).

A further *in vitro* study reported that AEA inhibited migration of the highly invasive metastatic breast cancer cell line (MDA-MB-231) (Grimaldi et al., 2006), but its effect on MCF-7 migration is still unknown. Whether inhibition of MAGL and FAAH impact MCF-7 cell proliferation and migration is still not well investigated.

6.2 Aim

The primary aim of this study was to investigate the functional impact of MAGL and FAAH inhibition on MCF-7 cell proliferation and migration.

6.3 Materials & Methods

6.3.1 Chemicals

The following table shows chemicals that were used in the assays described in this chapter:

Cells, and Chemicals or solutions	Company
Breast cancer cell line (MCF-7)	European collection of animal cell cultures, Porton down, Salisbury, UK
Dulbecco's Modified Eagles media (DMEM) with Ham-F12 (without supplements) L-glutamine (at a concentration of 200 mM), foetal bovine serum (FBS) Solution of 10X trypsin/EDTA (0.5 g/l porcine trypsin and 0.2g/l EDTA) Phosphate buffered saline (PBS) Doxorubicin Cytochalasin D	Sigma Aldrich, UK

The sources of other chemical used were identified in **Chapter 2**.

6.3.2 Cell Culture

All experiments were carried out in a class II vertical laminar flow cabinet (Thermofisher) after being thoroughly cleaned by 70% v/v industrial methylated spirit (IMS). MCF-7 cells were maintained in 75 cm^2 polystyrene cell culture flasks fitted with 0.22 µm filter caps (Nunc), containing 15 mL of growth media (DMEM, 10% FBS and L-glutamine (at a final concentration of 2 mM). Following that, cells were grown in a Sanyo CO_2 incubator at a temperature of 37 ^oC in a humidified atmosphere (95% air: 5% CO_2).

In order to culture cells for a longer time, cells need to be spilt regularly. Also, this step is necessary to prevent cell senescence that occurs when cell

density increases with time. To do so, the growth medium was removed by an aspirator, and then the cells were washed by adding 5 mL PBS. Following this, cell monolayers were disrupted with 2 mL of 0.05 g/L trypsin/0.02 g/L EDTA in PBS. PBS is a water-based salt buffer utilised to wash chelators from the culture prior to cell dissociation; it is not toxic to the cells. It sustains the physiological PH and osmolality of the cells; therefore, impeding cells from rupturing or shrivelling up. PBS also mirrors the osmolality of the body (isotonic) and it is not influenced by temperature fluctuations (Martin et al., 2006). Afterward, the flask was placed in the incubator for 2 min. After the incubation, 8 mL growth medium was added and then the cells were pipetted up and down several times. The cell suspension was transferred to a sterile Universal tube and then centrifuged at 150 g for 5 min. The supernatant layer was removed and 5 mL of warmed fresh growth media were added to the pellet. The passage step was conducted three times a week at a split ratio of 1:5. Finally, 1 mL of the resulting suspension was transferred to a fresh culture flask with 15 mL of fresh growth media depending on the splitting ratio.

To establish a bank of samples, the same procedure for splitting cells described in the paragraph above until centrifugation was carried out. After removing the supernatant, 5 mL of freezing medium (90% serum/10% DMSO) was added to the pellet. 1 mL of this suspension was transferred into each cryogenic vial. Vials were then placed in a Nalgene (propan-2-ol-based) cell freezing container and stored at -80 ^{o}C for 24 h. The frozen vials were transferred to liquid nitrogen for long term storage.

When needed, the frozen cells were taken from liquid nitrogen and quickly thawed via putting the vial for 1 min in a 37 ^{o}C water bath. Then, 1 mL of suspension was transferred into a 75 cm^2 fresh cell culture flask containing 15 mL of growth media.

6.3.3 Trypan blue viability assay

Trypan blue is a vital blue dye which is typically used as a cell stain to assess cell viability. This test is often carried out during the cell counting process, and it also can be used to determine cell viability rapidly and accurately. Trypan blue measures the proportion of dead cells, as the chromophore is negatively charged and does not interact with the cell except in case of membrane damage. Hence, cells that exclude the trypan blue dye are viable (Freshney, 1987). A TC10 automated cell counter (Bio-Rad, Hemel Hempstead, UK) was used to determine cell viability.

An equal proportion of trypan blue solution was mixed with an equal volume of cell suspension, where 10 µL of trypan blue in a small Eppendorf was mixed with 10 µL of cell suspension. This mixture was immediately pipetted onto the cell counter slides provided via BioRad. Then, the slide was inserted into the TC10 counter to give an immediate cell count for the cell suspension.

6.3.4 Preparation of MCF-7 cell plates

After MCF-7 cells reached 80-90 % confluency, the monolayer was disrupted and centrifuged as reported in the previous section. The supernatant layer was removed and 5 mL of fresh growth medium was added to the pellet. Trypan blue and the TC10 automated cell counter were used to assess cell

viability. Then, 5 x 10^4 cells/well were seeded into 96 well plates to determine cell proliferation, while 1.2 x 10^5 were grown in 12 well plates to assess cell viability or the influence of drugs.

6.3.5 Treatment of Cells

After the cells reached confluency in either 96 well plates or 12 well plates, the culture media was removed and replaced with fresh medium containing drugs for 24, 48 and 72 h. Doxorubicin was used as a positive control to inhibit the cell proliferation; a stock solution was prepared to 50 mM in distilled water and kept at -20 ^oC. It was then further diluted into growth medium to reach 500 nM, the final concentration. In addition, 1 µM FAAH (URB597, JNJ1661010 or PF3845) and 100 nM of MAGL (JJKK-068) inhibitors were used to assess the influence of FAAH and MAGL inhibition on cell proliferation. Inhibitors were diluted in growth medium to reach the final concentration. Cells treated with DMSO were used as a vehicle control at a final concentration of 0.001% (v/v) of culture volume.

6.3.6 Cell proliferation assays

6.3.6.1 MTT assay

MTT (3-(4,5-dimethylthiazol-2-yl)-2,5-diphenyltetrazolium bromide) is a water soluble tetrazolium salt, which is converted to an insoluble product (purple formazan) by decomposition of the tetrazolium ring by mitochondrial enzymes. This product accumulates in viable cells and can be detected by absorbance. Therefore, the mitochondrial dehydrogenase of viable cells can be quantified, but not dead cells. This assay is widely used to assess cell proliferation (see

figure 6.1)(Gerlier et al., 1986; Peng et al., 2005). After cell treatment, the old media was removed from 24 well plates and then washed twice with PBS. MTT solution was prepared by adding MTT to DMEM growth medium (a final concentration of 50 µM). 1 mL of this mixture was added to each well and then the plate was left in an incubator for 2 h. The media containing MTT was aspirated and the same equivalent volume from isopropanol (propan-2-ol) was added. The formazan product from MTT metabolism was dissolved in isopropanol by pipetting up and down. 200 µL from each 24 well was transferred to a 96 well plate. Absorbance was read at 570 nm using a SPECTRA MAX, 340pc microplate reader (Molecular Device, US).

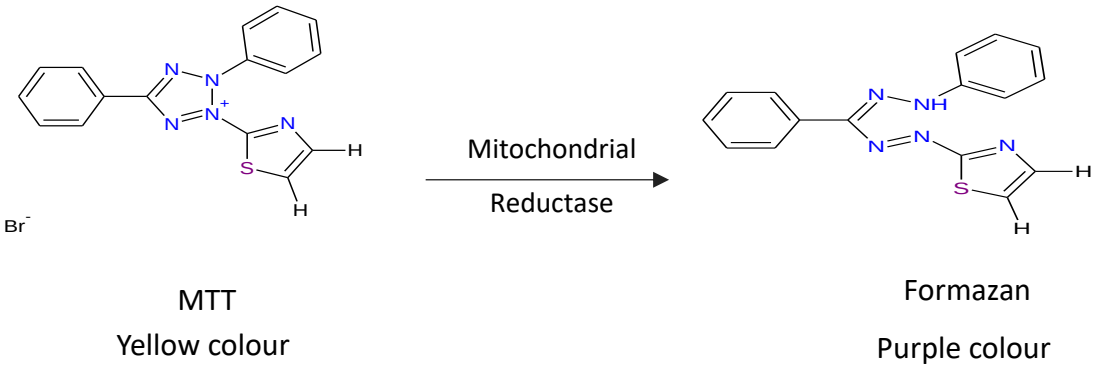

Figure 6.1. MTT (3-(4,5-dimethylthiazol-2-yl)-2,5-diphenyltetrazolium bromide) reduction to assess viable/proliferative cells.

6.3.6.2 Resazurin Reduction assay

The principle of the resazurin assay is based on the reduction of non-fluorescent resazurin into a resorufin product, a pink fluorescent molecule, by viable cells with active metabolism. The colour intensity is proportional to the cell activity. There are several advantages of using this assay, namely that it is sensitive, reproducible and not toxic meaning that the cells are still available after the addition of resazurin for further tests (see figure 6.2) (Riss et al., 2004).

Resazurin stock solution was prepared by dissolving 2.5 mg resazurin (Sigma-Aldrich, UK) in 2.5 mL of PBS to achieve 100 mM. The solution was filtered into a Universal tube, then 250 µL of it was diluted in 25 mL of PBS to achieve 100 µM. The solution was pre-warmed to 37 ^{o}C prior to addition to the cells. The cells were incubated with 200 µL of resazurin (100 µM) in PBS at 37 ^{o}C, 95% air: 5% CO2 for 1h. Then, the plate was read using a fluorescence plate reader Ex: 530-570 nm.

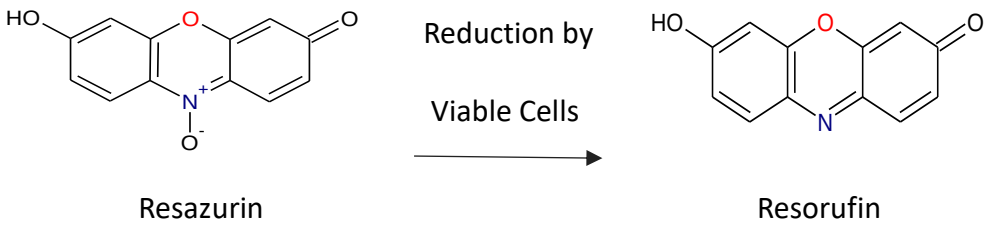

Figure 6.2. Resazurin reduction to assess viable/proliferative cells.

6.3.7 Harvesting cells for ABPP

The assay protocol to harvest MCF-7 cells for ABPP was adapted from Wei et al. (2006). MCF-7 cells were grown in a 172 cm^2 flask containing 30 mL of growth medium. After the cells reached 80-90 % confluency, the growth medium was aspirated and the cells were washed three times with 2 mL of cold PBS (flasks were kept in ice) before being harvested by scraping. The cell pellet was sonicated for 3 seconds in TE buffer and then centrifuged at 33 000 g for 45 min, at 4 °C to separate cytosol from the membranes. A volume of TE buffer equivalent to that of the cytosol was added to membrane pellets, and sonicated for 3 seconds for homogeneity. A Lowry assay was conducted to determine protein concentration as described in **Chapter 2**. Following that, the ABPP

assay was carried out as described previously in Chapter 2, where 25 µg of MCF-7 protein was loaded in each well.

6.3.8 Cell migration assay

Filamentous actin (F-actin) cytoskeleton plays an essential role in cell motility (Hayot et al., 2006), and cytochalasin D is a potent inhibitor of actin polymerization (Cooper, 1987). In order to validate our approach, cytochalasin D was used as a positive control to investigate the migratory potential of MCF-7 cancer cells.

6.3.8.1 Coating glass coverslips Poly-L-lysine for MCF-7

The procedure was performed to help cells attach to the coverslip for further staining. A 13 mm glass coverslip was inserted into a 12 well plate, 500 µL of 100X poly L-lysine was then added over each well. Afterwards, the plate was left in a cabinet for 2 h, and then each well was washed twice with sterile water. Finally, the plate was left in a cabinet for 1 h to dry, and then 100,000 cells were seeded in each well for 24 h (protocol and materials were adapted from Paul Millns). Then, cells were treated by two different concentrations of cytochalasin D (10 µM and 10 nM).

6.3.8.2 Rhodamine-Phalloidin Staining

Rhodamine-phalloidin is a fluorescent dye that is widely used to visualize actin localization in MCF-7 cells (Lovett et al., 2010) and other cells. Phalloidin is a highly selective probe binding with F-actin , while TRITC is a red-orange fluorescence dye providing brightness (Pierson, 1988). F-actin plays a vital role in cell morphology and motility (Isambert et al., 1995). DAPI (diamidino-2-phenylindole) is a fluorescent dye that binds to DNA in the cells, after which the

nuclear morphology can be compared. Apoptotic cells will produce high blue fluorescence with high permeability (Ndiaye et al., 2010). Therefore, rhodamine-phalloidin and DAPI stains were used to assess the cytochalasin D drug ability to disrupt F-actin at concentrations associated with low (if any) cytotoxicity.

After coating the glass coverslip, cells were rinsed with PBS three times to remove media components, then cells were fixed in 4% formaldehyde for 5 min at room temperature. Cells then were rinsed three times, followed by the permeabilization of cells in 0.15% Triton-X 100 in PBS for 2 min. Afterward, cells were incubated in the dye solution containing Rhodamine-phalloidin diluted 1:500 and DAPI diluted also 1:500 in PBS for 30 min at room temperature. Finally, cells were washed with PBS for 5 min three times to remove unbound phalloidin conjugate. Then, one drop of D. DABCO fluorescent mounting medium was added on a microscope slide, the coverslip containing stained cells was placed over mounting drop. The mounting medium containing 200 mg of DABCO (1,4-diazabicyclo-2-2-2-octane) was dissolved in 10 mL of the 1X PBS followed by the addition of 90 mL glycerol. The mounting medium protects cells from drying out in long term storage, and prevents photobleaching.

Finally, the F-actin and DAPI staining was analysed with a confocal laser scanning microscopy, equipped with a 3 Plan-Apochromat 40x1.3 oil objective (wavelengths were: λ_{exc}=488 nm and λ_{em}= 505 nm) (protocol and materials were adapted from Dr. Sally Wheatley)(Aleshcheva et al., 2013).

6.3.8.3 Cell exclusion zone migration assay

The assay method applied in this study was adapted from a published version (Mohammed et al., 2017). The cell exclusion zone device uses a 96 well plate with 'stopper' barriers that create a central cell-free detection zone for the cell migration experiment. Removing the stoppers allows the cells to migrate into the detection zone at the centre of each well. MCF-7 cells were seeded in a 96 well plate using a DMEM culture medium at a cell density of $10x10^4$ cells per 200 µL in order to reach 100% confluency on the next day. After 24 h and before the 96 well plate was removed from the device, the DMEM culture medium was aspirated and cells were washed by PBS (pre-warmed at 37 ^oC) to completely remove the medium components. Afterward, 200 µL of serum-free medium with diluted DMSO as a vehicle control or with inhibitors was added in each well. Serum-free medium was used to decrease proliferation rates to emphasise the role of cell migration. The plate was incubated at 37 ^oC: 5% CO_2 (v/v) for 3 h to allow cell migration into the central region. The migration was monitored by imaging at zero time (after 3 h of incubation) and after 24 h. Cytochalasin D (10 nM) was used as a positive control in this assay. Confocal microscope, equipped with a 1 Plan-Neofluar 10x0.30, was utilized to take the image setting camera of lenses to 2.5 magnification. The area of migrated cells was measured using FIJI software, and the difference between areas at the two time intervals indicated a quantitative signal of cell migration capacity.

6.3.9 Data Analysis

The data collected from cell viability/proliferation assay were analysed using GraphPad Prism software (7.04, US). Data are mean ± SEM of at least six

independent experiments. Statistical differences were determined by one-way ANOVA followed by Dunnett's multiple comparisons, as appropriate. A p value of <0.05 was considered as significant.

6.4 Results

6.4.1 Proliferation of the MCF-7 cells

6.4.1.1 Effects of different concentrations of FBS on cell proliferation.

Prior studies report that serum enhances the proliferation of MCF-7 cells, which in turn influences the sensitivity and resistance of these cells to drugs (Butler et al., 1981; Chappell et al., 2001). Therefore, in the initial experiment, the direct effects of serum on MCF-7 cell proliferation was examined by the MTT assay, with the intention of identifying a reliable concentration of FBS that maintains cell survival without significantly enhanced cells growth or division.

The cells were cultured in 24 well plates containing DMEM medium with different concentrations of FBS ranging from 0-10% for 24 h at 37 ^{o}C. It was found that the growth rate of MCF-7 was gradually increased with increasing FBS concentration. There was no significant difference in cell growth rate between cells cultured with 0.5% FBS compared with serum free conditions (0% FBS) (P>0.05). In contrast, there was a significant difference in cell growth of MCF-7 cells cultured in a medium with 10% FBS compared to cells cultured in 0% FBS (****P≤0.0001) (see figure 6.3), where 10% of serum enhanced cells growth by ~79% over control. However, it was found that 1% FBS maintained MCF-7 cells without significantly enhancing cell division, thus cell culture in medium containing 1% of FBS was used in subsequent experiments.

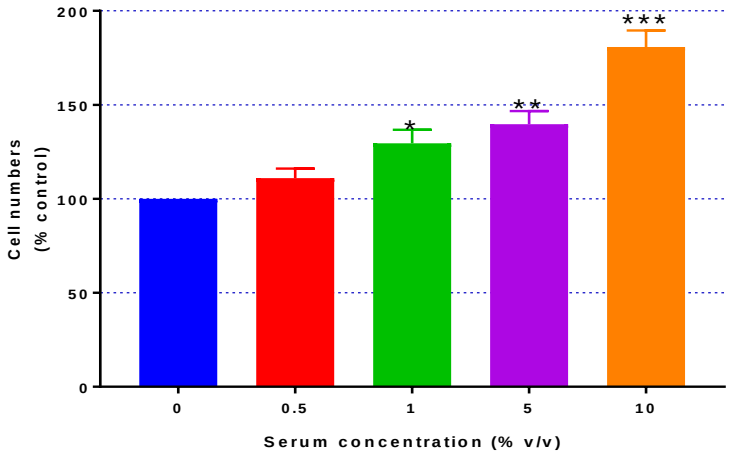

Figure 6.3. Effects of FBS concentration on MCF-7 cells. Data are scatterplots of triplicate data points from six independent experiments, normalized and expressed as a % control. Statistical analysis was performed using a one-way ANOVA with Dunnett's multiple comparisons test.

6.4.1.2 Effect of MAGL and FAAH inhibitors on MCF-7 cell proliferation.

FAAH inhibitors (MAFP, URB597, or JNJ1661010), and MAGL inhibitor JJKK-048 were investigated for influence on the MCF-7 cells growth cultured in a medium with low concentration of FBS (1% (v/v)) at different time points (24, 48 and 72 h) using MTT, Resazurin and Trypan blue assays. 500 nM doxorubicin was used as a positive control. A partial inhibition of MCF-7 cell proliferation was detected of 17% and 21 % by MTT staining, when the cells were incubated with Doxorubicin at either 24 h or 48 h, respectively. However, the inhibition was not statistically significant. On the other hand, 73% inhibition of MFC-7 proliferation was detected after 72 h incubation with Doxorubicin (****$P \leq 0.0001$). This indicates that Doxorubicin exerts a significant anti-proliferative effect after 3 days of incubation, and that was confirmed by three

assays (MTT, resazurin and Trypen blue). However, the level of inhibition with Doxorubicin detected by three different assays was varied. 56% inhibition of MCF-7 cell viability was detected by resazurin staining after 72 h incubation with Doxorubicin, while only 28% inhibition of MCF-7 cell viability was detected by Trypen blue under the same conditions. Statistical analysis of both colorimetric assays used paird t-test to analyse the differences between the two assay procedures. There was a significant difference between two assays, where MTT assay revealed an increase in percentage inhibition when compared to Resazurin (**$P \leq 0.01$). The increase in the percent inhibition using colorimetric reaction could be caused by how sensitive the dye is to react with viable cells, and it should be noted that the MTT dye is more sensitive than the Resazurin dye.

Furthermore, either at low (100 nM) or high concentration (1µM), none of the inhibitors tested in this study showed significant changes in MCF-7 cell growth rate relative to control even after 72 h incubation (see figure 6.4 and 6.5). These results were identical using three cell viability/proliferation assays: MTT, Resazurin and trypan blue.

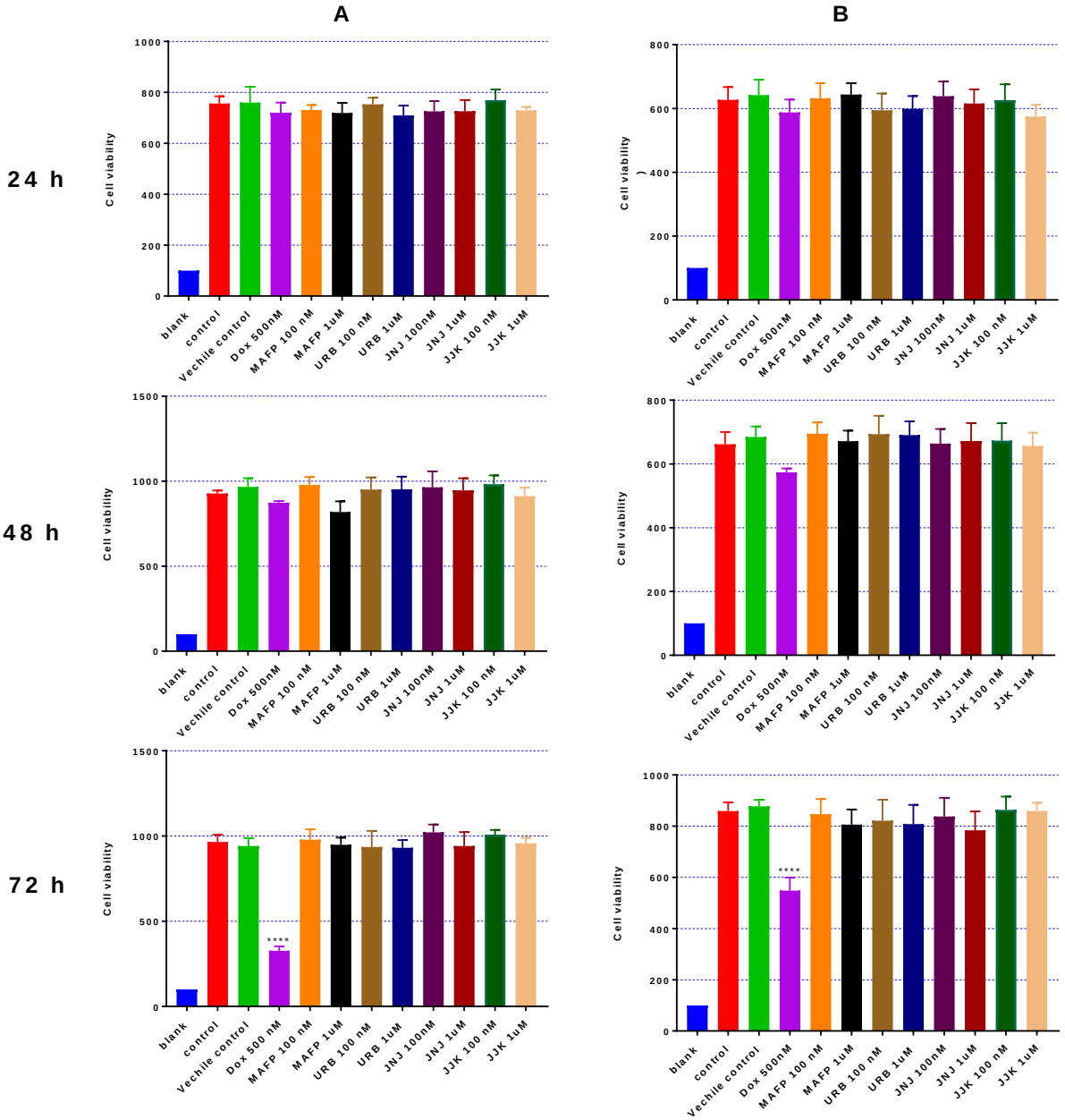

Figure 6.4.Effects of two different concentrations of MAGL and FAAH inhibitors on MCF-7 cells growth at different time points. MCF-7 cells were treated with two different concentrations of each inhibitor (100 nM and 1µM) for 24, 48 and 72 h. 500 nM of doxorubicin was used a positive control and 0.1 % of ethanol was used as a vehicle. Afterward, the cells growth were monitored using; A) MTT, and B) Resazurin. Data were collected in triplicate from six independent experiments, normalized and expressed as a % baseline. Statistical analysis was performed using a one-way ANOVA with Dunnett's multiple comparisons test.

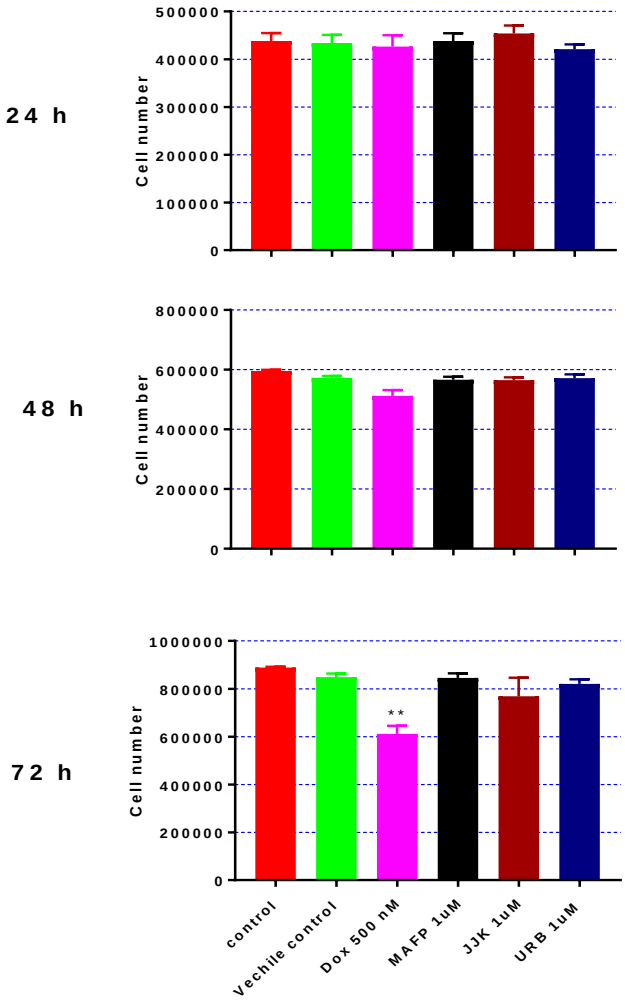

Figure 6.5. Effects of MAGL and FAAH inhibitors on MCF-7 cells growth at different time points monitored by trypan blue dye. Data were collected in triplicate from six independent experiments, normalized and expressed as a % control. Statistical analysis was performed using a one-way ANOVA with Dunnett's multiple comparisons test.

Following the observation that inhibition of MAGL and FAAH showed no effect on MCF-7 cells growth, a question was raised about whether these enzymes are expressed in these cells or not. Therefore, ABPP and immunoblotting assays were carried out to identify the activity and protein

expression, respectively, for MAGL and FAAH. From the ABPP assay, FAAH activity was detected in this MCF-7 cell line at a molecular mass of 62 kDa, and the band was inhibited in the presence of FAAH selective inhibitors (MAFP, URB597 and JNJ1661010), whereas MAGL activity was undetectable in these cells either in cytosol or membrane fractions (see figure 6.6). The results from immunoblotting were consistent with the results from ABPP. Immunoblot analysis revealed the presence of enzyme protein FAAH in MCF-7 but not MAGL (see figure 6.7). Note, the type of antibody and experiment condition was described in detail in **Chapter 5**.

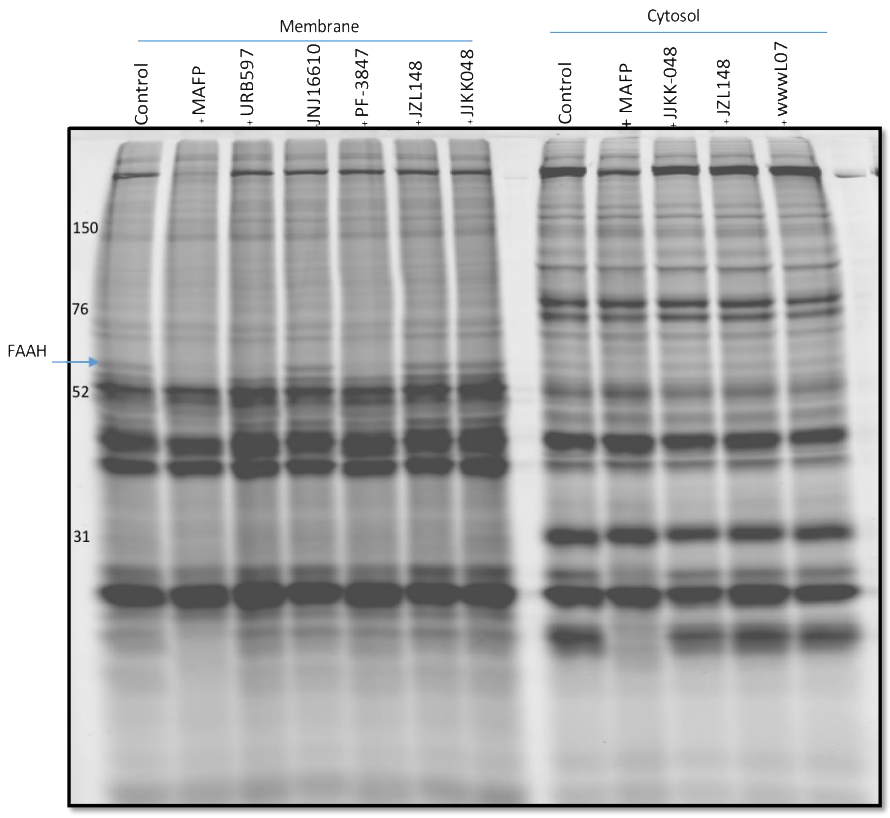

Figure 6.6. Investigation of MAGL and FAAH activities in MCF-7 cell line by competitive ABPP. MCF-7 cytosolic and membrane fractions were pre-incubated with DMSO or selective inhibitors for 15 min, followed by the addition of 500 nM of TAMRA-FP and resolved using SDS-PAGE (25 µg protein per lane. The experiment was repeated three times with very similar trends.

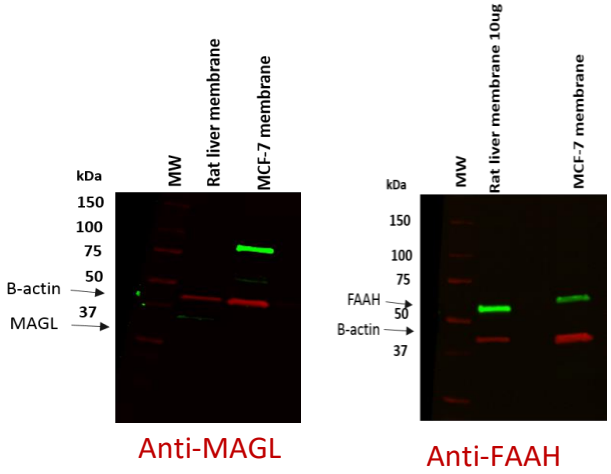

Figure 6.7: immunoblotting showed FAAH expression in MCF-7 cell line. Data represent immunostaining for each target protein and the reference protein β-actin. Molecular weight ladders can be seen in the far left hand lane on each blot. The experiment was repeated three times similar results.

Collectively, ABPP and immunoblotting revealed that FAAH was expressed in MCF-7 cells. A further investigation was conducted using combinations of the FAAH inhibitors with doxorubicin using Resazurin dye. There was no significant difference on the cell growth of MCF-7 treated with 500 nM of doxorubicin alone or mixed with 1 µM of either MAFP, URB579 or JNJ1661010 inhibitors ($P<0.05$). 100 nM of Doxorubicin showed significant reduction on MCF-7 cell viability($**** P \leq 0.0001$). However, when MCF-7 cells were treated with a lower concentration of doxorubicin (100 nM) in combination with 1 µM URB597 or JNJ1661010, these inhibitors showed

significant protective effects against doxorubicin (**P≤0.001), by 25 % compared to doxorubicin alone (see figure 6.8).

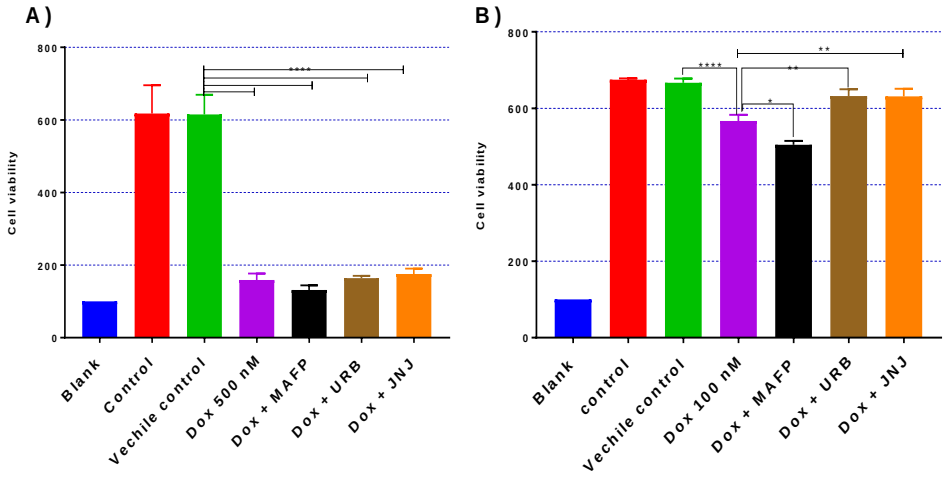

Figure 6.8. Assessing the protective effect of FAAH inhibitors on the MCF-7 cells growth. MCF-7 cells were treated with 1 µM of selective inhibitors mixed with either; A) 500 nM or B) 100 nM of doxorubicin for 72 h. Afterward, the cell growth of MCF-7 was measured by Resazurin dye. Data were collected in triplicate from six independent experiments, normalized and expressed as a % baseline. Statistical analysis was performed using a one-way ANOVA with Dunnett's multiple comparisons test (* $P \leq 0.05$, ** $P \leq 0.001$, **** $P \leq 0.0001$).

6.4.2 Migration of the MCF-7 cells

6.4.2.1 Cytochalasin D concentration effect on MCF-7 cells

Cytochalasin D was used a reference control in a migration study on MCF-7 cells at two different concentrations (10µM or 10nM), measuring F-actin staining by rhodamine- phallloidin and nuclei staining by DAPI. As a representative image showed, 10 µM cytochalasin D led to complete distribution of nuclei integrity and actin filaments in human MCF-7 cells, common apoptotic morphological changes. In contrast, it was observed that lower concentration of

cytochalasin D (10 nM) caused little disruption of F-actin in MCF-7 cells compared to control cells (see figure 6.9).

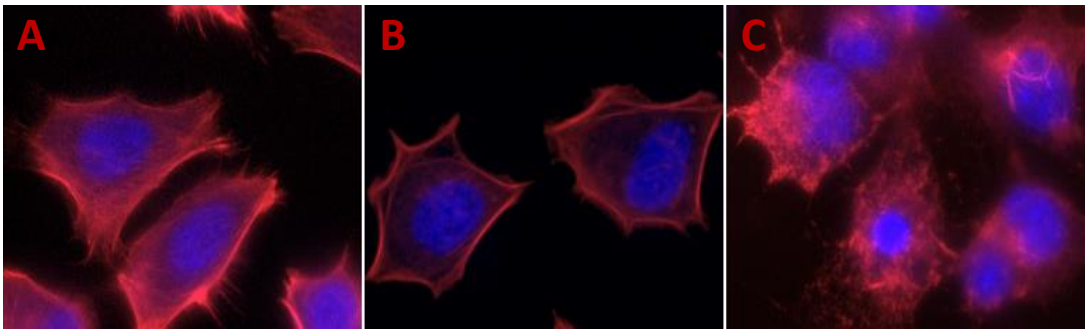

Figure 6.9: Fluorescent microscopy images of the distribution of actin polymerization in MCF-7 cells by Cytochalasin D. Cells were grown on a glass coverslip for 24 h until 80% confluence, washed and treated with: A) vehicle, B) 10 nM cytochalasin D or, C) 10 µM cytochalasin D for 16 h. Afterwards, cells were permeabilized with Triton-x-100 and stained with rhodamine-phalloidin to visualize the F-actin (red channel) and DAPI to highlight the nucleus (blue channel). This experiment was repeated three times and each time the images were identical.

6.4.2.2 Effect of FAAH inhibition on MCF-7 cell migration

Cells were allowed to migrate into an exclusion region of fixed diameter in the centre of the well. In the illustrative images shown, the difference in zone area in which MCF-7 cell migration occurred at 0 time (3.930 mm^2) and after 24 h (2.396 mm^2) was 1.53 mm^2 for control. The difference in areas at 0 time (3.930 mm^2) and 24 h (2.448 mm^2) was 1.48 mm^2 for cells treated with 1 µM URB597. In addition, the difference in areas at 0 time (3.930 mm^2) and 24 h (2.453 mm^2) was 1.48 mm^2 for the cells treated with 1 µM JNJ1661010. These data indicate that untreated and treated cells have similar migration rates. With 10 nM of cytochalasin D (positive control), the motility of MCF-7 ceased after 24 h.

I)

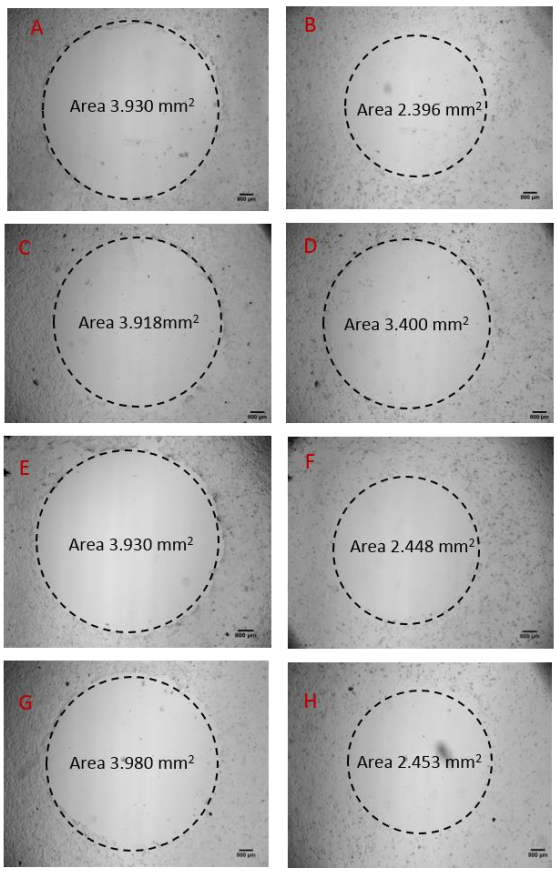

II)

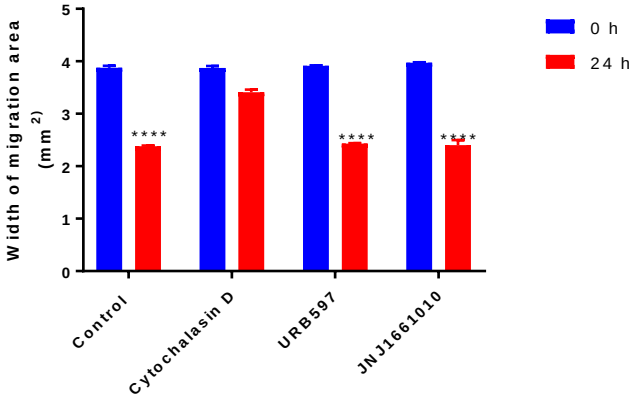

Figure 6.10.I and II. The inhibitory effect of FAAH on the MCF-7 cell migration process. I) The circular black line illustrates the empty area at time 0 h. A) the area of control group at 0 h (3.930 mm^2), B) the area of control group at 24 h, C) The area of treated cells with 10 nM cytochalasin D at 0 h (3.930 mm^2), D) the area of treated cells with 10 nM cytochalasin D at 24 h (3.400 mm^2), and the cells ceased migration into the empty area. E) the area of treated cells with 1 µM URB597 at 0 h (3.930 mm^2), F) the area of treated cells with 1 µM at 24 h (2.448 mm^2), G) The area of treated cells with 1 µM JNJ1661010 at 0 h(3.930 mm^2), F) the area of treated cell with 1 µM JNJ1661010 at 24 h (2.453 mm^2), clearly cells migrated rapidly into the empty area, (Scale bar = 800 µM). The experiment was repeated three times and each time the results were consistent. II) Migration area of 0 h and 24 h comparison.

6.5 Discussion

Inhibition of FAAH activity has no direct functional impact on human MCF-7 breast adenocarcinoma cell proliferation or migration.

6.5.1 Influence of selective FAAH inhibitors on MCF-7 proliferation rate

Proliferation can be defined as increased division and number of cells. Data from the current study provide evidence that URB597 or JNJ1661010 treatment, leading to FAAH inhibition, had no influence on the proliferation rate of MCF-7 cells. MCF-7 cells were adapted to grow in a low-serum culture medium (1%) to decrease oestrogen exposure from FBS, as described previously (Chappell et al., 2001) , and subsequently they grew at a reduced rate. This permits the cells to be used for experiments investigating the effects of selective FAAH and MAGL inhibitors on MCF-7 cells. It was reported that FBS contains steroid hormones as growth promoters such as insulin and estradiol according to the manufacture sheet from Sigma company and (Butler et al., 1981) , which stimulates oestrogen receptors on breast cancer cell line to enter the cell cycle (Dees et al., 1997).

Although FAAH inhibition did not appear to have any effects, these cells express FAAH enzyme abundantly as found by ABPP and immunoblotting. In agreement with our results, several studies reported the expression of FAAH in breast cancer cell lines (DI MARZO et al., 2001; Jessani et al., 2002; Li et al., 2013). Moreover, Jessani et al., (2002) found that, by using the ABPP technique, FAAH can be used a marker representative of differences in breast cancer cell behaviour. FAAH activity was exclusively detectable in the poorly invasive

breast cancer cell line (MCF-7), whereas its activity level was downregulated in the invasive breast carcinoma lines (MDA-MB-231) (Jessani et al., 2002).

However, FAAH inhibition, in the present study, was shown to prevent the reduction in cell viability. This effect was only observed when MCF-7 cancer cells were treated with a combination of FAAH inhibitors (URB597 or JNJ1661010) and low concentrations of an antineoplastic agent (doxorubicin, 100 nM). FAAH inhibitors showed increases in cell proliferation by 25% relative to the cells treated with doxorubicin alone. Doxorubicin actively interferes with the function of DNA leading to its damage and cell death (Thorn et al., 2011). The mechanism of FAAH inhibition observed in the current study can be possibly explained by the Li et al. (2013) published study. It was reported that inhibition of FAAH by URB597 and treatment by AEA activate the transcription factor NF-E2-related factor 2 (Nrf2), leading to induction of heme oxygenase-1 (HO-1)(Li et al., 2013). Ho-1 belongs to the rate limiting enzymes of heme catabolism and it is known also as a stress-responsive protein (Elbirt et al., 1999). As a result , activation of Nrf2/HO-1 pathway has been shown to have pro-proliferative and anti-apoptotic effects on MCF-7 cells (Li et al., 2013). Controversially, it was found that, using the MTT assay, treatment with AEA (more than 10 μM) exhibited antiproliferative effects in MCF-7 cells, leading to alteration in Ca^{2+} uptake in MCF-7 cells (Vercelli et al., 2014). These data suggest that at a low concentration AEA exerts a pro-proliferation effect, and at a high concentration, AEA exerts an anti-proliferative effect.

Changes in signalling for apoptosis or proliferation have been associated with drug resistance. Prior studies found that activation of Nrf2 signalling partially participates in the enhancement of acquired resistance to doxorubicin

(Zhong et al., 2013; Tsou et al., 2015). Taken together, FAAH selective inhibitor treatments, such as URB579 and JNJ1661010, may increase the expression of Nrf2 signalling and enhance resistance of MCF-7 cells to doxorubicin. Therefore, FAAH inhibition exerts cyto-protective effects on MCF-7 cells, which may eliminate it as a potential therapeutic target.

Furthermore, it was found that, from the current study, JZL184 and JJKK-048 had no effect on MCF-7 proliferation, consistent with the absence of MAGL activity and protein expression in these cells. In a study of a similar manner, MAGL activity was undetectable in MCF-7 nonaggressive breast cancer cells, while its activity was increased in an aggressive form of breast cancer (231MFP) (Nomura et al., 2010). It was suggested that MAGL activity could be one feature of advanced forms of breast cancer.

6.5.2 Influence of selective FAAH inhibitors on MCF-7 cell migration.

Cancer cell motility is one of the hallmarks of the transition to metastasis, which is mediated by the actin cytoskeleton (F-actin) (Laezza et al., 2008). Identifying the factors involved in the regulation of migratory activity of MCF-7 cells, in order to prevent metastasis, is an essential step in the development of breast cancer therapy.

Cytochalasin D is a mycotoxin that inhibits actin polymerization through the disruption of actin microfilaments (Cooper, 1987). It also arrests the cycle development at the point of the G1-S transition (Trendowski, 2015). Therefore, in the present study, Cytochalasin D was used as a positive control. It is found that at non-cytotoxic concentrations (10 nM), cytochalasin D was able to significantly decrease the levels of migration of MCF-7 cell line. The present

study is the first study to our knowledge to show that treatment of MCF-7 with selective FAAH inhibitors, URB597 and JNJ1661010, have no effect on the migration activity of these cells compared to cytochalasin D. These results were achieved despite abundant FAAH activity in MCF-7 cells. Previous studies reported that AEA inhibited the migration and invasion of MDA-MB-231 cells, a highly invasive human breast cancer cell, directly by impairing actin polymerization independent of CB receptor (Laezza et al., 2008), or through a CB_1 receptor dependent manner (Grimaldi et al., 2006). However, the effect of AEA treatment on MCF-7 cell migration, a less invasive cancer cell than MDA-MB-231, has not been determined yet. (Li et al., 2013) study examined the endogenous level of eCBs, and found that MCF-7 does not accumulate AEA. Therefore, it can be speculated that FAAH inhibition has no direct effect on MCF-7 cell migration, which may be due to the absence of AEA production in these cells.

A future investigation to assess the influence of FAAH inhibition on migratory activity of a highly invasive human breast cancer cell is warranted. In addition, it would be useful when considering measuring AEA and 2-AG in the medium of the MCF-7 cells to see if they are released. This helps to gain more understanding of the potential role of ECS in the proliferation and migratory activity of MCF-7.

Chapter 7 General Discussion

The endocannabinoid system has been identified as potentially vital in regulation of the cardiovascular system, particularly of vascular function but much less is known about its role in blood cells. Thus, the principal objective of this thesis was to achieve a greater understanding of the expression of MAGL and FAAH activities in different blood cells, as an essential prelude to investigating their potential roles in both physiological and pathological conditions in these entities.

Before beginning a full-scale characterisation of MAGL and FAAH activities in human blood cells, advantage was taken of access to rat vascular tissues to optimise the radiometric assay and ABPP approaches. This tissue is more freely available without the same ethical requirements associated with obtaining human tissues and allowed the assessment of enzyme activities in crude tissue homogenate containing a mixture of various enzymes making use of alternative substrates. Male Wistar rat mesenteric arteries were investigated in a collaboration with Dr Vanessa Ho (St George's, University of London), who had previously accumulated data suggesting a role for FAAH activity, in particular, in mesenteric vascular function. A primary finding from this study using both radiometric and ABPP assays was that FAAH activity in rat mesenteric activities changed with age of the animal, unlike MAGL, which suggests that turnover of N-acylethanolamines (such as AEA), but not monoacylglycerols (such as 2-AG), hydrolysis is influenced by age. Considering both our and Vanessa's studies suggests that increasing FAAH activity with age in mesenteric arteries is associated with endothelium dysfunction. Since AEA causes vasorelaxation of rat (Stanley et al., 2014a) and human (Stanley et al.,

2016) mesenteric arteries, this suggests targeting FAAH might function to limit the impact of vascular ageing. In a parallel study, the activity of these enzymes was also detectable in rat blood samples with higher activity levels compared to vascular tissues, implying an influence of blood cell and tissue activities on eCB responses.

As an alternative to the radiometric and ABPP assays, a spectrophotometric assay was described by Ulloa et al. (2010) as a precise and cheap assay for MAGL activity using the purified enzyme. However, we found this assay to be less useful when using complex sources, such as rat vascular tissue, as the substrate 1-ATG appeared to be hydrolysed not only by MAGL, but also other enzymes.

Following the appropriate ethical approval process, radiometric and ABPP approaches were used to study the expression profile of MAGL and FAAH in human blood samples from healthy volunteers of both sexes, a range of ages and BMIs. It was important to ensure all subjects were on the same baseline by avoiding eating, drinking alcohol and doing exercise prior to blood sampling. In these studies, MAGL and FAAH activities were reproducible within-subjects over three visits, and their activity levels were similar between males and females regardless of age, BMI and alcohol consumption. 2-OG hydrolysis profile in whole blood samples is relatively similar between two species, humans and rats.

FAAH activity was consistently stable within human subjects, while there was a potential variation between subjects (CV of 20%). This contrasts with a study which showed no difference between FAAH mRNA levels isolated from heathy

volunteers' whole blood samples regardless of age and gender (Tanaka et al., 2007). This may be a factor of the anucleate feature of platelets and erythrocytes, which contribute to FAAH activities and further demonstrates the need to measure enzyme activity levels instead of gene transcription.

Being able to measure MAGL and FAAH activities in human blood samples provides potentially useful biomarkers for clinical studies on humans. The assay and steps described in this thesis provide a basis for design of validated process steps, including the isolation of blood components followed by storage at -196 ^{o}C to minimize degradation of the enzyme activities. Thus, the studies described appear to have defined an acceptable strategy for measuring FAAH and MAGL enzyme activities in human blood for clinical studies, at least for basic research purposes *in vitro*.

A limiting factor on the speed of investigation on the endocannabinoid system is the lack of a reliable and cost-effective tool to detect enzyme activities. Based on the data in this thesis, FP-rhodamine has been shown to be a practical method to study the expression profile of serine hydrolase enzymes in human samples, as it is repeatable, simple, accurate, accessible and cost-effective. Further potential exploitation of the technique could focus on micro-scaling; whether it is possible to use a minute volume of blood samples; whether in ABPP, samples will continue to be scanned using a spectrophotometer before quantifying the enzymes or if there will be an alternative normalisation process possible in the future. If these technical questions are solvable, ABPP is a feasible assay that could be utilised as a diagnostic test in regular hospital pathology laboratories or even in the community (for the first step).

Our study also identified that platelets feature high MAGL activity expression compared to other blood fractions. This complements the reported role of MAGL in partially causing platelet aggregation, as described by Malorni et al. (2004) and Keown et al. (2010). This suggests any disruption of MAGL activity may cause clotting complication. Meanwhile, FAAH activity is expressed at much lower activity levels in platelets, which supports it lacking a function in platelet aggregation, as Fasia et al. (2003) reported. Whether enzyme inhibitors or natural mutations in these enzymes are associated with alterations in platelet function should be a subject of future investigation.

Erythrocytes, however, feature higher FAAH activity expression than platelets. It was previously reported that AEA induces death of erythrocytes (Bentzen et al., 2007). Taken together with our results, this raises the possibility that FAAH helps eliminate AEA from the extracellular space and subsequently extends erythrocyte lifespan.

These enzymes are distributed differently during the blood clotting process, potentially responding to vascular injury to maintain hemostasis. FAAH activity is released to the serum as a result of proteolysis of platelets or erythrocytes, or both, possibly contributing to metabolism of relaxatory AEA and other N-acylethanolamines, thereby inducing vasoconstriction and decreasing blood flow to the area. MAGL activity appears to be mildly decreased by the influence of proteins generated during clotting, such as thrombin. A scenario can be summarized as a clotting process changing the distribution of FAAH and MAGL enzymes, which might initiate vasoconstriction cascade of blood vessels and platelet aggregation, respectively, to ultimately lead to wound healing. Collectively, it is shown that activity level is a reliable marker able to provide

information on these enzymes, specifically FAAH used as platelet activation marker, in blood clotting. It should be considered that long-term therapy targeting these enzymes may inhibit platelet and erythrocyte function, hence caution is advisable for further clinical study.

After identifying FAAH and MAGL expression in different blood fractions, work was done to investigate further the functional impact of extended enzyme inhibition. Since long term investigations of anucleate erythrocytes and platelets is not possible, these studies were continued using breast cancer cells. Different stages of breast cancer have different enzyme expression profiles, as a study in this thesis showed that FAAH but not MAGL, activity is expressed in MCF-7. Meanwhile, MAGL was reportedly expressed in more aggressive breast cancer cells (Nomura et al., 2010).

Despite FAAH expression in these cells, pharmacological inhibition of FAAH by URB597 and JNJ1661010 had no effect on cell proliferation and migration. However, FAAH inhibitors exerted a minor protective effect, by increasing cell proliferation, but only when co-administrated with low concentrations of the antineoplastic agent doxorubicin. Therefore, it may suggest that FAAH inhibition is unsuitable as a therapeutic target for certain types of cancer, such as breast ductal carcinoma.

Limitations and future studies

Despite the ability of ABPP to detect MAGL activity in platelets (described in the section above), it failed to detect the low activity level of FAAH as described in animal tissues and human blood in Chapters 3, 4 and 5. When the activity level of FAAH is relatively high, for example in the MCF-7 cancer cell line, ABPP was able to detect its activity. To overcome this problem, a fluorescent irreversible probe selective for FAAH and MAGL can be used in the future study. For example, LEI-463 is a selective MAGL probe that visualizes MAGL activity in cancer cell lines and animal tissues, developed by Jiang et al. (2018 presented at ICRS 2018). Some other benefits of this approach include avoiding the need for blood separation, scaling down the volume of samples ideally to have pinprick blood samples.

From **Chapter 4**, a 20% variation of FAAH activity between subjects was observed. However, this study was not designed to investigate the correlation of FAAH activity in blood samples with other factors, and to-date there is no human study to have done so. Therefore, a correlation between circulating FAAH activity and factors such as age are worth considering in future studies. From our study, the correlation coefficient of -0.184 was calculated. Stdev of age was equal to 9.2, and Stdev of enzyme activity was equal to 9.7. These suggest that a pilot study can be done. According to (Julious, 2005) and (Moore et al., 2011) it is suggested that at least 12 participants should be included in each group, if we divided the age groups into three groups (younger adults, middle aged adults and older adults), an a priori sample size of 36 individuals was estimated. A future study would, therefore, need to recruit at least 36 individuals over a spread of ages to test the hypothesis of an age-related change in blood FAAH activities.

Data from **Chapter 4** suggested that high FAAH activity might play a role in maintaining erythrocyte lifespan**.** A previous study found that T-lymphocytes isolated from subjects with an FAAH gene variant (C386A polymorphism) have roughly a 50% reduction in protein and enzymatic activity compared to wild-type T-lymphocytes (Chiang et al., 2004)**.** Therefore, an interesting question arises here, whether expressing the polymorphism of FAAH affects erythrocyte lifespan. This would be a novel study, studying amino acid sequence alterations helps to recognize essential genetic changes, which may alter the lifespan of erythrocytes. The measurement of erythrocytes' lifespan can be taken by labelling a representative sample of erythrocytes by biotin, nonradioactive covalent label and then biotin-labelled erythrocytes quantified relative to the total erythrocytes by flow cytometry in percentage terms (Franco, 2012).

It has been proposed here that MAGL activity can be used as a potential biomarker for disease using ABPP as a diagnostic tool. Despite being around 20% variation between-subjects, MAGL activity could still be considered as a biomarker provided that the level of MAGL in subjects with disease is significantly higher or lower than in healthy subjects. One disorder that can be considered is migraine, which is the most prevalent neurological disorder, characterized by a unilateral hemicranial pulsating headache that usually has various symptoms, for example, sensory disturbances and nausea. It can occur due to a set of genetic, environmental and epigenetic factors (Ferroni et al., 2018; Greco et al., 2018).

MAGL and FAAH modify pain perception via regulating eCB tone, and an atypical pain threshold is also responsible for the onset of tension-type headaches. Looking more closely at the migraine pathogenesis, Calcitonin gene-

related peptide (CGRP), an inflammatory mediator, plays a critical role in the pathogenesis of migraine. It is secreted from sensory nerves, dilates and disturbs blood vessels, culminating in the secretion of other neuropeptides and increased pain impulses sent to the nucleus trigeminalis caudalis. As a result, this sends pain signals to brain centres (e.g. cortex and thalamus). In this pathway, NO plays a role in activating perivascular sensory afferent nerve fibres in the meninges to stimulate neuropeptides release. The root of migraine is an interrelation of internal and external triggers in thalamus and brainstem, the latter of which has the most AEA in CNS, regulating pain sensation (Greco et al., 2018).

Many studies have described the interaction of eCB with NO and CGRP as playing a critical role in migraine development in clinical studies, reviewed by (Greco et al., 2018; Leimuranta et al., 2018). In addition, platelets are also reported to contribute to the development of afferent sensitization by releasing inflammatory mediators at the site of tissue injury, where FAAH activity was higher in female migraineurs than healthy females (Cupini et al., 2006). Current standards of migraine care are at best moderately effective and, occasionally, not especially tolerable. In particular, prophylactic treatments (beta blockers, antiepileptic drugs) can lead to weight gain and cognitive disturbances (Greco et al., 2018).

MAGL and FAAH activities were high in animal migraine models, and it has been shown that blocking MAGL causes a reduction in pain behaviours (Leimuranta et al., 2018).

While there are global diagnostic criteria, migraine remains a complex disorder that is underdiagnosed, misdiagnosed and more effective therapeutic approaches

are impeded by the lack of appropriate biomarkers, which ultimately, may facilitate the goal of individualized medicine by helping clinicians to better diagnose migraine (Durham et al., 2013). CGRP levels in plasma, measured by enzyme linked immunosorbent assay, are the most relevant biomarker for migraine yet identified (Durham et al., 2013). However, there are several disadvantages of using this method as it is time-consuming and expensive (Lee et al., 2018). Since it is found in this thesis that MAGL activity can be easily visualized from platelet samples using ABPP, MAGL can be tested as a possible biomarker for migraine using ABPP for detection.

Conclusion

These novel results provide evidence that MAGL and FAAH activities are reproducible in human blood samples, and that their functional expression varies during normal patho/physiological processes, such as clotting. Furthermore, it was illustrated that there are no effects on MCF-7 cells caused by inhibiting FAAH or MAGL. These studies provide an acceptable practice method for ongoing clinical study using enzyme expression as a possible biomarker considering the ABPP technique as a diagnostic tool.

References

Aaltonen N, Kedzierska E, Orzelska-Górka J, Lehtonen M, Navia-Paldanius D, Jakupovic H*, et al.* (2016). In Vivo Characterization of the Ultrapotent Monoacylglycerol Lipase Inhibitor {4-[bis-(benzo [d][1, 3] dioxol-5-yl) methyl]-piperidin-1-yl}(1H-1, 2, 4-triazol-1-yl) methanone (JJKK-048). Journal of Pharmacology and Experimental Therapeutics 359**:** 62-72.

Aaltonen N, Savinainen JR, Ribas CR, Rönkkö J, Kuusisto A, Korhonen J*, et al.* (2013). Piperazine and piperidine triazole ureas as ultrapotent and highly selective inhibitors of monoacylglycerol lipase. Chemistry & biology 20**:** 379-390.

Adler DH, Cogan JD, Phillips JA, Schnetz-Boutaud N, Milne GL, Iverson T*, et al.* (2008). Inherited human cPLA 2α deficiency is associated with impaired eicosanoid biosynthesis, small intestinal ulceration, and platelet dysfunction. The Journal of clinical investigation 118**:** 2121-2131.

Aguado T, Monory K, Palazuelos J, Stella N, Cravatt B, Lutz B*, et al.* (2005). The endocannabinoid system drives neural progenitor proliferation. The FASEB journal 19**:** 1704-1706.

Ahn K, Johnson DS, Mileni M, Beidler D, Long JZ, McKinney MK*, et al.* (2009). Discovery and characterization of a highly selective FAAH inhibitor that reduces inflammatory pain. Chemistry & biology 16**:** 411-420.

Ahn K, Smith SE, Liimatta MB, Beidler D, Sadagopan N, Dudley DT*, et al.* (2011). Mechanistic and pharmacological characterization of PF-04457845: a highly potent and selective fatty acid amide hydrolase inhibitor that reduces inflammatory and noninflammatory pain. Journal of Pharmacology and Experimental Therapeutics 338**:** 114-124.

Aleshcheva G, Sahana J, Ma X, Hauslage J, Hemmersbach R, Egli M*, et al.* (2013). Changes in morphology, gene expression and protein content in chondrocytes cultured on a random positioning machine. PLoS One 8**:** e79057.

Alexander JP, & Cravatt BF (2005). Mechanism of carbamate inactivation of FAAH: implications for the design of covalent inhibitors and in vivo functional probes for enzymes. Chemistry & biology 12**:** 1179-1187.

Alhouayek M, & Muccioli G (2017). Pharmacological Aspects of Anandamide and 2-Arachidonoyglycerol as Bioactive Lipids. In Handbook of Cannabis and Related Pathologies. Elsevier, pp 616-629.

Anderson NL (2010). The clinical plasma proteome: a survey of clinical assays for proteins in plasma and serum. Clinical chemistry 56**:** 177-185.

Anderson NL, & Anderson NG (2002). The human plasma proteome history, character, and diagnostic prospects. Molecular & Cellular Proteomics 1**:** 845-867.

Andrews RK, & Berndt MC (2004). Platelet physiology and thrombosis. Thrombosis research 114**:** 447-453.

Ayakannu T, Taylor AH, Marczylo TH, Willets JM, & Konje JC (2013). The endocannabinoid system and sex steroid hormone-dependent cancers. International Journal of Endocrinology 2013.

Baenke F, Peck B, Miess H, & Schulze A (2013). Hooked on fat: the role of lipid synthesis in cancer metabolism and tumour development. Disease models & mechanisms 6**:** 1353-1363.

Baguley BC, & Leung E (2011). Heterogeneity of phenotype in breast cancer cell lines. In Breast Cancer-Carcinogenesis, Cell Growth and Signalling Pathways. InTech.

Baldassarri S, Bertoni A, Bagarotti A, Sarasso C, Zanfa M, Catani M*, et al.* (2008). The endocannabinoid 2 - arachidonoylglycerol activates human platelets through non - CB1/CB2 receptors. Journal of Thrombosis and Haemostasis 6**:** 1772-1779.

Basavarajappa BS, Saito M, Cooper TB, & Hungund BL (2003). Chronic ethanol inhibits the anandamide transport and increases extracellular anandamide levels in cerebellar granule neurons. European journal of pharmacology 466**:** 73-83.

Basavarajappa BS, Yalamanchili R, Cravatt BF, Cooper TB, & Hungund BL (2006). Increased ethanol consumption and preference and decreased ethanol sensitivity in female FAAH knockout mice. Neuropharmacology 50**:** 834-844.

Bátkai S, Pacher P, Osei-Hyiaman D, Radaeva S, Liu J, Harvey-White J*, et al.* (2004). Endocannabinoids acting at cannabinoid-1 receptors regulate cardiovascular function in hypertension. Circulation 110**:** 1996-2002.

Bátkai S, Rajesh M, Mukhopadhyay P, Hasko G, Liaudet L, Cravatt BF*, et al.* (2007). Decreased age-related cardiac dysfunction, myocardial nitrative stress, inflammatory gene expression, and apoptosis in mice lacking fatty acid amide hydrolase. American Journal of Physiology-Heart and Circulatory Physiology 293**:** H909-H918.

Baumeister S, & Musacchio A (2018). Investigation of the properties of Acyl Protein Thioesterases and their role in Ras depalmitoylationTechnische Universität Dortmund Dortmund.

Bearer E, Prakash J, & Li Z (2002). Actin dynamics in platelets. International review of cytology 217**:** 137-182.

Becker DM, Segal J, Vaidya D, Yanek LR, Herrera-Galeano JE, Bray PF*, et al.* (2006). Sex differences in platelet reactivity and response to low-dose aspirin therapy. Jama 295**:** 1420-1427.

Belfiore F (1980). B. Enzyme Regulation in the Arterial Wall. In Enzyme Regulation and Metabolic Diseases. Karger Publishers, pp 498-505.

Bentzen PJ, & Lang F (2007). Effect of anandamide on erythrocyte survival. Cellular Physiology and Biochemistry 20**:** 1033-1042.

Bertrand T, Augé F, Houtmann J, Rak A, Vallée F, Mikol V*, et al.* (2010). Structural basis for human monoglyceride lipase inhibition. Journal of molecular biology 396**:** 663-673.

Bisogno T, Howell F, Williams G, Minassi A, Cascio MG, Ligresti A*, et al.* (2003). Cloning of the first sn1-DAG lipases points to the spatial and temporal regulation of endocannabinoid signaling in the brain. The Journal of cell biology 163**:** 463-468.

Bisogno T, Ligresti A, & Di Marzo V (2005). The endocannabinoid signalling system: biochemical aspects. Pharmacology Biochemistry and Behavior 81**:** 224-238.

Björklund E, Norén E, Nilsson J, & Fowler CJ (2010). Inhibition of monoacylglycerol lipase by troglitazone, N‐arachidonoyl dopamine and the irreversible inhibitor JZL184: comparison of two different assays. British journal of pharmacology 161**:** 1512-1526.

Blankman JL, Simon GM, & Cravatt BF (2007). A comprehensive profile of brain enzymes that hydrolyze the endocannabinoid 2-arachidonoylglycerol. Chemistry & biology 14**:** 1347-1356.

Blednov YA, Cravatt BF, Boehm II SL, Walker D, & Harris RA (2007). Role of endocannabinoids in alcohol consumption and intoxication: studies of mice lacking fatty acid amide hydrolase. Neuropsychopharmacology 32**:** 1570.

Blüher M, Engeli S, Klöting N, Berndt J, Fasshauer M, Bátkai S*, et al.* (2006). Dysregulation of the peripheral and adipose tissue endocannabinoid system in human abdominal obesity. Diabetes 55**:** 3053-3060.

Bojesen IN, & Hansen HS (2003). Binding of anandamide to bovine serum albumin. Journal of lipid research 44**:** 1790-1794.

Bojesen IN, & Hansen HS (2005). Membrane transport of anandamide through resealed human red blood cell membranes. Journal of lipid research 46**:** 1652-1659.

Boldrup L, Wilson SJ, Barbier AJ, & Fowler CJ (2004). A simple stopped assay for fatty acid amide hydrolase avoiding the use of a chloroform extraction phase. Journal of biochemical and biophysical methods 60**:** 171-177.

Bolen A, Naren AP, Yarlagadda S, Beranova-Giorgianni S, Chen L, Norman D*, et al.* (2011a). The phospholipase A1 activity of lysophospholipase AI links platelet activation to LPA production during blood coagulation. Journal of lipid research**:** jlr. M013326.

Bolen AL, Naren AP, Yarlagadda S, Beranova-Giorgianni S, Chen L, Norman D*, et al.* (2011b). The phospholipase A1 activity of lysophospholipase AI links platelet activation to LPA production during blood coagulation. Journal of lipid research 52**:** 958-970.

Börsch-Haubold AG, Kramer RM, & Watson SP (1995). Cytosolic phospholipase A2 is phosphorylated in collagen-and thrombin-stimulated human platelets independent of protein kinase C and mitogen-activated protein kinase. Journal of Biological Chemistry 270**:** 25885-25892.

Bortolato M, Mangieri RA, Fu J, Kim JH, Arguello O, Duranti A*, et al.* (2007). Antidepressant-like activity of the fatty acid amide hydrolase inhibitor URB597 in a rat model of chronic mild stress. Biological psychiatry 62**:** 1103-1110.

Boyer J, Somma C, Vérine A, L'HÔTE C, Finidori J, Merger C*, et al.* (1981). Human Erythrocyte Monoester Lipase: Characterization and Radiochemical Assay of the Cell-Bound Enzyme in Normal Subjects*. The Journal of Clinical Endocrinology & Metabolism 53**:** 143-148.

Brantl SA, Khandoga AL, & Siess W (2014a). Activation of platelets by the endocannabinoids 2-arachidonoylglycerol and virodhamine is mediated by their conversion to arachidonic acid and thromboxane A2, not by activation of cannabinoid receptors. Platelets 25**:** 465-466.

Brantl SA, Khandoga AL, & Siess W (2014b). Mechanism of platelet activation induced by endocannabinoids in blood and plasma. Platelets 25**:** 151-161.

Brindley DN, & Pilquil C (2009). Lipid phosphate phosphatases and signaling. Journal of lipid research 50**:** S225-S230.

Bry K, Kuusi T, Andersson LC, & Kinnunen PK (1979). Monoacylglycerol hydrolase in human platelets. FEBS letters 106**:** 111-114.

Buczynski MW, Herman MA, Hsu K-L, Natividad LA, Irimia C, Polis IY*, et al.* (2016). Diacylglycerol lipase disinhibits VTA dopamine neurons during chronic nicotine exposure. Proceedings of the National Academy of Sciences 113**:** 1086-1091.

Butler WB, Kelsey WH, & Goran N (1981). Effects of serum and insulin on the sensitivity of the human breast cancer cell line MCF-7 to estrogen and antiestrogens. Cancer research 41**:** 82-88.

Byrnes JR, & Wolberg AS (2017). Red blood cells in thrombosis. Blood**:** blood-2017-2003-745349.

Cable JC, Tan GD, Alexander S, & O'Sullivan SE (2011). The activity of the endocannabinoid metabolising enzyme fatty acid amide hydrolase in subcutaneous adipocytes correlates with BMI in metabolically healthy humans. Lipids Health Dis 10**:** 10.1186.

Canobbio I, Cipolla L, Consonni A, Momi S, Guidetti G, Oliviero B*, et al.* (2013). Impaired thrombin-induced platelet activation and thrombus formation in mice lacking the Ca2+-dependent tyrosine kinase Pyk2. Blood 121**:** 648-657.

Catani MV, Gasperi V, Evangelista D, Agro AF, Avigliano L, & Maccarrone M (2010). Anandamide extends platelets survival through CB1-dependent Akt signaling. Cellular and molecular life sciences 67**:** 601-610.

Chappell J, Leitner JW, Solomon S, Golovchenko I, Goalstone ML, & Draznin B (2001). Effect of insulin on cell cycle progression in MCF-7 breast cancer cells Direct and potentiating influence. Journal of Biological Chemistry 276**:** 38023-38028.

Chau L-Y, & Tai H-H (1988). Monoglyceride and diglyceride lipases from human platelet microsomes. Biochimica et Biophysica Acta (BBA)-Lipids and Lipid Metabolism 963**:** 436-444.

Chaudhry R, & Babiker HM (2018). Physiology, Coagulation Pathways. In StatPearls [Internet]. StatPearls Publishing.

Chen B, Ge S-S, Zhao Y-C, Chen C, & Yang S (2016). Activity-based protein profiling: an efficient approach to study serine hydrolases and their inhibitors in mammals and microbes. RSC Advances 6**:** 113327-113343.

Chiang KP, Gerber AL, Sipe JC, & Cravatt BF (2004). Reduced cellular expression and activity of the P129T mutant of human fatty acid amide hydrolase: evidence for a link between defects in the endocannabinoid system and problem drug use. Human molecular genetics 13**:** 2113-2119.

Chicca A, Marazzi J, Nicolussi S, & Gertsch J (2012). Evidence for bidirectional endocannabinoid transport across cell membranes. Journal of biological chemistry**:** jbc. M112. 373241.

Cohen B, & Gibor Y (1980). Anemia and menstrual blood loss. Obstetrical and Gynecological Survey 35**:** 597-618.

Comşa Ş, Cimpean AM, & Raica M (2015). The story of MCF-7 breast cancer cell line: 40 years of experience in research. Anticancer research 35**:** 3147-3154.

Cooper JA (1987). Effects of cytochalasin and phalloidin on actin. The Journal of cell biology 105**:** 1473-1478.

Coriell LL (1979). [3] Preservation, storage, and shipment. In Methods in enzymology. Elsevier, pp 29-36.

Cortelazzo A, De Felice C, Pecorelli A, Belmonte G, Signorini C, Leoncini S*, et al.* (2014). Beta-actin deficiency with oxidative posttranslational modifications in Rett syndrome erythrocytes: insights into an altered cytoskeletal organization. PloS one 9**:** e93181.

Cote M, Matias I, Lemieux I, Petrosino S, Almeras N, Despres J*, et al.* (2007). Circulating endocannabinoid levels, abdominal adiposity and related cardiometabolic risk factors in obese men. International journal of obesity 31**:** 692.

Cravatt BF, Demarest K, Patricelli MP, Bracey MH, Giang DK, Martin BR*, et al.* (2001). Supersensitivity to anandamide and enhanced endogenous cannabinoid signaling in mice lacking fatty acid amide hydrolase. Proc Natl Acad Sci U S A 98**:** 9371-9376.

Cravatt BF, Giang DK, Mayfield SP, Boger DL, Lerner RA, & Gilula NB (1996). Molecular characterization of an enzyme that degrades neuromodulatory fatty-acid amides. Nature 384**:** 83-87.

Cravatt BF, Prospero-Garcia O, Siuzdak G, Gilula NB, Henriksen SJ, Boger DL*, et al.* (1995). Chemical characterization of a family of brain lipids that induce sleep. Science 268**:** 1506-1509.

Crawley J, Zanardelli S, Chion C, & Lane D (2007). The central role of thrombin in hemostasis. Journal of thrombosis and haemostasis 5**:** 95-101.

Cupini L, Bari M, Battista N, Argiro G, Finazzi-Agro A, Calabresi P*, et al.* (2006). Biochemical changes in endocannabinoid system are expressed in platelets of female but not male migraineurs. Cephalalgia 26**:** 277-281.

Dai X, Cheng H, Bai Z, & Li J (2017). Breast cancer cell line classification and its relevance with breast tumor subtyping. Journal of Cancer 8**:** 3131.

Das A, Dikshit M, & Nath C (2001). Profile of acetylcholinesterase in brain areas of male and female rats of adult and old age. Life sciences 68**:** 1545-1555.

Dashkevich N, Ovanesov M, Balandina A, Karamzin S, Shestakov P, Soshitova N*, et al.* (2012). Thrombin activity propagates in space during blood coagulation as an excitation wave. Biophysical journal 103**:** 2233-2240.

De Angelis V, Koekman AC, Weeterings C, Roest M, de Groot PG, Herczenik E*, et al.* (2014). Endocannabinoids control platelet activation and limit aggregate formation under flow.

De Fonseca FR, Navarro M, Gomez R, Escuredo L, Nava F, Fu J*, et al.* (2001). An anorexic lipid mediator regulated by feeding. Nature 414**:** 209.

De Petrocellis L, Bisogno T, Ligresti A, Bifulco M, Melck D, & Di Marzo V (2002). Effect on cancer cell proliferation of palmitoylethanolamide, a fatty acid amide interacting with both the cannabinoid and vanilloid signalling systems. Fundamental & clinical pharmacology 16**:** 297-302.

De Petrocellis L, Melck D, Palmisano A, Bisogno T, Laezza C, Bifulco M*, et al.* (1998). The endogenous cannabinoid anandamide inhibits human breast cancer cell proliferation. Proceedings of the National Academy of Sciences 95**:** 8375-8380.

Dees C, Askari M, Foster JS, Ahamed S, & Wimalasena J (1997). DDT mimicks estradiol stimulation of breast cancer cells to enter the cell cycle. Molecular Carcinogenesis: Published in cooperation with the University of Texas MD Anderson Cancer Center 18**:** 107-114.

Deutsch DG (2016). A personal retrospective: elevating anandamide (AEA) by targeting fatty acid amide hydrolase (FAAH) and the fatty acid binding proteins (FABPs). Frontiers in pharmacology 7**:** 370.

Deutsch DG, Omeir R, Arreaza G, Salehani D, Prestwich GD, Huang Z*, et al.* (1997). Methyl arachidonyl fluorophosphonate: a potent irreversible inhibitor of anandamide amidase. Biochemical pharmacology 53**:** 255-260.

Devedjiev Y, Dauter Z, Kuznetsov SR, Jones TL, & Derewenda ZS (2000). Crystal structure of the human acyl protein thioesterase I from a single X-ray data set to 1.5 Å. Structure 8**:** 1137-1146.

Di Cera E (2003). Thrombin interactions. Chest 124**:** 11S-17S.

Di Marzo V, Bifulco M, & De Petrocellis L (2004). The endocannabinoid system and its therapeutic exploitation. Nature reviews Drug discovery 3**:** 771.

DI MARZO V, MELCK D, ORLANDO P, BISOGNO T, ZAGOORY O, BIFULCO M*, et al.* (2001). Palmitoylethanolamide inhibits the expression of fatty acid amide hydrolase and enhances the anti-proliferative effect of anandamide in human breast cancer cells. Biochem J 358**:** 249-255.

Dinh T, Carpenter D, Leslie F, Freund T, Katona I, Sensi S*, et al.* (2002). Brain monoglyceride lipase participating in endocannabinoid inactivation. Proceedings of the National Academy of Sciences 99**:** 10819-10824.

Dlugos A, Childs E, Stuhr KL, Hillard CJ, & de Wit H (2012). Acute stress increases circulating anandamide and other N-acylethanolamines in healthy humans. Neuropsychopharmacology 37**:** 2416-2427.

Done SJ (2011). Breast Cancer-Recent Advances in Biology, Imaging and Therapeutics.

Durham P, & Papapetropoulos S (2013). Biomarkers associated with migraine and their potential role in migraine management. Headache: The Journal of Head and Face Pain 53**:** 1262-1277.

Edgemond WS, Hillard CJ, Falck J, Kearn CS, & Campbell WB (1998). Human platelets and polymorphonuclear leukocytes synthesize oxygenated derivatives of arachidonylethanolamide (anandamide): their affinities for cannabinoid receptors and pathways of inactivation. Molecular pharmacology 54**:** 180-188.

Elbirt KK, & Bonkovsky HL (1999). Heme oxygenase: recent advances in understanding its regulation and role. Proceedings of the Association of American Physicians 111**:** 438-447.

Ellis EF, Moore SF, & Willoughby KA (1995). Anandamide and delta 9-THC dilation of cerebral arterioles is blocked by indomethacin. American Journal of Physiology-Heart and Circulatory Physiology 269**:** H1859-H1864.

Engeli S, Böhnke J, Feldpausch M, Gorzelniak K, Janke J, Bátkai S*, et al.* (2005). Activation of the peripheral endocannabinoid system in human obesity. Diabetes 54**:** 2838-2843.

Erdozain AM, Rubio M, Valdizan EM, Pazos A, Meana JJ, Fernández-Ruiz J*, et al.* (2014). The endocannabinoid system is altered in the post‐mortem prefrontal cortex of alcoholic subjects. Addiction biology.

Everley PA, Gartner CA, Haas W, Saghatelian A, Elias JE, Cravatt BF*, et al.* (2007). Assessing enzyme activities using stable isotope labeling and mass spectrometry. Molecular & Cellular Proteomics 6**:** 1771-1777.

Fagundo AB, De la Torre R, Jiménez-Murcia S, Agüera Z, Pastor A, Casanueva FF*, et al.* (2013). Modulation of the endocannabinoids N-

Arachidonoylethanolamine (AEA) and 2-Arachidonoylglycerol (2-AG) on executive functions in humans.

Fanelli F, Di Lallo VD, Belluomo I, De Iasio R, Baccini M, Casadio E*, et al.* (2012). Estimation of reference intervals of five endocannabinoids and endocannabinoid related compounds in human plasma by two dimensional-LC/MS/MS. Journal of lipid research 53**:** 481-493.

Fasia L, Karava V, & Siafaka- Kapadai A (2003). Uptake and metabolism of [3H] anandamide by rabbit platelets. European Journal of Biochemistry 270**:** 3498-3506.

Fegley D, Gaetani S, Duranti A, Tontini A, Mor M, Tarzia G*, et al.* (2005). Characterization of the fatty acid amide hydrolase inhibitor cyclohexyl carbamic acid 3′ -carbamoyl-biphenyl-3-yl ester (URB597): effects on anandamide and oleoylethanolamide deactivation. Journal of Pharmacology and Experimental Therapeutics 313**:** 352-358.

Ferroni P, Barbanti P, Spila A, Fratangeli F, Aurilia C, Fofi L*, et al.* (2018). Circulating Biomarkers In Migraine. New Opportunities For Precision Medicine. Current medicinal chemistry.

Feuerecker M, Hauer D, Toth R, Demetz F, Hölzl J, Thiel M*, et al.* (2012). Effects of exercise stress on the endocannabinoid system in humans under field conditions. European journal of applied physiology 112**:** 2777-2781.

Fielding CJ (1981). Monoglyceride hydrolase activities of rat plasma and platelets. Their properties and roles in the activity of lipoprotein lipase. Journal of Biological Chemistry 256**:** 876-881.

Forget B, Coen KM, & Le Foll B (2009). Inhibition of fatty acid amide hydrolase reduces reinstatement of nicotine seeking but not break point for nicotine self-administration—comparison with CB 1 receptor blockade. Psychopharmacology 205**:** 613-624.

Fowler CJ, Doherty P, & Alexander SP (2017). Endocannabinoid turnover. In Advances in Pharmacology. Elsevier, pp 31-66.

Franco RS (2012). Measurement of red cell lifespan and aging. Transfusion medicine and hemotherapy 39**:** 302-307.

Freshney R (1987). Measurement of cytotoxicity and viability. Culture of animal cells 253**:** 254.

Gaoni Y, & Mechoulam R (1964). Isolation, structure, and partial synthesis of an active constituent of hashish. Journal of the American chemical society 86**:** 1646-1647.

Gasperi V, Avigliano L, Evangelista D, Oddi S, Chiurchiù V, Lanuti M*, et al.* (2014a). 2-Arachidonoylglycerol enhances platelet formation from human megakaryoblasts. Cell Cycle 13**:** 3938-3947.

Gasperi V, Ceci R, Tantimonaco M, Talamonti E, Battista N, Parisi A*, et al.* (2014b). The fatty acid amide hydrolase in lymphocytes from sedentary and active subjects. Medicine and science in sports and exercise 46**:** 24-32.

Gasperi V, Evangelista D, Chiurchiù V, Florenzano F, Savini I, Oddi S*, et al.* (2014c). 2-Arachidonoylglycerol modulates human endothelial cell/leukocyte interactions by controlling selectin expression through CB 1 and CB 2 receptors. The international journal of biochemistry & cell biology 51**:** 79-88.

Gerlier D, & Thomasset N (1986). Use of MTT colorimetric assay to measure cell activation. Journal of immunological methods 94**:** 57-63.

Ghafouri N, Tiger G, Razdan RK, Mahadevan A, Pertwee RG, Martin BR*, et al.* (2004). Inhibition of monoacylglycerol lipase and fatty acid amide hydrolase by analogues of 2 - arachidonoylglycerol. British journal of pharmacology 143**:** 774-784.

Gkini E, Anagnostopoulos D, Mavri-Vavayianni M, & Siafaka-Kapadai A (2009). Metabolism of 2-acylglycerol in rabbit and human platelets. Involvement of monoacylglycerol lipase and fatty acid amide hydrolase. Platelets 20**:** 376-385.

Godlewski G, Alapafuja SO, Bátkai S, Nikas SP, Cinar R, Offertáler L*, et al.* (2010). Inhibitor of fatty acid amide hydrolase normalizes cardiovascular function in hypertension without adverse metabolic effects. Chemistry & biology 17**:** 1256-1266.

Grazia Signorello M, Giacobbe E, Segantin A, Avigliano L, Sinigaglia F, Maccarrone M*, et al.* (2011). Activation of human platelets by 2-arachidonoylglycerol: role of PKC in NO/cGMP pathway modulation. Current neurovascular research 8**:** 200-209.

Greco R, Demartini C, Zanaboni AM, Piomelli D, & Tassorelli C (2018). Endocannabinoid System and Migraine Pain: An Update. Frontiers in neuroscience 12**:** 172.

Greten H, Levy RI, & Fredrickson DS (1969). Evidence for separate monoglyceride hydrolase and triglyceride lipase in post-heparin human plasma. Journal of lipid research 10**:** 326-330.

Grimaldi C, Pisanti S, Laezza C, Malfitano AM, Santoro A, Vitale M*, et al.* (2006). Anandamide inhibits adhesion and migration of breast cancer cells. Experimental cell research 312**:** 363-373.

Hansson AC, Bermúdez-Silva FJ, Malinen H, Hyytiä P, Sanchez-Vera I, Rimondini R*, et al.* (2007). Genetic impairment of frontocortical endocannabinoid degradation and high alcohol preference. Neuropsychopharmacology 32**:** 117-126.

Hayot C, Debeir O, Van Ham P, Van Damme M, Kiss R, & Decaestecker C (2006). Characterization of the activities of actin-affecting drugs on tumor cell migration. Toxicology and applied pharmacology 211**:** 30-40.

Herradón E, Martín M, & López‐Miranda V (2007). Characterization of the vasorelaxant mechanisms of the endocannabinoid anandamide in rat aorta. British journal of pharmacology 152**:** 699-708.

Heyman E, Gamelin F-X, Goekint M, Piscitelli F, Roelands B, Leclair E*, et al.* (2012). Intense exercise increases circulating endocannabinoid and BDNF levels in humans—possible implications for reward and depression. Psychoneuroendocrinology 37**:** 844-851.

Hillard CJ (2000). Endocannabinoids and vascular function. Journal of Pharmacology and Experimental Therapeutics 294**:** 27-32.

Hirabayashi T, & Shimizu T (2000). Localization and regulation of cytosolic phospholipase A 2. Biochimica et Biophysica Acta (BBA)-Molecular and Cell Biology of Lipids 1488**:** 124-138.

Ho WS, & Randall M (2007). Endothelium‐dependent metabolism by endocannabinoid hydrolases and cyclooxygenases limits vasorelaxation to anandamide and 2‐arachidonoylglycerol. British journal of pharmacology 150**:** 641-651.

Hoffbrand V, & Moss P (2011) *Essential haematology*. vol. 28. John Wiley & Sons.

Hoover HS, Blankman JL, Niessen S, & Cravatt BF (2008). Selectivity of inhibitors of endocannabinoid biosynthesis evaluated by activity-based protein profiling. Bioorganic & medicinal chemistry letters 18**:** 5838-5841.

Howley ET (2001). Type of activity: resistance, aerobic and leisure versus occupational physical activity. Medicine & Science in Sports & Exercise 33**:** S364-S369.

Huggins JP, Smart TS, Langman S, Taylor L, & Young T (2012). An efficient randomised, placebo-controlled clinical trial with the irreversible fatty acid amide hydrolase-1 inhibitor PF-04457845, which modulates endocannabinoids but fails to induce effective analgesia in patients with pain due to osteoarthritis of the knee. PAIN® 153**:** 1837-1846.

HUNGUND BL, & BASAVARAJAPPA BS (2004). Role of Endocannabinoids and Cannabinoid CB1 Receptors in Alcohol‐Related Behaviors. Annals of the New York Academy of Sciences 1025**:** 515-527.

Isambert H, Venier P, Maggs AC, Fattoum A, Kassab R, Pantaloni D*, et al.* (1995). Flexibility of actin filaments derived from thermal fluctuations. Effect of bound nucleotide, phalloidin, and muscle regulatory proteins. Journal of Biological Chemistry 270**:** 11437-11444.

J Alvarez-Jaimes L, & A Palmer J (2011). The role of endocannabinoids in pain modulation and the therapeutic potential of inhibiting their enzymatic degradation. Current pharmaceutical biotechnology 12**:** 1644-1659.

Jagger JE, Bateman RM, Ellsworth ML, & Ellis CG (2001). Role of erythrocyte in regulating local O2delivery mediated by hemoglobin oxygenation. American Journal of Physiology-Heart and Circulatory Physiology 280**:** H2833-H2839.

Jensen EC (2012). The basics of western blotting. The Anatomical Record: Advances in Integrative Anatomy and Evolutionary Biology 295**:** 369-371.

Jessani N, Liu Y, Humphrey M, & Cravatt BF (2002). Enzyme activity profiles of the secreted and membrane proteome that depict cancer cell invasiveness. Proceedings of the National Academy of Sciences 99**:** 10335-10340.

Jha R, & Rizvi SI (2009). Age-dependent decline in erythrocyte acetylcholinesterase activity: correlation with oxidative stress. Biomed Pap Med Fac Univ Palacky Olomouc Czech Repub 153**:** 195-198.

Jian W, Edom R, Weng N, Zannikos P, Zhang Z, & Wang H (2010). Validation and application of an LC–MS/MS method for quantitation of three fatty acid ethanolamides as biomarkers for fatty acid hydrolase inhibition in human plasma. Journal of Chromatography B 878**:** 1687-1699.

Jordà MA, Verbakel SE, Valk PJ, Vankan-Berkhoudt YV, Maccarrone M, Finazzi-Agro A*, et al.* (2002). Hematopoietic cells expressing the peripheral cannabinoid receptor migrate in response to the endocannabinoid 2-arachidonoylglycerol. Blood 99**:** 2786-2793.

Julious SA (2005). Sample size of 12 per group rule of thumb for a pilot study. Pharmaceutical Statistics: The Journal of Applied Statistics in the Pharmaceutical Industry 4**:** 287-291.

Jun D, Kuca K, Hronek M, & Opletal L (2006). Effect of some acetylcholinesterase reactivators on human platelet aggregation in vitro. Journal of Applied Toxicology: An International Journal 26**:** 258-261.

Kaczocha M, Glaser ST, Chae J, Brown DA, & Deutsch DG (2010). Lipid droplets are novel sites of N-acylethanolamine inactivation by fatty acid amide hydrolase-2. Journal of Biological Chemistry 285**:** 2796-2806.

Kamat SS, Camara K, Parsons WH, Chen D-H, Dix MM, Bird TD*, et al.* (2015). Immunomodulatory lysophosphatidylserines are regulated by ABHD16A and ABHD12 interplay. Nature chemical biology 11**:** 164.

Karbarz MJ, Luo L, Chang L, Tham C-S, Palmer JA, Wilson SJ*, et al.* (2009). Biochemical and biological properties of 4-(3-phenyl-[1, 2, 4] thiadiazol-5-yl)-piperazine-1-carboxylic acid phenylamide, a mechanism-based inhibitor of fatty acid amide hydrolase. Anesthesia & Analgesia 108**:** 316-329.

Karlsson M, Reue K, Xia Y-R, Lusis AJ, Langin D, Tornqvist H*, et al.* (2001). Exon–intron organization and chromosomal localization of the mouse monoglyceride lipase gene. Gene 272**:** 11-18.

Kathuria S, Gaetani S, Fegley D, Valiño F, Duranti A, Tontini A*, et al.* (2003). Modulation of anxiety through blockade of anandamide hydrolysis. Nature medicine 9**:** 76.

Keith JM, Apodaca R, Xiao W, Seierstad M, Pattabiraman K, Wu J*, et al.* (2008). Thiadiazolopiperazinyl ureas as inhibitors of fatty acid amide hydrolase. Bioorganic & medicinal chemistry letters 18**:** 4838-4843.

Keown OP, Winterburn TJ, Wainwright CL, Macrury SM, Neilson I, Barrett F*, et al.* (2010). 2‐arachidonyl glycerol activates platelets via conversion to arachidonic acid and not by direct activation of cannabinoid receptors. British journal of clinical pharmacology 70**:** 180-188.

Kim I, Yetley EA, & Calvo MS (1993). Variations in iron-status measures during the menstrual cycle. The American journal of clinical nutrition 58**:** 705-709.

Kono M, Matsumoto T, Imaeda T, Kawamura T, Fujimoto S, Kosugi Y*, et al.* (2014). Design, synthesis, and biological evaluation of a series of piperazine ureas as fatty acid amide hydrolase inhibitors. Bioorganic & medicinal chemistry 22**:** 1468-1478.

Kottahachchi D, Gooneratne L, Jayasekera A, Muth-Pawlak D, Moulder R, Imanishi SY*, et al.* (2015). Quantitative analysis of the erythrocyte membrane proteins in polycythemia vera patients treated with hydroxycarbamide. EuPA Open Proteomics 7**:** 43-53.

Kramer R, Roberts E, Manetta J, Hyslop P, & Jakubowski J (1993). Thrombin-induced phosphorylation and activation of Ca (2+)-sensitive cytosolic phospholipase A2 in human platelets. Journal of Biological Chemistry 268**:** 26796-26804.

Kunos G, Járai Z, Bátkai S, Goparaju SK, Ishac EJ, Liu J*, et al.* (2000). Endocannabinoids as cardiovascular modulators. Chemistry and physics of lipids 108**:** 159-168.

Labar G, Bauvois C, Borel F, Ferrer JL, Wouters J, & Lambert DM (2010a). Crystal structure of the human monoacylglycerol lipase, a key actor in endocannabinoid signaling. Chembiochem 11**:** 218-227.

Labar G, Wouters J, & Lambert D (2010b). A review on the monoacylglycerol lipase: at the interface between fat and endocannabinoid signalling. Current medicinal chemistry 17**:** 2588-2607.

Laezza C, Pisanti S, Malfitano AM, & Bifulco M (2008). The anandamide analog, Met-F-AEA, controls human breast cancer cell migration via the RHOA/RHO kinase signaling pathway. Endocrine-related cancer 15**:** 965-974.

Laitinen T, Navia-Paldanius D, Rytilahti R, Marjamaa JJ, Karizkova J, Parkkari T*, et al.* (2013). Mutation of Cys242 of human monoacylglycerol lipase disrupts balanced hydrolysis of 1-and 2-monoacylglycerols and selectively impairs inhibitor potency. Molecular pharmacology**:** mol. 113.090795.

Lal I, Dittus K, & Holmes CE (2013). Platelets, coagulation and fibrinolysis in breast cancer progression. Breast Cancer Research 15**:** 207.

Lambert DM, Vandevoorde S, Jonsson K-O, & Fowler CJ (2002). The palmitoylethanolamide family: a new class of anti-inflammatory agents? Current medicinal chemistry 9**:** 663-674.

Lang E, Bissinger R, Gulbins E, & Lang F (2015). Ceramide in the regulation of eryptosis, the suicidal erythrocyte death. Apoptosis 20**:** 758-767.

Lanz C, Mattsson J, Stickel F, Dufour J-F, & Brenneisen R (2018). Determination of the Endocannabinoids Anandamide and 2-Arachidonoyl Glycerol with Gas Chromatography-Mass Spectrometry: Analytical and Preanalytical Challenges and Pitfalls. Medical Cannabis and Cannabinoids 1**:** 9-18.

Lazzarin N, Valensise H, Bari M, Ubaldi F, Battista N, Finazzi-Agro A*, et al.* (2004). Fluctuations of fatty acid amide hydrolase and anandamide levels during the human ovulatory cycle. Gynecological endocrinology 18**:** 212-218.

Leboffe L, di Masi A, Trezza V, Polticelli F, & Ascenzi P (2017). Human serum albumin: A modulator of cannabinoid drugs. IUBMB life 69**:** 834-840.

Lee H, & Blaufox M (1985). Blood volume in the rat. J Nucl Med 26**:** 72-76.

Lee MJ, Lee S-Y, Cho S, Kang E-S, & Chung C-S (2018). Feasibility of serum CGRP measurement as a biomarker of chronic migraine: a critical reappraisal. The journal of headache and pain 19**:** 53.

Lee TTY, Hill MN, Hillard CJ, & Gorzalka BB (2013). Temporal changes in N‐acylethanolamine content and metabolism throughout the peri‐adolescent period. Synapse 67**:** 4-10.

Leimuranta P, Khiroug L, & Giniatullin R (2018). Emerging Role of (Endo)Cannabinoids in Migraine. Front Pharmacol 9**:** 420.

Leslie CC (2015). Cytosolic phospholipase A2: physiological function and role in disease. Journal of lipid research**:** jlr. R057588.

Lev-Lehman E, Deutsch V, Eldor A, & Soreq H (1997). Immature human megakaryocytes produce nuclear-associated acetylcholinesterase. Blood 89**:** 3644-3653.

Li H, Wood J, Whitten K, Vadivel S, Seng S, Makriyannis A*, et al.* (2013). Inhibition of fatty acid amide hydrolase activates Nrf2 signalling and induces heme oxygenase 1 transcription in breast cancer cells. British journal of pharmacology 170**:** 489-505.

Lian J, Nelson R, & Lehner R (2017). Carboxylesterases in lipid metabolism: from mouse to human. Protein & cell**:** 1-18.

Litvinov RI, & Weisel JW (2017). Role of red blood cells in haemostasis and thrombosis. ISBT science series 12**:** 176-183.

Liu J, Wang L, Harvey-White J, Osei-Hyiaman D, Razdan R, Gong Q*, et al.* (2006). A biosynthetic pathway for anandamide. Proceedings of the National Academy of Sciences 103**:** 13345-13350.

Liu Y, Patricelli MP, & Cravatt BF (1999). Activity-based protein profiling: The serine hydrolases. Proceedings of the National Academy of Sciences 96**:** 14694-14699.

Long JZ, Li W, Booker L, Burston JJ, Kinsey SG, Schlosburg JE*, et al.* (2009a). Selective blockade of 2-arachidonoylglycerol hydrolysis produces cannabinoid behavioral effects. Nature chemical biology 5**:** 37-44.

Long JZ, Nomura DK, Vann RE, Walentiny DM, Booker L, Jin X*, et al.* (2009b). Dual blockade of FAAH and MAGL identifies behavioral processes regulated by endocannabinoid crosstalk in vivo. Proceedings of the National Academy of Sciences 106**:** 20270-20275.

Lord CC, Thomas G, & Brown JM (2013). Mammalian alpha beta hydrolase domain (ABHD) proteins: lipid metabolizing enzymes at the interface of cell signaling and energy metabolism. Biochimica et Biophysica Acta (BBA)-Molecular and Cell Biology of Lipids 1831**:** 792-802.

Lovett DH, Cheng S, Cape L, Pollock AS, & Mertens PR (2010). YB-1 alters MT1-MMP trafficking and stimulates MCF-7 breast tumor invasion and metastasis. Biochemical and biophysical research communications 398**:** 482-488.

Lowry OH, Rosebrough NJ, Farr AL, & Randall RJ (1951). Protein measurement with the Folin phenol reagent. The Journal of biological chemistry 193**:** 265-275.

Maccarrone M, Attinà M, Bari M, Cartoni A, Ledent C, & Finazzi‐Agrò A (2001a). Anandamide degradation and N‐acylethanolamines level in wild‐type and CB1 cannabinoid receptor knockout mice of different ages. Journal of neurochemistry 78**:** 339-348.

Maccarrone M, Bari M, Battista N, & Finazzi-Agrò A (2002a). Estrogen stimulates arachidonoylethanolamide release from human endothelial cells and platelet activation. Blood 100**:** 4040-4048.

Maccarrone M, Bari M, Del Principe D, & Finazzi-Agrò A (2003a). Activation of human platelets by 2-arachidonoylglycerol is enhanced by serotonin. Thromb Haemost 89**:** 340-347.

Maccarrone M, Bari M, Di Rienzo M, Finazzi-Agrò A, & Rossi A (2003b). Progesterone activates fatty acid amide hydrolase (FAAH) promoter in human T lymphocytes through the transcription factor Ikaros Evidence for a synergistic effect of leptin. Journal of Biological Chemistry 278**:** 32726-32732.

Maccarrone M, Bari M, Lorenzon T, Bisogno T, Di Marzo V, & Finazzi-Agrò A (2000a). Anandamide uptake by human endothelial cells and its regulation by nitric oxide. Journal of Biological Chemistry 275**:** 13484-13492.

Maccarrone M, Bari M, Menichelli A, Del Principe D, & Agrò AF (1999). Anandamide activates human platelets through a pathway independent of the arachidonate cascade. FEBS letters 447**:** 277-282.

Maccarrone M, Bari M, Menichelli A, Giuliani E, Del Principe D, & Finazzi‐Agrò A (2001b). Human platelets bind and degrade 2‐arachidonoylglycerol, which activates these cells through a cannabinoid receptor. European Journal of Biochemistry 268**:** 819-825.

Maccarrone M, Bisogno T, Valensise H, Lazzarin N, Fezza F, Manna C*, et al.* (2002b). Low fatty acid amide hydrolase and high anandamide levels are associated with failure to achieve an ongoing pregnancy after IVF and embryo transfer. Molecular human reproduction 8**:** 188-195.

Maccarrone M, De Felici M, Bari M, Klinger F, Siracusa G, & Finazzi‐Agrò A (2000b). Down‐regulation of anandamide hydrolase in mouse uterus by sex hormones. European Journal of Biochemistry 267**:** 2991-2997.

Maccarrone M, Valensise H, Bari M, Lazzarin N, Romanini C, & Finazzi-Agrò A (2001c). Progesterone up-regulates anandamide hydrolase in human lymphocytes: role of cytokines and implications for fertility. The journal of Immunology 166**:** 7183-7189.

Malorni W, Bari M, Straface E, Battista N, Matarrese P, Finazzi-Agrò A*, et al.* (2004). Morphological evidence that 2-arachidonoylglycerol is a true agonist of human platelets. Thrombosis and haemostasis 91**:** 1159-1161.

Mander L, & Liu H-W (2010) *Comprehensive natural products II: Chemistry and Biology*. vol. 1. Elsevier.

Mangieri RA, Hong K-IA, Piomelli D, & Sinha R (2009). An endocannabinoid signal associated with desire for alcohol is suppressed in recently abstinent alcoholics. Psychopharmacology 205**:** 63-72.

Marco EM, Echeverry-Alzate V, Lopez-Moreno JA, Gine E, Penasco S, & Viveros MP (2014). Consequences of early life stress on the expression of endocannabinoid-related genes in the rat brain. Behavioural pharmacology 25**:** 547-556.

Martín Giménez VM, Noriega SE, Kassuha DE, Fuentes LB, & Manucha W (2018). Anandamide and endocannabinoid system: an attractive therapeutic approach for cardiovascular disease. Therapeutic advances in cardiovascular disease**:** 1753944718773690.

Martin N, Pirie A, Ford L, Callaghan C, McTurk K, Lucy D*, et al.* (2006). The use of phosphate buffered saline for the recovery of cells and spermatozoa from swabs. Science & justice: journal of the Forensic Science Society 46**:** 179-184.

McKinney MK, & Cravatt BF (2003). Evidence for distinct roles in catalysis for residues of the serine-serine-lysine catalytic triad of fatty acid amide hydrolase. Journal of Biological Chemistry 278**:** 37393-37399.

Melck D, De Petrocellis L, Orlando P, Bisogno T, Laezza C, Bifulco M*, et al.* (2000). Suppression of nerve growth factor Trk receptors and prolactin

receptors by endocannabinoids leads to inhibition of human breast and prostate cancer cell proliferation. Endocrinology 141**:** 118-126.

Melck D, Rueda D, Galve-Roperh I, De Petrocellis L, Guzmán M, & Di Marzo V (1999). Involvement of the cAMP/protein kinase A pathway and of mitogen‐activated protein kinase in the anti‐proliferative effects of anandamide in human breast cancer cells. FEBS letters 463**:** 235-240.

Mindukshev IV, Krivoshlyk VV, Ermolaeva EE, Dobrylko IA, Senchenkov EV, Goncharov NV*, et al.* (2007). Necrotic and apoptotic volume changes of red blood cells investigated by low-angle light scattering technique. Journal of Spectroscopy 21**:** 105-120.

Mohammed OJ, Latif ML, & Pratten MK (2017). Diabetes-induced effects on cardiomyocytes in chick embryonic heart micromass and mouse embryonic D3 differentiated stem cells. Reproductive Toxicology 69**:** 242-253.

Moore CG, Carter RE, Nietert PJ, & Stewart PW (2011). Recommendations for planning pilot studies in clinical and translational research. Clinical and translational science 4**:** 332-337.

Mor M, Rivara S, Lodola A, Plazzi PV, Tarzia G, Duranti A*, et al.* (2004). Cyclohexylcarbamic acid 3 '-or 4 '-substituted biphenyl-3-yl esters as fatty acid amide hydrolase inhibitors: Synthesis, quantitative structure− activity relationships, and molecular modeling studies. Journal of medicinal chemistry 47**:** 4998-5008.

Morris CB (1995). Cryopreservation of animal and human cell lines. In Cryopreservation and Freeze-Drying Protocols. Springer, pp 179-187.

Muccioli GG (2010). Endocannabinoid biosynthesis and inactivation, from simple to complex. Drug discovery today 15**:** 474-483.

Mulvihill MM, & Nomura DK (2013). Therapeutic potential of monoacylglycerol lipase inhibitors. Life sciences 92**:** 492-497.

Murillo-Rodríguez E, Vázquez E, Millán-Aldaco D, Palomero-Rivero M, & Drucker-Colin R (2007). Effects of the fatty acid amide hydrolase inhibitor URB597 on the sleep-wake cycle, c-Fos expression and dopamine levels of the rat. European journal of pharmacology 562**:** 82-91.

Mustard JF, Kinlough-Rathbone RL, & Packham MA (1989). [1] Isolation of human platelets from plasma by centrifugation and washing. Methods in enzymology 169**:** 3-11.

Nachman RL, & Ferris B (1972). Studies on the proteins of human platelet membranes. Journal of Biological Chemistry 247**:** 4468-4475.

Nakajima Y, Furuichi Y, Biswas KK, Hashiguchi T, Kawahara K-i, Yamaji K*, et al.* (2006). Endocannabinoid, anandamide in gingival tissue regulates the periodontal inflammation through NF‐κB pathway inhibition. FEBS letters 580**:** 613-619.

Ndiaye D, Patel V, Demas A, LeRoux M, Ndir O, Mboup S*, et al.* (2010). A non-radioactive DAPI-based high-throughput in vitro assay to assess Plasmodium falciparum responsiveness to antimalarials—increased sensitivity of P. falciparum to chloroquine in Senegal. The American journal of tropical medicine and hygiene 82**:** 228-230.

Noma A, & Kita M (1976). Purification of monoacylglycerol hydrolase from human post-heparin plasma. FEBS letters 61**:** 42-45.

Nomura DK, Hudak CS, Ward AM, Burston JJ, Issa RS, Fisher KJ*, et al.* (2008). Monoacylglycerol lipase regulates 2-arachidonoylglycerol action and arachidonic acid levels. Bioorganic & medicinal chemistry letters 18**:** 5875-5878.

Nomura DK, Long JZ, Niessen S, Hoover HS, Ng S-W, & Cravatt BF (2010). Monoacylglycerol lipase regulates a fatty acid network that promotes cancer pathogenesis. Cell 140**:** 49-61.

Nomura DK, Morrison BE, Blankman JL, Long JZ, Kinsey SG, Marcondes MCG*, et al.* (2011a). Endocannabinoid hydrolysis generates brain prostaglandins that promote neuroinflammation. Science 334**:** 809-813.

Nomura DK, Morrison BE, Blankman JL, Long JZ, Kinsey SG, Marcondes MCG*, et al.* (2011b). Endocannabinoid hydrolysis generates brain prostaglandins that promote neuroinflammation. Science**:** 1209200.

O'Sullivan SE, Kendall DA, & Randall MD (2004). Heterogeneity in the mechanisms of vasorelaxation to anandamide in resistance and conduit rat mesenteric arteries. British journal of pharmacology 142**:** 435-442.

O'Sullivan SE, Kendall DA, & Randall MD (2005). Vascular effects of Δ9-tetrahydrocannabinol (THC), anandamide and N-arachidonoyldopamine (NADA) in the rat isolated aorta. European journal of pharmacology 507**:** 211-221.

O'Sullivan SE, Kendall DA, & Randall MD (2009). Time-Dependent Vascular Effects of Endocannabinoids Mediated by Peroxisome Proliferator-Activated Receptor Gamma (PPAR. PPAR research 2009.

Oddi S, Fezza F, Pasquariello N, D'Agostino A, Catanzaro G, De Simone C*, et al.* (2009). Molecular identification of albumin and Hsp70 as cytosolic anandamide-binding proteins. Chemistry & biology 16**:** 624-632.

Ollis DL, Cheah E, Cygler M, Dijkstra B, Frolow F, Franken SM*, et al.* (1992). The α/β hydrolase fold. Protein Engineering, Design and Selection 5**:** 197-211.

Osborne CK, Hobbs K, & Trent JM (1987). Biological differences among MCF-7 human breast cancer cell lines from different laboratories. Breast cancer research and treatment 9**:** 111-121.

Palabrica T, Lobb R, Furie BC, Aronovitz M, Benjamin C, Hsu Y-M*, et al.* (1992). Leukocyte accumulation promoting fibrin deposition is mediated in vivo by P-selectin on adherent platelets. Nature 359**:** 848.

Palta S, Saroa R, & Palta A (2014). Overview of the coagulation system. Indian journal of anaesthesia 58**:** 515.

Pan B, Wang W, Long JZ, Sun D, Hillard CJ, Cravatt BF*, et al.* (2009). Blockade of 2-arachidonoylglycerol hydrolysis by selective monoacylglycerol lipase inhibitor 4-nitrophenyl 4-(dibenzo [d][1, 3] dioxol-5-yl (hydroxy) methyl) piperidine-1-carboxylate (JZL184) enhances retrograde endocannabinoid signaling. Journal of Pharmacology and Experimental Therapeutics 331**:** 591-597.

Parker LA, Rock EM, & Limebeer CL (2011). Regulation of nausea and vomiting by cannabinoids. British journal of pharmacology 163**:** 1411-1422.

Parolaro D, Massi P, Rubino T, & Monti E (2002). Endocannabinoids in the immune system and cancer. Prostaglandins, Leukotrienes and Essential Fatty Acids (PLEFA) 66**:** 319-332.

Pascual AC, Gaveglio VL, Giusto NM, & Pasquaré SJ (2013). Aging modifies the enzymatic activities involved in 2‐arachidonoylglycerol metabolism. BioFactors 39**:** 209-220.

Pastor A, Farré M, Fitó M, Fernandez-Aranda F, & de la Torre R (2014). Analysis of ECs and related compounds in plasma: artifactual isomerization and ex vivo enzymatic generation of 2-MGs. Journal of lipid research 55**:** 966-977.

Patinkin D, Milman G, Breuer A, Fride E, & Mechoulam R (2008). Endocannabinoids as positive or negative factors in hematopoietic cell migration and differentiation. European journal of pharmacology 595**:** 1-6.

Patricelli MP, Lovato MA, & Cravatt BF (1999). Chemical and mutagenic investigations of fatty acid amide hydrolase: evidence for a family of serine hydrolases with distinct catalytic properties. Biochemistry 38**:** 9804-9812.

Paul A, Kendall DA, & Alexander SP (2005). A spectrophotometric assay for fatty acid amide hydrolase suitable for high-throughput screening. Biochemical pharmacology 69**:** 1187-1193.

Peng L, Wang B, & Ren P (2005). Reduction of MTT by flavonoids in the absence of cells. Colloids and Surfaces B: Biointerfaces 45**:** 108-111.

Pertwee R, Howlett A, Abood ME, Alexander S, Di Marzo V, Elphick M*, et al.* (2010). International Union of Basic and Clinical Pharmacology. LXXIX. Cannabinoid receptors and their ligands: beyond CB1 and CB2. Pharmacological reviews 62**:** 588-631.

Pertwee RG (2008). The therapeutic potential of drugs that target cannabinoid receptors or modulate the tissue levels or actions of endocannabinoids. In Drug Addiction. Springer, pp 637-686.

Pertwee RG (2014). Elevating endocannabinoid levels: pharmacological strategies and potential therapeutic applications. Proceedings of the Nutrition Society 73**:** 96-105.

Pertwee RG, & Ross R (2002). Cannabinoid receptors and their ligands. Prostaglandins, Leukotrienes and Essential Fatty Acids (PLEFA) 66**:** 101-121.

Petrocellis LD, Cascio MG, & Marzo VD (2004). The endocannabinoid system: a general view and latest additions. British journal of pharmacology 141**:** 765-774.

Pierson ES (1988). Rhodamine-phalloidin staining of F-actin in pollen after dimethylsulphoxide permeabilization. Sexual Plant Reproduction 1**:** 83-87.

Piomelli D, Tarzia G, Duranti A, Tontini A, Mor M, Compton TR*, et al.* (2006). Pharmacological profile of the selective FAAH inhibitor KDS‐4103 (URB597). CNS drug reviews 12**:** 21-38.

Piyanova A, Lomazzo E, Bindila L, Lerner R, Albayram O, Ruhl T*, et al.* (2015). Age-related changes in the endocannabinoid system in the mouse hippocampus. Mechanisms of ageing and development 150**:** 55-64.

Pratt PF, Hillard CJ, Edgemond WS, & Campbell WB (1998). N-arachidonylethanolamide relaxation of bovine coronary artery is not mediated by CB1 cannabinoid receptor. American Journal of Physiology-Heart and Circulatory Physiology 274**:** H375-H381.

Prinz H (2010). Hill coefficients, dose–response curves and allosteric mechanisms. Journal of chemical biology 3**:** 37-44.

Raichlen DA, Foster AD, Seillier A, Giuffrida A, & Gerdeman GL (2013). Exercise-induced endocannabinoid signaling is modulated by intensity. European journal of applied physiology 113**:** 869-875.

Ramsey JM, Cooper JD, Penninx BW, & Bahn S (2016). Variation in serum biomarkers with sex and female hormonal status: implications for clinical tests. Scientific reports 6**:** 26947.

Randall M (2007). Endocannabinoids and the haematological system. British journal of pharmacology 152**:** 671-675.

Randall MD, Alexander SP, Bennett T, Boyd EA, Fry JR, Gardiner SM*, et al.* (1996). An endogenous cannabinoid as an endothelium-derived vasorelaxant. Biochemical and biophysical research communications 229**:** 114-120.

Randall MD, Harris D, Kendall DA, & Ralevic V (2002). Cardiovascular effects of cannabinoids. Pharmacology & therapeutics 95**:** 191-202.

Reggio PH (2010). Endocannabinoid binding to the cannabinoid receptors: what is known and what remains unknown. Current medicinal chemistry 17**:** 1468-1486.

Riss T, Moravec R, Niles A, Duellman S, Benink H, Worzella T*, et al.* (2004). Cell Viability Assays.

Robertson JG (2005). Mechanistic basis of enzyme-targeted drugs. Biochemistry 44**:** 5561-5571.

Romero J, Hillard C, Calero M, & Rabano A (2002). Fatty acid amide hydrolase localization in the human central nervous system: an immunohistochemical study. Molecular brain research 100**:** 85-93.

Rowley JW, & Weyrich AS (2013). Coordinate expression of transcripts and proteins in platelets. Blood 121**:** 5255-5256.

Rubio M, de Miguel R, Fernández-Ruiz J, Gutiérrez-López D, Carai MA, & Ramos JA (2009). Effects of a short-term exposure to alcohol in rats on FAAH enzyme and CB 1 receptor in different brain areas. Drug and alcohol dependence 99**:** 354-358.

Ruggeri ZM (2003). Von Willebrand factor, platelets and endothelial cell interactions. Journal of thrombosis and haemostasis : JTH 1**:** 1335-1342.

Rusjan PM, Wilson AA, Mizrahi R, Boileau I, Chavez SE, Lobaugh NJ*, et al.* (2013). Mapping human brain fatty acid amide hydrolase activity with PET. Journal of Cerebral Blood Flow & Metabolism 33**:** 407-414.

Sabrkhany S, Griffioen AW, & oude Egbrink MG (2011). The role of blood platelets in tumor angiogenesis. Biochimica et Biophysica Acta (BBA)-Reviews on Cancer 1815**:** 189-196.

Sankaran VG, & Weiss MJ (2015). Anemia: progress in molecular mechanisms and therapies. Nature medicine 21**:** 221.

Sarzani R, Bordicchia M, Salvi F, Cola G, Franchi E, Battistoni I*, et al.* (2008). A human fatty acid amide hydrolase (FAAH) functional gene variant is associated with lower blood pressure in young males. American journal of hypertension 21**:** 960-963.

Savinainen J, Saario S, & Laitinen J (2012). The serine hydrolases MAGL, ABHD6 and ABHD12 as guardians of 2‐arachidonoylglycerol signalling through cannabinoid receptors. Acta physiologica 204**:** 267-276.

Savinainen JR, Patel JZ, Parkkari T, Navia-Paldanius D, Marjamaa JJ, Laitinen T*, et al.* (2014). Biochemical and pharmacological characterization of the human lymphocyte antigen B-associated transcript 5 (BAT5/ABHD16A). PLoS One 9**:** e109869.

Scalvini L, Piomelli D, & Mor M (2015). Monoglyceride lipase: Structure and inhibitors. Chemistry and physics of lipids.

Schlosburg JE, Blankman JL, Long JZ, Nomura DK, Pan B, Kinsey SG*, et al.* (2010). Chronic monoacylglycerol lipase blockade causes functional antagonism of the endocannabinoid system. Nature neuroscience 13**:** 1113-1119.

Schreiber D, Harlfinger S, Nolden BM, Gerth CW, Jaehde U, Schömig E*, et al.* (2007). Determination of anandamide and other fatty acyl ethanolamides in human serum by electrospray tandem mass spectrometry. Analytical biochemistry 361**:** 162-168.

Scotchie JG, Savaris RF, Martin CE, & Young SL (2015). Endocannabinoid regulation in human endometrium across the menstrual cycle. Reproductive sciences 22**:** 113-123.

Sebastiani P, Thyagarajan B, Sun F, Honig LS, Schupf N, Cosentino S*, et al.* (2016). Age and sex distributions of age‐related biomarker values in healthy older adults from the Long Life Family Study. Journal of the American Geriatrics Society 64**:** e189-e194.

Senis YA, Tomlinson MG, García A, Dumon S, Heath VL, Herbert J*, et al.* (2007). A comprehensive proteomics and genomics analysis reveals novel transmembrane proteins in human platelets and mouse megakaryocytes including G6b-B, a novel immunoreceptor tyrosine-

based inhibitory motif protein. Molecular & Cellular Proteomics 6**:** 548-564.

Setty BY, Chen D, & Stuart MJ (1996). Sickle red blood cells stimulate endothelial cell production of eicosanoids and diacylglycerol. The Journal of laboratory and clinical medicine 128**:** 313-321.

Sharma R, Chisti Y, & Banerjee UC (2001). Production, purification, characterization, and applications of lipases. Biotechnology advances 19**:** 627-662.

Shearer JA, Coker SJ, & Carswell HV (2018). Detrimental effects of 2-arachidonoylglycerol on whole blood platelet aggregation and on cerebral blood flow after a focal ischemic insult in rats. American Journal of Physiology-Heart and Circulatory Physiology 314**:** H967-H977.

Sieber SA, & Cravatt BF (2006). Analytical platforms for activity-based protein profiling–exploiting the versatility of chemistry for functional proteomics. Chemical communications**:** 2311-2319.

Signorello MG, Giacobbe E, & Leoncini G (2011a). Activation by 2‐arachidonoylglycerol of platelet p38MAPK/cPLA2 pathway. Journal of cellular biochemistry 112**:** 2794-2802.

Signorello MG, Giacobbe E, Passalacqua M, & Leoncini G (2011b). The anandamide effect on NO/cGMP pathway in human platelets. Journal of cellular biochemistry 112**:** 924-932.

Signorello MG, Giacobbe E, Passalacqua M, & Leoncini G (2013). The 2-arachidonoylglycerol effect on myosin light chain phosphorylation in human platelets. Biochimie 95**:** 1620-1628.

Signorello MG, & Leoncini G (2016). Regulation of cAMP Intracellular Levels in Human Platelets Stimulated by 2‐Arachidonoylglycerol. Journal of cellular biochemistry 117**:** 1240-1249.

Sim DS, Dilks JR, & Flaumenhaft R (2007). Platelets possess and require an active protein palmitoylation pathway for agonist-mediated activation and in vivo thrombus formation. Arteriosclerosis, thrombosis, and vascular biology 27**:** 1478-1485.

Simon GM, & Cravatt BF (2010). Activity-based proteomics of enzyme superfamilies: serine hydrolases as a case study. Journal of Biological Chemistry 285**:** 11051-11055.

Singh J, Petter RC, Baillie TA, & Whitty A (2011). The resurgence of covalent drugs. Nature reviews Drug discovery 10**:** 307.

Sipe JC, Chiang K, Gerber AL, Beutler E, & Cravatt BF (2002). A missense mutation in human fatty acid amide hydrolase associated with problem drug use. Proceedings of the National Academy of Sciences 99**:** 8394-8399.

Sipe JC, Scott TM, Murray S, Harismendy O, Simon GM, Cravatt BF*, et al.* (2010). Biomarkers of endocannabinoid system activation in severe obesity. PloS one 5**:** e8792.

Smith M, Braem B, & Davis K (1980). Human platelet acetylcholinesterase: the effects of anticholinesterases on platelet function. Thrombosis and haemostasis 42**:** 1615-1619.

Snider NT, Walker VJ, & Hollenberg PF (2010). Oxidation of the endogenous cannabinoid arachidonoyl ethanolamide by the cytochrome P450 monooxygenases: physiological and pharmacological implications. Pharmacological reviews 62**:** 136-154.

Somma-Delpero C, Valette A, Lepetit-Thevenin J, Nobili O, Boyer J, & Verine A (1995). Purification and properties of a monoacylglycerol lipase in human erythrocytes. The Biochemical journal 312 (Pt 2)**:** 519-525.

Sparling P, Giuffrida A, Piomelli D, Rosskopf L, & Dietrich A (2003). Exercise activates the endocannabinoid system. Neuroreport 14**:** 2209-2211.

Spector AA, & Fletcher JE (1978). Fatty acid binding by serum albumin. In Albumin: structure, biosynthesis, function. Pergamon Press, Oxford-New York, pp 51-60.

Spiecker M, Darius H, & Liao JK (2000). A functional role of IκB-ε in endothelial cell activation. The Journal of Immunology 164**:** 3316-3322.

Spieles G, Kresin M, Loges K, Sputtek A, Heschel I, & Rau G (1995). The effect of storage temperature on the stability of frozen erythrocytes. Cryobiology 32**:** 366-378.

Stanke-Labesque F, Mallaret M, Lefebvre B, Hardy G, Caron F, & Bessard G (2004). 2-Arachidonoyl glycerol induces contraction of isolated rat aorta: role of cyclooxygenase-derived products. Cardiovascular research 63**:** 155-160.

Stanley C, & O'Sullivan SE (2014a). Vascular targets for cannabinoids: animal and human studies. British journal of pharmacology 171**:** 1361-1378.

Stanley C, & O'Sullivan S The vasorelaxant effects of anandamide in the human mesenteric artery. 175.

Stanley CP, Hind WH, Tufarelli C, & O'Sullivan SE (2016). The endocannabinoid anandamide causes endothelium-dependent vasorelaxation in human mesenteric arteries. Pharmacological Research 113**:** 356-363.

Stanley CP, & O'Sullivan SE (2014b). Cyclooxygenase metabolism mediates vasorelaxation to 2-arachidonoylglycerol (2-AG) in human mesenteric arteries. Pharmacological Research 81**:** 74-82.

Stone NL, Millar SA, Herrod PJ, Barrett DA, Ortori CA, Mellon VA*, et al.* (2018). An Analysis of Endocannabinoid Concentrations and Mood Following Singing and Exercise in Healthy Volunteers. Frontiers in behavioral neuroscience 12.

Sugiura T, Kodaka T, Nakane S, Miyashita T, Kondo S, Suhara Y*, et al.* (1999). Evidence That the Cannabinoid CB1 Receptor Is a 2-Arachidonoylglycerol Receptor Structure-Activity Relationship of 2-Arachidonoylglycerol, Ether-linked Analogues, and Related Compounds. Journal of Biological Chemistry 274**:** 2794-2801.

Sugiura T, & Waku K (2002). Cannabinoid receptors and their endogenous ligands. The Journal of Biochemistry 132**:** 7-12.

Sutton CW (2012). The role of targeted chemical proteomics in pharmacology. British journal of pharmacology 166**:** 457-475.

Swystun LL, & Liaw PC (2016). The role of leukocytes in thrombosis. Blood**:** blood-2016-2005-718114.

Tanaka M, Yanagihara I, Takahashi H, Hamaguchi M, Nakahira K, & Sakata I (2007). The mRNA expression of fatty acid amide hydrolase in human whole blood correlates with sepsis. Journal of endotoxin research 13**:** 35-38.

Tantimonaco M, Ceci R, Sabatini S, Catani MV, Rossi A, Gasperi V*, et al.* (2014). Physical activity and the endocannabinoid system: an overview. Cellular and molecular life sciences 71**:** 2681-2698.

Taschler U, Radner FP, Heier C, Schreiber R, Schweiger M, Schoiswohl G*, et al.* (2011). Monoglyceride lipase deficiency in mice impairs lipolysis and attenuates diet-induced insulin resistance. Journal of Biological Chemistry 286**:** 17467-17477.

Thorn CF, Oshiro C, Marsh S, Hernandez-Boussard T, McLeod H, Klein TE*, et al.* (2011). Doxorubicin pathways: pharmacodynamics and adverse effects. Pharmacogenetics and genomics 21**:** 440.

Toczek M, Baranowska-Kuczko M, Grzęda E, Pędzińska-Betiuk A, Weresa J, & Malinowska B (2016). Age-specific influences of chronic administration of the fatty acid amide hydrolase inhibitor URB597 on

cardiovascular parameters and organ hypertrophy in DOCA-salt hypertensive rats. Pharmacological Reports 68**:** 363-369.

Trendowski M (2015). Using cytochalasins to improve current chemotherapeutic approaches. Anti-Cancer Agents in Medicinal Chemistry (Formerly Current Medicinal Chemistry-Anti-Cancer Agents) 15**:** 327-335.

Tsou S-H, Chen T-M, Hsiao H-T, & Chen Y-H (2015). A critical dose of doxorubicin is required to alter the gene expression profiles in MCF-7 cells acquiring multidrug resistance. PloS one 10**:** e0116747.

Turcotte C, Zarini S, Jean S, Martin C, Murphy RC, Marsolais D*, et al.* (2017). The endocannabinoid metabolite prostaglandin E2 (PGE2)-Glycerol inhibits human neutrophil functions: involvement of its hydrolysis into PGE2 and EP Receptors. The Journal of Immunology**:** 1601767.

Ueda N, Yamanaka K, Terasawa Y, & Yamamoto S (1999). An acid amidase hydrolyzing anandamide as an endogenous ligand for cannabinoid receptors. FEBS letters 454**:** 267-270.

Ulloa NM, & Deutsch DG (2010). Assessment of a spectrophotometric assay for monoacylglycerol lipase activity. The AAPS journal 12**:** 197-201.

V Catani M, Gasperi V, Catanzaro G, Baldassarri S, Bertoni A, Sinigaglia F*, et al.* (2010). Human platelets express authentic CB1 and CB2 receptors. Current neurovascular research 7**:** 311-318.

Valk P, Verbakel S, Vankan Y, Hol S, Mancham S, Ploemacher R*, et al.* (1997). Anandamide, a natural ligand for the peripheral cannabinoid receptor is a novel synergistic growth factor for hematopoietic cells. Blood 90**:** 1448-1457.

Vanhoutte P, Shimokawa H, Feletou M, & Tang E (2017). Endothelial dysfunction and vascular disease–a 30th anniversary update. Acta Physiologica 219**:** 22-96.

Vercelli C, Barbero R, Cuniberti B, Racca S, Abbadessa G, Piccione F*, et al.* (2014). Transient receptor potential vanilloid 1 expression and functionality in mcf-7 cells: a preliminary investigation. Journal of breast cancer 17**:** 332-338.

Vérine A, Benkirane M, Meignen J, & Boyer J (1989). Lipoprotein lipase in rat heart—II. influence of apolipoproteins and nutritional factors on tri-di-and monoacylglycerol lipase activities in post-heparin effluents. Comparative Biochemistry and Physiology Part B: Comparative Biochemistry 94**:** 19-25.

Vogeser M, Hauer D, Christina Azad S, Huber E, Storr M, & Schelling G (2006). Release of anandamide from blood cells. Clinical Chemical Laboratory Medicine 44**:** 488-491.

Wagner C, Steffen P, & Svetina S (2013). Aggregation of red blood cells: from rouleaux to clot formation. arXiv preprint arXiv:13101483.

Wei BQ, Mikkelsen TS, McKinney MK, Lander ES, & Cravatt BF (2006). A second fatty acid amide hydrolase with variable distribution among placental mammals. Journal of Biological Chemistry 281**:** 36569-36578.

Willems LI, Overkleeft HS, & van Kasteren SI (2014). Current developments in activity-based protein profiling. Bioconjugate chemistry 25**:** 1181-1191.

Wojtukiewicz MZ, Sierko E, Hempel D, Tucker SC, & Honn KV (2017). Platelets and cancer angiogenesis nexus. Cancer and Metastasis Reviews 36**:** 249-262.

Wong DA, Kita Y, Uozumi N, & Shimizu T (2002). Discrete role for cytosolic phospholipase A2α in platelets: studies using single and double mutant mice of cytosolic and group IIA secretory phospholipase A2. Journal of Experimental Medicine 196**:** 349-357.

Xu J, Gu W, Ji K, Xu Z, Zhu H, & Zheng W (2018). Sequence analysis and structure prediction of ABHD16A and the roles of the ABHD family members in human disease. Open biology 8**:** 180017.

Yapa U, Prusakiewicz JJ, Wrightstone AD, Christine LJ, Palandra J, Groeber E*, et al.* (2012). High-performance liquid chromatography-tandem mass spectrometry assay of fatty acid amide hydrolase (FAAH) in blood: FAAH inhibition as clinical biomarker. Analytical biochemistry 421**:** 556-565.

Yu Z, Friso G, Miranda J, Burlingame AL, Patel MJ, Lo‐Tseng T*, et al.* (1997). Structural characterization of human hemoglobin crosslinked by bis (3, 5‐dibromosalicyl) fumarate using mass spectrometric techniques. Protein science 6**:** 2568-2577.

Zechner R, Kienesberger PC, Haemmerle G, Zimmermann R, & Lass A (2009). Adipose triglyceride lipase and the lipolytic catabolism of cellular fat stores. Journal of lipid research 50**:** 3-21.

Zhang D, Saraf A, Kolasa T, Bhatia P, Zheng GZ, Patel M*, et al.* (2007). Fatty acid amide hydrolase inhibitors display broad selectivity and inhibit multiple carboxylesterases as off-targets. Neuropharmacology 52**:** 1095-1105.

Zhong Y, Zhang F, Sun Z, Zhou W, Li ZY, You QD*, et al.* (2013). Drug resistance associates with activation of Nrf2 in MCF‐7/DOX cells, and wogonin reverses it by down‐regulating Nrf2‐mediated cellular defense response. Molecular carcinogenesis 52**:** 824-834.

Appendix. 1.

Volunteer's questionnaires (1) for first visit:

Name:……

……

Today's date:……..

Blood pressure…….m mHg

Weight:…….. kg

Gender: ☐ Female ☐ Male

Height ……metres

1 Please state your age in years (e.g. 25 years old)

……

2 In the last **3 days,** have you taken any medication, including aspirin or other pain killers or any vitamins?

☐ Yes ☐ No

If yes, please specify the name(s) of the medication you took:…….

3 In the last **3 months**, have you consulted a doctor for a health problem, had surgery or medical treatment?

☐ Yes ☐ No

If yes, please give more information:……..

4 In the last **3 months,** have you had a vaccination?

☐ Yes ☐ No

If yes, please indicate which one you received:……

5 Do you **drink alcohol**?

☐ Yes ☐ No

If yes, when did you have your last alcoholic beverage?.....

How many units of alcohol do you drink **per week**?.....

[3/4 can (~250 ml) of regular beer with 5% alcohol content]

[1 small glass (~100 ml) of wine with 12% alcohol content]

[1 pub measure (~30 ml) of spirits with 40% alcohol content]

6 Do you **smoke cigarettes?**

☐ Yes ☐ No

If yes, when did you have your last cigarette?.....

About how many cigarettes do you smoke in a typical day?

☐ 1-10 ☐ 11-20 ☐ More than 20

7 **Physical activity**: How much time (per week) do you spend on each of the following?

		none	**<30 min per week**	**30-60 min per week**	**1-3 h per week**	**>3 h per week**
1	Walking	0	1	2	3	4
2	Bicycling (including stationary exercise bikes)	0	1	2	3	4
3	Aerobic exercise equipment (Stairmaster, rowing, skiing machine, etc.)	0	1	2	3	4
4	Other exercise (specify)	0	1	2	3	4

Please circle/tick one number for each question

And when did you last do some exercise?

.....

8 Caffeine consumption

Roughly how many caffeinated drinks do you consume per week? Please make your best estimate.

Items	Days (0-7)	Servings
Coffee		
Tea		
Soft drinks		
Energy drink (e.g. Red Bull)		
Chocolate		

Under “days”, please indicate how many days per week you normally consume the items (answer from 0 to 7 days per week), and under “servings” indicate how many servings of each item you consume on a typical day (e.g. if you have 4 cup of tea, enter 4 under the servings column)

Appendix. 2.

Short volunteer questionnaire (2) for second and third visits:

Please select “yes” or “no” for the following questions. In the last 48 hours:

	Yes	No
• Did you smoke?		
• Did you get stress because of exam, family issues……..etc?		
• For women, are you on menstrual cycle?		
• Did you take any medication such as aspirin?		
• Do you have a cold or any other infection?		

Thank you for your participation

Appendix. 3.

Correlation analysis between enzyme activity in blood samples from healthy subjects (Chapter 4) and factors such as body mass index (BMI), age and systolic blood pressure (SBP)

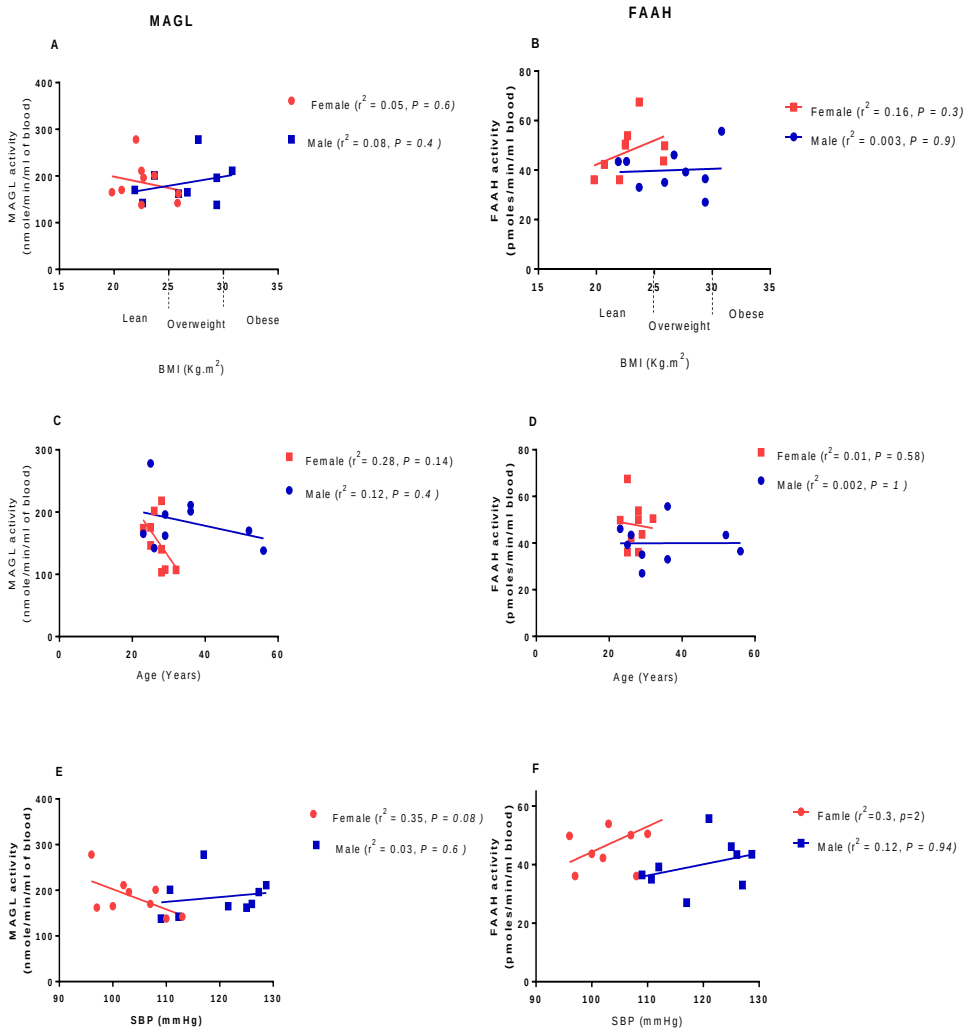

MAGL activity in platelet samples and FAAH activity in erythrocyte samples, and age (A and B), BMI (C and D) and SBP (E and F) in heathy subjects. Analysed using linear regression.

Linear regression analysis failed to show significant correlations between enzyme activities and either age, BMI or SBP (P>0.1).

Appendix. 4.

Direct line/e-mail
+44 (0) 115 8230514
karen.wright@nottingham.ac.uk

The University of Nottingham

Faculty of Medicine and Health Sciences

Research Ethics Committee
School of Life Sciences
University of Nottingham
E Floor, Medical School
Queen's Medical Centre
Nottingham
NG7 2UH

11/05/16

Dear Steve

Ethics Reference No: A190316SA
Study Title: Endocannabinoid hydrolases in human blood
Chief Investigator/Supervisor: Steve Alexander
Lead Investigator/Student: Saoirse O'Sullivan, Nuha Anajirih
Duration of Study: Approximately 3 Months **No of Subjects:**18 (nine female and nine male)

Thank you for your recent application which was considered by the Committee.

The following documents were received:

- Application Form
- Participant Information Sheet
- Poster
- 2 Questionnaires

These have been reviewed and are satisfactory. The study is approved.

Approval is given on the understanding that the Conditions of Approval set out below are followed.

1. You must follow the protocol agreed and inform the Committee of any changes in writing.
2. You must notify the Chair of any serious or unexpected event.
3. This study is approved for the period of active recruitment requested. The Committee also provides a further 5 year approval for any necessary work to be performed on the study which may arise in the process of publication and peer review.
4. An End of Project Progress Report is completed and returned when the study has finished.

Yours sincerely

K. Wright

Dr Vincent Wilson
Chair, School of Life Sciences, Research Ethics Committee

The University of Nottingham

Faculty of Medicine and Health Science, School of Life Sciences

Endocannabinoid metabolism in human blood

Nuha Anajirih, Dr. Steve Alexander, Dr. Saoirse O'Sullivan

Could you help us to learn more about Endocannabinoid metabolism in human blood?

The endocannabinoid system is a group of specialized lipids, their receptors, and the enzymes that produce and degrade them. Through direct and indirect actions, endocannabinoids are known to modulate and influence a variety of physiological systems, including pain, inflammation, energy balance, sleep health, stress responses, mood, and memory. The enzymes that hydrolase endocannabinoids are known as serine hydrolases. When these enzymes do not work properly, they cause various type of disease. We observed that the level of these enzymes are variable between subjects .

we would like a blood sample from healthy volunteers

We aim to gain better understating of distribution of serine hydrolysis in human blood

The activity level of serine hydrolase is influenced by dietary intake. Thus, you will be asked to fast 8 hours prior to blood test

participants will receive a free breakfast

Are you in good health?

Please get in touch for more information

Email: mbxna6@nottingham.ac.uk

Appendix.5.

Direct line/e-mail
+44 (0) 115 8230514
karen.wright@nottingham.ac.uk

12/02/18

The University of Nottingham

Faculty of Medicine and Health Sciences

Research Ethics Committee
School of Life Sciences
University of Nottingham
E Floor, Medical School
Queen's Medical Centre
Nottingham
NG7 2UH

Dear Dr Alexander

Ethics Reference No: 408031/SA – Dr Steve Alexander
Study Title: Endocannabinoid hydrolases in human blood fractions: the effects of platelet aggregation.
Principle Investigators: Dr Steve Alexander, School of Life Sciences
Duration of Study: Approximately 6 Weeks **No of Subjects:** 8 Males

Thank you for your email, dated 22/12/17 responding to the issues raised by the Committee and the following documents were received:

- Updated application form
- Responses to comments raised by the committee.

These have been reviewed and your study is now approved.

Approval is given on the understanding that the Conditions of Approval set out below are followed.

1. You must follow the protocol agreed and inform the Committee of any changes in writing.
2. You must notify the Chair of any serious or unexpected event.
3. This study is approved for the period of active recruitment requested. The Committee also provides a further 5 year approval for any necessary work to be performed on the study which may arise in the process of publication and peer review.
4. An End of Project Progress Report is completed and returned when the study has finished.

Yours sincerely

pp K Wright

Dr Vincent Wilson
Chair, School of Life Sciences, Research Ethics Committee

- Could you help us to learn more about endocannabinoid metabolism in human blood?

Who is eligible ?

- Male
- Healthy

What is involved in this study?

1. Blood sampling
2. Fasting 8 hours (overnight) prior to the blood taking
3. Abstaining from strenuous exercise for the preceding 12 hours
4. Abstaining from alcohol intake for the previous 24 hours

The University of Nottingham
UNITED KINGDOM · CHINA · MALAYSIA

Free breakfast will be offered

If you are interested, please contact me and an explanation about this project will be provided

Nuha Abdulaziz
mbxna6@Nottingham.ac.uk